An investigation into the mechanisms by which *bim* gene expression is regulated in sympathetic neurons

ROSIE HUGHES

A thesis submitted for the Degree of Doctor of Philosophy

Institute of Child Health

University College London

2009

Declaration

I, Rosie Hughes, confirm that the work presented in this thesis is my own. Where work has been derived from other sources, I confirm that this has been indicated in this thesis.

Signed **Date**

Abstract

Neuronal apoptosis plays a critical role in development and disease. Developing sympathetic neurons require nerve growth factor (NGF) for their survival and die by apoptosis in its absence. Studies with sympathetic neurons have provided important insights into the molecular mechanisms of neuronal apoptosis and the signalling pathways that regulate the cell death programme in neurons. Bim is a BH3-only member of the Bcl-2 family that increases in level after NGF withdrawal and which is required for NGF withdrawal-induced death. Regulation of *bim* expression is complex and remains incompletely understood.

By analysing the DNA sequence of the rat *bim* promoter I identified a conserved inverted CCAAT box (ICB) that is bound by the heterotrimeric transcription factor NF-Y *in vitro* and in chromatin. Interestingly, mutational analysis revealed that the ICB is critical for the induction of a *bim*-LUC reporter construct following NGF withdrawal. Use of a well-characterised dominant negative NF-YA mutant (YA13 m29) showed that NF-Y is required for *bim* promoter activity and its induction following NGF withdrawal. Overexpression of YA13 m29 also demonstrated that NF-Y activity is essential for the expression of the endogenous Bim protein and that NF-Y is important for apoptosis following NGF withdrawal. Furthermore, I found that the transcriptional coactivators CBP/p300 are required for the activation of *bim*-LUC following NGF withdrawal and that CBP/p300 may interact with NF-Y to enhance *bim* transcription.

In addition to this, the prosurvival MEK/ERK pathway has been found to inhibit *bim* expression independently of the PI3-K/Akt pathway. 3' RACE and experiments in sympathetic neurons with a new *bim*-LUC+3'UTR reporter construct revealed that this negative regulation is mediated through the *bim* 3' UTR. Mutational analysis and RNA stability experiments have been employed to further investigate this mechanism.

Acknowledgements

I would especially like to thank my supervisor Dr. Jonathan Ham for his project ideas, guidance and continued enthusiasm throughout my PhD. I would also like to thank all past and present members of the MHCB unit, in particular Vanessa, Becky, Mark and Francesca, for their advice in the lab and for the many fun times.

Table of contents

Table of figures

Abbreviations

APAF-1	apoptotic protease activating factor-1
ARE	AU-rich element
Bad	Bcl-2 antagonist of cell death
Bak	Bcl-2 antagonist killer
Bax	Bcl-2 associated x protein
Bcl-2	B-cell CLL/Lymphoma-2
Bcl-xL	Bcl-2 related gene, long isoform
BDNF	brain-derived neurotrophic factor
Bid	BH3 interacting domain death agonist
Bim	Bcl-2 interacting mediator of cell death
Bmf	Bcl-2 modifying factor
CBP	CREB-binding protein
ChIP	chromatin immunoprecipitation
CHOP	CCAAT/enhancer binding protein homologous protein
Co-IP	co-immunoprecipitation
CREB	cAMP response element binding protein
DIABLO	direct IAP-binding protein with low pI
DISC	death-inducing signalling complex
EMSA	electrophoretic mobility shift assay
ERK	extracellular signal-regulated kinase
FADD	Fas-associated death domain
FLIP	FLICE-inhibitory protein
FOXO3a	Forkhead box O3a
gpIgG	guinea pig immunoglobulin G
Hrk/Dp5	harakiri/death protein 5
IAP	inhibitor of apoptosis protein
ICB	inverted CCAAT box
JNK	c-Jun N-terminal kinase

MAPK	mitogen activated protein kinase
Mcl-1	myeloid cell leukaemia-1 protein
MEK	MAPK/extracellular signal-regulated kinase kinase
MLK	mixed-lineage kinase
MOMP	mitochondrial outer membrane permeabilisation
NGF	nerve growth factor
NT-3	neurotrophin-3
NF-Y	nuclear factor-Y
PI3-K	phosphoinositide 3-kinase
PUMA	p53-upregulated modulator of apoptosis
qPCR	quantitative polymerase chain reaction
RT-PCR	reverse transcriptase polymerase chain reaction
SMAC	second mitochondria-derived activator of caspase
TNFR	tumour necrosis factor receptor
TrkA	tropomyosin-related kinase A
XIAP	X-linked inhibitor of apoptosis protein
3′ RACE	3′ rapid amplification of cDNA ends
3′ UTR	3′ untranslated region

Chapter 1: Introduction

1.1 Introduction to apoptosis

Apoptosis is a specific form of programmed cell death, in which a series of evolutionarily-conserved biochemical events leads to a characteristic morphology and death. Apoptotic cell death can be distinguished from necrosis, a form of traumatic cell death that results from a wide variety of acute cellular injuries. Cells undergoing apoptosis display several morphological characteristics that include the loss of membrane asymmetry and attachment, cytoplasmic shrinkage, blebbing of the plasma membrane, chromatin condensation and nuclear fragmentation (Kerr *et al*., 1972). The chromosomal DNA in apoptotic cells is cleaved by an endonuclease between nucleosomes. The resulting fragments run as a ladder of bands on an agarose gel, whereas the DNA from necrotic cells usually runs as a smear (Wyllie *et al*., 1980). Following cell death, apoptotic cells are removed in an orderly manner by neighbouring phagocytes and this process, unlike necrosis, does not initiate an inflammatory response. Apoptosis is an important process in mammalian development, and in normal tissue homeostasis, as well as in disease, where the dysregulation of apoptotic pathways causes a number of human pathologies.

Apoptosis is perhaps the best-studied form of programmed cell death. Other modes of programmed cell death include autophagy, which involves the degradation of intracellular components through the lysosome (Schwartz *et al*., 1993). There are also examples of non-apoptotic programmed cell death that occur in a caspase-independent fashion (Kroemer and Martin, 2005). For example, caspase-independent cell death can be mediated by AIF (apoptosis-inducing factor) (Susin *et al*., 1999).

The molecular mechanisms of apoptosis have been the subject of much investigation over recent years. It is now apparent that the cell death programme involves many different genes that, together, tightly control the initiation and execution of apoptosis across a number of species. However, many of the detailed mechanisms that regulate this important form of cell death still remain to be elucidated.

1.2 Apoptotic pathways

Apoptosis can be initiated by a diverse range of intracellular and extracellular signals, such as DNA damage, hormones, or the withdrawal of cytokines or growth factors. The first phase of apoptosis depends on the nature of the death signal to be integrated. Therefore, depending on the type of apoptotic stimulus, the initiation phase of apoptosis can proceed via one of two major pathways, the extrinsic pathway and the intrinsic pathway (Figure 1.1).

1.2.1 The extrinsic pathway

The extrinsic pathway is activated when proapoptotic ligands bind to specialised cell surface receptors termed 'death receptors'. Death receptors belong to the tumour necrosis factor (TNF) receptor superfamily (Locksley *et al*., 2001). The best characterised examples are Fas (CD95/Apo1), TNF receptor 1 (p55/CD120a), TRAMP (WSL-1/Apo3/DR3/LARD), TRAIL-R1 (DR4) and TRAIL-R2 (DR5/Apo2/KILLER) (Tartaglia *et al*., 1993; Dhein *et al*., 1995; Kitson *et al*., 1996; Bodmer *et al*., 1997; MacFarlane *et al*., 1997; Pan *et al*., 1997). Fas ligand (CD95 ligand) binds Fas, TNFα and TNFβ bind to TNFR1, TWEAK (Apo3 ligand) binds to TRAMP and TRAIL (Apo2 ligand) is the ligand for both TRAIL-R1 and TRAIL-R2 (Pan *et al*., 1997; Ashkenazi and Dixit 1998; Marsters *et al*., 1998). Upon ligand binding, death receptors recruit adaptor proteins such as Fas-associated death domain (FADD) or TNFR-associated death domain (TRADD), and these interactions are mediated by a single death domain (DD) located on the intracellular side of the death receptor (Ashkenazi and Dixit, 1998). FADD also recruits caspase-8 and caspase-10 to form the death-inducing signalling complex (DISC). Once assembled, the DISC induces the activation of caspase-8, which directly activates other members of the caspase family (in type I cells) or which cleaves Bid and thereby triggers the release of proapoptotic factors from the mitochondria and the subsequent activation of more downstream effector caspases (type II cells) (Wajant, 2002).

Figure 1.1 The intrinsic and extrinsic pathways of apoptosis.

The intrinsic pathway is initiated when Bcl-2 family proteins integrate apoptotic stimuli and regulate the release of apoptogenic factors from the mitochondria. Mitochondrial outer membrane permeabilisation (MOMP) leads to the release of cytochrome *c* and the activation of APAF1, which together with dATP and caspase-9, form the apoptosome. Here, caspase-9 is activated and this activates the downstream effector caspases, caspase-3 and caspase-7. The extrinsic pathway is initiated following the binding of a death ligand to a death receptor, for example Fas ligand to Fas. Fas then recruits FADD, which together with caspase-8 and caspase-10, forms the DISC. Activated caspase-8 cleaves Bid to initiate the intrinsic pathway and also activates the downstream effector caspases, caspase-3 and caspase-7. The intrinsic and extrinsic pathways merge at this point and activated caspase-3 and activated caspase-7 cleave a series of protein substrates to execute cell death. In the absence of apoptotic stimuli the caspase cascade is inhibited by the negative regulators XIAP and FLIP. Adapted from Riedl and Salvesen (2007) and Youle and Strasser (2008).

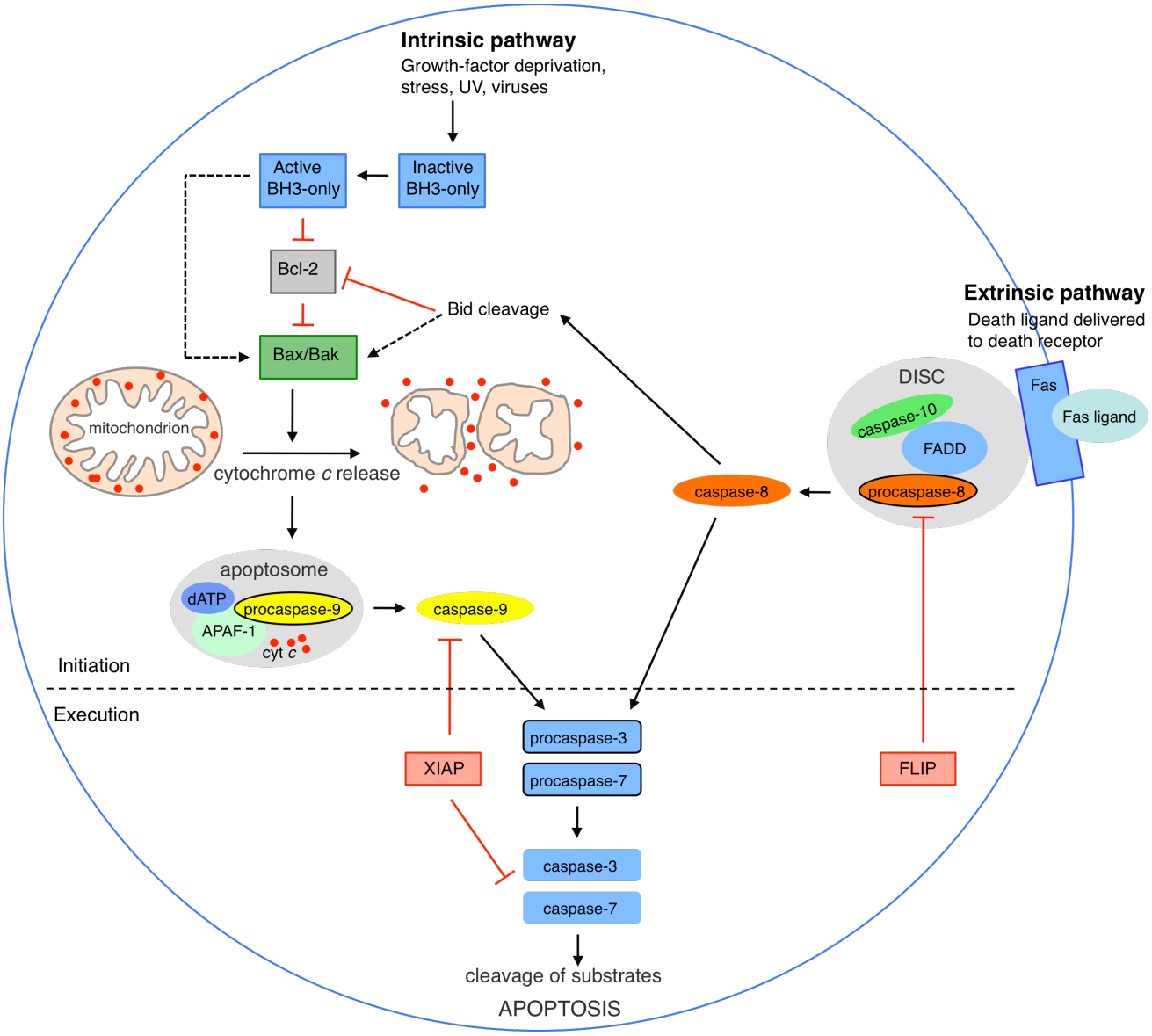
Intrinsic pathway
Growth-factor deprivation, stress, UV, viruses
Active BH3-only
Inactive BH3-only
Bcl-2
Bid cleavage
Bax/Bak
mitochondrion
cytochrome c release
apoptosome
dATP
procaspase-9
APAF-1
cyt c
caspase-9
Initiation
Execution
XIAP
procaspase-3
procaspase-7
caspase-3
caspase-7
cleavage of substrates
APOPTOSIS
Extrinsic pathway
Death ligand delivered to death receptor
DISC
caspase-10
FADD
procaspase-8
Fas
Fas ligand
caspase-8
FLIP

1.2.2 The intrinsic pathway

The intrinsic pathway of apoptosis, also known as the mitochondrial pathway, hinges on the balance of activity between proapoptotic and antiapoptotic members of the Bcl-2 family. When cells are exposed to apoptotic stimuli, Bcl-2 family proteins regulate the permeabilisation of the mitochondrial outer membrane (MOMP) via a mechanism that is not well understood (Chipuk and Green, 2008). MOMP facilitates the release of apoptogenic factors from the mitochondrial intermembrane space into the cytoplasm (Chipuk *et al*., 2006). These include SMAC/DIABLO (second mitochondria-derived activator of caspase/direct IAP-binding protein with low pI) and cytochrome *c*. Cytochrome *c* and the cytosolic adaptor protein APAF-1 (apoptotic protease activating factor 1), along with dATP, form a large protein structure, the apoptosome (Acehan *et al*., 2002). Once formed, the apoptosome recruits and induces the activation of caspase-9, which then activates downstream effector caspases (Riedl and Salvesen, 2007).

There is, however, some cross-talk between the extrinsic and intrinsic pathways. For example in type II cells, the BH3-only protein Bid is cleaved by caspase 8 (activated by the extrinsic pathway) and truncated Bid subsequently translocates to the mitochondria to activate the intrinsic pathway (Luo *et al*., 1998). The intrinsic and extrinsic pathways then merge downstream during the proteolytic caspase cascade that leads to the execution of apoptosis.

1.2.3 Caspases: structure, activation and substrates

Apoptotic caspases are cysteine proteases that can either be initiator (apical) caspases or effector (executioner caspases). At least 14 distinct mammalian caspases have now been identified (Shi, 2004). The initiator caspases include caspase-2, caspase-8, caspase-9 and caspase-10, and the effector caspases include caspase-3, caspase-6 and caspase-7. Caspases are synthesised as single-chain catalytically-inactive zymogens that must undergo proteolytic cleavage for apoptosis to proceed (Shi, 2004). Initiator caspases contain N-terminal prodomains of around 90 amino acids that are important for their function, compared to only 20-30 important residues in the prosequence of effector caspases (Yan and Shi, 2005). Effector caspase zymogens are activated by their intrachain cleavage, mediated by a specific initiator caspase. For example, procaspase-3

is activated through internal cleavage by caspase-9, which separates the large and small subunits (Yan and Shi, 2005). Intrachain cleavage increases the catalytic activity of the effector caspase by several orders of magnitude (Shi, 2004). Initiator caspases undergo autocatalytic intrachain cleavage, but this only enhances their catalytic activity by a modest degree, compared to the activation of effector caspases (Stennicke and Salvesen, 1999; Srinivasula *et al*., 2001). For instance, caspase-9 is only marginally more active compared to procaspase-9, but upon association with the apoptosome, its catalytic activity increases up to 2000-fold (Rodriguez and Lazebnik, 1999; Srinivasula *et al*., 2001). The effector caspases in turn execute cell death by organising the degradation of cellular organelles (Yuan and Horvitz, 2004). The effector caspases are selective proteases, but they cleave a large number of polypeptides during apoptosis. A few examples include: ICAD, the inhibitor of the caspase-activated DNase (CAD), which cleaves chromosomal DNA between nucleosomes, the cytoplasmic proteins Gelsolin and Gas-2, the nuclear proteins Lamin A and Lamin B_1 and a range of protein kinases such as PKN, MEKK-1 and Mst1 kinase (Kaufmann, 1989; Lazebnik *et al*., 1993; Brancolini *et al*., 1995; Erhardt *et al*., 1997; Kothakota *et al*., 1997; Kamada *et al*., 1998; Takahashi *et al*., 1998). This process leads to the characteristic morphology that apoptotic cells share and subsequently dead cells are removed by neighbouring phagocytes in a process termed efferocytosis (deCathelineau and Henson, 2003).

1.2.4 Inhibitors of caspases

Activation of caspases by death receptor-associated scaffolds can be regulated by FLIP (FLICE-inhibitory protein), which can bind the prodomains of procaspase-8 and -10, thereby inhibiting their recruitment to CD95/Fas and TFNR1-induced activation complexes (Han *et al*., 1997; Inohara *et al*., 1997; Irmler *et al*., 1997; Srinivasula *et al*., 1997). Caspase activity can also be regulated by interactions with IAPs (inhibitor of apoptosis proteins). Eight distinct mammalian IAPs have now been described: XIAP (X-linked inhibitor of apoptosis protein), c-IAP1 (cellular-inhibitor of apoptosis protein 1), c-IAP2 (cellular-inhibitor of apoptosis protein 2), ML-IAP (melanoma-inhibitor of apoptosis protein)/Livin, ILP-2 (inhibitor of apoptosis like protein-2), NAIP (neuronal apoptosis inhibitor protein), Bruce/Apollon and survivin. XIAP, c-IAP1 and c-IAP2 bind

to, and inhibit, active caspase-3 and -7 at sub-nanomolar (XIAP) to submicromolar (c-IAP-1 and c-IAP-2) concentrations (Deveraux *et al*., 1997; Roy *et al*., 1997; Duckett *et al*., 1998). They also bind to procaspase-9 and prevent its activation (Deveraux *et al*., 1998). Upon induction of apoptosis, Smac/Diablo is released into the cytosol, where it interacts with multiple IAPs and counters their inhibitory effect (Chai *et al*., 2000; Wilkinson *et al*., 2004). IAPs contain at least one BIR (baculoviral IAP repeat) domain, which are important for their inhibitory function (Hinds *et al*., 1999; Sun *et al*., 1999; Sun *et al*., 2000).

1.3 The Bcl-2 family

The intrinsic pathway of apoptosis depends on the Bcl-2 (B-cell CLL/Lymphoma 2) family of proteins, which regulate the release of proapoptotic factors from the mitochondrial intermembrane space (Figure 1.1).

1.3.1 Bcl-2 family subgroups

The Bcl-2 family can be divided into three main groups, based on how many of the four BH (Bcl-2 homology) domains they share (Figure 1.2A).

Antiapoptotic Bcl-2 proteins, for example Bcl-2, Bcl-xL (Bcl-2 related gene, long isoform) and Mcl-1 (myeloid cell leukaemia 1) contain BH domains 1-4 and are often, but not always, associated with the outer mitochondrial membrane. This interaction is facilitated by the transmembrane domain (TM), that many of the other Bcl-2 relatives also share (Figure 1.2A). The function of the antiapoptotic Bcl-2 proteins is to engage and inhibit the proapoptotic Bcl-2 proteins (Chipuk and Green, 2008).

The multi-domain proapoptotic Bcl-2 proteins include Bax (Bcl-2 associated x protein) and Bak (Bcl-2 antagonist killer 1). Bax and Bak contain BH domains 1-3 and are directly responsible for mitochondrial outer membrane permeabilisation (MOMP) (Leber *et al*., 2007). Bax and Bak are essential for MOMP, because their combined deletion renders cells resistant to multiple apoptotic insults and inhibits the release of cytochrome *c* from the mitochondria (Lindsten *et al*., 2000; Wei *et al*., 2001). However, the exact mechanism by which Bax and Bak induce MOMP is still unclear. It was originally thought that Bax and Bak function in a redundant, parallel fashion (Wei *et al*.,

Figure 1.2 The Bcl-2 family.

(A) The Bcl-2 family comprises three sub-groups that contain between one and four Bcl-2 homology (BH) domains. Antiapoptotic Bcl-2 family members have four BH domains. The proapoptotic sub-family contains BH domains 1-3. The BH3-only sub-group comprises proapoptotic proteins that share only the BH3 domain in common with the other sub-groups. Most members of the Bcl-2 family contain a transmembrane domain (TM) and are therefore typically associated with membranes. Adapted from Taylor *et al*. (2008).

(B) The antiapoptotic protein neutralisation model. The BH3-only proteins Bid, Bim and Puma can bind and neutralise all antiapoptotic Bcl-2 members. A combination of other BH3-only proteins is required to promote apoptosis since each can neutralise only a subset of antiapoptotic proteins, for example Bad can bind to Bcl-2, Bcl-xL and Bcl-W, whereas Noxa can bind to Mcl-1 and A1. Adapted from Chipuk and Green (2008).

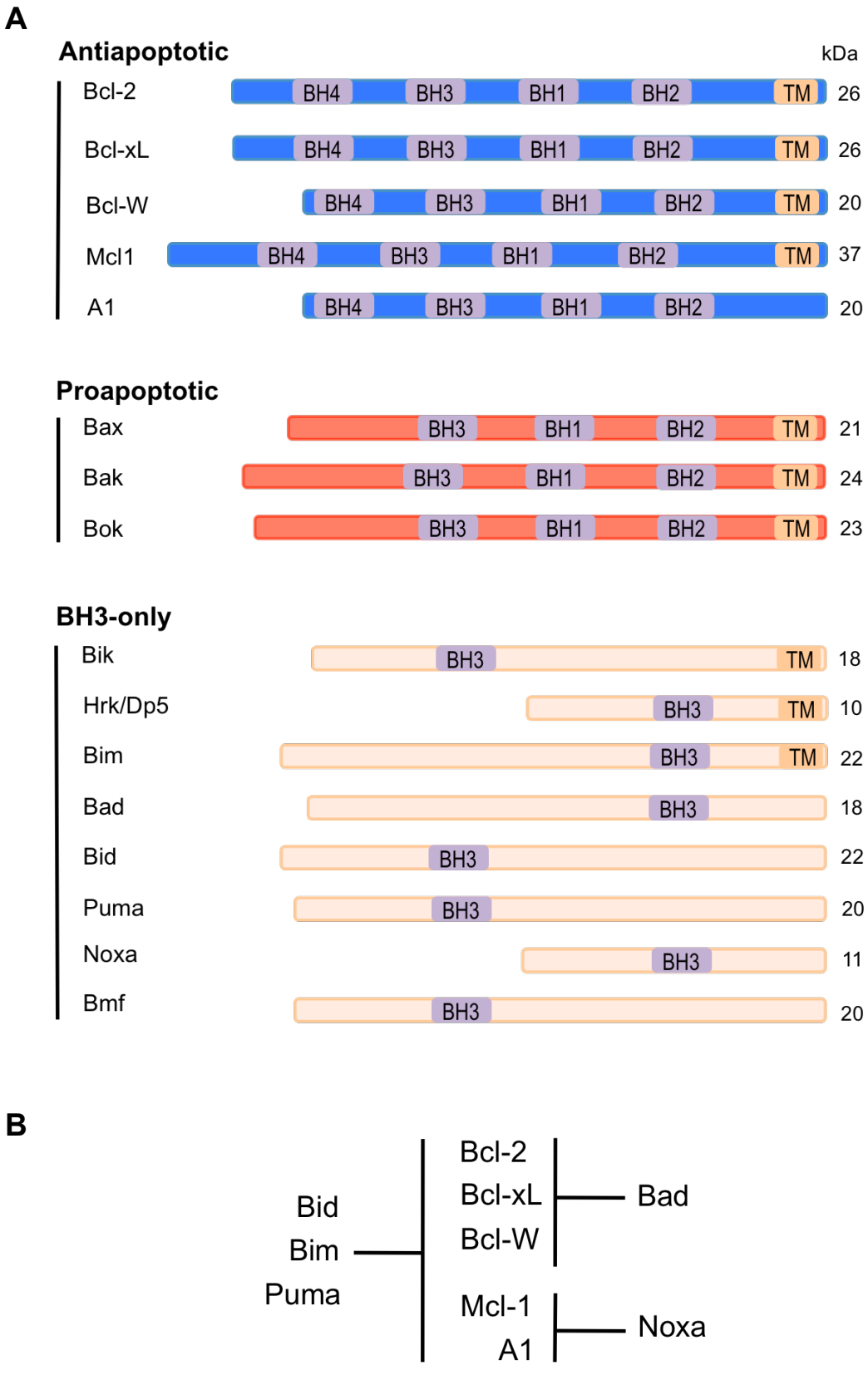
A
Antiapoptotic
kDa
Bcl-2
BH4
BH3
BH1
BH2
TM
26
Bcl-xL
26
Bcl-W
20
Mcl1
37
A1
20
Proapoptotic
Bax
21
Bak
24
Bok
23
BH3-only
Bik
18
Hrk/Dp5
10
Bim
22
Bad
18
Bid
22
Puma
20
Noxa
11
Bmf
20
B
Bid
Bim
Puma
Bcl-2
Bcl-xL
Bcl-W
Bad
Mcl-1
A1
Noxa

2001), whereas now it has become evident that the two proteins require different mechanisms of activation (Leber *et al*., 2007), although Bax is the better studied of the two. In the absence of apoptotic stimuli, Bax is a monomeric protein that is primarily cytosolic or loosely bound to membranes (Antonsson *et al*., 2001). Upon activation, through protein-protein interactions with other Bcl-2 family members, Bax translocates to the mitochondria and forms higher order oligomers (Wolter *et al*., 1997; Gross *et al*., 1998; Antonsson *et al*., 2000). Suzuki *et al*. (2000) first analysed the 3D structure of Bax and demonstrated that cytosolic Bax has its C-terminus (TM domain) inserted into its hydrophobic groove (the canonical BH3 binding site), which would prevent its dimerisation with BH3-only proteins. The authors showed, however, that to be able to insert into the mitochondrial outer membrane, Bax must undergo a conformational change that displaces the C-terminal TM domain from the hydrophobic pocket (Suzuki *et al*., 2000). It is thought that outer membrane permeabilisation occurs after Bax and/or Bak form multiple oligomers that insert into the lipid bilayer, thus forming aqueous channels (Leber *et al*., 2007). Additionally, there is some evidence that other proteins may be involved, for example it has been proposed that Bak is held in check by VDAC2 (Cheng *et al*., 2003).

The third sub-group of the Bcl-2 family comprises the BH3-only proapoptotic proteins (Figure 1.2A). The BH3-only proteins are so-called because they share only the BH3 domain in common with their Bcl-2 relatives. Examples include Bid (BH3 interacting domain death agonist), Hrk/Dp5 (Harakiri/Death protein 5) and Bim (Bcl-2 interacting mediator of cell death). BH3-only proteins function as integrators of stress signalling pathways within the cell and they directly activate the intrinsic pathway through protein-protein interactions with their Bcl-2 family relatives (Bouillet and Strasser, 2002).

1.3.2 The direct activation and the indirect activation models

The exact nature of the protein-protein interactions that result in the activation of Bax and Bak, and thus initiate MOMP, remain unclear. In fact, this subject is highly controversial and central to much debate over recent years. Current evidence suggests that BH3-only proteins activate Bax and Bak, either by indirectly antagonising antiapoptotic proteins

(the indirect activation model) or through direct binding to Bax and Bak (the direct activation/hierarchy model) (Galonek and Hardwick, 2006).

The indirect activation model is based on the idea that in healthy cells Bax and Bak are sequestered by antiapoptotic Bcl-2 family members, such as Bcl-2 and Mcl-1, and following apoptotic stimuli, BH3-only proteins engage the antiapoptotic proteins, thereby releasing Bax and Bak (which are then free to induce MOMP). Several BH3-only proteins can only bind certain prosurvival Bcl-2 proteins, for example Noxa and Hrk/Dp5, whereas Puma, Bid and Bim can engage all of the prosurvival proteins (Figure 1.2B) (Chen *et al*., 2005; Willis and Adams, 2005; Willis *et al*., 2007). It appears that different combinations of BH3-only proteins are required depending on which prosurvival relatives are expressed in a certain cell type. For example, in sympathetic neurons, the antiapoptotic proteins Bcl-2 and Bcl-xL inhibit the release of cytochrome *c* and protect against NGF withdrawal-induced death (Frankowski *et al*., 1995; Greenlund *et al*., 1995; Whitfield *et al*., 2001). Following NGF withdrawal, only three BH3-only proteins are upregulated: Hrk/Dp5, Puma and Bim, and cytochrome *c* release and cell death is dependent on Bax (Deckwerth *et al*., 1996; Imaizumi *et al*., 1997; Harris and Johnson, 2001; Putcha *et al*., 2001; Whitfield *et al*., 2001; Besirli *et al*., 2005). One problem with the indirect activation model is that not all of the proapoptotic effector proteins (Bax and Bak) appear to be sequestered by antiapoptotic proteins (Sedlak *et al*., 1995; Hsu and Youle, 1997; Cheng *et al*., 2003). Also, much data concerning interactions between the BH3-only proteins and the prosurvival proteins has been generated by the use of synthetic BH3 domain peptides that often lack secondary structure (Chen *et al*., 2005; Kuwana *et al*., 2005). It remains unclear whether these fragments recapitulate the activity of the full-length proteins.

The direct activation model is built around the idea that certain BH3-only proteins can directly bind to and activate Bax and Bak. Initially, it was shown that Bid could induce the oligomerisation of Bak (Wei *et al*., 2000). Following this, it was reported, again using BH3 peptides, that Bid, Puma and Bim can directly induce the activation of Bax and Bak and cytochrome *c* release (Letai *et al*., 2002; Kuwana *et al*., 2005). This sub-set of BH3-only proteins was thus termed ‘activator’ proteins and the remaining BH3-only proteins (for example Noxa and Hrk/Dp5) were classified as

'sensitisers'. Based on these findings, the direct activation model was adapted into a hierarchical structure whereby, following apoptotic stimuli 'sensitisers' bind to proapoptotic Bcl-2 proteins which then release the 'activators', which in turn bind to and induce the activation of Bax and Bak (Galonek and Hardwick, 2006). However, experimental evidence for this model is also mixed. It has not been demonstrated that the 'activators' can bind to Bax and Bak with strong affinity and therefore it is generally accepted that a direct interaction is not essential for apoptosis to proceed (Chipuk and Green, 2008). In addition, the *bim*/*bid* double knockout mouse does not recapitulate the major apoptotic phenotype of the *bak*/*bax* double knockout mouse (Willis *et al*., 2007). Furthermore, Willis *et al*. (2007) used fibroblast knockout cell lines lacking Bim and Bid (and an absence of appreciable levels of Puma) to demonstrate that apoptosis via the intrinsic pathway can still be achieved in the absence of so-called 'activators'.

Several studies have established a mechanism for Bcl-2 family protein-protein interactions, in which the α-helical BH3 domain of the proapoptotic proteins inserts into a hydrophobic groove formed by the juxtaposition of the BH1-3 domains of the antiapoptotic Bcl-2 proteins (Sattler *et al*., 1997). In further support of the direct-activation model, Gavathiotis *et al*. (2008) used a 'hydrocarbon stapling' method to overcome the loss of alpha-helical structure when BH3 peptides are synthetically produced without their parent protein. The authors showed that a Bim SAHB (stabilised α-helix of Bcl-2 domains) could directly engage Bax, but it did not bind to the canonical BH3 binding site, instead Bim SAHB bound to a homologous hydrophobic cleft on the other side of Bax (Gavathiotis *et al*., 2008). They demonstrated that Bim SAHB binding to Bax induced its oligomerisation and the release of cytochrome *c in vitro*, and this was inhibited by mutagenesis of key residues at this new interface (Gavathiotis *et al*., 2008).

As a further level of complexity to the debate, Merino *et al*. (2009) generated mice that had the Bim BH3 domain replaced by that of Bad, Noxa, or Puma. They demonstrated that the mutant proteins could engage the usual prosurvival relatives but could no longer bind to Bax. The authors concluded that the proapoptotic activity of Bim is not simply caused by its ability to engage prosurvival relatives or only by its ability to bind Bax (Merino *et al*., 2009). Taken together, mounting evidence supports an integrated model, whereby apoptosis can proceed via the indirect model, but for maximal

execution of apoptosis to proceed then Bim (and possibly other BH3-only proteins) transiently engages and directly activates Bax (Merino *et al*., 2009).

1.3.3 Regulation of BH3-only proteins

BH3-only proteins function as the integrators of prosurvival and proapoptotic stimuli within the cell and are thus tightly regulated by a number of upstream signalling pathways. For example, *hrk/dp5* is a direct target of the c-Jun N-terminal kinase (JNK)/c-Jun pathway in sympathetic neurons and cerebellar granule neurons, and is transcriptionally upregulated after survival factor withdrawal (Ma *et al*., 2007; Towers *et al*., 2009). Growth factors induce the phosphorylation of Bad at Ser112, Ser136 and Ser155, which allows the chaperone protein 14-3-3 to bind and sequester phosphorylated Bad in the cytoplasm (Datta *et al*., 2000). After growth factor withdrawal Bad is dephosphorylated and can therefore interact with other Bcl-2 family members (Datta *et al*., 2000). A number of protein kinases have been proposed to mediate Bad phosphorylation including Akt, Rsk, PAK, p70S6K and PKA (Datta *et al*., 2000). Bad can also be phosphorylated at Ser128 by JNKs (Donovan *et al*., 2002; Konishi *et al*., 2002). Phosphorylation at Ser128 inhibits the interaction of Bad with 14-3-3, thereby increasing its proapoptotic activity (Donovan *et al*., 2002). The *noxa* and *puma* genes are both direct targets of p53 (Jeffers *et al*., 2003; Shibue *et al*., 2003; Villunger *et al*., 2003). When thymocytes were cultured from WT, $p53^{-/-}$ and $puma^{-/-}$ mice that had been exposed to γ radiation, $p53^{-/-}$ cells were completely protected, however $puma^{-/-}$ cells were also significantly protected compared to the WT cells (Villunger *et al*., 2003). Recently it has been shown that *puma* is also a direct target of the JNK/c-Jun pathway in Huh-7 cells (a human hepatacytoma cell line) (Cazanave *et al*., 2009). Less is known about the BH3-only protein Bmf. In healthy cells Bmf interacts with DLC2 (dynein light chain 2) and is then sequestered to myosin V motors (Puthalakath *et al*., 2001). Following apoptotic stimuli, Bmf is released and it is then free to translocate and bind to Bcl-2 family members (Puthalakath *et al*., 2001). Like Bad and Bim, Bmf is an intrinsically unstructured protein and upon binding to Bcl-2 family relatives only the BH3 domain becomes structured (Hinds *et al*., 2007). It is thought that most BH3-only proteins are unstructured (Hinds *et al*., 2007). BH3-only proteins can also be regulated further

downstream in the apoptotic pathway: following death receptor activation Bid is cleaved by caspase-8 to generate tBid (truncated Bid), which activates Bid by exposing its BH3 domain (Li *et al*., 1998). While full-length Bid is localised to the cytosol, tBid translocates to the mitochondria and has been shown to directly interact with Bax (Wei *et al*., 2000; Kuwana *et al*., 2002; Kuwana *et al*., 2005). Furthermore, in type II cells such as hepatocytes, loss of *bid* renders cells resistant to Fas-induced apoptosis (Yin *et al*., 1999; Jost *et al*., 2009). Finally, Bim is a target of a number of regulatory mechanisms, which will be discussed in detail later in this chapter.

It is also of interest that many of the BH3-only single knockout mice, such as *bad*$^{-/-}$, do not have a major apoptotic phenotype. This may be because there is a level of redundancy displayed between certain BH3-only proteins in different cell types (Chipuk and Green, 2008).

1.4 Apoptosis in flies and worms

Apoptosis was first recognised as a normal physiological process in the nematode worm *Caenorhabditis elegans* (*C. elegans*) (Ellis and Horvitz, 1986). Genetic studies have since demonstrated that the apoptotic pathway shares considerable similarity among mammals, flies and worms (Figure 1.3). In *C. elegans,* four genes, *egl-1*, *ced-9*, *ced-4* and *ced-3*, function in sequence to regulate the initiation and execution of apoptosis (Putcha and Johnson, 2004). CED-3 is a member of the caspase family and is essential for apoptosis in nematodes, functioning both as an initiator and an effector caspase (Ellis *et al*., 1991). In cells that die by apoptosis during worm development, the BH3-only homologue EGL-1 binds to CED-9, and thereby releases CED-4 (Figure 1.3). CED-9 is functionally and structurally similar to the mammalian prosurvival proteins, Bcl-2 and Bcl-xL. CED-4 induces the activation of CED-3 and is the functional orthologue of the mammalian protein, Apaf-1 (Yang *et al*., 1998). In *Drosphila melanogaster* (the fruit fly), *Dapaf-1* is almost identical, in terms of sequence similarity, to *Apaf-1*. Dapaf-1 activates Dronc, an initiator caspase in flies. Dronc then cleaves and activates DrICE (Figure 1.3). *Drosophila* also has Bcl-2-like proteins: the proapoptotic Bcl-2 family homologue Debcl/Drob-1/dBorg-1/dBok inhibits the antiapoptotic Bcl-2 homologue

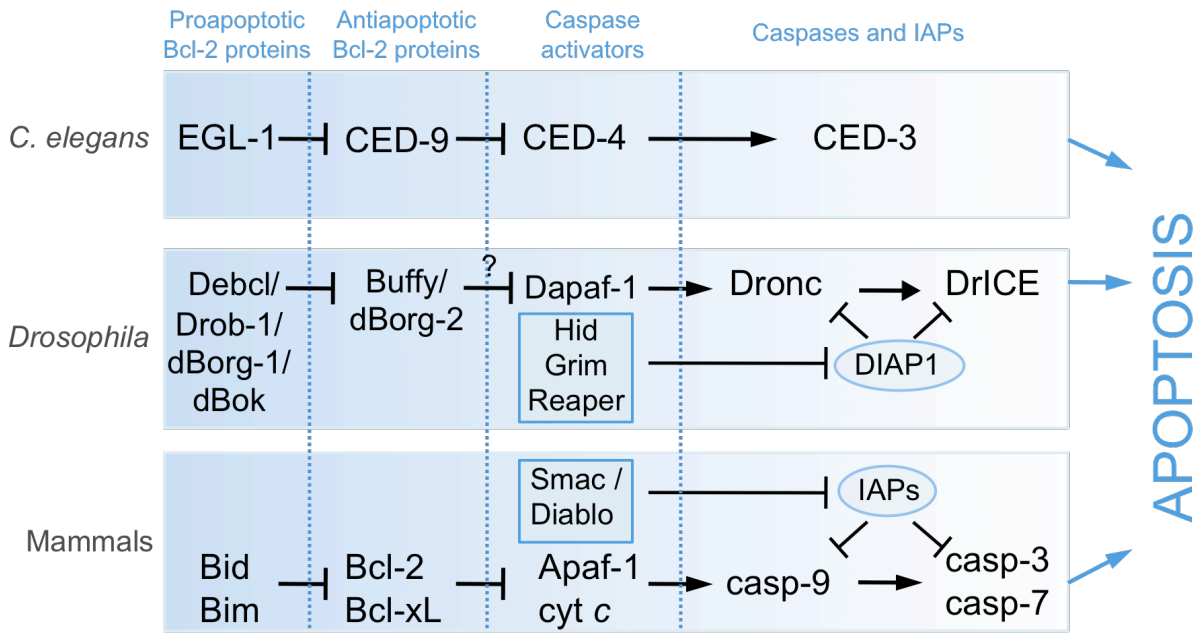

Figure 1.3 The apoptotic pathway is conserved in *C. elegans*, *Drosophila* and mammals.

Mammalian BH3-only proteins, such as Bid and Bim, are homologous to EGL-1 in *C. elegans*. CED-9 is functionally and structurally similar to the mammalian prosurvival proteins, Bcl-2 and Bcl-xL. The Drosophila Bcl-2-like proteins include the proapoptotic protein Debcl/Drob-1/dBorg-1/dBok, which inhibits the antiapoptotic protein Buffy/dBorg-2. Proteins that initiate the activation of caspases include Apaf-1 and cytochrome *c* in mammals, Dapaf-1 in Drosophila and CED-4 in *C. elegans*. The apoptotic pathway in *Drosophila* and mammals includes the initiator caspases, Dronc and caspase-9, respectively, which cleave and activate the effector caspases, DrICE, and caspase-3 and caspase-7, respectively. In *C. elegans* CED-3 functions both as the initiator and the effector caspase. In mammals caspases can be inhibited by IAPs, which can be inhibited by Smac/Diablo. In Drosophila, caspases can be inhibited by DIAP1, which can be inhibited by Hid/Grim/Reaper. However, the mechanism by which the caspase inhibitors, IAPs and DIAP1 are regulated, are not conserved across species. Adapted from Yan and Shi (2005).

Buffy/dBorg-2 (Figure 1.3) (Danial and Korsmeyer, 2004). Additionally, *Drosophila* has IAP proteins, DIAP1, DIAP2 and dBruce.

However, despite the striking similarity in conservation between apoptotic pathways across species, some of the underlying mechanisms are quite different. For example, the regulation of caspases in *Drosophila* and mammals is completely dissimilar (Yan and Shi, 2005). In mammals, XIAP inhibits the catalytic activity of caspase-9, whereas in *Drosophila*, DIAP1 has no effect on the catalytic activity of Dronc (Yan *et al*., 2004). DIAP1 acts as an E3 ubiquitin ligase to target Dronc for degradation via the proteasome (Wilson *et al*., 2002; Chai *et al*., 2003). Other differences include the mechanism by which CED-9 inactivates CED-4, by directly binding to it, whereas in mammals Bcl-xL and Bcl-2 do not directly engage Apaf-1. Furthermore, there is only limited data to support a role for cytochrome *c* in apoptosis in *Drosophila* (Arama *et al*., 2006).

1.5 Apoptosis in development and disease

1.5.1 Apoptosis during mammalian development

The death of cells by apoptosis is critical for normal mammalian development. For instance, mice with a deletion of *caspase-3* die prematurely due to a large excess of post-mitotic, terminally-differentiated cells in their central nervous system, that would normally be culled before that developmental stage by apoptosis (Kuida *et al*., 1996). The development of an organ or tissue is often the result of a pruning process in which an organ or tissue is sculpted from a mass of cells by apoptosis. A classic example is in vertebrate limb bud development, during which apoptosis removes the cells between the developing digits (Saunders, 1966). This developmental process can be arrested by treatment with different caspase inhibitors (Milligan *et al*., 1995). In the immune system, apoptosis eliminates immature B lymphocytes and T lymphocytes that are ineffective and also those that elicit an autoimmune response (Werlen *et al*., 2003). Apoptosis also occurs extensively in the nervous system, where around half of the total number of neurons formed by neurogenesis die by apoptosis during development (Oppenheim, 1991).

1.5.2 Apoptosis in disease

Apoptosis is associated with a wide range of human pathologies that can be broadly categorised into two groups: those in which there is an increase in cell survival (or diseases associated with an inhibition of apoptosis), and those in which there is an increase in cell death (hyper-active apoptosis).

The development of cancers is associated with the inhibition of apoptosis. Generally, due to the sensitivity of the intrinsic pathway, more tumours arise through defective signalling in the intrinsic pathway than the extrinsic pathway (Johnstone *et al*., 2002). A common cause of tumourigenesis is the mutation of genes that regulate cell proliferation and cell death or survival, such as *ras*, *c-myc* or *p53*. Another crucial factor in tumourigenesis is the balance between proapoptotic and antiapoptotic Bcl-2 family members. *Bcl-2* is upregulated in a range of neoplastic conditions and its overexpression has been shown to protect different cell types from a wide range of apoptotic insults (Shimizu *et al*., 1995; Gajewski and Thompson, 1996; Ibrado *et al*., 1997). For example, the *bcl-2* gene was originally identified as a translocated gene in follicular lymphoma (Tsujimoto *et al*., 1984; Bakhshi *et al*., 1985; Cleary *et al*., 1986) and the overexpression of *bcl-2* in Eμ-*bcl-2*/*myc* transgenic mice accelerates lymphomagenesis (Strasser *et al*., 1990). Other pathologies associated with an inhibition of apoptosis include a range of autoimmune conditions and certain viral infections (Reed 2002).

Many neurodegenerative diseases are characterised by the gradual loss of specific sets of neurons. These include Alzheimer's disease, amyotrophic lateral sclerosis, Parkinson's disease, retinitis pigmentosa and different forms of cerebellar degeneration (Thompson, 1995). There is increasing evidence to suggest that apoptosis is a mechanism by which neuronal cells die in a number of these conditions and neurons often die by apoptosis in cell culture and animal models of human neurodegenerative disorders (Yankner, 1996; Estus *et al*., 1997; Nijhawan *et al*., 2000; Yuan and Yankner, 2000; Tatton *et al*., 2003; LeBlanc, 2005; Cottet and Schorderet, 2009). Additionally, apoptosis is one of the mechanisms by which neurons die following an acute injury to the nervous system, such as traumatic brain injury or stroke (Charriaut-Marlangue *et al*., 1996; Martin, 1998).

Due to the numerous studies that support a relevant role for apoptosis in the aetiology of many diseases, the development of pharmacologic agents has recently been focused on targeting different stages of the apoptotic pathway. Drugs that inhibit apoptosis include the small molecule JNK inhibitor D-JNK-1, demonstrated to be an effective neuroprotectant in models of stroke (Borsello *et al*., 2003). In addition, a number of caspase inhibitors have been developed, for example the pan-caspase inhibitor IDN-6556, which has been tested for use during liver transplantations, (Baskin-Bey *et al*., 2007; Masuoka *et al*., 2009). Chemotherapy drugs that activate apoptosis often do so from upstream, for example Cisplatin induces apoptosis by damaging DNA and thereby activating p53, which in turn activates the transcription of *puma* and other proapoptotic genes (Alderden *et al*., 2006; Jiang *et al*., 2006; Yu and Zhang, 2008). However, more recently specific activators of the intrinsic pathway have been developed, for example the BH3-mimetic ABT-737 that binds prosurvival proteins such as Bcl-2 and induces Bax/Bak-dependent killing (Oltersdorf *et al*., 2005; van Delft *et al*., 2006). Additionally, a number of studies demonstrate that IAP proteins are elevated in almost all human malignancies (Tamm *et al*., 2000; Yang *et al*., 2003; Tamm *et al*., 2004). Therefore, a number of Smac mimetics have now been developed, which bind IAP proteins and abrogate their inhibitory activity (Varfolomeev *et al*., 2007; Vucic and Fairbrother, 2007).

1.6 Neuronal apoptosis

1.6.1 Apoptosis in the developing mammalian nervous system

Many types of developing vertebrate neurons are thought to compete for the limiting amounts of neurotrophic factors that their target tissues secrete. Cells that fail to acquire sufficient amounts of neurotrophin subsequently die by apoptosis (Oppenheim, 1991). This process is important for establishing neuronal populations of the correct size and for eliminating neurons that have made inappropriate connections (Barde, 1989; Yuan and Yankner, 2000).

Developmental neuronal apoptosis has been particularly well studied in the developing peripheral nervous system. During development, cells of the neural crest give rise to post-ganglionic sympathetic neurons. In this process, neural crest cells migrate ventrally from the margins of the dorsal neural tube to form a column of sympathetic

ganglion primordia that then coalesce to form sympathetic ganglia and eventually establish the superior cervical ganglion (SCG) (Glebova and Ginty, 2005). During late embryonic and early postnatal development, sympathetic neurons depend on nerve growth factor (NGF) for survival (Figure 1.4). NGF signalling is critical for sympathetic neuron development as *ngf*$^{-/-}$ knockout mice show almost complete loss of sympathetic neurons (Crowley *et al*., 1994). In addition, sympathetic neurons do not only require NGF. For example, *nt-3*$^{-/-}$ knockout mice only retain half of the sympathetic neurons that would normally survive (Ernfors *et al*., 1994; Farinas *et al*., 1994). NT-3 is required as an intermediate target-derived factor that mediates proximal sympathetic axon extension (Glebova and Ginty, 2005).

1.6.2 Models for studying NGF withdrawal-induced apoptosis

Developing sympathetic neurons isolated from early postnatal rats retain their dependence on NGF *in vitro* and can therefore be kept in culture for extended periods in its presence (Martin *et al*., 1988). In the absence of NGF, cultured sympathetic neurons die by apoptosis, usually within 24-48 hours, displaying all the classic hallmarks associated with this form of programmed cell death (Deckwerth and Johnson, 1993; Edwards and Tolkovsky, 1994; Estus *et al*., 1994) (Figure 1.5B). Early studies with sympathetic neurons demonstrated that apoptosis requires *de novo* gene expression, as cell death in this context can be blocked by inhibitors of RNA and protein synthesis (Martin *et al*., 1988) (Figure 1.5A). NGF withdrawal activates the intrinsic pathway of apoptosis in sympathetic neurons (Neame *et al*., 1998; Putcha *et al*., 2002, Wright *et al*., 2007) (Figure 1.1). In addition, a number of genes have now been demonstrated to be critical regulators of apoptosis in sympathetic neurons (section 1.6.3). A major advantage of the sympathetic neuron model is that its cell biology is extremely well defined *in vitro* and *in vivo*. Thus, sympathetic neurons have become a classic model for studying neuronal apoptosis.

The rat pheochromocytoma cell line (PC12) has also been used extensively to study neuronal apoptosis (Greene and Tischler, 1976; Pittman *et al*., 1993). PC12 cells,

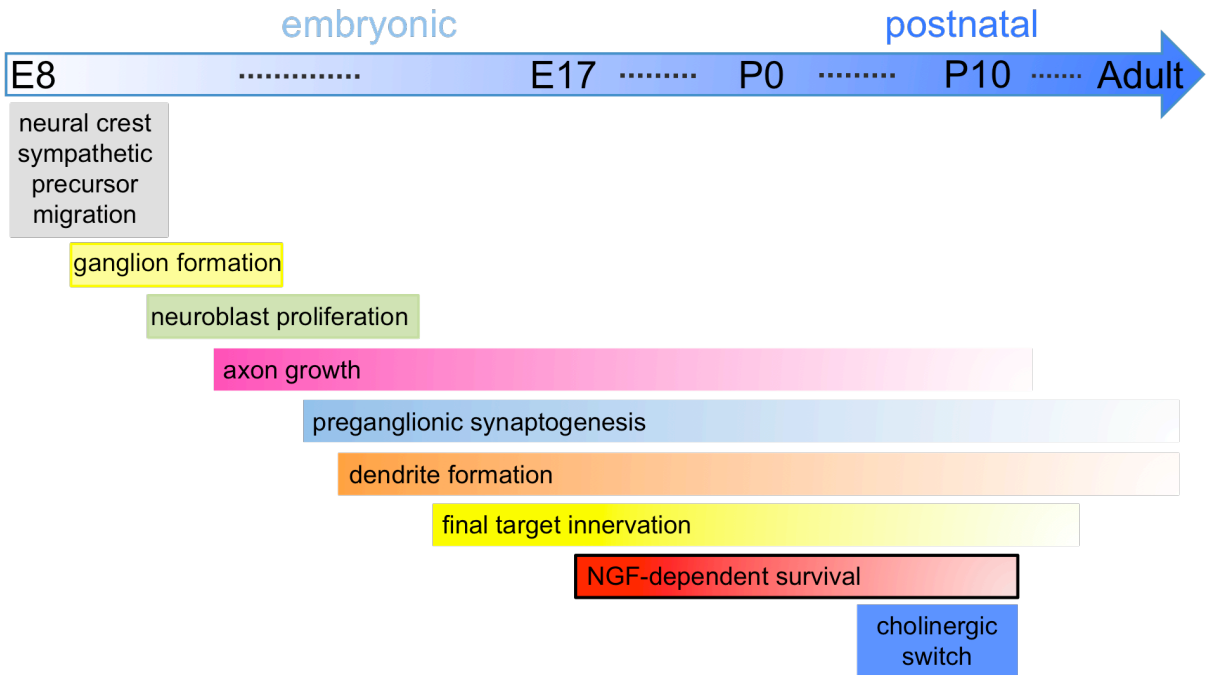

Figure 1.4 Order of events during development of the sympathetic nervous system in mouse.

Embryonic (E) time points and postnatal (P) time points are approximate. Sympathetic neurons are dependent on NGF for their survival from approximately E17 through to P10. NGF is also required for sympathetic axon growth into peripheral target organs, but the extent of this requirement varies greatly between target organs (Glebova and Ginty, 2004). Adapted from Glebova and Ginty (2005).

and their subline PC6-3 cells, can be routinely cultured and then differentiated into a neuronal-phenotype in low-serum conditions together with NGF (Figure 1.5C). Like sympathetic neurons, the withdrawal of NGF from cultures of neuronally differentiated PC12 cells results in cell death by apoptosis in a transcription-dependent manner (Pittman *et al*., 1993) (Figure 1.5). PC12 cells provide a suitable alternative to primary cells for studying cell death induced by growth factor deprivation. This is important for experiments in which large cell populations are required, as one of the major limitations to the sympathetic neuron model is that only around 12,000 cells can be isolated from each 1-day-old rat (Whitfield *et al*., 2004).

Additionally, there are several other model systems used for studying apoptosis in neuronal cells. For example, cerebellar granule neurons (CGNs) can be isolated from the cerebellum of postnatal rats and mice and maintained *in vitro* in medium containing 10% serum and depolarising concentrations of KCl (25 mM) (Bilimoria and Bonni, 2008). Subsequently, apoptosis can be induced by KCl/serum deprivation (Gallo *et al*., 1987; D'Mello, 1993). Spinal motoneurons can also be used for studying apoptosis, since they can be isolated from E14 rats and E12.5 mice and maintained in the presence of neurotrophic factors such as BDNF and GDNF and therefore apoptosis can be induced following growth factor withdrawal (Henderson *et al*., 1995).

1.6.3 The NGF withdrawal-induced death pathway

NGF-dependent sympathetic neurons and neuronally differentiated PC12 cells are well characterised models of neuronal apoptosis and a considerable amount has been learned about the role of Bcl-2 family members, caspases, IAP proteins and the signalling pathways that regulate the cell death programme using these systems.

One of the first genes involved in this pathway, to be identified, was the basic/leucine zipper transcription factor c-Jun, a member of the AP-1 family (Estus *et al*., 1994; Ham *et al*., 1995). Following NGF withdrawal, *c-jun* mRNA and protein levels increase rapidly and microinjection of a c-Jun antibody, the expression of a c-Jun dominant-negative protein, or the conditional knockout of the *c-jun* gene, protects sympathetic neurons against NGF withdrawal-induced death (Estus *et al*., 1994; Ham *et*

Figure 1.5 Models for studying NGF withdrawal-induced apoptosis.

A) Schematic of nerve growth factor withdrawal-induced death in neuronal models. Developing sympathetic neurons are dependent on NGF for their survival, as are neuronally differentiated PC6-3 cells. In both systems, withdrawal of NGF results in cell death by apoptosis. This can be prevented by the use of inhibitors of transcription and protein synthesis, actinomycin-D and cycloheximide, respectively. This demonstrates that apoptosis requires *de novo* gene expression.

B) Sympathetic neurons were isolated from 1-day-old rats and maintained in the presence of NGF for 5-7 days. Following NGF withdrawal for 16 hours, the cells begin to display apoptotic changes. By 48 hours after NGF withdrawal, most of the cells are dead. The scale bar represents 50 μm.

C) PC6-3 stock cells can be differentiated into a neuronal phenotype when cultured in the presence of NGF for 7 days. Differentiated PC6-3 cells undergo apoptosis when NGF is withdrawn. The scale bar represents 50 μm.

A

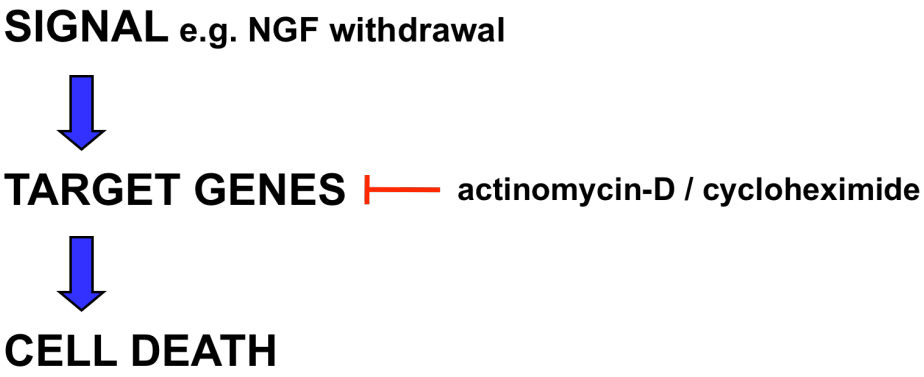
SIGNAL e.g. NGF withdrawal
TARGET GENES
actinomycin-D / cycloheximide
CELL DEATH

B

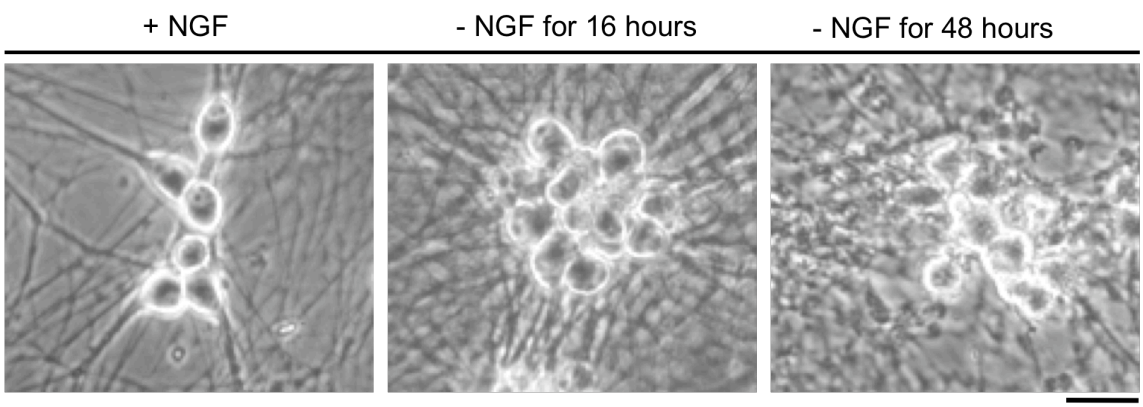
Sympathetic neurons
+ NGF
- NGF for 16 hours
- NGF for 48 hours

C

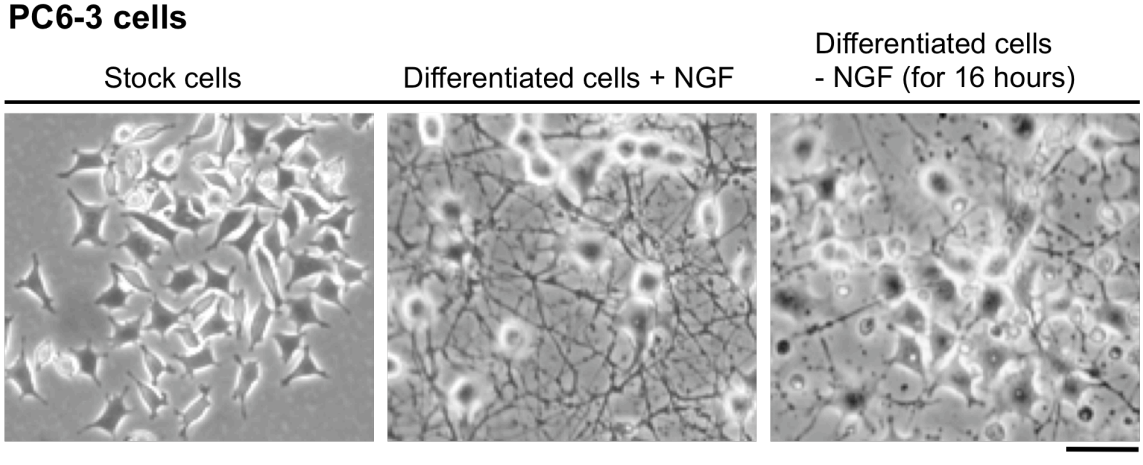
PC6-3 cells
Stock cells
Differentiated cells + NGF
Differentiated cells
- NGF (for 16 hours)

al., 1995; Palmada *et al*., 2002). Furthermore, c-Jun is phosphorylated by JNKs, which are activated following NGF withdrawal and JNK activity is required for NGF withdrawal-induced death (Ham *et al*., 1995; Xia *et al*., 1995; Virdee *et al*., 1997; Eilers *et al*., 1998; Harding *et al*., 2001). Early studies with c-Jun and the JNK pathway implicated the mitochondria and thus the intrinsic pathway, which is now known to be activated by NGF-withdrawal in sympathetic neurons and neuronally differentiated PC12 cells. Following NGF withdrawal, cytochrome *c* is released from the mitochondrial intermembrane space into the cytosol, where it is required for NGF withdrawal-induced death (Neame *et al*., 1998; Deshmukh and Johnson, 1998). Apoptosis in this setting can be blocked by the microinjection of neutralising antibodies to cytochrome *c* (Neame *et al*., 1998). The expression of a c-Jun dominant-negative protein inhibits the release of cytochrome *c* after NGF withdrawal, and the overexpression of MEKK1, which activates the JNK pathway, induces the release of cytochrome *c* and apoptosis in the presence of NGF (Whitfield *et al*., 2001). These findings demonstrated that JNK/c-Jun signalling is critical for the cell death programme activated by NGF withdrawal in sympathetic neurons.

Two downstream targets of the JNK/c-Jun pathway in sympathetic neurons and neuronally differentiated PC12 cells are the BH3-only proteins Bim and Hrk/Dp5 (Harris and Johnson, 2001; Whitfield *et al*., 2001; Towers *et al*., 2009). The expression of Hrk/Dp5 is largely restricted to the nervous system (Imaizumi et al., 1997). *Hrk/dp5* mRNA and protein levels increase when cells are deprived of NGF, and peak at around 18 hours following NGF withdrawal (Imaizumi *et al*., 1997; Towers *et al*., 2009). The induction of *hrk/dp5* mRNA requires mixed-lineage kinase (MLK) and JNK activity, AP-1 activity and a conserved c-Jun/ATF-2 binding site in the *hrk/dp5* promoter (Towers *et al*., 2009). Furthermore, the overexpression of Hrk/Dp5 in microinjected sympathetic neurons induces apoptosis (Imaizumi *et al*., 1997). However, sympathetic neurons isolated from *hrk/dp5*$^{-/-}$ mice die only marginally slower than wild type neurons after NGF withdrawal (Imaizumi *et al*., 2004). It is now apparent that Hrk/Dp5 makes a more minor contribution to the apoptotic pathway in these cells compared to Bim (Ham *et al*., 2005). Bim is also a target of survival signalling by the PI3-K/Akt and the MEK/ERK pathways in these cells, but this will be discussed later in this chapter.

Another BH3-only protein that is transcriptionally upregulated in NGF-deprived sympathetic neurons is Puma (Besirli *et al*., 2005). Puma is a p53 target following DNA-damage in sympathetic neurons (Wyttenbach and Tolovsky, 2006) and ΔNp73, a truncated form of the p53 family member p73, can protect sympathetic neurons against NGF withdrawal-induced death (Pozniak *et al*., 2000). Conversely, another member of the p53 family, TAp63 increases in level after NGF withdrawal and is required for NGF withdrawal-induced death *in vitro* (Jacobs et al., 2005). However, it remains unclear exactly how Puma is regulated following NGF withdrawal. It is possible that the transcription of *puma* is activated by TAp63 and/or by c-Jun, since *puma* has recently been demonstrated to be a c-Jun target gene (Cazanave *et al*., 2009).

The prolyl hydroxylase EglN3/SM-20 also increases in expression during NGF withdrawal-induced death and its overexpression leads to apoptosis in the presence of NGF in microinjected sympathetic neurons (Wax *et al*., 1994; Lipscomb *et al*., 1999). Surprisingly, the induction of EglN3/SM-20 in neuronally differentiated PC12 cells, leads to an increase in the total amount of cytochrome *c* as well as its release into the cytosol (Straub *et al*., 2003). In addition, loss of *egln3/sm-20* significantly protects sympathetic neurons from cell death following NGF withdrawal (Schlisio *et al*., 2008).

Two antiapoptotic Bcl-2 family proteins appear to be important in this pathway, Bcl-2 and Bcl-xL. The levels of *bcl-2* and *bcl-xl* mRNA decrease following NGF withdrawal in sympathetic neurons and the overexpression of either protein can inhibit the release of cytochrome *c* and protect against NGF withdrawal-induced death (Frankowski *et al*., 1995; Greenlund *et al*., 1995; Whitfield *et al*., 2001). Also, sympathetic neurons isolated from Bcl-2 deficient mice die more rapidly than the wild type cells (Greenlund *et al*., 1995).

Apoptosis induced by NGF deprivation is dependent on the proapoptotic multidomain protein Bax, which translocates from the cytosol to the mitochondrial outer membrane following NGF withdrawal in sympathetic neurons (Deckwerth *et al*., 1996; Putcha *et al*., 1999). *Bax*$^{-/-}$ mice have over two fold more sympathetic neurons compared to wild type mice and are resistant to NGF withdrawal-induced apoptosis *in vitro* (Deckwerth *et al*., 1996). Interestingly, knockout of the related Bak protein has no effect on NGF withdrawal-induced death (Putcha *et al*., 2002). This may be because

sympathetic neurons, like hippocampal neurons and CGNs, cultured *in vitro* express N-Bak and not Bak (Sun *et al*., 2001; Uo *et al*., 2005). N-Bak is a neuron-specific splice variant of Bak that lacks the BH1 and BH2 domains and thus cannot function as a multi-domain proapoptotic Bcl-2 protein (Sun *et al*., 2001; Uo *et al*., 2005)

Looking further downstream in the NGF withdrawal-induced death pathway, it has been demonstrated that caspases are critical effectors of cell death. Treatment of NGF-deprived sympathetic neurons and neuronally differentiated PC12 cells with caspase inhibitors, such as zVAD-fmk and BAF, prevents apoptosis (Deshmukh *et al*., 1996; Park *et al*., 1998). Moreover, caspase-3 plays a key role in this context, since sympathetic neurons isolated from *caspase-3* deficient mice are protected from cell death (Wright *et al*., 2007). In addition to the macromolecular synthesis that occurs following NGF withdrawal there is another pathway that does not require new protein synthesis: the development of competence to die in response to cytochrome *c* (Deshmukh and Johnson, 1998). For instance, the microinjection of cytochrome *c* into the cytosol of sympathetic neurons does not induce cell death in the presence of NGF (Deshmukh and Johnson, 1998). This is because NGF deprivation allows the cells to become competent to die (Deshmukh and Johnson, 1998). It is now known that the activity of the caspase inhibitor XIAP must decrease for apoptosis to proceed following cytochrome *c* release, since XIAP-deficient neurons die rapidly following the injection of cytochrome *c* as do cells that have been coinjected with Smac/Diablo together with cytochrome *c* (Deshmukh *et al*., 2002). In fact, XIAP protein levels decrease rapidly in sympathetic neurons following NGF withdrawal (Potts *et al*., 2003).

1.7 Trk receptor signalling

1.7.1 Trk receptors

The survival, differentiation and growth of developing vertebrate neurons depends on the availability of specific neurotrophins that are secreted by the target cells that the neurons innervate. Trk (tropomyosin-related kinase) receptors, a family of three receptor tyrosine kinases, are the major class of neurotrophin cell-surface receptor (Kaplan *et al*., 1991). TrkA is the receptor for NGF, TrkB is the receptor for BDNF (brain-derived neurotrophic factor) and NT-4 (neurotrophin-4) and TrkC is the receptor for NT-3 (neurotrophin-3)

(Figure 1.6). However, there is some crossover between receptors. NT-3 can bind to TrkA and TrkB, but with lower affinity than the primary ligands for these receptors and also with lower affinity than the binding of NT-3 to TrkC (Huang and Reichardt, 2003). Similarly, NT-4 can also bind to TrkC with lower affinity (Huang and Reichardt, 2003).

Members of the Trk family of tyrosine kinase receptors are differentially expressed in neurons of the central nervous system and the peripheral nervous system (Huang and Reichardt, 2003). Sympathetic neurons express relatively high levels of the TrkA receptor and low levels of the TrkC receptor (Belliveau *et al*., 1997). NGF is the primary neurotrophin for TrkA and a classic example of a target-derived neurotrophic factor (Levi-Montalcini, 1987). The binding of NGF to axon terminals initiates local as well as retrograde signalling to cell bodies (Glebova and Ginty, 2005). In the case of retrograde signalling, NGF-TrkA complexes are internalised and then transported from axon terminals to the cell body of neurons (Riccio *et al*., 1997; Watson *et al*., 1999; Kuruvilla *et al*., 2000; Lonze *et al*., 2002; Delcroix *et al*., 2003; Ye *et al*., 2003; Heerssen *et al*., 2004). As further evidence that NGF-TrkA signalling is critical to sympathetic neuron development, *TrkA*$^{-/-}$ knockout mice have virtually no postganglionic sympathetic neurons, a phenotype that is shared with *ngf*$^{-/-}$ knockout mice (Crowley *et al*., 1994; Smeyne *et al*., 1994; Fagan *et al*., 1996).

1.7.2 Survival and death signalling via TrkA

Trk receptors have intrinsic tyrosine kinase activity and can thus autophosphorylate (Barbacid, 1995). Following the binding of NGF to TrkA, several tyrosine residues are phosphorylated within its intracellular cytoplasmic tail, which then serve as docking sites for the recruitment of a number of different binding proteins (Fruman *et al*., 1998; Qian *et al*., 1998). NGF signalling activates several different intracellular signalling pathways, often via the small GTP-binding protein Ras. Ras signalling is responsible for between 40% and 60% of neurotrophin-dependent survival (Kaplan and Miller, 2000). In sympathetic neurons, the two major effectors of Ras-activated survival signalling are the PI3-K (PI3-Kinase)/Akt and the MEK (MAPK (mitogen activated protein kinase) extracellular signal-regulated kinase kinase) / ERK (extracellular signal-regulated kinase)

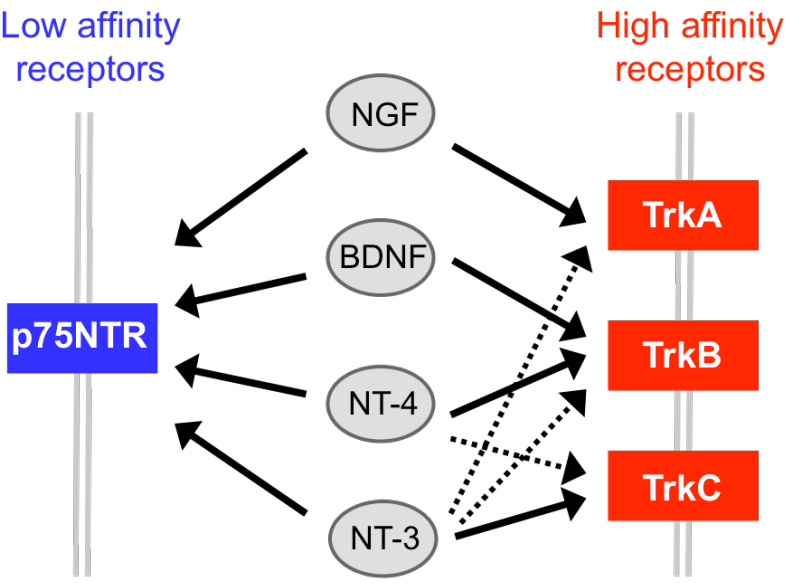

Figure 1.6 Neurotrophins and their receptors.

The neurotrophins and their primary receptors are shown in bold arrows whereas weaker interactions are shown in dashed arrows. All four neurotrophins bind to p75NTR. TrkA is the receptor for NGF, TrkB is the receptor for BDNF and NT-4 and TrkC is the receptor for NT-3. NT-3 can also bind to TrkA and TrkB, but with lower affinity than it binds to TrkC. NT-4 can also bind to TrkC but with lower affinity than it binds to TrkB. Adapted from Gilbert (2006).

pathways (Dudek *et al*., 1997; Crowder and Freeman, 1998; Klesse *et al*., 1999). Activated Akt can directly inhibit neuronal apoptosis by phosphorylating proapoptotic proteins or the transcription factors that regulate them (Kaplan and Miller, 2000). For example, in sympathetic neurons activated Akt phosphorylates the transcription factor FOXO3a, which is sequested by the chaperone protein 14-3-3 in the cytoplasm, and therefore phosphorylated FOXO3a cannot translocate into the nucleus and activate the transcription of *bim* (Figure 1.8; Gilley *et al*., 2003). MEK/ERK signalling includes both the MEK1/2/ERK1/2 and the MEK5/ERK5 pathways. In sympathetic neurons both signalling pathways are stimulated in response to NGF and both can be activated downstream from Ras (Kaplan and Miller, 2000; Wang and Tournier, 2006). Recent studies have found that the deletion of the *erk5* gene results in a significant increase in apoptosis in neonatal sympathetic neurons (Finegan *et al*., 2009).

Additionally, in sympathetic neurons NGF signalling leads to the phosphorylation of CREB (cAMP response element binding protein) on Ser133 (Riccio *et al*., 1997; Riccio *et al*., 1999). CREB can be activated by multiple kinases (Kaplan and Miller, 2000), and studies have shown that CREB is a critical mediator of NGF-dependent gene expression in sympathetic neurons (Riccio *et al*., 1999). Knockout experiments highlighted the critical role that CREB plays in neuronal development, since the loss of *creb* resulted in the decreased survival of sympathetic and sensory neurons and a significant impairment in the process of axon elongation (Lonze *et al*., 2002). Furthermore, in sympathetic neurons CREB activates the transcription of the prosurvival *bcl-2* gene (Riccio *et al*., 1999).

The prosurvival MEK/ERK and PI3-K/Akt pathways act to suppress apoptosis and therefore the removal of NGF results in the loss of survival signals. However, NGF withdrawal also induces the activation of a major proapoptotic pathway in sympathetic neurons, the MLK/JNK/c-Jun pathway (Figure 1.8; Estus *et al*., 1994; Ham *et al*., 1995; Xia *et al*., 1995; Eilers *et al*., 1998; Eilers *et al*., 2001; Harding *et al*., 2001; Whitfield *et al*., 2001).

1.7.3 p75 neurotrophin receptor

In addition to Trk receptors, there is another class of neurotrophin cell surface receptor, the p75 neurotrophin receptor (p75NTR) (Kaplan and Miller, 1997). All four neurotrophins bind to p75NTR with similar affinity (Figure 1.6; Rodriguez-Tebar *et al*., 1992). The loss of p75 results in an increased number of sympathetic neurons in neonatal mice, but not in adult mice, thereby indicating that p75NTR is important for cell death during development (Bamji *et al*., 1998; Brennan *et al*., 1999). A number of studies have implicated BDNF, and possibly NT-4, as the ligands that bind p75NTR and facilitate cell death during development (Bamji *et al*., 1998; Brennan *et al*., 1999; Deppmann *et al*., 2008; Majdan *et al*., 2001). Moreover, this has led to the proposal of a feed-forward loop in which target-derived NGF favours the emergence of a subset of neurons that have enhanced NGF signalling (Deppmann *et al*., 2008). These high NGF-TrkA signalling neurons can then kill neighbouring neurons that have low retrograde NGF-TrkA signalling, via the p75NTR receptor, since NGF promotes TrkA expression and controls the expression of BDNF and NT-4 in sympathetic neurons (Deppmann *et al*., 2008).

1.8 Bim

1.8.1 Bim structure and function

Bim is a BH3-only member of the Bcl-2 family. The exonic structure of *bim* is conserved across species and alternative splicing of exons 3 and 4 results in the generation of several different Bim isoforms (Figure 1.7). The major Bim variants include Bim_{EL}, Bim_{L} and Bim_{S} (Figure 1.7B), which differ in their potency. Bim_{EL} is the major isoform expressed in neuronal cells including cerebellar granule neurons (CGNs), dorsal root ganglion (DRG) neurons and sympathetic neurons (Putcha *et al*., 2001; Whitfield *et al*., 2001).

Bim is an unstructured polypeptide (Hinds *et al*., 2007), and its binding specificity, like that of the other BH3-only proteins, appears to be defined only by its BH3 domain (Chen *et al*., 2005). The proapoptotic function of Bim is critical for apoptosis via the intrinsic pathway, since Bim is one of just three BH3-only proteins that can sequester all five of their prosurvival relatives (Figure 1.2B; Chen *et al*., 2005). In

Figure 1.7 Structure of the *bim* gene and the major Bim isoforms.

(A) The exonic structure of the *bim* gene. The structure of *bim* is highly conserved between species: mouse, rat and human share an identical arrangement of exons 1-6 with longer introns present in human. Coloured boxes indicate coding regions whereas white boxes indicate untranslated regions. Exon 1 is untranslated and the ATG start codon for translation is located 14 nucleotides from the beginning of exon 2 (O'Connor *et al*., 1998).

(B) The major Bim isoforms. Exon 3 contains an ERK1/2 docking domain (FSF) and ERK1/2 phosphorylation sites including Ser65. Exon 4 encodes the region that can bind DLC1 and JNK phosphorylation sites including Thr56 in Bim_L. The BH3 domain lies between amino acids 150-159 in exon 5, and is critical for the induction of apoptosis (Boyd *et al*., 1995). Exon 6 contains the hydrophobic transmembrane domain (TM) between amino acids 179-194, which is important for localisation to intracytoplasmic membranes (Kroemer, 1997). The *bim* mRNA encodes Bim_{EL} which is 194 amino acids (aa) long. Exon 3 is spliced out to produce Bim_L (140 amino acids) and exon 3 and exon 4 are spliced out to produce Bim_S (110 amino acids). Adapted from Bouillet *et al*. (2001a) and Ley *et al*. (2005a).

A

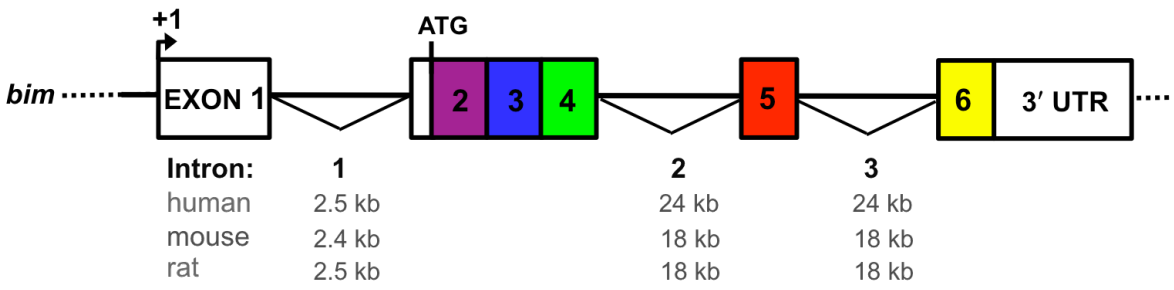
+1
ATG
bim
EXON 1
2
3
4
5
6
3′ UTR
Intron:
1
2
3
human
2.5 kb
24 kb
24 kb
mouse
2.4 kb
18 kb
18 kb
rat
2.5 kb
18 kb
18 kb

B

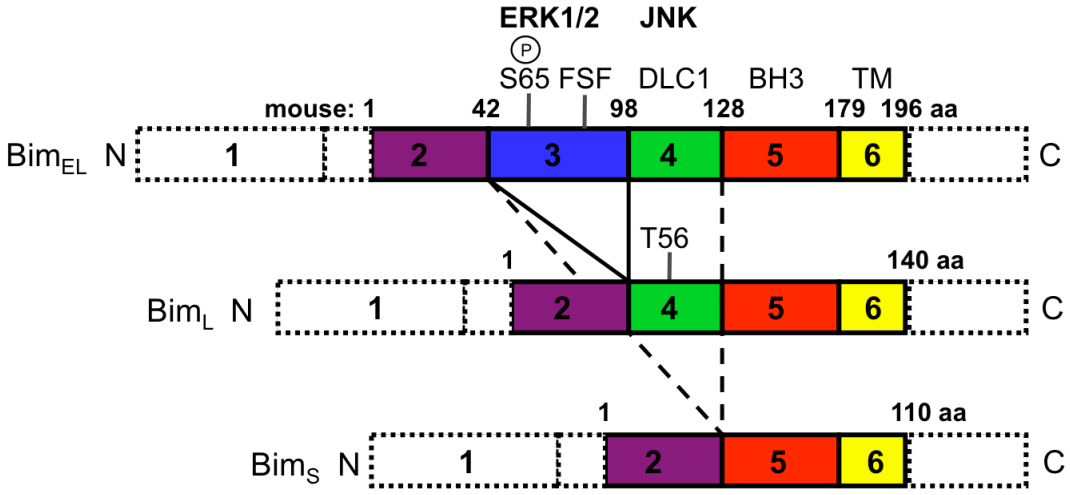
ERK1/2
JNK
P
S65 FSF
DLC1
BH3
TM
mouse: 1
42
98
128
179
196 aa
Bim$_{EL}$ N
1
2
3
4
5
6
C
T56
1
140 aa
Bim$_{L}$ N
1
2
4
5
6
C
1
110 aa
Bim$_{S}$ N
1
2
5
6
C

addition, there is mounting evidence that Bim can also directly induce MOMP by binding to and activating Bax (Letai *et al*., 2002; Kuwana *et al*., 2005; Gavathiotis *et al*., 2008).

Bim is important for apoptosis in many cell types, for example in cerebellar granule neurons deprived of KCl, lymphocytes deprived of cytokines such as IL2, or fibroblasts deprived of serum (Putcha *et al*., 2001; Bouillet *et al*., 2002; Ewings *et al*., 2007). In sympathetic neurons *bim* RNA and Bim protein levels increase following NGF withdrawal and peak at around 16 hours later (Putcha *et al*., 2001; Whitfield *et al*., 2001). The overexpression of Bim_{EL} in sympathetic neurons is sufficient to induce the release of cytochrome *c* and apoptosis in the presence of NGF, whereas the microinjection of *bim* antisense oligonucleotides significantly protects the cells from NGF withdrawal-induced death (Whitfield *et al*., 2001; Gilley *et al*., 2003). Moreover, sympathetic and sensory neurons isolated from $bim^{-/-}$ knockout mice are significantly protected from trophic factor-induced death (Whitfield *et al*., 2001; Coultas *et al*., 2007).

Bim deficient mice have markedly increased haematopoietic cell numbers with two to four fold increases in the number of myeloid and lymphoid cells (Bouillet *et al*., 1999). Bim loss also prevents polycystic kidney disease (PKD) and other degenerative conditions caused by abnormal apoptosis induced by the knockout of *bcl-2* (Bouillet *et al*., 2001b). Furthermore, Bim has also been demonstrated to play a role in retinal neuron death during development and also in cell culture and animal models of Alzheimer's disease and Parkinson's disease (Biswas *et al*., 2007a; Doonan *et al*., 2007; McKerman and Cotter, 2007; Perier *et al*., 2007).

1.8.2 Transcriptional regulation of *bim*

A number of different transcriptional mechanisms have been reported to regulate *bim* expression. In sympathetic neurons or PC12 cells dependent on NGF for survival, transcriptional control of *bim* involves at least three different signalling pathways (Figure 1.8). A number of studies have supported a critical role for MLK-JNK-c-Jun signalling in *bim* regulation. For instance, the overexpression of a dominant negative c-Jun protein or treatment with the MLK inhibitor CEP-1347 reduces *bim* induction following NGF deprivation in sympathetic neurons (Harris and Johnson, 2001; Whitfield *et al*., 2001).

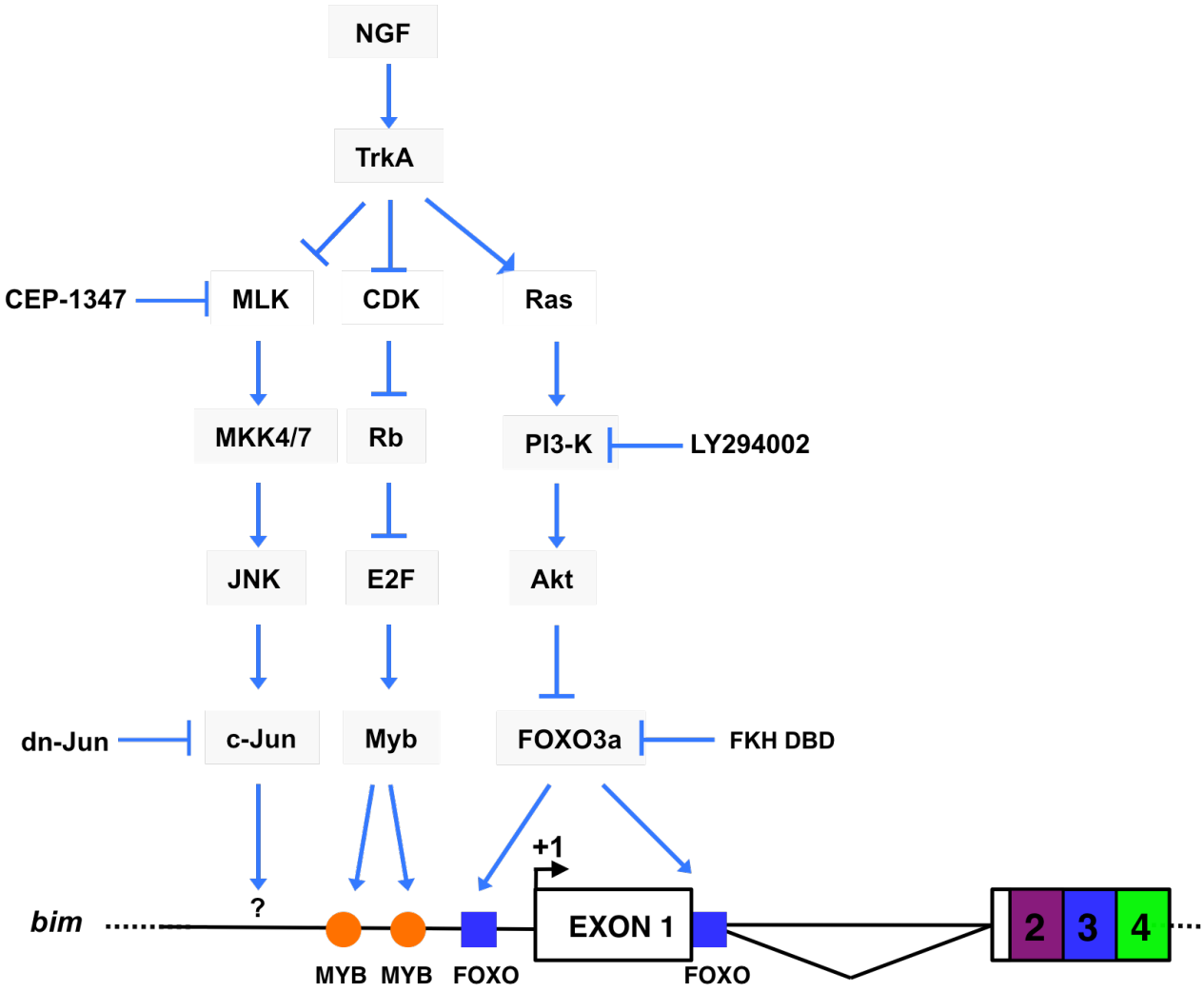

Figure 1.8 Transcriptional regulation of *bim* in sympathetic neurons.

Withdrawal of NGF activates the proapoptotic MLK/JNK/c-Jun pathway, which contributes to the induction of *bim* by a mechanism that is currently unknown. The JNK pathway can be inhibited by the MLK inhibitor CEP-1347 or by the expression of dominant negative c-Jun. NGF withdrawal leads to the activation of Cdk4 and the de-repression of the *b-myb* and *c-myb* genes. The Myb proteins bind to myb sites (indicated by circles) and activate *bim*. NGF withdrawal also leads to a decrease in the prosurvival activity of PI3-K/Akt. This leads to the dephosphorylation and nuclear translocation of FOXO3a, which subsequently binds to FOXO sites (indicated by squares). This pathway can be inhibited by the PI3-K/Akt inhibitor LY294002 and the expression of the mutant FKH DBD (Gilley *et al*., 2003).

Additionally, the increase in Bim protein levels after NGF withdrawal is reduced in sympathetic neurons isolated from *jun*^{AA} knockin mice, in which the *c-jun* gene lacks activating Ser63/Ser73 phosphorylation sites (Besirli *et al*., 2005). *Bim* is also a target of FOXO transcription factors in sympathetic neurons and neuronal PC12 cells (Figure 1.8). Following NGF withdrawal, FOXO3a translocates into the nucleus and binds to two conserved FOXO sites, thereby contributing to activation of *bim* transcription (Gilley *et al*., 2003). Mutation of these sites, in the context of a *bim*-LUC reporter construct, greatly reduces *bim* promoter activation following NGF withdrawal and the overexpression of constitutively active FOXO3a can activate *bim*-LUC in the presence of NGF and induce endogenous Bim expression (Gilley *et al*., 2003). Furthermore, FOXO activity contributes to the NGF withdrawal-induced death of sympathetic neurons (Gilley *et al*., 2003). More recently, a third transcriptional pathway has been reported to regulate *bim* expression in neuronal PC12 cells (Figure 1.8). NGF deprivation leads to the activation of Cdk4, which in turn phosphorylates members of the Rb family, leading to the dissociation of Rb family members and chromatin modifiers from a complex with E2F, and to de-repression of the *b-myb* and *c-myb* genes. The Myb transcription factors then bind to Myb sites in the *bim* promoter and activate *bim* transcription (Biswas *et al*., 2005).

Some of the signalling pathways and transcription factors that regulate *bim* transcription are cell type-specific whereas other mechanisms appear to be more general. For example, in pro-B and T cells, trophic factor deprivation and inhibition of PI3-K activity cause FOXO3a dephosphorylation, induction of Bim expression and FOXO3a-dependent apoptosis (Dijkers *et al*., 2000, Dijkers *et al*., 2002; Stahl *et al*., 2002). On the other hand, the ER stress-induced activation of *bim* transcription involves different mechanisms. Puthalakath *et al*. (2007) showed that Bim is essential for ER stress-induced apoptosis in a range of cell types. The authors found that ER stress activates *bim* transcription and this activation does not involve FOXO3a but the stress-induced transcription factor CHOP (CCAAT/enhancer binding protein homologous protein). Furthermore, CHOP-C/EBPα can activate a *bim*-LUC reporter construct via a consensus CHOP-C/EBPα site located within intron 1 of the *bim* gene (Puthalakath *et al*., 2007). However, when this region of intron 1 (exon 1c) was deleted in the context of our *bim*-

LUC reporter construct, there was no significant change in the induction of *bim*-LUC following NGF withdrawal, suggesting that this CHOP-C/EBPα binding site is not important for the activation of *bim* following NGF withdrawal in sympathetic neurons (Gilley and Ham, 2005).

1.8.3 Post-transcriptional regulation of *bim*

Although transcriptional control is the predominant means of regulating gene expression is eukaryotes, a number of mechanisms exist whereby a gene is subject to important supplementary control between its initial transcription and protein synthesis.

Alternative splicing results in the generation of a number of different Bim isoforms that consequently vary in their potency (O'Connor *et al*., 1998; U *et al*., 2001; Liu *et al*., 2002; Marani *et al*., 2002; Chen *et al*., 2004).

Additionally, recent data has implicated *bim* as a target for regulation via mRNA stability and translation. Matsui *et al*. (2007) found that exposure to cytokines leads to the destabilisation of *bim* mRNA via AU-rich elements within a 1 kb section of the 3′ UTR in the Baf-3 cell line. Furthermore, *bim* has now been added to the fast-expanding list of transcripts that are targets for regulation by miRNAs. Ventura *et al*. (2008) found that mice with a conditional knockout of miR-17~92 die shortly after birth and that loss of miR-17~92 results in increased levels of Bim and inhibition of B cell development. This is consistent with the observation that Bim is important for controlling lymphocyte apoptosis (O'Connor *et al*., 1998; Bouillet *et al*., 1999; Bouillet *et al*., 2001b; Ventura *et al*., 2008). Most recently, Terasawa *et al*. (2009) showed that *bim* mRNA expression is suppressed by miR-221 and miR-222, both of which are induced by NGF-stimulation in PC12 cells via the ERK1/2 pathway. As further evidence to support *bim* as a miRNA target, Su *et al*. (2009) found that in embryonic stem cells deficient for Ago1-4 (core effectors of the miRNA pathway) Bim protein levels were significantly elevated.

1.8.4 Post-translational regulation of Bim

Over the last decade a great deal has been discovered about the post-translational mechanisms that regulate the Bim protein. The major splice variants of Bim vary in their proapoptotic potency due to the different post-translational mechanisms that govern their

activity (Ley *et al*., 2005a). Bim_S is the most potent isoform with no post-translational mechanisms to restrain it and possibly for this reason it is less frequently expressed than the other two major isoforms Bim_L and Bim_{EL}, whereas Bim_{EL} is the most tightly regulated isoform (O'Reilly *et al*., 2000; Ley *et al*., 2005a).

Bim_L and Bim_{EL} both retain exon 4 of the *bim* gene, which encodes a binding site for dynein light chain-1 (DLC1 or LC8), a component of the dynein motor complex (Figure 1.7B). Bim_L and Bim_{EL} can therefore bind to, and be sequestered by, the DLC1 component of the dynein motor complex (Puthalakath *et al*., 1999). However, this interaction appears only to be relevant in certain cell types (Shinjyo *et al*., 2001; Gomez-Bougie *et al*., 2005; Ley *et al*., 2005a). Lei and Davis (2003) showed that JNK-mediated phosphorylation of Bim, at Thr56 in the DLC1 binding motif, can disrupt the interaction between Bim_L and DLC1 leading to increased proapoptotic activity in the HEK 293T cell line. In addition, another mechanism for the phosphorylation of Bim by JNK has been described for neuronal cells: following NGF withdrawal, Bim_{EL} is phosphorylated by JNK at Ser65, which leads to interactions with Pin1 that stabilise Bim_{EL} and thereby potentiate neuronal apoptosis (Putcha *et al*., 2003; Becker *et al*., 2004; Bonni and Becker, 2006).

Bim_{EL} is the only isoform to retain exon 3 of the *bim* gene (Figure 1.7B). Initially it was shown that Bim_{EL} is phosphorylated by the MEK/ERK pathway in neuronal PC12 cells maintained in the presence of NGF (Biswas and Greene, 2002). Ley *et al*. (2003) also demonstrated the ERK-mediated phosphorylation of Bim_{EL} in serum-treated fibroblasts. Later studies showed that the region of the Bim protein, encoded by exon 3, contains an ERK1/2 docking site via which the MEK1/2/ERK1/2 pathway promotes the phosphorylation of Bim_{EL} at Ser65 and other sites, which leads to its degradation via the proteasome (Figure 1.7; Luciano *et al*., 2003; Ley *et al*., 2004; Marani *et al*., 2004; Ley *et al*., 2005b; Ewings *et al*., 2007). Moreover, Ewings *et al*. (2007) showed that the ERK1/2-dependent phosphorylation of Bim_{EL} leads to the dissociation of Bim_{EL} from complexes with Mcl-1 and Bcl-xL. The authors also demonstrated that mutations in the BH3 domain cause increased turnover of Bim_{EL}. This work supports a model in which active ERK1/2 phosphorylates Bim_{EL} and phosphorylated Bim_{EL} dissociates from prosurvival proteins and in this unbound state is a target for degradation

(Ewings *et al*., 2007). It has also been suggested that phosphorylation of Bim by ERK 1/2 inhibits its interaction with Bax (Harada *et al*., 2004).

The mechanism by which Bim_{EL} is targeted for degradation by the proteasome is not completely understood. Initially, Akiyama *et al*. (2003) proposed that the E3 ligase responsible for Bim_{EL} degradation is Cbl. However, it was subsequently demonstrated that Cbl is, in fact, not required (Wiggins *et al*., 2007). Recently, Dehan *et al*. (2009) showed that the F-box protein betaTrCP binds and promotes the proteasomal degradation of phosphorylated Bim_{EL}. Furthermore, it has now been demonstrated that Bim (primarily Bim_{EL}) is a target of the Cullin 2/Elonginβ-c/s ubiquitin-protein ligase complex and degradation by this pathway appears to be promoted by Drg binding to Bim isoforms (Ambrosini *et al*., 2009).

1.9 Aims of this thesis

The Bcl-2 family, BH3-only protein Bim plays an important role in NGF withdrawal-induced death in sympathetic neurons, as well as in several other models of apoptosis. Although the roles of c-Jun and FOXO3a in regulating *bim* transcription have previously been studied by our group, there is still a considerable amount to be learned about the molecular mechanisms by which *bim* gene expression is controlled.

In this study, I will examine the role of the region of the *bim* promoter proximal to the major transcriptional start site and investigate how it controls *bim* basal promoter function and contributes to the activation of *bim* following NGF withdrawal. This work will focus on a conserved NF-Y-binding CCAAT box that is located just upstream from the major transcriptional start site in the rat *bim* gene. In addition, I will study how *bim* expression is regulated by the MEK/ERK signalling pathway in sympathetic neurons and I will investigate the role of the *bim* 3′ UTR in this regulation.

Chapter 2: Materials and Methods

2.1 Materials

All stock chemicals, compounds, enzymes and other reagents were supplied by Sigma-Aldrich unless stated otherwise.

Table 1: Buffers and Solutions

BUFFER/SOLUTION	COMPONENTS
6 X DNA loading buffer	0.25% w/v bromophenol blue 0.25% w/v xylene cyanol 20% v/v glycerol 50 mM EDTA
LB medium	1% w/v bacto-tryptone (Difco, BD Biosciences Co.) 0.5% w/v yeast extract (Difco, BD Biosciences Co.) 17 mM NaCl (Fisher Scientific Inc.)
LB agar	LB medium 1.5% bacto-agar (Difco, BD Biosciences Co.)
ChIP buffer A	5 mM PIPES-NaOH pH 8.0 85 mM KCl 0.5 mM PMSF 2% v/v Sigma mammalian protease inhibitor cocktail
ChIP SDS lysis buffer	1% w/v SDS 10 mM EDTA 50 mM Tris-HCl pH 8.0 0.5 mM PMSF 2% v/v Sigma mammalian protease inhibitor cocktail
ChIP dilution buffer	0.01% w/v SDS 1.1% v/v Triton X-100 1.2 mM EDTA 16.7 mM Tris-HCl pH 8.0

	167 mM NaCl 0.5 mM PMSF 2% v/v Sigma mammalian protease inhibitor cocktail
ChIP low salt wash buffer	0.1% w/v SDS 5 mM EDTA 10 mM Tris-HCl pH 8.0 150 mM NaCl
ChIP 300 mM high salt wash buffer	0.1% w/v SDS 1% w/v Triton X-100 2 mM EDTA 20 mM Tris-HCl pH 8.0 300 mM NaCl
ChIP LiCl wash buffer	0.25 M LiCl 1% IGEPAL-CA630 1 mM EDTA 10 mM Tris-HCl pH 8.0 1% w/v deoxycholic acid sodium salt
ChIP elution buffer	1% w/v SDS 5 mM EDTA 10 mM Tris-HCl pH 8.0 300 mM NaCl
Co-IP buffer A	10 mM Hepes pH 7.9 10 mM KCl 0.1 mM EDTA 0.1 mM EGTA 1 mM DTT 0.5 mM PMSF 2% v/v Sigma mammalian protease inhibitor cocktail

Co-IP buffer C	20 mM Hepes pH 7.9 1 mM EDTA 1 mM EGTA 1 mM DTT 1 mM PMSF 25% v/v glycerol 2% v/v Sigma mammalian protease inhibitor cocktail
Co-IP non-denaturing lysis buffer	1% v/v Triton-X100 50 mM Tris-HCl pH 7.4 300 mM NaCl 5 mM EDTA 0.02% v/v NaN_3 pH 7.4 1 mM PMSF 2% v/v Sigma mammalian protease inhibitor cocktail
TE buffer	10 mM Tris-HCl pH 8.0 1 mM EDTA
TM buffer	100 mM Tris-HCl pH 8.0 50 mM $MgCl_2$
GTP C1 buffer	12.5 mM Hepes pH 7.9 10% v/v glycerol 100 mM KCl 1 mM EDTA
Hypotonic buffer	0.1% v/v Triton-X100 20 mM Hepes pH 7.6 20% v/v glycerol 1 mM DTT 10 mM NaCl 1.5 mM $MgCl_2$ 0.2 mM EDTA 0.5 mM PMSF

	25 mM NaF
	25 mM β-glycerol phosphate
	2% v/v Sigma mammalian protease inhibitor cocktail
Hypertonic buffer	hypotonic buffer
	500 mM NaCl
Whole cell extract buffer	0.1% v/v NP40 (VWR International)
	250 mM KCl
	50 mM Hepes pH 7.9
	10% v/v glycerol
	0.2 mM EDTA
	0.2 mM EGTA
	4 mM NaF
	4 mM Na orthovanadate
	1 mM DTT
	2% v/v Sigma mammalian protease inhibitor cocktail
SDS gel sample buffer	2 mM β-mercaptoethanol
	60 mM Tris-HCl pH 6.8
	0.01% w/v bromophenol blue
	2% w/v SDS
SDS gel running buffer (1X)	192 mM glycine (VWR International)
	25 mM Tris base
	0.1% w/v SDS
Stacking gel buffer	0.5 M Tris-HCl pH 6.8
	0.4% w/v SDS
Resolving gel buffer	1.5 M Tris-HCl pH 8.8
	0.4% w/v SDS
Transfer buffer (1X)	39 mM glycine
	48 mM Tris base
	20% v/v methanol
	0.037% w/v SDS

Stripping buffer	50 mM β-mercaptoethanol 62.5 mM Tris-HCl pH 6.8 2% w/v SDS

This table lists the components of the buffers and solutions that were prepared in this study.

2.2 Methods

2.2.1 Cloning

All oligonucleotide primers were custom-designed using MacVector 6.5.3 sequence analysis software (MacVector Inc.) and synthesised by Sigma-Aldrich. DNA sequencing was carried out by GATC Biotech and the sequences were analysed using FinchTV (Geospiza Inc.) and MacVector 6.5.3 software.

2.2.1.1 3′ Rapid amplification of cDNA ends (3′ RACE)

3′ RACE was used to define the end point of the rat *bim* 3′ UTR for subsequent cloning. RACE was performed on rat lung poly A+ RNA with the Marathon cDNA Amplification Kit (all components were from Clontech, Takara Bio Co.).

First-strand synthesis was carried out in a volume of 5 μl with 1 μg of rat lung poly A+ RNA and the cDNA synthesis primer at a concentration of 2 μM (the cDNA synthesis primer is a modified lock-docking oligo (dT) primer that positions itself at the 3′ end of a poly-A tail). The mixture was incubated at 70ºC for 2 minutes and following a brief chill on ice the following components were added up to a volume of 10 μl: 20 units of AMV (Avian Myeloblastosis Virus) reverse transcriptase and 1 mM dNTPs in 5 X first-strand buffer. Following a 1 hour incubation at 42ºC, the mixture was placed on ice for 2 minutes to terminate first strand synthesis.

Second-strand synthesis was performed on the first-strand synthesis reaction product in a volume of 80 μl with 5 X second-strand reaction buffer, 0.2 μM dNTPs and 20 X second-strand enzyme cocktail. After incubation at 16ºC for 1.5 hours, 6 units of T4 DNA polymerase was added and the reaction was incubated for a further 45 minutes at 16ºC. Second-strand synthesis was terminated by the addition of 4 μl of an EDTA/glycogen mix. The cDNA was extracted with 100 μl of phenol:chloroform: isoamyl alcohol (25:24:1) followed by chloroform:isoamyl alcohol (24:1). Following the addition of a 0.5 X volume of 4 M ammonium acetate, the cDNA was precipitated with ethanol, pelleted by high-speed centrifugation, washed with 80% ethanol, air dried and dissolved in 10 μl of sterile water.

Adaptor ligation was carried out on the double stranded cDNA in order to ligate the Marathon cDNA adaptor sequence to each end of the cDNA (the cDNA must have the adaptor terminal structure for RACE to proceed). The cDNA was incubated with the Marathon cDNA adaptor at 1 μM and 5 X DNA ligation buffer plus 400 units of T4 DNA ligase, in a volume of 10 μl. The ligation was incubated at 16ºC overnight followed by inactivation at 70ºC for 5 minutes. The library of adaptor double stranded (ds) cDNA was then used for RACE PCR.

3′ RACE PCR was carried out on the adaptor ds cDNA with the *bim*-specific primer 5′-CTTCTGGTGTTTTGAGGTCTGTGGAC-3′ at 0.2 μM, the AP1 primer (the AP1 primer anneals to the adaptor sequence at the cDNA ends) at 0.2 μM, 50 X Advantage 2 Polymerase mix and 10 X cDNA PCR buffer, in a volume of 50 μl. PCR conditions were 95ºC for 2 minutes followed by 35 cycles of 95ºC for 30 seconds, 64ºC for 30 seconds and 68ºC for 3 minutes.

PCR products were visualised on a 2.5% agarose gel containing ethidium bromide at 0.5 μg/ml. Bands of the correct size were cloned into pGEM-T using the pGEM-T Easy Vector System as specified by the manufacturer (Promega Corporation). The sequenced clones were analysed in order to determine the end point of the rat *bim* 3′ UTR.

2.2.1.2 Plasmid constructs

The *bim*-LUC reporter was constructed by Dr. Jonathan Gilley (Gilley *et al*., 2003). It consists of a 5.2 kb fragment, containing the region immediately 5′ to the rat *bim* initiator codon, sub-cloned into pGL3-Basic (Promega Corporation).

The *bim*-LUC CCAAT (-) construct was generated using the complementary oligonucleotide primers 5′-GAGCCCGCGGTGAGCTCGCGCCGGAGCGGG-3′ and 5′-CCCGCTCCGGCGCGAGCTCACCGCGGGCTC-3′. The altered bases (underlined) create four point mutations in the inverted CCAAT box. Mutagenesis was carried out using the QuikChange II XL site-directed mutagenesis kit (Stratagene Corporation). Here, the desired mutations are incorporated by polymerase chain reaction (PCR). The PCR products are then treated with the restriction endonuclease DpnI to digest the methylated, non-mutated parental DNA template. The remaining

double stranded DNA is then transformed into XL10-Gold ultracompetent cells (Stratagene). PCR components were: 50 ng of template (*bim*-LUC), 0.2 μM complementary primers, 0.2 μM dNTPs, 2.5 units of *PfuTurbo* DNA polymerase and 10 X reaction buffer, in a volume of 50 μl. PCR conditions were 95ºC for 2 minutes followed by 18 cycles of 95ºC for 50 seconds, 60ºC for 50 seconds and 68ºC for 15 minutes. DNA sequencing confirmed that the mutations had been incorporated correctly.

The *bim*-LUC+3′UTR reporter was generated by PCR amplification of the rat *bim* 3′ UTR from a restriction fragment cloned from the PAC clone 215h9. 215h9 was obtained from the rat P1 artificial chromosome (PAC) library RPC131 (generated by P. Y. Woon and P. de Jong, UK Human Genome Mapping Project Resource Centre, Cambridge, UK). Primers were used to generate the 3′ UTR in two fragments. For fragment 1 the primers were 5′-CTCACTAGTCAGGAGCTTCGTGCAG-3′ and 5′-CTCCTACAAGGCACAAAACCCG-3′. For fragment 2 the primers were 5′-CTATACGGATGTCCCTGTACTGTATC-3′ and 5′-CTCACTAGTCATGAGAGCT AGTCGCAA-3′. These primers add SpeI restriction sites to the 5′ end of fragment 1 and the 3′ end of fragment 2. PCR reactions were carried out with the following components: 50 ng of template (PAC clone 215h9), 0.2 μM complementary primers, 0.2 μM dNTPs, 2.5 units of *PfuTurbo* DNA polymerase and 10 X reaction buffer, in a volume of 50 μl. PCR conditions were 95ºC for 2 minutes followed by 25 cycles of 95ºC for 30 seconds, 56ºC for 45 seconds and 72ºC for 3 minutes. Fragments 1 and 2 were cloned into pGEM-T using the pGEM-T Easy Vector System for sequence confirmation and then the 3′ UTR was assembled in pBluescript SK (Stratagene Corporation) using a unique BglII restriction site within the 4.2-kb region to link fragments 1 and 2. The 3′ UTR was excised using SpeI and sub-cloned into *bim*-LUC, using an XbaI restriction site downstream of the Luciferase reporter gene and upstream of the SV40 late poly (A) signal. There was originally one other XbaI site present in *bim*-LUC (within intron 1) that was mutated to leave the XbaI site used here as unique. Mutagenesis was performed using the QuikChange II XL site-directed mutagenesis kit as described previously. Microinjection experiments were carried out to confirm that mutating this site had no effect on *bim*-LUC. To generate *bim*-LUC+3′UTR (F2),

fragment 2 was excised from pGEM-T using the 3′ SpeI site (incorporated by PCR) and a SpeI site within pGEM-T (located just upstream of the 5′ end of fragment 2) and sub-cloned into *bim*-LUC.

The *bim*-LUC+3′UTR(4xAREmut) construct was generated using the following complementary primer pairs: 5′-GCCACTTCCGTTTTGTAAATATGTA CCTCCTTAGCTCAGTTGCTCC-3′ and 5′-GGAGCAACTGAGCTAAGGAGG TACATATTTACAAAACGGAAGTGGC-3′, 5′-CCTGTTTCCTCCTTCCAGTGTTG TATATATCTGACTATGTATTAGATTAGG-3′ and 5′-CCTAATCTAATACATAGT CAGAATATATACAACACTGGAAGGAGGAAACAGG-3′, 5′-GCTGTAACTTGT AGAGTCATTGTATATGTATTTTCTGCTTATGTAATGTCTTACG-3′ and 5′-CG TAAGACATTACATAAGCAGAAAATACATATACAATGACTCTACAAGTTACA GC-3′. Three rounds of mutagenesis successfully incorporated point mutations into the four conserved AU-rich elements (AREs) within the rat *bim* 3′ UTR (mutated bases are underlined). Mutagenesis was carried out using the QuikChange II XL site-directed mutagenesis kit as described previously.

YA13 m29 was kindly provided by Dr. Roberto Mantovani (University of Milan, Italy). YA13 m29 is a dominant negative mutant of the NF-YA subunit (Mantovani *et al*., 1994) cloned into the expression vector pSG5 (Stratagene Corporation).

The expression vector for p300 was supplied by Upstate (Millipore Corporation). It is human p300 cDNA cloned into pCMVβ (CMVp300). The expression vector pcDNA3.1 (Invitrogen Corporation), which is also under the control of the CMV promoter, was used as an empty vector control.

The expression vector for CBP was kindly provided by Professor Tony Kouzarides (The Gurdon Institute, Cambridge). It is mouse CBP cDNA cloned into pRc/RSV (pRc/RSV-mCBP). The expression vector pBJ9Ω, which is also under the control of the RSV promoter, was used as an empty vector control (also supplied by T. Kouzarides).

2.2.1.3 Restriction endonuclease digests

Restriction endonucleases (Promega Corporation) were used to cleave double stranded DNA. Typically, restriction digests were performed in a volume of 30 µl on 0.2-1.5 µg of substrate DNA, with a 2-10 fold excess of enzyme over DNA. The digests were incubated for 2 hours at 37ºC (or the temperature that was optimal for each enzyme) and resolved by agarose gel electrophoresis.

2.2.1.4 Ligations

Typically, 3:1, 1:1 and 0:1 insert to vector ratios were set up for each ligation. When ligations were carried out with 3 fragments (for cloning of the *bim*-LUC+3′UTR reporter) the ratio was 3:3:1, 1:1:1 and 0:0:1. The following equation was used to calculate the required amount of insert for a 3:1 ligation:

$$ng_{\text{insert required}} = [(50\ ng_{\text{vector}} \times kb_{\text{insert}})/kb_{\text{vector}}] \times 3$$

For the ligation reaction, 1 unit of T4 DNA ligase (Promega Corporation) was mixed with the calculated amount of insert, 50 ng of vector and 10 X T4 ligase buffer, in a total volume of 10 µl. The reaction was left overnight at 16ºC before transformation into competent cells.

2.2.1.5 Agarose gel electrophoresis of DNA

To analyse DNA by agarose gel electrophoresis, DNA samples were prepared in 6 X DNA loading buffer (Table 1) and resolved on 0.5-2.5% agarose gels (depending on the size of the DNA to be visualised). Agarose gels were prepared in 1 X TBE (National Diagnostics Inc.) plus 0.5 µg/ml of ethidium bromide. Images were captured using a UVIdoc gel documentation system (UVItec Ltd.) and quantitated using ImageQuant image analysis software (GE Healthcare Ltd.).

To purify DNA from agarose gels, the DNA fragment of interest was excised under UV light and then purified using the QIAquick gel extraction kit (QIAGEN Ltd.) as specified by the manufacturer.

2.2.1.6 Transformation of chemocompetent bacteria

For routine cloning, subcloning efficiency DH5α competent cells (Invitrogen Corporation) were used for bacterial transformation as follows: competent cells were thawed on ice and 50 µl of cells was aliquoted into a chilled 14 ml tube per transformation. Up to 5 µl (1-10 ng) of plasmid DNA was mixed into each transformation reaction and the cells were incubated on ice for 30 minutes. Control transformations were regularly carried out using pUC19 DNA as a positive control and no-DNA as a negative control. The cells were heat shocked for 30 seconds in a 42ºC water bath and then placed on ice for 2 minutes. Up to 950 µl of pre-warmed LB medium was added to each tube and the cells were incubated for 1 hour with shaking (225-250 rpm) at 37ºC. Transformation reactions were spread onto pre-warmed selective plates (for example LB agar + 100 µg/ml of ampicillin) and the plates were incubated overnight at 37ºC. Individual colonies were then selected for analysis.

For cloning of large or difficult constructs, high efficiency XL10-Gold ultracompetent cells were used (Stratagene Corporation). Transformations were carried out using the method described for DH5α competent cells, but with the following modification: 2 µl of β-mercaptoethanol was added to each aliquot of competent cells for 10 minutes on ice prior to the addition of the plasmid DNA.

2.2.2 Isolation of plasmid DNA

Large quantities of purified plasmid DNA, for microinjection, were isolated as follows: A single bacterial colony was picked and inoculated into 2 ml of LB medium containing 100 µg/ml of ampicillin (or the relevant selective antibiotic) for 5 hours at 37ºC with shaking (225-250 rpm). The starter culture was then transferred into 150 ml of LB medium containing 100 µg/ml of ampicillin and incubated for a further 16 hours at 37ºC with shaking. The Plasmid DNA was isolated using the Genopure plasmid maxi kit (Roche Diagnostics Corporation) for high copy number plasmids, as described by the manufacturer.

For small quantities of DNA, used for cloning, a single bacterial colony was picked and inoculated into 2 ml of LB broth containing 100 μg/ml of ampicillin and incubated overnight at 37ºC with shaking (225-250 rpm). The plasmid DNA was isolated using the QIAprep spin miniprep kit (QIAGEN Ltd.) as described by the manufacturer.

The concentration of the plasmid DNA was determined using a NanoDrop spectrophotometer (Nanomodel ND-1000). A 260 nm / 280 nm absorbance ratio of 1.8 is accepted as pure for DNA (if the ratio is significantly lower it may indicate the presence of protein, phenol or other contaminants).

2.2.3 Isolation of RNA

Total RNA was isolated from sympathetic neurons cultured for 7 days *in vitro* using the QIAGEN RNeasy mini kit with some modifications: Neurons from 2 coverslips (approximately 1.6 X 10^4 cells) for each treatment (for example; +NGF, +NGF +U0126, -NGF) were washed into 1.5 ml microfuge tubes using ice-cold PBS (-). Cells were spun down briefly to remove PBS (-) and resuspended by vortexing for 1 minute in 350 μl of buffer RLT. 350 μl of 70% ethanol was added to the homogenised lysate before mixing well. The sample was applied to an RNeasy mini column and centrifuged for 15 seconds at 8000 x g. 350 μl of buffer RW1 was then added to the RNeasy spin column, which was centrifuged for 15 seconds at 8000 x g. An on-column DNase digestion was then performed to eliminate genomic DNA contamination using DNase I from the RNase-free DNase set (QIAGEN Ltd.). Another 350 μl of buffer RW1 was added to the RNeasy spin column to wash the RNA, which was then spun for 15 seconds at 8000 x g. 500 μl of buffer RPE was applied to the column and centrifuged for 15 seconds at 8000 x g followed by another 500 μl of buffer RPE, which was centrifuged for 2 minutes at 8000 x g, and a further 1 minute at full speed to dry the membrane. The RNA was eluted from the column in 50 μl of RNase-free sterile water. 1 μl of the ribonuclease inhibitor RNaseOUT (Invitrogen) was added to each sample. Isolation of RNA was carried out at room

temperature, but the procedure was carried out rapidly and all RNA samples were stored at -80ºC.

RNA was concentrated, if necessary, by addition of 5 µg of glycogen and 5 µl of 3 M sodium acetate (pH 5.3), in a 5 X volume of ice-cold ethanol at -20ºC overnight. The samples were pelleted by centrifugation for 20 minutes at 15,700 x g at 4ºC and the pellet was washed in 500 µl of ice-cold 70% ethanol. The samples were centrifuged for a further 5 minutes at 15,700 x g at 4ºC and the pellet was air dried for 2-3 minutes before being resuspended in an appropriate volume of RNase-free sterile water.

The concentration of isolated RNA was determined using a NanoDrop spectrophotometer (model ND-1000). A 260 nm / 280 nm absorbance ratio of 2 is accepted as pure for RNA (if the ratio is significantly lower it may indicate the presence of protein, phenol or other contaminants).

2.2.4 cDNA synthesis

cDNA was synthesised from isolated RNA samples using M-MLV (Moloney Murine Leukaemia Virus) reverse transcriptase (Invitrogen Corporation). Up to 5 µg of total RNA was incubated with 1 mM dNTPs and 500 ng of oligo $(dT)_{12-18}$ for 5 minutes at 65ºC followed by the addition of 5 X M-MLV first strand buffer, 0.01 M DTT and 1 µl of RNaseOUT (Invitrogen Corporation). The mixture was incubated for 2 minutes at 37ºC before the addition of 200 units of M-MLV reverse transcriptase and incubation for 50 minutes at 37ºC. The reaction was inactivated by incubation for 15 minutes at 70ºC.

2.2.5 Cell culture

2.2.5.1 Sympathetic neuron culture

Primary sympathetic neurons were cultured from the superior cervical ganglia (SCG) of 1-day-old Sprague-Dawley rats bred at the Biological Services Unit, UCL, as described previously (Whitfield *et al*., 2004). In brief, SCGs were isolated using sterilised Dumont no. 5 forceps (Agar Scientific Ltd.) and dissociated by enzymatic

treatment in a 0.025% trypsin solution followed by a 0.1% collagenase solution (collagenase type II, Worthington Biochemical Corporation) for 30 minutes at 37ºC, respectively. SCGs were further dissociated, mechanically, using a P1000 Gilson pipetman. The cell suspension was collected by centrifugation (200 x g for 10 minutes at room temperature) and pre-plated in SCG+ medium for 2 hours on an uncoated tissue culture dish. This step allows non-neuronal cells, such as Schwann cells and fibroblasts, to attach and therefore the cell suspension is enriched for sympathetic neurons (Deckwerth and Johnson, 1993). The neurons were then collected by centrifugation, as previously, and counted in trypan blue solution using a modified Fuchs-Rosenthal haemocytometer. Between 6,000-8,000 neurons were plated in 80 µl of SCG+ medium on 13 mm glass coverslips (VWR international Ltd.) coated with poly-$_L$-lysine and laminin. Each coverslip was placed in a 3.5 cm dish and after 2 hours, cells were flooded with 2 ml of SCG+ medium. Cells were maintained in 10% v/v CO_2 at 37ºC and refed with fresh SCG+ medium at 1, 2 and 5 days in culture and subsequently every 3 days. SCG+ medium was SCG medium (DMEM medium (D6546, Sigma) containing 10% foetal calf serum, 2 mM glutamine and penicillin-streptomycin) supplemented with 2.5S NGF (Cedarlane Laboratories Ltd.) at 50 ng/ml and the antimitotic agents fluorodeoxyuridine and uridine at a final concentration of 20 µM.

2.2.5.2 PC6-3 cell culture

PC6-3 cells, a subline of the PC12 (rat pheochromocytoma) cell line (Pittman *et al*., 1993), were maintained in 5% v/v CO_2 at 37ºC on 9 cm dishes coated with rat type I collagen (Upstate Biotechnology Inc.) at 2.5 µl/ml in PBS (-).

Undifferentiated PC6-3 cells were maintained in stock medium (RPMI 1640 medium (21875, Gibco), containing 10% horse serum, 5% foetal calf serum, 2 mM glutamine and penicillin-streptomycin). Cells were passaged once a week (usually at 1:10). To passage the cells, old medium was discarded, the cells were washed in 5 ml of PBS (Gibco, Invitrogen Corporation) and the cells were incubated with 2 ml of 1xTrypsin/EDTA (Gibco, Invitrogen Corporation) for 5 minutes. Stock medium was

added up to 10 ml and cells were collected by centrifugation (800 x g for 5 minutes at room temperature).

PC6-3 cells were differentiated into a neuronal phenotype for 5-7 days in differentiation medium (RPMI 1640 medium containing 2% horse serum, 1% foetal calf serum, 2 mM glutamine and penicillin-streptomycin) supplemented with NGF (Promega Corporation) at 100 ng/ml. Typically, cells were seeded for differentiation at a density of 1 X 10^6 per 9 cm dish.

2.2.5.3 NGF withdrawal and use of chemical inhibitors

In NGF withdrawal experiments, neurons were rinsed twice with medium (without NGF) and then re-fed with medium containing an anti-NGF antibody at 100 ng/ml (Chemicon International Inc.). The PI3-K inhibitor LY294002 was used at a concentration of 50 μM and the MEK/ERK inhibitor U0126 at a concentration of 10 μM (both compounds from Promega Corporation). The RNA synthesis inhibitor actinomycin-D was used at a concentration of 0.1 μg/ml. In rat sympathetic neurons, *bim* mRNA levels peak at 16 hours following withdrawal of NGF (Whitfield *et al*., 2001). Therefore, treatment with chemical inhibitors and withdrawal of NGF was carried out for 16 hours. When actinomycin-D was used in conjunction with U0126, cells were either pre-treated with U0126 for 16 hours prior to the addition of actinomycin-D or U0126 and actinomycin-D were added at the same time. Following the addition of actinomycin-D, RNA was isolated from the cells over a time course. Chemical inhibitors were dissolved in DMSO and therefore equal volumes of DMSO were added to control (untreated) cells in each case.

2.2.6 Microinjection

Microinjection experiments were carried out using an Axiovert 200 inverted microscope (Carl Zeiss Ltd.) fitted with a heated stage and CO_2 chamber, using an Eppendorf transjector (model 5246) and micromanipulator (model 5171). Needles used for microinjection were pulled from borosilicate glass capillaries (Intracel Ltd.) using a Kopf Instruments gravity puller (model 720).

Sympathetic neurons were cultured *in vitro* for 5-7 days prior to microinjection. Between 125 and 150 cells were injected per coverslip and each injection experiment was repeated at least 3 times. Plasmids were injected into the nucleus of each cell and typically over 90% of cells survived injection.

2.2.6.1 Dual luciferase assays

Neurons were injected with luciferase reporter constructs in 0.5 X PBS (-Ca^{2+}, -Mg^{2+}) at a concentration of 10 ng/µl, with the exception of *bim*-LUC+3'UTR and its derivatives, which were injected at 14 ng/µl to allow an equivalent copy number for this larger construct. The *Renilla* luciferase expression construct pRL-TK (Promega Corporation) was added to injection mixes at 5 ng/µl to control for injection efficiency (it is not activated by NGF withdrawal). The expression vector for the NF-YA mutant (YA13 m29) or the control empty vector pSG5 were injected at 20 ng/µl. The expression vector for p300, p300 in pCMVβ, or the control empty vector pcDNA3.1 were injected at 50 ng/µl. Luciferase assays were performed using the Dual-luciferase reporter assay system (Promega Corporation) and a Lumat LB9507 luminometer (Berthold Technologies Ltd.). M1/M2 readings were produced by normalising *Firefly* output to *Renilla* output.

2.2.6.2 Antibody co-injection experiments

The p300 (C-20:Sc-585 X) and CBP (C-20:Sc-583 X) rabbit polyclonal antibodies (Santa Cruz Biotechnology Inc.) were diluted in PBS (-Ca^{2+}, -Mg^{2+}) and centrifuged in Microcon YM-3 centrifugal filters (Millipore Corporation) to remove sodium azide. Antibodies were injected at a final concentration of 1 µg/µl and purified rabbit immunoglobulin in PBS (Jackson ImmunoResearch Laboratories, Inc) was used as a control.

2.2.6.3 Cell survival assays

Neurons were injected with the YA13 m29 expression vector or the control empty vector (pSG5) at 200 ng/µl, along with 5 µg/µl of Texas red dextran (70,000 MW; Molecular Probes, Invitrogen Corporation) as a marker for injected cells. Following

withdrawal of NGF, the number of viable, morphologically-normal, injected cells was determined at time 0, 24, 48 and 72 hours. Viable cells were counted in a blinded manner using a Zeiss Axiovert 200 inverted fluorescence microscope.

2.2.6.4 Microinjection for immunocytochemistry

Neurons were injected with the YA13 m29 expression vector or the control empty vector (pSG5) at 20 ng/μl along with 2.5 μg/μl of purified guinea pig IgG (Jackson ImmunoResearch Inc.) as a marker for injected cells. Cells were fixed and stained as described in 2.2.12.

2.2.7 Semi-quantitative RT-PCR

RNA was isolated from sympathetic neurons and reverse transcribed as described in 2.2.3 and 2.2.4. 50 ng of cDNA was used per 50 μl PCR reaction containing 0.2 mM dNTPs, oligonucleotide primers at 0.4 μM and 0.05 U/μl of REDTaq DNA polymerase in 1 X REDTaq PCR buffer (all from Sigma-Aldrich Corporation). Primer pairs were as follows: *bim* 5′-CTACCAGATCCCCACTTTTC-3′ and 5′-GCCCTCCTTCGTGT AAGTCTC-3′ and *neurofilament-M* 5′-ACGCTGGACTCGCTGGGCAA-3′ and 5′-GCGAGCGCGCTGCGCTTGTA-3′. PCR conditions were 95ºC for 2 minutes followed by 30 or 35 cycles of 95ºC for 30 seconds, 56ºC for 20 seconds and 72ºC for 1 minute. PCR products were visualised by agarose gel electrophoresis as described previously. Images were captured using a UVIdoc gel documentation system (UVItec Ltd.) and quantitated using ImageQuant image analysis software (GE Healthcare Ltd.) Samples were analysed at 30 and 35 cycles and the average mRNA levels were calculated. Relative *bim* mRNA levels were calculated by normalising to the control *neurofilament-M*.

2.2.8 Real-time quantitative PCR (qPCR)

RNA was isolated from sympathetic neurons and reverse transcribed as described previously. A *bim* specific primer and probe set was designed using the PrimerExpress software v2.0 (Applied Biosystems Inc.): *bim* forward primer 5′-CCAGGCCTT

CAACCATTATCTC-3′, *bim* reverse primer 5′-GCGCAGATCTTCAGGTTCCT-3′ and *bim* probe 5′-TGCAATGGCTTCCATAAGGCCAGTCTCA-3′. A number of forward primer, reverse primer and probe concentrations were tested to determine the optimal primer and probe concentration for measuring *bim* mRNA expression in my cDNA samples. The combination of 300 nM forward primer and 900 nM reverse primer concentration was optimal as it produced the lowest cycle threshold (C_T) value and the highest reaction Rn value (the Rn value is a measure of the fluorescent signal). The optimal probe concentration was 200 nM since this was the lowest concentration that did not affect the C_T value. *Glyceraldehyde-3-phosphate dehydrogenase* (Gapdh) and *Hypoxanthine phosphoribosyltransferase 1* (Hprt 1) were used as house-keeping (control) genes. Pre-optimised *Gapdh* (Rn99999916_S1) and *Hprt 1* (Mn00446968_m1) primer/probe sets were ordered from Applied Biosystems. *Bim* qPCR reactions were set up with 300 nM forward primer, 900 nM reverse primer, 200 nM probe and 1 X Taqman universal mastermix (Applied Biosystems Inc.) *Gapdh* and *Hprt 1* reactions were set up with 1 X *Gapdh* or *Hprt 1* primer/probe set and 1 X Taqman universal mastermix. PCR conditions were 95ºC for 20 seconds, followed by 40 cycles of 95ºC for 1 second and 60ºC for 20 seconds.

In order to analyse the data using the $2^{-\Delta\Delta CT}$ relative quantitation method (Livak and Schmittgen, 2001), *bim* qPCR reactions must be equally efficient to *Gapdh* and *Hprt 1* (in terms of the rate of amplification of the transcript). Therefore, a standard curve was generated first to determine the qPCR efficiency at low and high cDNA concentrations (0.39 ng to 50 ng). *Bim*, *Gapdh* and *Hprt 1* were efficient at low and high cDNA concentrations, with correlation coefficients of 0.9986, 0.9999 and 0.9951, respectively. The efficiency of each reaction was calculated using the formula: PCR efficiency = $(10^{(1/-s)})$-1 (Ginzinger, 2002) where s is the gradient of the standard curve and a slope of 3.3 equals 100% PCR efficiency. The efficiency of the *bim*, *Gapdh* and *Hprt 1* reactions were all 99%, therefore the $2^{-\Delta\Delta CT}$ relative quantitation method could be used to determine the relative expression level of *bim* mRNA (where *bim* mRNA levels are calculated relative to *Gapdh* or *Hprt 1* mRNA levels).

2.2.9 Chromatin immunoprecipitation (ChIP)

Chromatin immunoprecipitation (ChIP) was performed as described by Alberts *et al*. (1998) with a number of modifications. A chromatin immunoprecipitation assay kit from Upstate (Millipore Corporation) was used along with some additional buffers and reagents. All buffers used for ChIP are described in Table 1. PC6-3 cells were differentiated by plating at a density of 1 X 10^6 cells (per 9 cm dish) in the presence of NGF and after 7 days the density had reached approximately 4 X 10^6 cells (per 9 cm dish). The differentiated cells were kept in the presence of NGF or withdrawn from NGF for 16 hours before fixing with formaldehyde (37% formaldehyde was added to the culture medium to a final concentration of 1%) for 3 hours at room temperature to cross link proteins and DNA. 1.5 M glycine was added to 100 mM for a further 10 minutes to quench the reaction. The medium was removed and cells were rinsed in ice-cold PBS (-) plus 0.5 mM PMSF and 2% Sigma mammalian protease inhibitor cocktail before being scraped off the dishes in 2 ml of the PBS solution. Cells were pooled for +NGF or -NGF and pelleted by centrifugation at 400 x g for 4 minutes at 4ºC. Each pellet was resuspended in buffer A + 0.5% NP40 and incubated for 10 minutes at 4ºC on a rocking platform (Stuart Scientific Co.). The lysates were pelleted by centrifugation at 400 x g for 4 minutes at 4ºC, re-suspended in 2 ml of buffer A (-NP40), rocked for a further 10 minutes and centrifuged at 1200 x g for 5 minutes at 4ºC. The pellets were resuspended in 0.8 ml of ChIP SDS lysis buffer so that cells were at a concentration of approximately 1 X 10^7 nuclei/200 µl of buffer. The samples were incubated on ice for 10 minutes before sonication with a Bandelin ultrasonic homogeniser (model HD2070) using a 3 mm microtip and 50% power. Each lysate was sonicated for 12 pulses of 20 seconds, with 30 seconds on ice between each pulse (to produce DNA fragments approximately 200-1000 bp long). The fragmented chromatin was then centrifuged at 15,700 x g for 10 minutes at 4ºC and the supernatant, containing the chromatin, was recovered. The chromatin was divided into 200 µl aliquots (as samples for immunoprecipitation) and then diluted 10 fold in ChIP dilution buffer.

Lysates were pre-cleared to remove proteins binding non-specifically by incubation with 20 µl of 50% protein A/G-agarose (without DNA, Santa Cruz

Biotechnology Inc.) in ChIP dilution buffer plus 10 μg/μl of BSA at 4ºC for 1 hour with rotation. The agarose beads were pelleted by centrifugation for 2 minutes at 100 x g and the pre-cleared chromatin was recovered. 4 μg of each antibody for immunoprecipitation (for example p300 C-20:Sc-585 X) was added to each tube, which was then incubated overnight at 4ºC with rotation. Millipore Bim (AB17003) and Santa Cruz MyoD (M-318:Sc-760 X) antibodies were used as negative controls. To recover the immune complexes, 15 μl of protein A/G-agarose (in ChIP dilution buffer plus BSA at 10 μg/μl) was added to each sample for 2 hours at 4ºC with rotation. The beads were pelleted and washed twice (for 5 minutes and 15 minutes at room temperature) in each of the following buffers: ChIP low salt wash buffer, ChIP 300 mM high salt wash buffer, ChIP LiCl wash buffer and twice with TE buffer. After the final wash, the beads were pelleted, re-suspended in 500 μl of ChIP elution buffer by vortexing and incubated at 65ºC overnight to reverse the cross links and release the immune complexes from the beads. 100 μg of glycogen was added and samples were treated with RNase A at 40 μg/μl for 1 hour at 37ºC followed by proteinase K at 40 μg/μl for 2 hours at 56ºC. The samples were extracted with 500 μl of phenol:chloroform:isoamyl alcohol followed by chloroform:isoamyl alcohol. This step was repeated and then the DNA was precipitated with ethanol, pelleted by high-speed centrifugation, washed with 70% ethanol, air dried and dissolved in 40 μl of TE buffer.

ChIP samples were analysed by semi-quantitative PCR using Taq DNA polymerase and CoralLoad PCR buffer (QIAGEN Ltd.). To detect binding of NF-Y to the inverted CCAAT box in the rat *bim* promoter the following primer pair was used: *bim* forward primer 5′-CAGGCCAAGTCACTAGGGTAAACAC-3′ and *bim* reverse primer 5′-GAATCCGGTGACTGCAACGACAA-3′. The same primer pair was used to detect binding of p300 and CBP to this region. PCR conditions were 95ºC for 2 minutes, followed by 25 or 30 cycles of 95ºC for 30 seconds, 60ºC for 30 seconds and 72ºC for 30 seconds. PCR products were run on non-denaturing 8% polyacrylamide gels (8% acrylamide/bis solution, 1 X TBE, 0.04% APS and 0.2% TEMED) in 1 X TBE at 180 V for 2 hours and stained with SYBR Green 1 (Sigma Aldrich Corporation). Images were captured using a UVIdoc gel documentation system (UVItec Ltd.) and quantitated using ImageQuant image analysis software (GE

Healthcare Ltd.). Samples were analysed between 25 and 30 cycles and the average amount of *bim* promoter DNA, precipitated by each antibody, was calculated.

2.2.10 Co-Immunoprecipitation (Co-IP)

All buffers used for Co-IP are described in Table 1. A 50% slurry of protein A/G-agarose (without DNA, Santa Cruz Biotechnology Inc.) was prepared in PBS (-) and added to a 1.5 ml microfuge tube containing 2 μg of the specific antibody (for example p300 C-20:Sc-585 X) resuspended in 500 μl ice-cold PBS (-). This was also repeated for the non-specific control, purified rabbit immunoglobulin in PBS (Jackson ImmunoResearch Laboratories, Inc). The mixtures were incubated at 4ºC for 90 minutes on an orbital tube rotator (Stuart Scientific Co.). The beads were collected by centrifugation at 15,700 x g for 2 seconds at 4ºC. The supernatant containing the unbound antibody was removed and the beads were resuspended in 1 ml of non-denaturing lysis buffer. The tubes were inverted 3 to 4 times to mix and the beads were collected by centrifugation at 15,700 x g for 2 seconds at 4ºC. The beads were washed in 1 ml of non-denaturing lysis buffer and the beads collected as described in the previous step. The antibody-bound beads were then stored at 4ºC for up to 6 hours prior to use.

Around 80 μg of nuclear lysate was added to each tube containing specific or control antibody-bound beads. The mixture was incubated at 4ºC for 2 hours with rotation. The beads were then collected by centrifugation at 15,700 x g for 2 seconds at 4ºC and the supernatant was removed. The beads were resuspended in 1 ml of ice-cold wash buffer, the tubes inverted for 4 to 6 times to mix, and the beads were collected by centrifugation at 15,700 x g for 2 seconds at 4ºC. This wash step was repeated 3 times and the final supernatant was removed to leave the beads in approximately 15 μl of wash buffer (containing the immune complexes). The beads were resuspended in 30 μl of SDS gel sample buffer, boiled for 5 minutes at 100ºC and analysed by immunoblotting (as described in 2.2.13).

2.2.10.1 Preparation of nuclear extracts for Co-IP

PC6-3 cells were differentiated by plating at a density of 1 X 10^6 cells (per 9 cm dish) in the presence of NGF for 7 days. Nuclear lysates were prepared from differentiated PC6-3 cells maintained in NGF and differentiated PC6-3 cells 16 hours following NGF withdrawal. To prepare nuclear extracts the cells were washed twice in ice-cold PBS (-) and then scraped off the dishes in 2 ml of PBS (per 9 cm dish). Cells were pooled for +NGF or -NGF and pelleted by centrifugation at 400 x g for 5 minutes at 4ºC. Each pellet was resuspended in 200 µl of buffer A and then incubated on ice for 15 minutes, prior to the addition of 10% NP40 to each lysate (15 µl of 10% NP40 per 200 µl lysate). Samples were vortexed for 15 seconds and then incubated for 15 minutes at 4ºC on an orbital tube rotator. The lysates were pelleted by centrifugation at 15,700 x g for 30 seconds, resuspended in 200 µl of ice-cold buffer C and then incubated at 4ºC on an orbital shaker (Stuart Scientific Co.) at 150 rpm. After 1 hour the lysate was vortexed for 30 seconds and then spun down for 10 minutes at 15,700 x g at 4ºC. The supernatant was removed and this was the nuclear extract.

2.2.11 Electrophoretic mobility shift assay (EMSA)

Oligonucleotide pairs used for EMSA experiments were as follows: *bim* CCAAT wt 5'-CTAGCCCGCGGTGATTGGGCGCCGGAG-3' and 5'-CTAGCTCCGGCGCCCAA TCACCGCGGG-3' and *bim* CCAAT mut 5'-CTAGCCCGCGGTGAGCTCG CGCGGAG-3' and 5'-CTAGCTCCGGCGCGAGCTCACCGCGGG-3' (the mutated bases of the ICB are underlined). Oligonucleotides for a CCAAT box in the rat GTP Cyclohydrolase I gene were used as a positive control: GTP C1 WT 5'-CTAGGCTCGGCCAATGAGAACGCCT-3' and 5'-CTAGAGGCGTTCTCATT GGCCCGAGC-3' and GTP C1 mut 5'-CTAGCTCGGGGAGCTGAGAACGCCT-3' and 5'-CTAGAGGCGTTCTCAGCTCCCCGAGC-3' (Kapatos *et al*., 2000). Oligonucleotide pairs were annealed as follows; 2 µg of each oligonucleotide was mixed together with 10 µl of TM buffer (Table 1) and 80 µl of sterile water, incubated for 10 minutes at 80ºC and then slow cooled to room temperature. The 5' overhangs of

annealed oligonucleotides were labelled by filling in with Klenow polymerase (Roche Diagnostics Ltd.) and [α-^{32}P]dCTP (3000 Ci/mmol; PerkinElmer Inc.).

20 µl binding reactions were set up in GTP C1 binding buffer (Table 1) plus 1 µg of poly (dI-dC) and 5 µg of BSA using 5 µg of cytoplasmic or nuclear extract from PC6-3 cells and 10 µg of whole cell extract from sympathetic neurons. Supershift experiments were carried out by incubating samples on ice with antibodies (4 µg) for 2 hours. A Santa Cruz antibody against NF-YA (H-209: Sc-10779 X) was used along with c-Jun (H-79: Sc-1694 X) or Fra-2 (L-15: Sc-171 X) antibodies as negative controls (also from Santa Cruz Biotechnology Inc.). Samples were incubated with 0.4 ng of ^{32}P-labelled oligonucleotide for 15 minutes at room temperature and loaded onto a 5%, native polyacrylamide gel (5% acrylamide/bis solution, 0.25 X TBE, 0.04 % APS and 0.2% TEMED) in 0.25 X TBE. Electrophoresis was carried out at 180 V for 2 hours using a vertical gel electrophoresis apparatus (Whatman, model V15-17). After electrophoresis, the gel was fixed in a 10 % acetic acid / 10 % methanol solution for 20 minutes and dried at 80ºC under vacuum using a Biorad gel dryer (model 583). The bands were visualised by exposing the gel to MXB X-ray film (Kodak Ltd).

2.2.11.1 Preparation of protein extracts for EMSA experiments

Nuclear and cytoplasmic lysates were prepared from undifferentiated PC6-3 cells, differentiated PC6-3 cells maintained in NGF and differentiated PC6-3 cells 16 hours following NGF withdrawal. Protein extracts were prepared by a method based on that described by Wong *et al*. (1999): cells were washed twice in ice-cold PBS (-) (Gibco, Invitrogen Corporation) and left to swell for 5 minutes on ice in 500 µl (per 9 cm dish) of hypotonic buffer (Table 1). Cells were scraped into a single cell suspension and the nuclei pelleted at 200 x g at 4ºC for 10 minutes. The supernatant was removed and this was the cytoplasmic extract. The pellet was resuspended in a 5 X volume of hypertonic buffer (Table 1). The suspension was rocked for 1 hour at 4ºC in an orbital tube rotator and then spun at 15,700 x g in a microcentrifuge for 5 minutes at 4ºC. The final supernatant was removed and this was the nuclear extract.

Whole cell extracts were prepared from sympathetic neurons (cultured for 7 days *in vitro*) that were maintained in medium containing NGF or following NGF

withdrawal for 16 hours using a method based on Schwarz *et al*., 1993: neurons from 4 coverslips for each treatment were washed into 1.5 ml microfuge tubes (+ and –NGF, respectively) with ice cold PBS (-). Cells were spun down briefly to remove PBS (-) and resuspended in 30 μl of whole extract buffer (Table 1). Extracts were left for 20 minutes on ice and then spun in a microcentrifuge at 15,700 x g for 30 minutes at 4ºC and the supernatant was collected.

Protease and phosphatase inhibitors were added to the protein extract buffers just before use and all protein extracts were stored at -80ºC. Protein concentration was determined using the Biorad protein assay kit (Biorad Laboratories Inc.), which is based on the method of Bradford (1976), with γ-globulin as a standard.

2.2.12 Immunocytochemistry

Neurons were fixed in 4% paraformaldehyde at room temperature for 20 minutes, washed in PBS (-) 3 times and permeabilised either in Triton X-100 (0.5% Triton X-100 in PBS (-) for 5 minutes at room temperature) or in methanol (ice-cold MeOH for 15 minutes) according to the primary antibody that was used. After washing, blocking was carried out in 50% goat serum (Sigma-Aldrich Corporation) in 1% BSA in PBS (-) at room temperature for 30 minutes. After washing, cells were incubated in primary antibody for 1 hour at room temperature at a dilution of 1:100 or 1:250 (in 1% BSA in PBS). Cells were washed as detailed above and incubated in a FITC-conjugated secondary antibody (and a rhodamine anti-guinea pig IgG secondary antibody if neurons were microinjected) diluted 1:750 in 1% BSA in PBS, for 45 minutes at room temperature. Coverslips were washed again and the nuclei were then stained with Hoechst 33342 dye at 1 μg/ml for 10 minutes at room temperature. After washing three times in distilled water, coverslips were mounted onto glass slides in Citifluor AF1 glycerol/PBS solution and sealed using clear nail varnish. Slides were stored at 4ºC and viewed on a Zeiss Axioplan 2 fluorescence microscope (x63 magnification using Zeiss Immersol oil) and cells were scored in a blinded manner whenever possible. Secondary-only controls were carried out to confirm the specificity of primary antibodies and all antibodies used for immunofluorescence are listed in Table 2.

Table 2: Antibodies used for immunofluorescence

Antibody	Supplier	Dilution	Permeabilisation
NF-YA H-209: Sc-10779	Santa Cruz	1:250	Triton X-100
Bim # 2819	Cell Signalling	1:100	Triton X-100
p300 C-20:Sc-585	Santa Cruz	1:100	Methanol
CBP C-20:Sc-583	Santa Cruz	1:100	Methanol

This table lists the primary antibodies used for immunofluorescence, together with the working dilution and method of permeabilisation used for each antibody.

2.2.13 Immunoblotting

Sympathetic neurons were cultured for 7 days *in vitro* and whole cell extracts were prepared as follows: neurons from 4 coverslips for each treatment (for example; + NGF, +NGF +U0126, -NGF) were washed into 1.5 ml microfuge tubes using ice-cold PBS (-). Cells were spun down briefly to remove PBS (-) and lysed in 30 µl of SDS gel sample buffer (Table 1) by incubating at 100ºC for 15 minutes. Lysates were stored at -80ºC and boiled for a further 5 minutes prior to loading. Protein concentration was determined using the Biorad protein assay kit (Biorad Laboratories Inc.) with γ-globulin as a standard.

Proteins were separated on a 12% SDS-polyacrylamide gel (Stacking gel: 4% acrylamide/bis solution, 0.125 M Tris-HCl pH 6.8, 0.1% SDS, 0.05% APS and 0.2% TEMED. Resolving gel: 12% acrylamide/bis solution, 0.375 M Tris-HCl pH 8.8, 0.1% SDS, 0.05% APS and 0.2% TEMED) in 1 X SDS gel running buffer (Table 1) at 120 V for 80 minutes using a Mini-PROTEIN III electrophoresis tank (Biorad laboratories Inc.). Proteins were transferred to Immobilon-*P* (Millipore Corporation) using the Biorad Mini-PROTEIN III transfer system in 1x transfer buffer (Table 1) at 35 V for 2 hours.

Membranes were blocked for 1 hour at room temperature in 1 X TBS containing 0.1% Tween-20 and 5% non-fat milk powder (blocking solution).

Membranes were incubated overnight at 4ºC in primary antibody diluted in blocking solution at 1:1000 (Table 3). Excess antibody was removed by washing 6 times for 10 minutes in TBS containing 0.1% Tween-20 (TBS-T). The membranes were incubated in horseradish peroxidase-conjugated secondary antibodies diluted 1:3500 in TBS-T (Table 3), washed as previously and then proteins were detected with the chemiluminescent reagent, ECL (Amersham Biosciences Ltd). The bands were visualised by exposure to MXB X-ray film (Kodak Ltd.) and scanned images were then quantitated using ImageQuant image analysis software (GE Healthcare Ltd.). For re-probing, membranes were stripped of bound proteins for 30 minutes at 50ºC in stripping buffer (Table 1). All antibodies used for immunoblotting are listed in Table 3.

Table 3: Antibodies used for immunoblotting

Antibody	Supplier	Dilution	Secondary Ab
p44/42 (ERK1/2) # 9102	Cell Signalling	1:1000	Anti-rabbit HRP (1:3500)
Phospho-p44/42 (phospho-ERK1/2) (Thr 202/Tyr 204) # 9101S	Cell Signalling	1:1000	Anti-rabbit HRP (1:3500)
AKT # 9272	Cell Signalling	1:1000	Anti-rabbit HRP (1:3500)
Phospho-AKT (Ser 473) # 9271S	Cell Signalling	1:1000	Anti-rabbit HRP (1:3500)

This table lists the antibodies, together with their working dilution and secondary antibody that were used for immunoblotting.

2.2.14 Statistical analysis

In each set of experiments data is normalised to a control sample in the presence of NGF (for example, *bim*-LUC +NGF). All data are presented as the mean ± S.E. of

multiple experiments. The Paired Student's T-test (for two-tailed distributions) was used as a test for statistical significance. *** represents a p-value of less than 0.001, ** represents a p-value of less than 0.01 and * represents a p-value of less than 0.05. P-values less than 0.05 were considered as a statistically significant difference. All statistical comparisons were carried out using Microsoft Excel 2003.

For microinjection, the relative induction of a DNA construct was calculated by dividing the normalised luciferase activity in the presence of NGF by the normalised luciferase activity in the absence of NGF.

Chapter 3: The role of NF-Y in regulating *bim* gene expression in sympathetic neurons.

3.1 Introduction

Bim is a potent proapoptotic protein in many different cell types and its expression is tightly regulated by a number of transcriptional and post-translational mechanisms. Regulation of *bim* appears to vary between cell types, but in models of neuronal cell death, in which the cells are dependent on NGF for survival, transcriptional control of *bim* involves at least three pathways (Figure 1.8). *Bim* mRNA and Bim protein levels increase when sympathetic neurons are deprived of NGF and overexpression of Bim_{EL} in these cells can induce cytochrome *c* release and apoptosis (Putcha *et al*., 2001; Whitfield *et al*., 2001). A number of studies suggest that activation of the MLK-JNK-c-Jun pathway is a key event for *bim* upregulation in sympathetic neurons: the overexpression of a dominant negative c-Jun protein reduces the increase in *bim* mRNA and protein levels that occurs after NGF withdrawal (Whitfield *et al*., 2001); the MLK inhibitor CEP-1347 inhibits the increase in *bim* mRNA level (Harris and Johnson, 2001); the jun^{AA} knock-in mutation reduces the increase in Bim protein level after NGF withdrawal (Besirli *et al*., 2005). Furthermore, sympathetic neurons and sensory neurons isolated from $bim^{-/-}$ knockout mice are partially protected against cell death following withdrawal of NGF, indicating that *bim* is required for NGF withdrawal-induced death (Whitfield *et al*., 2001; Coultas *et al*., 2007). In addition to this, Gilley *et al*. (2003) identified two conserved FOXO sites that flank the *bim* proximal promoter and showed, by microinjection of a *bim*-LUC reporter construct, that mutation of these sites greatly reduces *bim* promoter activation following NGF withdrawal in sympathetic neurons. *Bim* is also a target for PI3-K signalling and overexpression of constitutively active FOXO3a can induce Bim expression (Gilley *et al*., 2003). Moreover, FOXO activity contributes to the NGF deprivation-induced death of sympathetic neurons (Gilley *et al*., 2003). Finally, Biswas *et al*. (2005) identified two Myb binding sites in the *bim* promoter and, using neuronally differentiated PC12 cells, showed that *bim* is a target of a Cdk4-E2F pathway that leads to the de-repression of E2F-regulated *myb* genes and the induction of *bim*

following NGF withdrawal. These studies have provided detailed information on how *bim* is regulated following growth factor withdrawal. However, the role of the region of the *bim* promoter proximal to the major transcriptional start site and how it controls basal promoter function and contributes to the activation of *bim* following NGF withdrawal still remains to be elucidated. Since *bim* has a TATA-less promoter, I was interested to establish what factor(s) govern its basal promoter function and how these regulate *bim* expression following NGF deprivation in sympathetic neurons. One candidate that I have investigated is NF-Y.

Nuclear factor-Y (NF-Y), also known as CBF or CP-1 (and HAP 2/3/5 in yeast), is a heteromeric transcription factor of 70 kDa that is formed by the interaction of three subunits NF-YA, NF-YB and NF-YC. All three subunits contain core domains, conserved through evolution, that are sufficient for subunit interactions and DNA binding (Hooft van Huijsduijen *et al*., 1990; Sinha *et al*., 1995). Interestingly, the activation domains are less well conserved and in yeast, the activation domain is encoded by a fourth subunit (HAP4) with no apparent homologues in other species (Forsburg and Guarente, 1989; Hooft van Huijsduijen *et al*., 1990; Gusmaroli *et al*., 2001). The NF-YB and NF-YC core regions are highly homologous to histones H2A and H2B, respectively, and their dimerisation, facilitated through strong histone fold motif interactions, is a prerequisite for NF-YA association (Caretti *et al*., 1999). The NF-YB/NFY-C dimer is important for protein-protein interactions and the alpha-C (αC) helix of NF-YC is a docking site for c-MYC and p53 (Figure 3.1; Izumi *et al*., 2001; Romier *et al*., 2003; Imbriano *et al*., 2005). NF-YA has two subdomains, an N-terminal region responsible for contacting the NF-YB/NF-YC dimer (NF-YA1) and a C-terminal region that is responsible for sequence specific DNA binding (NF-YA2) (Figure 3.1; Olesen and Guarente, 1990; Mantovani *et al*., 1994; Romier *et al*., 2003).

The NF-Y trimer, once formed, recognises and binds to the CCAAT box element. CCAAT boxes can be found in the forward (CCAAT) or reverse, inverted (ATTGG) orientation (known as an inverted CCAAT box, or a Y box) and are present in around 30% of eukaryotic promoters (Bucher, 1990). The canonical CCAAT box is composed of a strictly conserved central pentanucleotide sequence, CCAAT or

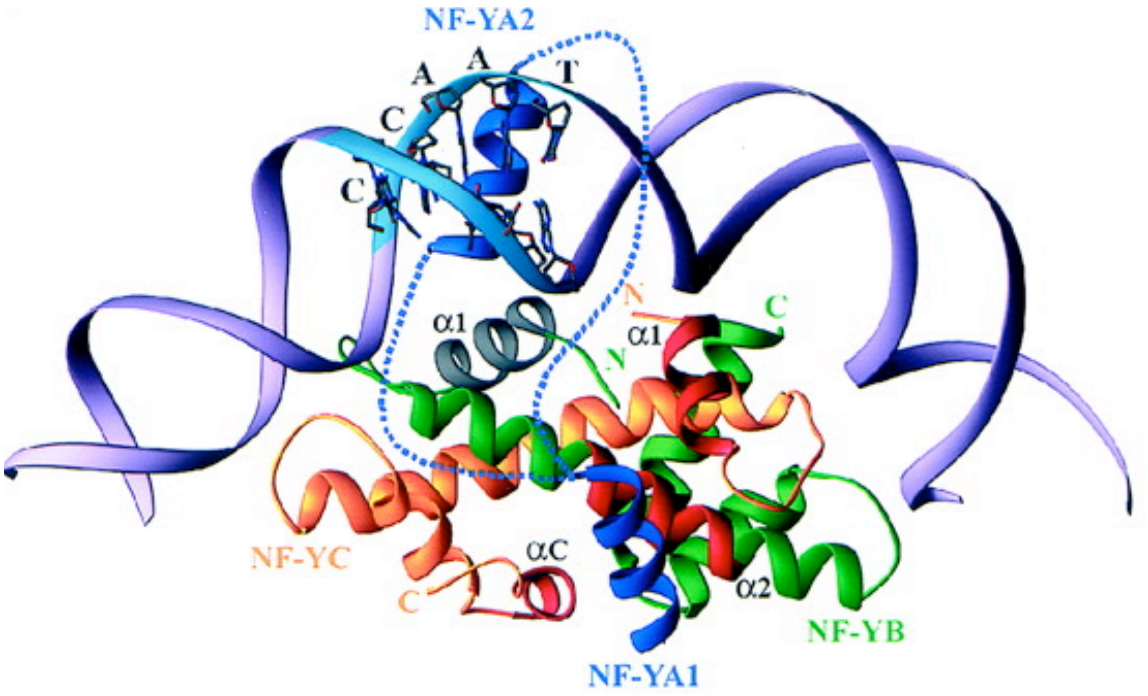

Figure 3.1 Model of the NF-Y/CCAAT complex.

Model of how the transcription factor NF-Y binds to and distorts the DNA. The NF-Y/CCAAT complex was modelled following analysis of the crystal structure of the NF-YB-NF-YC dimer, as resolved by x-ray crystallography. The DNA backbone is shown as ribbons (purple) with the CCAAT pentanucleotide labelled. NF-YA is shown in blue, NF-YB is shown in green and NF-YC is shown in orange. The two alternative positions for the linker connecting the two subdomains of NF-YA (NF-YA1 and NF-YA2) are shown as a blue dotted line. Taken from Romier *et al*. (2003).

ATTGG, with a highly preferred 5′ and 3′ surrounding sequence (Bucher, 1990). The frequency of CCAAT boxes appears to be higher in TATA-less promoters, particularly in the reverse ATTGG orientation. In promoters with a TATA box, the CCAAT box is typically located between -80 and -100 bp upstream of the major transcriptional start site, whereas in TATA-less promoters, it is usually found closer to the +1 signal (-66 on average) (Mantovani, 1998). The CCAAT box is often found as a single copy element. Multiple CCAAT boxes can be found in the same promoter, but in every case they are separated by at least 27 base pairs (Mantovani, 1999). Studies in a variety of experimental systems have validated the importance of CCAAT box elements for the transcriptional activation of different genes. However, there appears to be some variability in the extent of CCAAT dependence between different classes of promoter. TATA-less promoters, containing only one or two other activator sites, seem to require an intact CCAAT whereas TATA-containing promoters, that have other powerful transcriptional activator binding sites, are less dependent (Mantovani *et al*., 1992; Liberati *et al*., 1998).

NF-Y binds to the CCAAT box, in the forward or reverse orientation, with high specificity and affinity (Kim and Sheffery, 1990; Bi *et al*., 1997). Specific DNA binding involves both minor and major groove interactions and upon NF-Y binding, the DNA bends by approximately 60° to 80° (Figure 3.1; Ronchi *et al*., 1995; Liberati *et al*., 1998). This distortion of the DNA can facilitate protein-protein interactions between distally binding factors, since they are brought together in space (Mantovani *et al*., 1999). Analysis of the NF-Y crystal structure revealed that the bound NF-Y trimer spans a considerable distance along the DNA (Figure 3.1; Romier *et al*., 2003). This is consistent with previous biochemical data that suggested that a region of 24-26 base pairs is occupied by NF-Y (Liang and Maity, 1998; Liberati *et al*., 1998; Mantovani *et al*., 1998).

NF-Y sites are often found in the proximal promoter regions of many genes where they play a critical role in transactivation. However, a recent study, using chromatin immunoprecipitation (ChIP) on chip analysis, revealed that NF-Y sites are not confined to the core promoters of genes, with around 40% located outside (Testa *et al*., 2005). This suggests that that the NF-Y mediated transcriptional network is quite complex.

One function of NF-Y is to govern basal transcription and NF-Y has been reported to associate with the TATA-box binding protein (TBP), TBP-associated factors (TAFs) and TFIID (Bellorini *et al*., 1997; Frontini *et al*., 2002). Through these interactions NF-Y can facilitate preinitiation complex formation in the absence of a TATA box and recruit RNA polymerase II to the promoter (Kabe *et al*., 2005).

The major role of NF-Y is to cooperate with other transcriptional activators located close by and therefore CCAAT boxes are usually flanked by at least one other functional promoter element. The CCAAT box and the flanking element(s) are often precisely spaced to allow the binding factors to interact on the same side of the DNA helix (Mantovani 1999). NF-Y can markedly increase the affinity of a neighbouring factor, such as SP-1, for the DNA (Wright *et al*., 1995). Yoshida *et al*. (2000) showed that the basic leucine zipper protein ATF6 is induced by endoplasmic reticulum (ER) stress and binds cooperatively with NF-Y to induce the unfolded protein response (UPR). They found that when they mutated the CCAAT box, ATF6 could no longer bind to its target consensus sequence (Yoshida *et al*., 2000). NF-Y can also recruit the coactivator p300/CBP to DNA to potentiate transcription and NF-Y can be acetylated by p300 (Li *et al*., 1998; Salsi *et al*., 2003).

A number of groups have reported that p53/NF-Y complexes modulate the activity of cell cycle promoters that are involved in the DNA damage response (Yun *et al*., 1999; Manni *et al*., 2001; Imbriano *et al*., 2005). Upon DNA damage the p53/NF-Y complex recruits histone deacetylases (HDACs) and releases histone acetyltransferases (HATs), resulting in the repression of key cell cycle control genes (Imbriano *et al*., 2005). In contrast, mutant p53/NF-Y complexes cause aberrant cell cycle regulation by activating proliferative genes, and this is a critical point in their gain-of-function, in response to DNA damage (Di Agostino *et al*., 2006; Peart and Prives, 2006).

NF-Y function is primarily regulated through interactions with different transcription factors and transcriptional cofactors. However, the activity of the NF-Y trimer appears to be governed by post-translational modification of the NF-YA subunit. NF-YA is a target for ubiquitination and acetylation (Manni *et al*., 2008). NF-YA can also be phosphorylated and a phosphorylation-deficient mutant form of NF-YA has significantly reduced DNA-binding activity (Yun *et al*., 2003).

Functional studies have, so far, defined the importance of NF-Y in proliferation and control of the cell cycle. A conditional deletion of both *NF-YA* alleles, in primary mouse embryonic fibroblasts, led to a block in cell cycle progression, indicating that NF-Y dependent transcription is essential during early mouse development (Bhattacharya *et al*., 2003). Abrogation of NF-Y function by the stable expression of an NF-YA dominant negative in mouse NIH 3T3 fibroblasts also resulted in a loss of cell cycle progression (Hu and Maity, 2000).

In the work described in this chapter, I have investigated the role of an inverted CCAAT box and NF-Y in the regulation of *bim* transcription in sympathetic neurons.

3.2 Results

3.2.1 The *bim* proximal promoter contains an inverted CCAAT box that is conserved across species.

To start to investigate how the region of the *bim* promoter proximal to the transcriptional start site regulates *bim* expression, I used the ConSite software to scan the promoter for potential transcription factor binding sites. The ConSite website uses phylogenetic footprinting and transcription factor binding profiles to detect transcription factor binding sites within genomic sequences (Lenhard *et al*., 2003). I identified an inverted CCAAT box (ICB) that is located 29 base pairs or 54 base pairs upstream from the major transcriptional start site in rat and human *bim*, respectively (Figure 3.2A). ConSite predicts that a number of transcription factors can bind to the ICB, including the most common CCAAT-binding factor, NF-Y (Figure 3.2B). NF-Y binds with strong affinity to the central pentanucleotide sequence (CCAAT or ATTGG) and has a highly preferred 5′ and 3′ surrounding sequence (Figure 3.2C). The 16 base pair region of the *bim* promoter, that includes the central ATTGG, is highly conserved across human, rat and mouse and is a near perfect match to the consensus of an NF-Y binding site (Figure 3.2C).

3.2.2 NF-Y binds to the *bim* ICB in the presence of NGF and following NGF withdrawal.

To investigate whether NF-Y can bind to the ICB in the *bim* promoter, I carried out some electrophoretic mobility shift assays (EMSAs) (Figure 3.3). To identify potential NF-Y binding complexes, oligos containing a previously identified CCAAT box in the rat GTP hydrolase gene (Kapatos *et al*., 2000) were used as a positive control (Figure 3.3A and B). Initial EMSA experiments were performed with nuclear extracts from neuronally differentiated PC6-3 cells that had been treated with NGF for 7 days. The nuclear extracts contained proteins that bound the ICB and this binding (marked NF-Y complex) was abolished by point mutations in the ATTGG consensus (mutant probes) (Figure 3.3A). To determine whether the specific protein complexes contained NF-Y, antibodies

Figure 3.2 Identification of an inverted CCAAT box in the *bim* promoter.

(A) Alignment of the proximal promoter sequences for the rat, mouse and human *bim* genes. The inverted CCAAT box (ICB) is located 29 bp or 54 bp upstream of the transcriptional start site in rat and human, respectively. The asterisks indicate bases that are conserved across all three species.

(B) Transcription factors that can potentially bind to the ICB in the human and rat *bim* promoters identified using ConSite, http://www.phylofoot.org/consite.

(C) The binding profile of NF-Y to an ICB (Jaspar database, http://jaspar.gene.reg.net). The probability of different nucleotides at each position of an ICB, bound by NF-Y, is shown (where 116 NF-Y binding ICB consensus sequences were analysed, adapted from the Jaspar database). An alignment between the rat, mouse and human *bim* genes shows that there is a high level of conservation in this area.

A

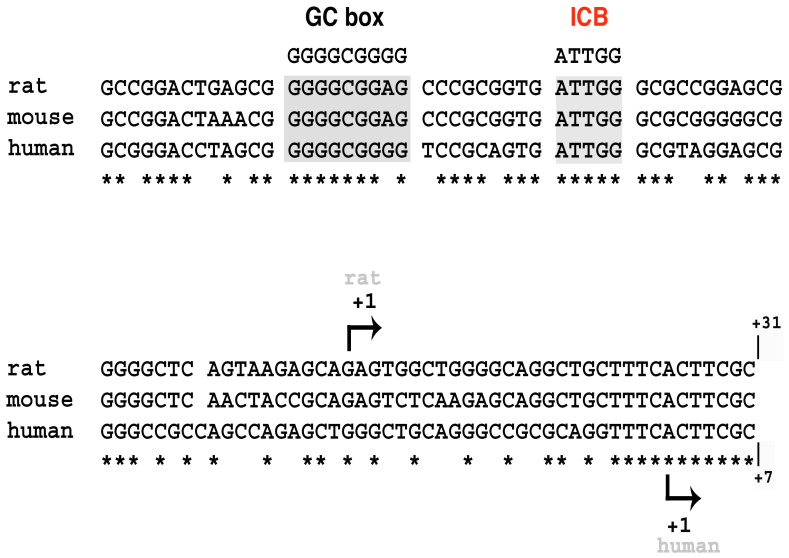

B

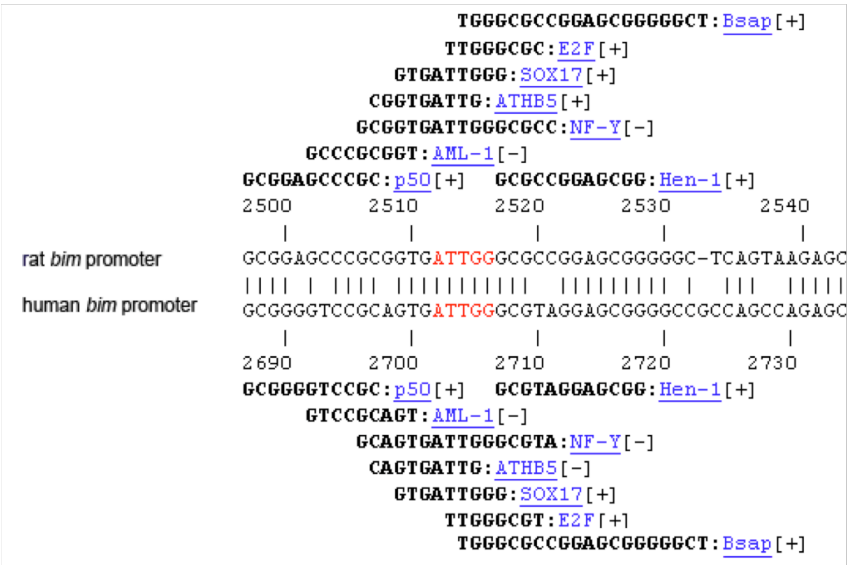

C

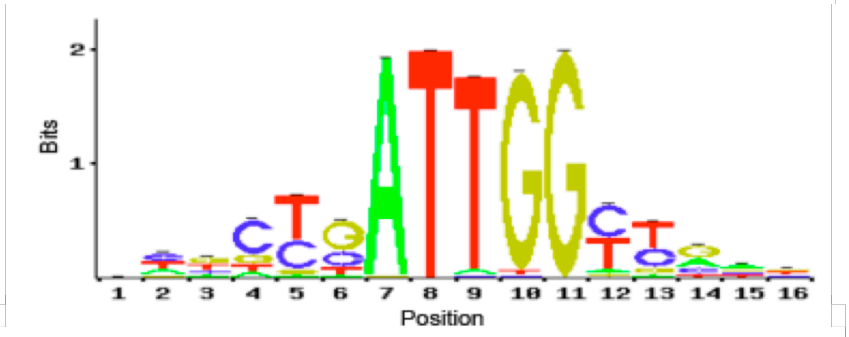

A	[	27	24	12	10	2	4	115	0	3	0	0	5	3	33	41	18	]
C	[	29	47	22	73	42	33	0	0	1	1	0	56	41	25	26	27	]
G	[	35	9	43	20	6	65	1	0	0	113	116	4	14	51	33	37	]
T	[	25	36	39	13	66	14	0	116	112	2	0	51	58	7	16	34	]

Bim promoter

Human	[	G	C	A	G	T	G	A	T	T	G	G	G	C	G	T	A	]
Rat	[	G	C	G	G	T	G	A	T	T	G	G	G	C	G	C	C	]
Mouse	[	G	C	G	G	T	G	A	T	T	G	G	G	C	G	C	G	]

specific to the NF-YA subunit or to c-Jun (as a negative control) were added to the binding reactions. The c-Jun antibody did not alter the binding pattern observed whereas the NF-Y antibody supershifted (marked SS) the entire protein complex, thereby confirming that the protein complex bound to the *bim* CCAAT probe was NF-Y (Figure 3.3B). The binding of NF-Y to the *bim* ICB was similar to the binding of NF-Y to the GTP C1 positive control probe, which behaved in an identical fashion when antibodies against the NF-Y complex were added (Figure 3.2B). To investigate whether NF-Y present in sympathetic neurons could bind to the *bim* ICB, EMSA experiments were performed with whole cell extracts prepared from sympathetic neurons maintained in the presence of NGF (+NGF) or withdrawn from NGF (-NGF) for 16 hours (Figure 3.3C). Extracts from sympathetic neurons maintained in the presence of NGF reproduced the binding pattern that was observed with extracts from differentiated PC6-3 cells in Figure 3.3B, and binding did not change following NGF withdrawal (Figure 3.3C). The protein complexes were successfully supershifted with the NF-YA antibody but not with a Fra-2 antibody, which was used as a negative control. It is of interest to note that when oligos were tested, in preliminary experiments, that were 5 nucleotides shorter at the 5′ end and 3′ end than those used in Figure 3.3, no specific binding was observed. This confirms that the sequences flanking the highly conserved ATTGG are required for NF-Y binding, consistent with previous reports (Mantovani, 1998; Bucher, 1999). However, it is still not known whether these distal bases are specifically recognised by NF-Y, or are simply necessary for proper distortion of the DNA for NF-Y binding, or both (Romier *et al*., 2003).

To confirm that NF-Y can bind to the endogenous *bim* promoter, I performed some chromatin immunoprecipitation (ChIP) assays using the NF-YA antibody that had been used in EMSA experiments, together with an antibody against the myogenic regulatory factor MyoD as a negative control. ChIP is a powerful method for confirming *in vivo* DNA binding sites of transcription factors, but a large number of cells are required in conventional ChIP assays, therefore neuronally differentiated PC6-3 cells were used instead of sympathetic neurons. PC6-3 cells were differentiated in the presence of NGF for 7 days and then either maintained in the presence of NGF (+NGF)

Figure 3.3 NF-Y can bind to the ICB in the promoter of *bim*.

(A) Oligonucleotides used for EMSA experiments. Point mutations were introduced into the CCAAT box consensus sequence in order to abolish binding and therefore identify specific complexes. The mutated bases are underlined.

(B) EMSA comparing *bim* CCAAT probes to the GTP C1 positive control probes, with nuclear extracts from PC6-3 cells differentiated in the presence of NGF for 7 days. An NF-YA antibody (H-209: Sc-10779 X) was used to supershift the NF-Y/CCAAT box complex and a c-Jun antibody (H-79: Sc-1694 X) was used as a negative control.

(C) EMSA with *bim* CCAAT probes and whole cell extracts from sympathetic neurons maintained in the presence of NGF (+NGF) or withdrawn from NGF (-NGF) for 16 hours. An NF-YA antibody (H-209: Sc-10779 X) was used to supershift the NF-Y/CCAAT box complex and a Fra-2 antibody (L-15: Sc-171 X) was used as a negative control.

Several experiments were performed in each case and representative results are shown. Free probe and the NF-Y complexes are indicated.

A

bim CCAAT WT	5′-CTAGCCCGCGGTGATTGGGCGCCGGA-3′
bim CCAAT mut	5′-CTAGCCCGCGGTGAGCTCGCGCCGGA-3′
GTP C1 WT	5′-CTAGCTCGGGCCAATGAGAACGCCT-3′
GTP C1 mut	5′-CTAGCTCGGGGAGCTGAGAACGCCT-3′

B

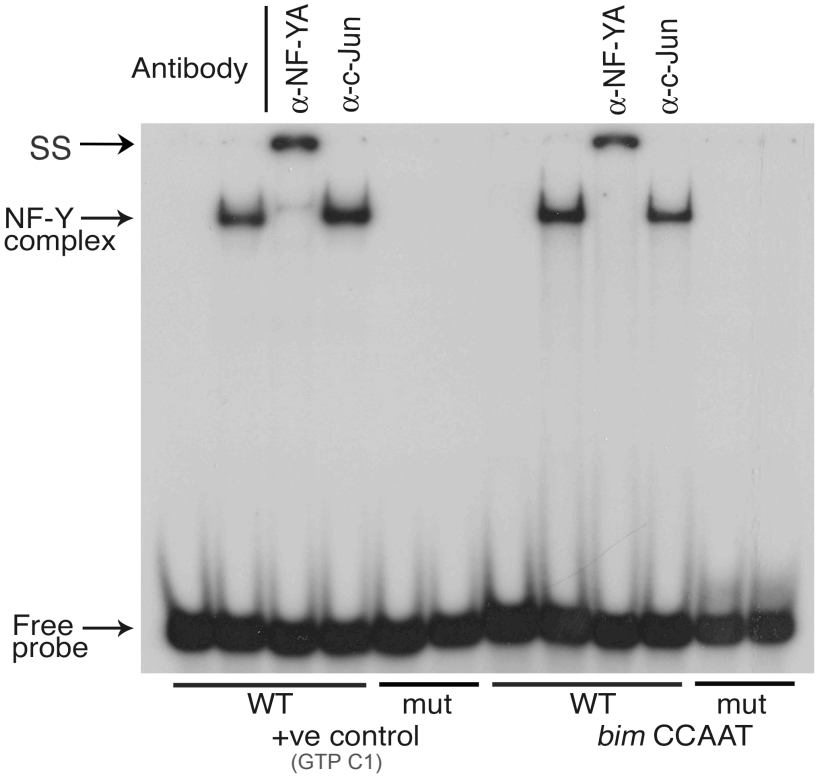

C

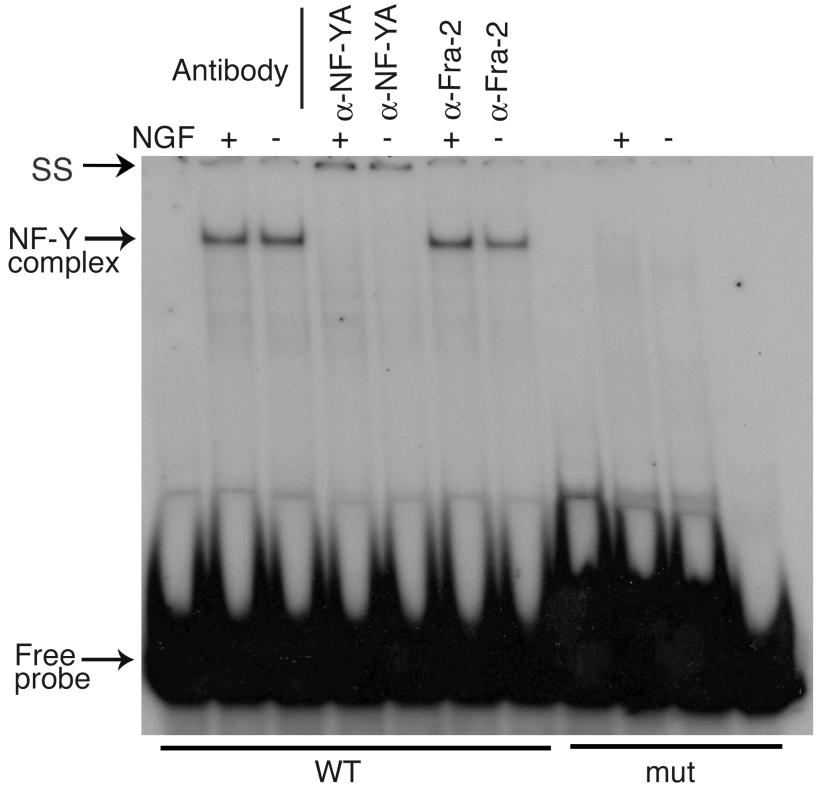

or withdrawn from NGF (-NGF) for 16 hours. The binding of NF-Y to the ICB in the *bim* promoter was studied by PCR amplification of the immunoprecipitated chromatin samples, using PCR primers that amplify a 331 base pair region surrounding the ICB (Figure 3.4A). This region does not contain any other potential NF-Y binding sites. The negative control antibody to MyoD, immunoprecipitated background levels of *bim* promoter chromatin, however this was significantly enriched by the antibody against NF-YA in cells maintained in the presence of NGF and following NGF withdrawal (Figure 3.4B and C). Therefore, NF-Y is bound to the ICB in the rat *bim* promoter in the presence of NGF and following NGF withdrawal for 16 hours, with no significant change in the affinity of NF-Y binding following withdrawal of NGF.

3.2.3 The ICB is critical for *bim* promoter function and contributes to the activation of *bim* transcription following NGF withdrawal.

A *bim*-LUC reporter construct is significantly activated following withdrawal of NGF in microinjected sympathetic neurons (Gilley *et al*., 2003). *Bim*-LUC consists of 2.5 kb of the rat *bim* promoter, the non-coding exon 1 and the 2.5 kb intron 1 cloned upstream of the firefly luciferase gene (Figure 3.5A). To determine whether the ICB is important for *bim* promoter activity point mutations were introduced into the ATTGG pentamer, within our *bim*-LUC reporter construct (Figure 3.5A). The point mutations within the *bim*-LUC CCAAT(-) reporter construct are the same as those incorporated into the *bim* CCAAT mutant oligos in EMSA experiments (Figure 3.3), therefore the binding of NF-Y to the *bim* promoter, in the context of *bim*-LUC CCAAT(-), should be abolished. To compare their activity the *bim*-LUC and *bim*-LUC CCAAT(-) constructs were microinjected into the nuclei of sympathetic neurons, together with the control *Renilla* luciferase construct, pRL-TK. The injected cells were then either maintained in the presence of NGF (+NGF) or withdrawn from NGF (-NGF) for 16 hours, after which time relative luciferase activity was determined by the dual luciferase assay (Gilley *et al*., 2003; Pajak *et al*., 2003). Mutation of the ICB resulted in an 80% decrease in basal promoter activity when *bim*-LUC and *bim*-LUC CCAAT(-) basal levels were compared (Figure 3.5B). Following NGF withdrawal for 16 hours, the *bim*-LUC reporter was activated significantly (Figure

Figure 3.4 NF-Y is bound to the endogenous *bim* promoter in the presence of NGF and following NGF withdrawal.

PC6-3 cells were differentiated in the presence of NGF for 7 days. The neuronally differentiated cells were then either maintained in the presence of NGF (+NGF) or withdrawn from NGF (-NGF) for 16 hours. After 16 hours, the cells were cross-linked with 1% formaldehyde and chromatin immunoprecipitations were performed using the NF-YA antibody (H-209: Sc-10779 X) or a MyoD antibody (M-318: Sc-760 X) as a negative control.

(A) PCR primers were designed that flank the inverted CCAAT box in the rat *bim* promoter (the approximate locations of forward and reverse primers are shown by the filled arrows).

(B) ChIP samples were analysed by semi-quantitative PCR and a representative image is shown. The 1Kb+ DNA ladder was used as a molecular weight marker.

(C) PCR was quantitated at 25 cycles and the average amount of *bim* promoter DNA, precipitated by each antibody, was calculated. ChIP was performed 4 times and data is presented as the mean ± S.E. There is a significant increase in the amount of *bim* promoter DNA precipitated by the NF-YA antibody in both + NGF (*) and - NGF (**) conditions, compared to the negative control antibody.

A

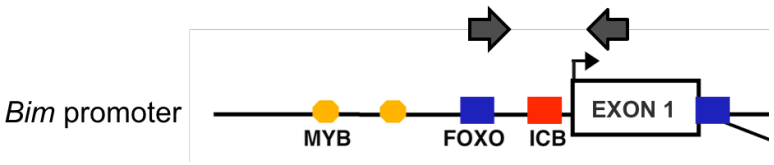
Bim promoter
MYB
FOXO
ICB
EXON 1

B

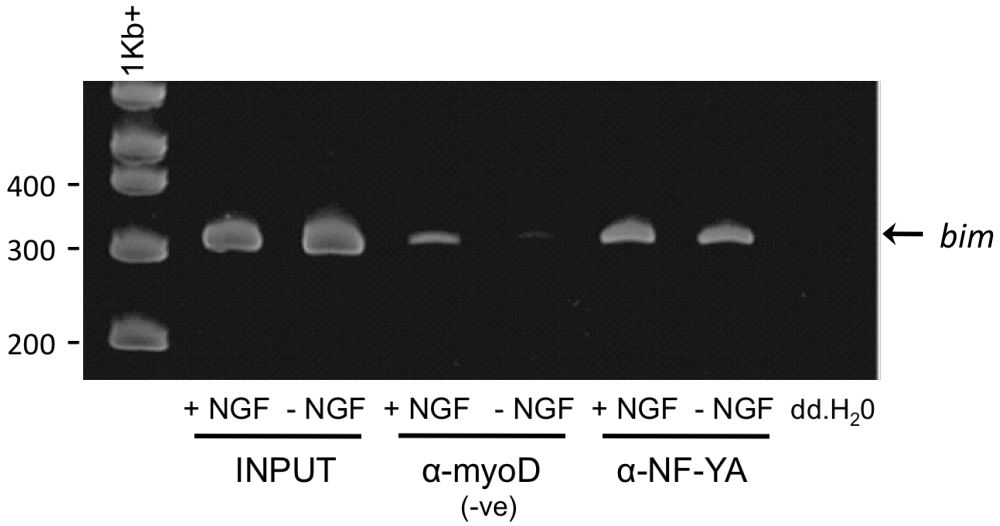
1Kb+
400
300
200
bim
+ NGF - NGF + NGF - NGF + NGF - NGF dd.H20
INPUT
α-myoD
(-ve)
α-NF-YA

C

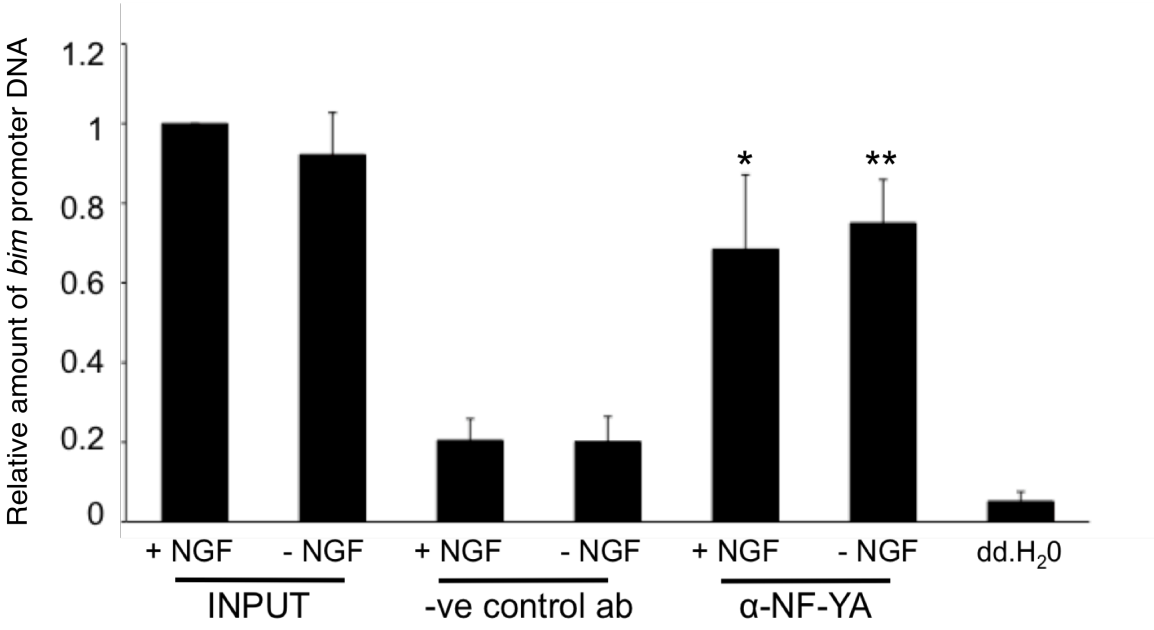
Relative amount of bim promoter DNA
1.2
1
0.8
0.6
0.4
0.2
0
*
**
+ NGF - NGF + NGF - NGF + NGF - NGF dd.H20
INPUT
-ve control ab
α-NF-YA

3.5B) (*bim*-LUC is typically activated 2 fold following NGF withdrawal, Gilley *et al*., 2003). The basal levels of the two constructs, in the presence of NGF, were then set to 1 and the induction factors of the constructs compared (Figure 3.5C). This comparison shows that the mutation of the ICB significantly decreases the induction of the *bim* promoter following NGF withdrawal, from 2.3 fold to 1.5 fold. Taken together, these results suggest that the ICB is critical for *bim* basal promoter activity and contributes to the induction of *bim* following NGF withdrawal in sympathetic neurons.

3.2.4 NF-Y is required for *bim* promoter activity and its induction following NGF withdrawal.

To establish whether NF-Y binding is required for *bim* promoter function (and not only an intact CCAAT box), sympathetic neurons were microinjected with the YA13 m29 expression vector (Figure 3.6). YA13 m29 is a dominant negative mutant of the NF-YA subunit (Mantovani *et al*., 1994). It can bind to the other NF-Y subunits but not to DNA and thus acts by forming inactive trimers with NF-YB and NF-YC. The YA13 m29 construct was microinjected into sympathetic neurons along with guinea pig IgG (gp IgG), as a marker for the injected cells, and after 24 hours the cells were stained with an antibody against NF-YA to detect YA13 m29 (and endogenous NF-YA). NF-YA immunostaining was considerably brighter in the nuclei of injected cells (Figure 3.6A), and approximately >90% of injected cells expressed high levels of NF-YA. Therefore, YA13 m29 is efficiently expressed in microinjected sympathetic neurons, where it localises to the nucleus. Sympathetic neurons were then co-microinjected with YA13 m29, or the control empty vector pSG5, along with the *bim*-LUC reporter and pRL-TK. The injected cells were either maintained in the presence of NGF (+NGF) or withdrawn from NGF (-NGF) for 16 hours, after which time relative luciferase activity was determined by the dual luciferase assay (Figure 3.6B). Expression of YA13 m29 completely obliterated the induction of *bim*-LUC following NGF withdrawal and caused a significant decrease in the basal level of *bim*-LUC, compared to the control pSG5 (Figure 3.6B). This demonstrates that NF-Y activity is required for the activation of *bim*-LUC following NGF withdrawal in sympathetic neurons.

Figure 3.5 The ICB is critical for basal promoter function and contributes to the induction of *bim* transcription following NGF withdrawal.

Sympathetic neurons were microinjected with *bim*-LUC or *bim*-LUC CCAAT (-) (both at 10 ng/μl) together with pRL-TK at 5 ng/μl (to control for injection efficiency). The cells were maintained in medium containing NGF (+NGF) or withdrawn from NGF (-NGF) for 16 hours, after which time luciferase activity was measured. Microinjection experiments were carried out 5 times and data is presented as the mean ± S.E.

(A) Structure of the *bim*-LUC and *bim*-LUC CCAAT (-) reporter constructs. The *bim*-LUC reporter contains 2.5 kb of the rat *bim* promoter, the non-coding Exon 1 and the 2.5 kb intron 1 cloned upstream of the firefly luciferase gene. The location of conserved FOXO binding sites, Myb binding sites and the ICB are shown. The *bim*-LUC CCAAT (-) construct contains 4 point mutations within the ICB consensus that were introduced by site-directed mutagenesis.

(B) *Bim*-LUC is activated significantly following NGF withdrawal (**). Mutation of the ICB significantly decreases the basal promoter level of *bim*-LUC (***).

(C) The basal levels of *bim*-LUC and *bim*-LUC CCAAT (-) were normalised to 1 and the induction factors of the two constructs were compared. Mutation of the ICB significantly decreases the induction of *bim*-LUC following NGF withdrawal (*).

A

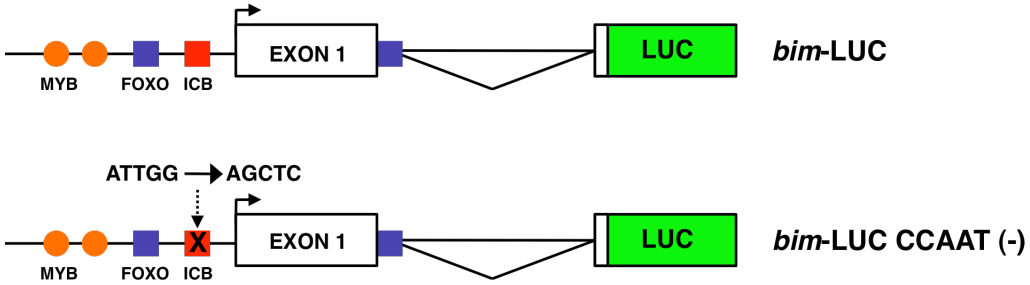
MYB
FOXO
ICB
EXON 1
LUC
bim-LUC
ATTGG
AGCTC
X
MYB
FOXO
ICB
EXON 1
LUC
bim-LUC CCAAT (-)

B

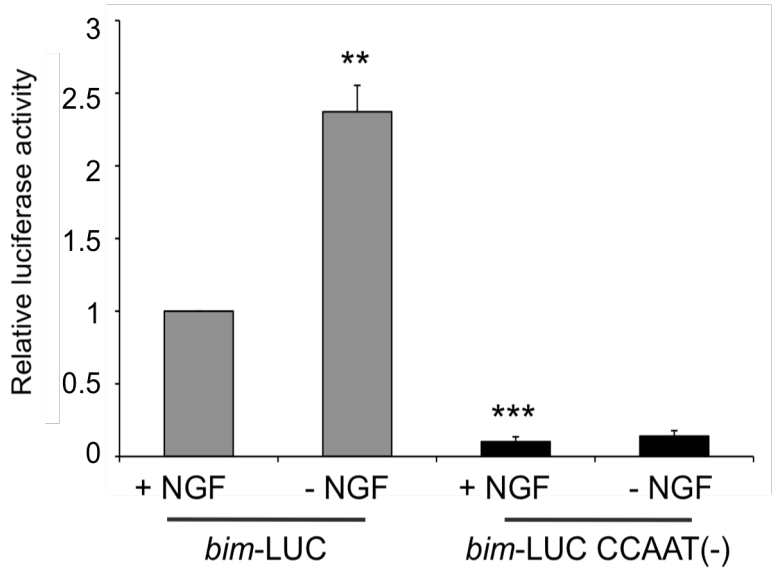
Relative luciferase activity
3
2.5
2
1.5
1
0.5
0
**
***
+ NGF
- NGF
+ NGF
- NGF
bim-LUC
bim-LUC CCAAT(-)

C

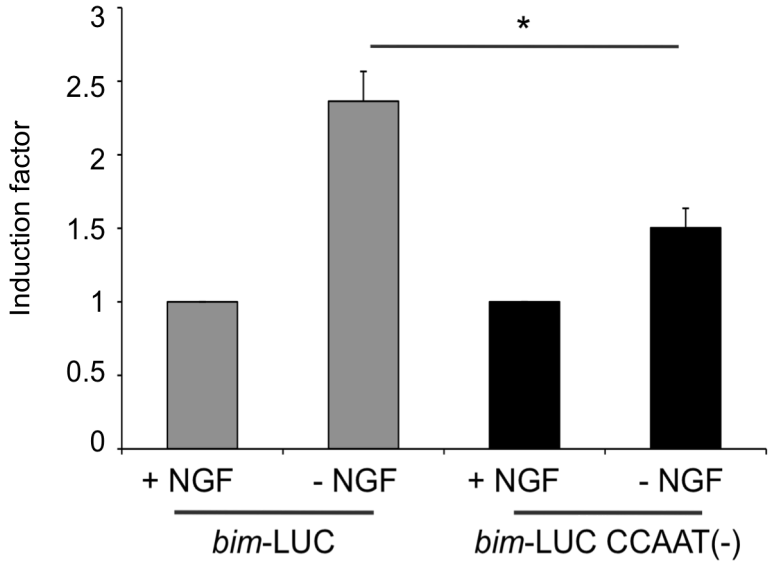
Induction factor
3
2.5
2
1.5
1
0.5
0
*
+ NGF
- NGF
+ NGF
- NGF
bim-LUC
bim-LUC CCAAT(-)

Figure 3.6 NF-Y is required for *bim* promoter activity and its induction following NGF withdrawal.

(A) Immunocytochemistry showing that the NF-YA dominant negative mutant, YA13 m29, localises to the nucleus in microinjected sympathetic neurons. Cells were injected with the YA13 m29 expression vector at 20 ng/μl along with 2.5 μg/μl of guinea pig IgG (gp IgG). After 24 hours, neurons were fixed and then stained with Hoechst dye, to visualise the nuclei, and antibodies to gp IgG (to identify injected cells) and NF-YA (H-209: Sc-10770) to detect YA13 m29. Several experiments were performed and representative images are shown. The bar represents 20 μm.

(B) Co-microinjection of YA13 m29 with *bim*-LUC. Sympathetic neurons were microinjected with *bim*-LUC at 10 ng/μl along with pRL-TK (5 ng/μl), plus YA13 m29 or the control empty vector pSG5 at 20 ng/μl. The cells were maintained in medium containing NGF (+NGF) or withdrawn from NGF (-NGF) for 16 hours, after which time luciferase activity was measured. Microinjection experiments were carried out 4 times and data is presented as the mean ± S.E. *Bim*-LUC is activated significantly following NGF withdrawal when co-injected with pSG5 (**). When *bim*-LUC is co-injected with YA13 m29, there is a significant decrease in basal promoter level (*) and the induction of *bim*-LUC, following NGF withdrawal, is lost.

A

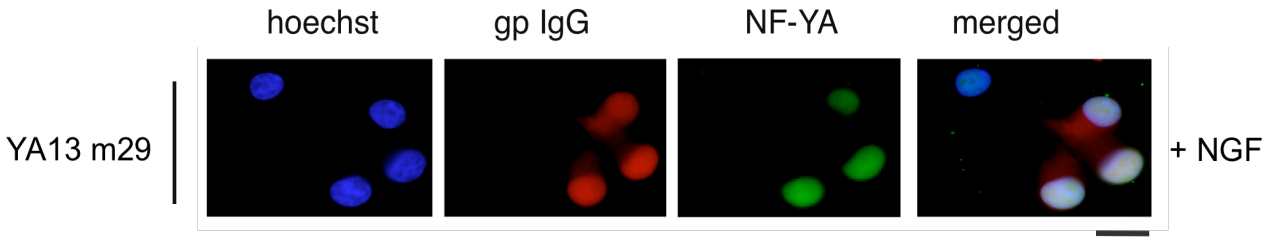
hoechst
gp IgG
NF-YA
merged
YA13 m29
+ NGF

B

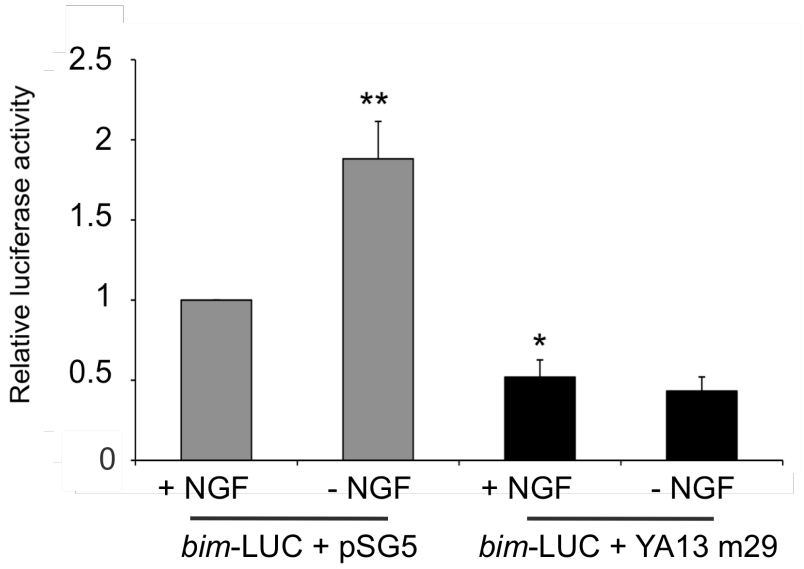
Relative luciferase activity
2.5
2
1.5
1
0.5
0
**
*
+ NGF
- NGF
+ NGF
- NGF
bim-LUC + pSG5
bim-LUC + YA13 m29

3.2.5 NF-Y activity is required for Bim expression and contributes to apoptosis in NGF-deprived sympathetic neurons.

To investigate whether NF-Y activity is required for endogenous Bim expression I studied the effect of YA13 m29 on Bim protein levels (Figure 3.7). Sympathetic neurons were microinjected with the YA13 m29 construct, or the control empty vector pSG5, along with gp IgG as a marker. The injected cells were either maintained in the presence of NGF (+NGF) or withdrawn from NGF (-NGF) for 16 hours after which time the cells were fixed and stained and Bim expression was visualised with an anti-Bim antibody. Bim is present in the cytoplasm at low levels in the presence of NGF, but strongly increases in level following NGF withdrawal (Figure 3.7A). Following NGF deprivation almost 60% of the cells expressed high Bim levels, when injected with the control pSG5 (Figure 3.7B). However, when the cells were injected with the YA13 m29 construct the number of cells expressing high levels of Bim was significantly reduced to 10% (Figure 3.7B). Therefore, when NF-Y activity is inhibited by over-expression of the dominant negative NF-YA subunit, YA13 m29, endogenous Bim expression is markedly reduced.

Finally, to investigate the role of NF-Y in programmed cell death, sympathetic neurons were microinjected with the YA13 m29 construct, or the control pSG5, together with Texas red dextran (as a marker for the injected cells). The neurons were then either maintained in the presence of NGF (+NGF) or withdrawn from NGF (-NGF). Following NGF withdrawal the number of viable injected cells was counted at time 0, 24, 48 and 72 hours. Cells were considered viable if they were morphologically normal and still retained Texas red dextran in the nucleus (Figure 3.8A). Cell death kinetics are shown in Figure 3.8B. There was no significant difference between neurons microinjected with YA13 m29 or pSG5, when the cells were maintained in the presence of NGF, although there was a trend towards more cell death with the YA13 m29 expression vector. Following NGF withdrawal, the number of viable cells injected with the pSG5 control was below 20% at 72 hours, this is consistent with previous studies (Whitfield *et al*., 2001; Gilley *et al*., 2003). Cells that were injected with YA13 m29 were partially protected from cell death at 48 and 72 hours following NGF withdrawal. The number of viable cells injected with YA13 m29 at 72 hours following NGF withdrawal was almost

Figure 3.7 NF-Y activity is required for expression of the endogenous Bim protein.

(A) Immunocytochemistry showing that YA13 m29 reduces Bim expression in microinjected sympathetic neurons. Cells were injected with the YA13 m29 construct or the control empty vector pSG5 at 20 ng/μl along with 2.5 μg/μl of guinea pig IgG (gp IgG). The cells were maintained in medium containing NGF (+NGF) or withdrawn from NGF (-NGF) for 16 hours. Following NGF withdrawal, neurons were fixed and then stained with Hoechst dye, to visualise the nuclei, and antibodies to gp IgG (to identify injected cells) and Bim (Cell Signalling #2819). In the presence of NGF cells either expressed no Bim protein or low levels of Bim protein, whereas following NGF withdrawal many cells expressed high levels of Bim protein. Therefore, cells were scored as no/low Bim staining (comparable to +NGF conditions) or high Bim staining. The orange arrow indicates a sympathetic neuron injected with pSG5 that is expressing high levels of Bim protein. The white arrow indicates a sympathetic neuron injected with YA13 m29 that is expressing low levels of Bim protein. Representative images are shown. The bar represents 20 μm.

(B) Quantitation of immunocytochemistry in Figure 3.7A. Immunocytochemistry experiments were carried out 6 times and data is presented as the mean ± S.E. Microinjection of the YA13 m29 construct significantly decreases Bim expression following NGF withdrawal compared to the control pSG5 (**).

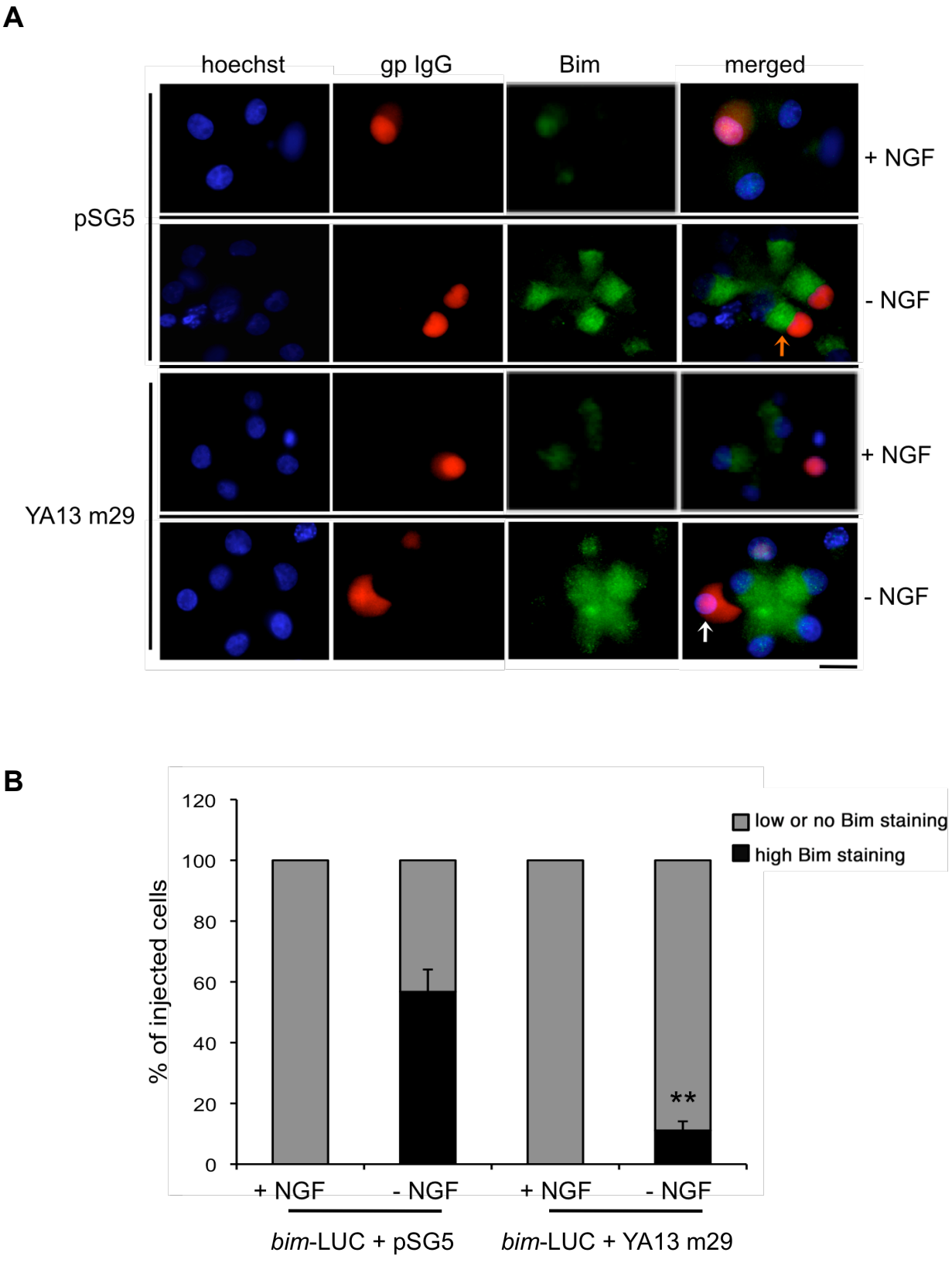
A
hoechst
gp IgG
Bim
merged
pSG5
+ NGF
- NGF
YA13 m29
+ NGF
- NGF
B
120
100
80
60
40
20
0
% of injected cells
low or no Bim staining
high Bim staining
**
+ NGF
- NGF
+ NGF
- NGF
bim-LUC + pSG5
bim-LUC + YA13 m29

2-fold that of the control (Figure 3.8C). This data provides evidence that NF-Y is important for cell death in NGF-deprived sympathetic neurons.

Figure 3.8 NF-Y activity contributes to cell death following NGF withdrawal in sympathetic neurons.

Sympathetic neurons were injected with the YA13 m29 construct or the control empty vector pSG5 at 200 ng/μl, along with 5 μg/μl of Texas red dextran as a marker for injected cells. The cells were maintained in medium containing NGF (+NGF) or withdrawn from NGF (-NGF). Following withdrawal of NGF, the number of viable, morphologically-normal, injected cells was determined at time 0, 24, 48 and 72 hours. Viable cells were counted in a blinded manner.

(A) Examples of sympathetic neurons injected with pSG5, along with Texas red dextran, and either maintained in medium containing NGF (+NGF) or withdrawn from NGF (-NGF) for 48 hours. The bar represents 10 μm.

(B) The number of viable injected cells at time 0, 24, 48 and 72 hours following NGF withdrawal. Cell survival assays were carried out 4 times and data is presented as the mean ± S.E.

(C) The number of viable injected cells at 72 hours following NGF withdrawal (as in Figure 3.8B). Microinjection of the YA13 m29 construct significantly increases the percentage of viable cells at 72 hours -NGF compared to the control pSG5 (*).

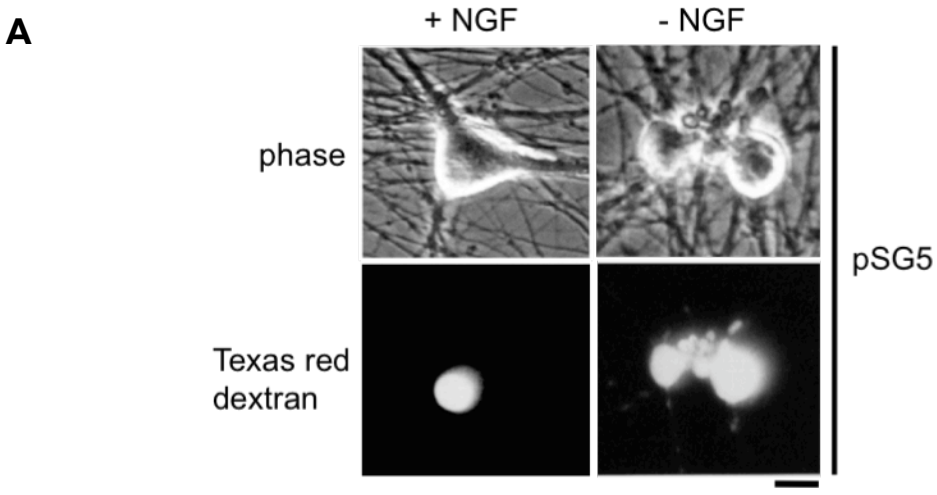

B

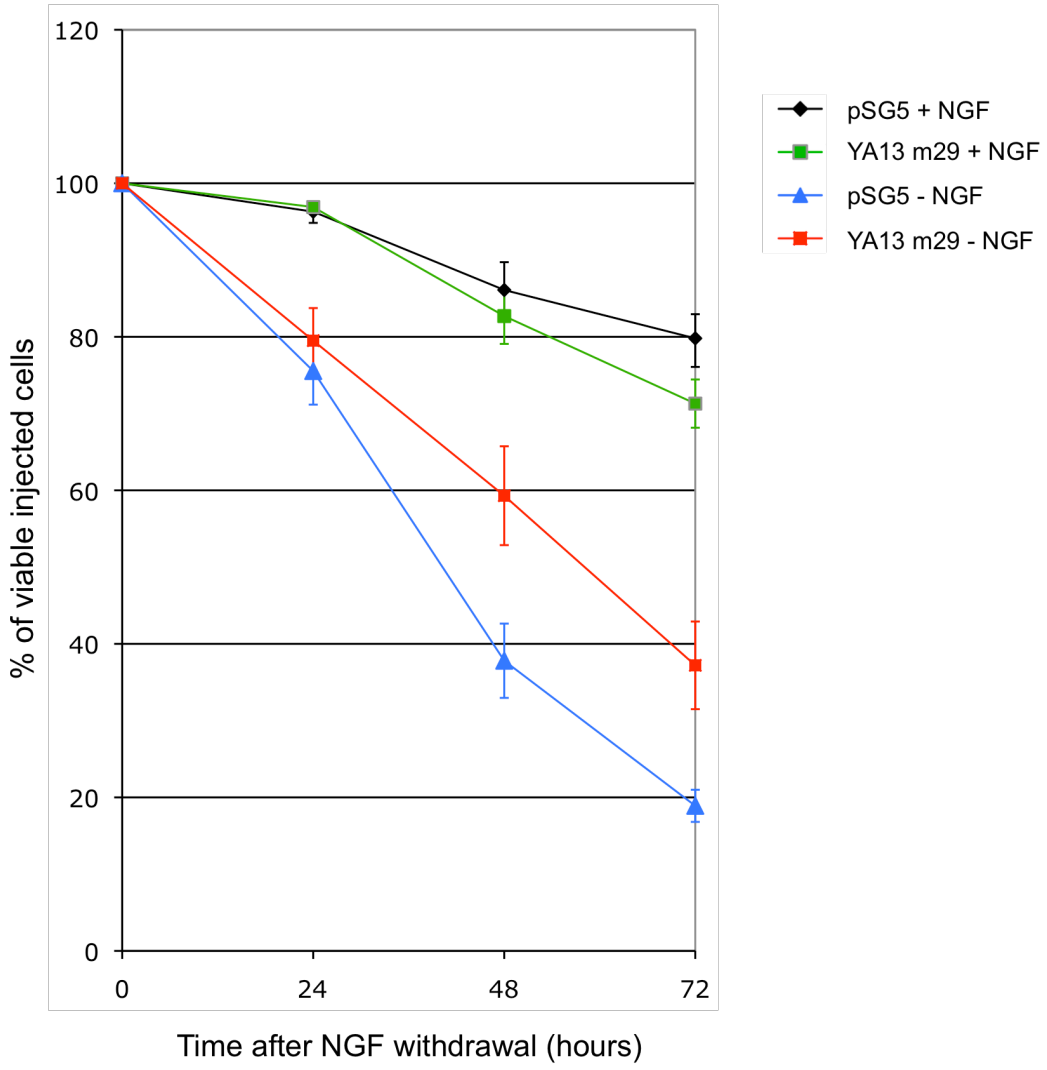
120
100
80
60
40
20
0
% of viable injected cells
0
24
48
72
Time after NGF withdrawal (hours)
pSG5 + NGF
YA13 m29 + NGF
pSG5 - NGF
YA13 m29 - NGF

C

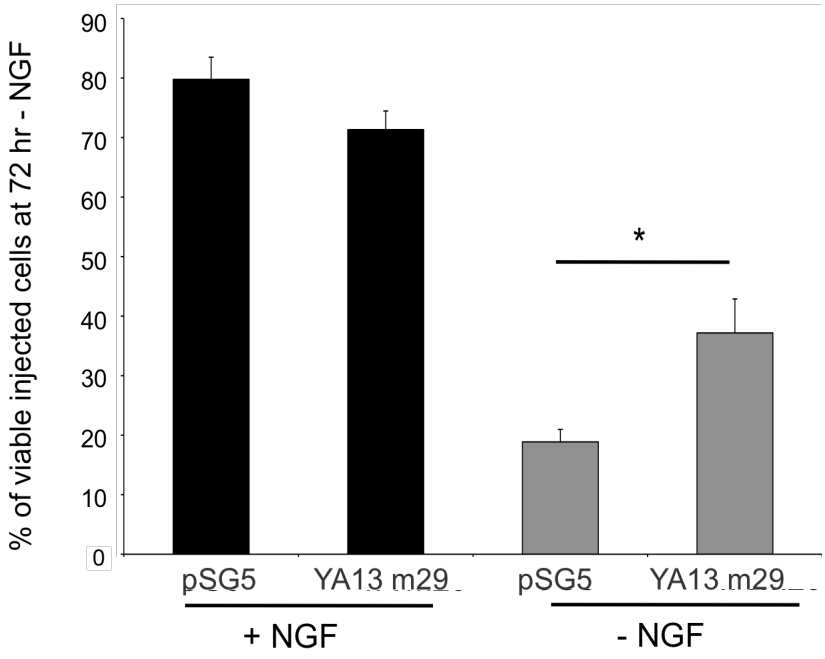
90
80
70
60
50
40
30
20
10
0
% of viable injected cells at 72 hr - NGF
*
pSG5
YA13 m29
pSG5
YA13 m29
+ NGF
- NGF

3.3 Discussion

In sympathetic neurons the level of *bim* RNA increases substantially following NGF withdrawal, reaching a peak at 16 hours minus NGF (Whitfield *et al*., 2001; Gilley *et al*., 2003). I have shown that the *bim* promoter proximal to the major transcriptional start site contains a conserved inverted CCAAT box (ICB) that is bound by the transcription factor NF-Y. To investigate whether the ICB is functionally important, I microinjected sympathetic neurons with a previously characterised *bim*-LUC reporter construct (Gilley *et al*., 2003), and a construct in which the ICB consensus was mutated, *bim*-LUC CCAAT (-). These experiments provide evidence that the ICB is critical, in the context of the *bim*-LUC reporter construct, for the basal function of the rat *bim* promoter. Even though there was an 80% decrease in the basal promoter activity when the ICB was mutated, the *bim* promoter is still functionally active, since in preliminary experiments I found that when I overexpressed constitutively active FOXO3a in the presence of NGF, the *bim*-LUC CCAAT (-) construct was still efficiently activated (*bim*-LUC CCAAT (-): 2.4 fold induction; *bim*-LUC: 2.3 fold induction, n=3, unpublished data). This is the first *bim* promoter element that has been shown to be important for basal promoter function and since the *bim* promoter does not contain a TATA box, it is likely that the NF-Y-binding-ICB plays an important role in pre-initiation complex assembly as reported for other TATA-less promoters (Bellorini *et al*., 1997; Frontini *et al*., 2002; Kabe *et al*., 2005). Also, microinjection experiments showed that the ICB contributes to *bim* activation following NGF withdrawal. Therefore, there are now a number of promoter elements including the ICB, the FOXO sites, the Myb sites and a number of AP1 sites (R. Randall, J. Gilley, R. Hughes and J. Ham, unpublished data) that are important for *bim* activation following NGF withdrawal. Whether these promoter elements somehow cooperate for full activation of *bim* is explored in the next chapter.

The heterotrimeric transcription factor NF-Y has so far been identified as a key regulator of a number of genes, most commonly those involved in the cell cycle (Hu and Maity, 2000; Bhattacharya *et al*., 2003). To establish whether NF-Y activity is required for *bim* promoter function, sympathetic neurons were microinjected with a dominant negative mutant of the NF-YA subunit, YA13 m29 (Mantovani *et al*., 1994). The YA13 m29 expression vector has been used in a number of studies to inhibit NF-Y activity (Su

et al., 2005; Di Agostino *et al*., 2006; Xu *et al*., 2006; Benatti *et al*., 2008). The YA13 m29 construct was co-microinjected into sympathetic neurons where it significantly decreased *bim* basal promoter activity. Furthermore, expression of YA13 m29 completely abolished activation of our *bim*-LUC reporter construct following NGF withdrawal. It is interesting that when NF-Y activity is inhibited, the induction of *bim*-LUC following NGF deprivation is completely lost, whereas mutating the ICB, in the context of *bim*-LUC, simply reduces the fold activation of the construct. Around 30% of eukaryotic promoters harbour CCAAT box elements in their promoters and it is likely that many of these bind NF-Y (Bucher 1990; Mantovani 1999). Therefore, expression of YA13 m29 could affect any NF-Y-binding CCAAT boxes located in other genes that are activated following NGF withdrawal and there may even be additional CCAAT boxes in the *bim* gene, located outside of the proximal promoter.

In addition to the effect on the *bim*-LUC reporter construct, YA13 m29 expression almost completely inhibits Bim protein expression following NGF withdrawal. Therefore, NF-Y activity is critical for endogenous Bim expression in sympathetic neurons. Importantly, expression of YA13 m29 partially protects sympathetic neurons from NGF-withdrawal induced apoptosis. The level of protection seen by inhibiting NF-Y activity is similar to the effect of a complete *bim* knockout on neuronal survival. Whitfield *et al*. (2001) isolated sensory neurons from $bim^{-/-}$ mice and at 48 hours after NGF deprivation only 10% of the wild type cells were viable, compared to almost 40% of the $bim^{-/-}$ cells. Additionally, Coultas *et al*. (2007) isolated sympathetic neurons from $bim^{-/-}$ mice and they found that the number of viable cells following NGF deprivation corroborated this data. Here, inhibition of NF-Y activity almost entirely reproduces this effect, with almost 40% of cells surviving at 72 hours following NGF withdrawal. This partial protection is probably due to the fact that the other BH3-only proteins that increase in level after NGF withdrawal, Puma and DP5, can partially compensate for the loss of Bim (Putcha and Johnson 2004; Ham *et al*., 2005). This idea is supported by the observation that knockout of the *puma* gene alone has a similar effect to the loss of Bim (Wyttenbach and Tolkovsky, 2006). Importantly, my data indicates that NF-Y is a significant regulator of apoptosis in sympathetic neurons.

Interestingly, ChIP experiments showed that NF-Y is bound to the *bim* promoter in the presence of NGF and following NGF withdrawal, with no apparent change in binding affinity for the ICB. This suggests that NF-Y may activate the transcription of *bim* by recruiting other DNA binding transcription factors or transcriptional co-factors that are regulated by NGF. For example, following withdrawal of NGF, FOXO3a translocates from the cytoplasm into the nucleus and binds to the two conserved FOXO sites (Fig 3.9; Gilley *et al*., 2003). This hypothesis will be addressed in the next chapter.

Inhibition of NF-Y activity reproduces the loss of *bim* activation that is observed, following NGF withdrawal, when the two conserved FOXO sites or the two Myb sites are mutated (Gilley *et al*., 2003; Biswas *et al*., 2005). In addition, the overexpression of a dominant negative c-Jun protein and the mutation of a number of AP1 sites in the *bim* promoter also abolish the activation of *bim* following NGF withdrawal (Whitfield *et al*., 2001; Randall *et al*., unpublished data). Taken together, these findings indicate that each of the promoter elements and their transcriptional activators are necessary, but not sufficient, for the activation of *bim* in neurons. Activation of individual pathways is sufficient for *bim* induction, but under physiological conditions, following NGF withdrawal, induction of multiple proapoptotic pathways appears to be essential. For example, when *bim* expression is induced following the inhibition of PI3-K activity (resulting in FOXO activation), or by the overexpression of Mybs, *bim* levels are considerably less than that following NGF withdrawal (Gilley *et al*., 2003; Biswas *et al*., 2005). The lack of redundancy that is displayed between activating pathways is yet another means by which *bim* expression is stringently regulated in neurons.

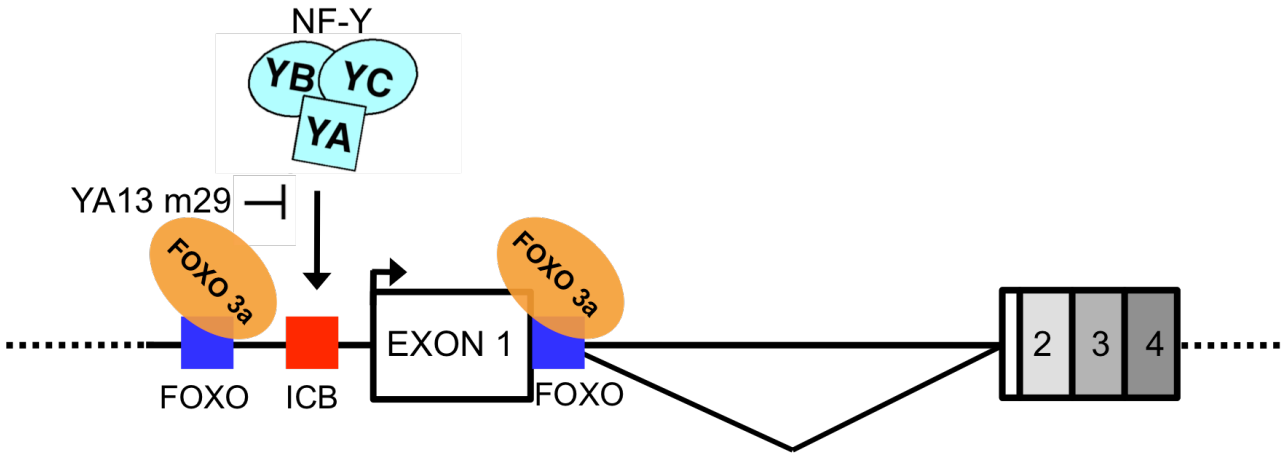

Figure 3.9 Model of the transcriptional activation of the *bim* promoter in sympathetic neurons.

The transcription factors that bind to the *bim* proximal promoter in sympathetic neurons. The NF-Y trimer is bound to the ICB. However, this can be inhibited by the dominant negative mutant YA13 m29. Following NGF withdrawal, FOXO3a translocates into the nucleus and binds to the two FOXO sites, thereby contributing to activation of *bim* transcription (Gilley *et al*., 2003). Loss of NF-Y activity inhibits activation of *bim* transcription following NGF withdrawal and partially protects sympathetic neurons against cell death.

Chapter 4: The role of CBP/p300 in activating *bim* gene expression in sympathetic neurons.

4.1 Introduction

Transcriptional control of *bim* involves at least three signalling pathways in sympathetic neurons. The prosurvival PI3-K/Akt pathway inhibits *bim* transcription in the presence of NGF by phosphorylating FOXO3a and thereby preventing its nuclear translocation (Gilley *et al*., 2003). The proapoptotic JNK/c-Jun pathway also activates *bim* transcription following NGF withdrawal although the precise mechanism remains to be established (Harris and Johnson, 2001; Whitfield *et al*., 2001; Besirli *et al*., 2005). In addition the CDK4/Rb/E2F/Myb pathway contributes to *bim* activation following NGF deprivation (Biswas *et al*., 2005). Finally, in the previous chapter I identified an inverted CCAAT box (ICB) in the *bim* proximal promoter that is bound by the transcription factor NF-Y. I found that the NF-Y-binding-CCAAT box is essential for *bim* basal promoter activity and expression of the YA13 m29 mutant protein inhibits activation of *bim* transcription and reduces Bim protein expression following NGF withdrawal. Thus, inhibition of NF-Y activity increased survival of NGF-deprived sympathetic neurons. It is clear that NF-Y is necessary for *bim* activation following NGF withdrawal, but the mechanism by which NF-Y functions, and is regulated in this context, has yet to be elucidated, since NF-Y is bound to the ICB in the presence and absence of NGF.

The transcriptional activation of a promoter can require the assembly of a number of regulatory multiprotein complexes, often involving the global transcriptional coactivators CBP/p300. CREB-binding protein (CBP) and p300 are two distinct but highly homologous proteins that play a critical role in the transcriptional activation of a multitude of target genes. Studies have shown that p300 and CBP perform overlapping and unique functions. Mice completely lacking p300 or CBP and mice with one null *p300* allele and one null *cbp* allele die during embryogenesis (Yao *et al*., 1998; Tanaka *et al*., 2000). This suggests that the total amount of p300 and CBP is important during development and that p300 and CBP are present in the cell at limiting concentrations. Therefore a relatively small decrease in the concentration of CBP/p300 can be

deleterious, for example in the human Rubinstein-Taybi syndrome where loss of one *cbp* allele results in developmental defects (Petrij *et al*., 1995). In addition to this, it is apparent that CBP and p300 have unique cellular functions in some systems. For example, $cbp^{+/-}$ mice show a number of multilineage defects in haematopoietic differentiation, which are not found in $p300^{+/-}$ mice (Kung *et al*., 2000; Kasper *et al*., 2006). CBP/p300 have been implicated in a wide range of cellular processes such as proliferation and cell cycle control (Giles *et al*., 1998; Goodman and Smolik, 2000). Studies have also highlighted the importance of CBP/p300 in programmed cell death, with an emphasis on p53-dependent apoptosis. For example, the expression of the adenovirus E1A oncoprotein, which targets CBP/p300, or the expression of a dominant-negative version of p300, inhibits p53-dependent apoptosis (Avantaggiati *et al*., 1997; Gu *et al*., 1997). Furthermore, a number of reports have described *p300* and *cbp* as tumour suppressor genes, and the disruption of either *p300* or *cbp* is associated with a range of human malignancies from leukaemias to solid tumours (Iyer *et al*., 2004).

CBP and p300 are universal transcriptional coactivators. They can interact with over 350 viral and mammalian proteins of which 196 are encoded by essential genes in mice (Kasper *et al*., 2006). For instance, CBP/p300 can interact with c-Jun and the Myb proteins (Lee *et al*., 1996; Giordano and Avantaggiati, 1999; Bessa *et al*., 2001). CBP/p300 stimulate target gene expression, following their recruitment to promoters by DNA binding transcription factors, through a number of different mechanisms. They can act as a 'bridge' to connect sequence-specific transcription factors to the basal transcription machinery (Shikama *et al*., 1997; Chan and La Thangue, 2001). The large size of CBP and p300 allows multiple proteins to bind to them simultaneously, thereby facilitating their role as a 'scaffold' for different components of a transcriptional multi-protein complex. A well-characterised example is the interferon-beta (IFN-β) enhanceosome. Here, regulatory proteins including c-Jun/ATF-2 and NF_kB are recruited to the *IFN-β* promoter where they create a stereospecific interaction surface for the recruitment of CBP/p300 and the basal transcription machinery (Kim *et al*., 1998; Merika *et al*., 1998; Wathelet *et al*., 1998; Yie *et al*., 1999). The formation of this stable complex promotes pre-initiation complex formation and allows multiple rounds of transcription to proceed (Kim *et al*., 1998; Merika *et al*., 1998; Wathelet *et al*., 1998; Yie *et al*., 1999).

Thirdly, CBP/p300 possess intrinsic histone acetyltransferase (HAT) activity, thereby linking transcription and chromatin remodelling. CBP/p300 can acetylate the four core histones (Bannister and Kouzarides, 1996; Ogryzko *et al*., 1996; Das *et al*., 2009), but in addition to chromatin it seems that the major targets of acetylation by CBP/p300 are transcription factors (Li *et al*., 1998; Martinez-Balbas *et al*., 1998; Shikama *et al*., 2000). The list of transcription factors known to be acetylated by CBP/p300 is expanding and it has been shown that acetylation usually increases the DNA binding activity of the target protein (Soutogloou *et al*., 2000; Inoue *et al*., 2007). For example, NF-Y can recruit p300 and is itself a target for acetylation by the coactivator (Faniello *et al*., 1999; Li *et al*., 1998). FOXO3a can also interact with p300 and is acetylated by p300, but only when FOXO3a is in a dephosphorylated state (Mahmud *et al*., 2002; Perrot and Rechler, 2005).

CBP and p300 play a critical role as integrators of multiple signal transduction pathways within the nucleus, yet relatively little is understood concerning their regulation. CBP/p300 are phosphoproteins and their phosphorylation appears to be under the control of the cell cycle, also both proteins contain protein kinase A (PKA) sites that contribute to their regulation (Yang *et al*., 1996; Perkins *et al*., 1997; Ait-Si-Ali *et al*., 1998; Xu *et al*., 1998). More recent findings have suggested that CBP/p300 become hyper-phosphorylated upon cellular stress, for example under hypoxic conditions (Zakrzewska *et al*., 2005).

CBP/p300 can activate the transcription of a multitude of target genes. Since they can interact with the different regulatory factors, Myb, c-Jun, NF-Y and FOXO3a, that govern *bim* promoter activation, I was interested to establish whether they are important for *bim* activation following NGF withdrawal in sympathetic neurons.

4.2 Results

4.2.1 CBP and p300 are localised to the nucleus of sympathetic neurons in the presence of NGF and following NGF withdrawal.

To investigate if CBP and p300 are important for activation of the *bim* promoter, I first had to confirm that they are expressed in sympathetic neurons. I carried out immunocytochemistry experiments on sympathetic neurons that were either maintained in the presence of NGF or deprived of NGF for 16 hours. CBP and p300 localise to the nucleus of sympathetic neurons where they stained brightly in the presence of NGF and following NGF withdrawal with no apparent change in expression level (Figure 4.1A and B). Approximately 95% of sympathetic neurons expressed high levels of CBP and p300 (in +NGF and -NGF conditions). CBP and p300 were not present in the nucleolus of sympathetic neurons (Figure 4.1A and B). This staining pattern was also observed by Mikecz *et al*. (2000) who used the same p300 (C-20: Sc-585) and CBP (C-20: Sc-583) antibodies to study the co-localisation of CBP and p300 at RNA polymerase II-rich sites within the nucleus of different cell lines and found that nuclear substructure localisation of CBP/p300 is restricted to PML (promyelocytic leukaemia) protein-containing domains (Mikecz *et al*., 2000).

I also carried out some control immunocytochemistry experiments using sympathetic neurons to confirm that in the absence of a primary antibody (secondary-only control) there was no specific staining (Figure 4.1C). This is an important experiment as I have used the same FITC-conjugated secondary antibody for all immunocytochemistry experiments in this study.

4.2.2 The ICB is required for activation of the *bim* promoter by p300.

I have hypothesised that for efficient activation of the *bim* promoter the coactivators CBP and/or p300 may be required. Furthermore, studies with p300 and CBP knockout mice have suggested that p300 and CBP are present at limiting concentrations in cells (Yao *et al*., 1998; Tanaka *et al*., 2000). Therefore, if my hypothesis is correct, overexpression of p300 or CBP should activate the *bim* promoter. Sympathetic neurons were co-microinjected with pRc/RSV-mCBP or the control empty vector pBJ9Ω, or CMVp300 or

Figure 4.1 CBP and p300 are expressed in sympathetic neurons.

(A) Immunocytochemistry showing that CBP is expressed in sympathetic neurons where it localises to the nucleus. Neurons were maintained in medium containing NGF (+NGF) or withdrawn from NGF (-NGF) for 16 hours, after which time the cells were fixed and then stained with Hoechst dye, to visualise the nuclei, and an antibody to CBP (C-20: Sc-583).

(B) Immunocytochemistry showing that p300 is expressed in sympathetic neurons where it localises to the nucleus. Neurons were maintained in medium containing NGF (+NGF) or withdrawn from NGF (-NGF) for 16 hours, after which time the cells were fixed and then stained with Hoechst dye, to visualise the nuclei, and an antibody to p300 (C-20: Sc-585).

(C) Immunocytochemistry control showing that there is no specific staining observed in the absence of a primary antibody. Neurons were maintained in medium containing NGF (+NGF) and then fixed and stained with Hoechst dye, to visualise the nuclei, and a secondary antibody without the prior addition of a primary antibody.

Several experiments were performed in each case and representative images are shown. The bar represents 20 μm.

A

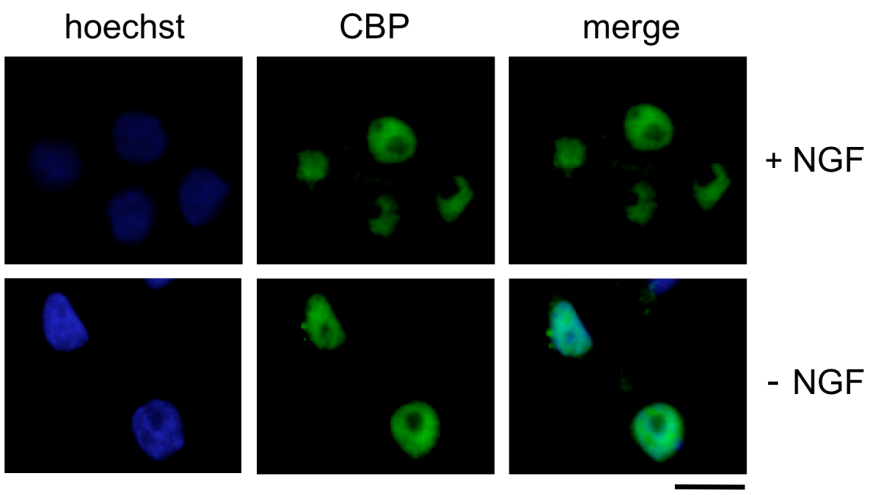
hoechst
CBP
merge
+ NGF
- NGF

B

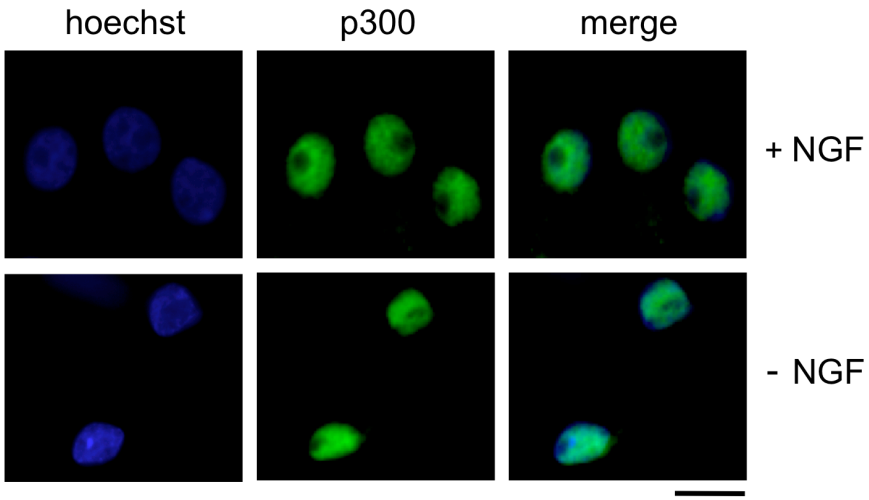
hoechst
p300
merge
+ NGF
- NGF

C

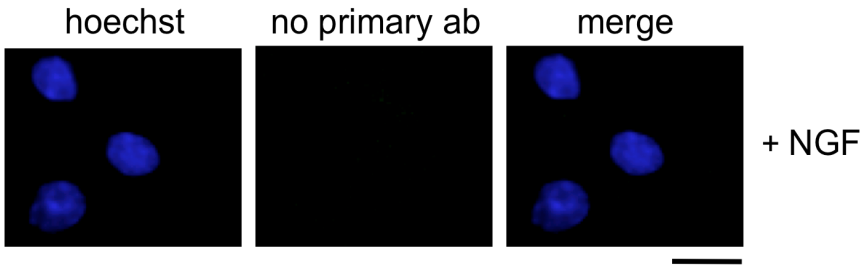
hoechst
no primary ab
merge
+ NGF

the control empty vector pcDNA3.1, together with the *bim*-LUC reporter construct (Figure 4.2A). *Bim*-LUC was significantly activated by overexpression of CBP or p300 (Figure 4.2A). To determine if the inverted CCAAT box (ICB) in the *bim* promoter, studied in Chapter 3, is important for activation of *bim* by CBP/p300, sympathetic neurons were co-microinjected with CMVp300, or the control empty vector pcDNA3.1, along with the *bim*-LUC CCAAT (-) construct (Figure 4.2B). Overexpression of p300 did not activate *bim*-LUC CCAAT (-) (Figure 4.2B). Therefore, the ICB must be intact for p300 to activate the *bim*-LUC reporter construct.

4.2.3 CBP and p300 are important for activation of the *bim* promoter in sympathetic neurons.

It has been demonstrated previously that the microinjection of specific antibodies can be used as a suitable alternative to conventional protein knockdown techniques (Arias *et al*., 1994; Towers *et al*., 2009). I co-injected antibodies specific to p300 or CBP together with the *bim*-LUC reporter construct to determine whether CBP or p300 are required for *bim* promoter activation (Figure 4.3). *Bim*-LUC was not significantly activated following NGF withdrawal when antibodies against p300 or CBP were co-injected, compared to the control rabbit IgG. This suggests that both p300 and CBP are important for efficient activation of the *bim* promoter following NGF withdrawal in sympathetic neurons.

4.2.4 Binding of CBP and p300 to the *bim* promoter increases after NGF withdrawal.

To confirm that p300 and CBP can bind to the endogenous *bim* promoter, I performed some chromatin immunoprecipitation (ChIP) assays using the p300 and CBP antibodies that had been used in antibody co-injection experiments, along with antibodies against MyoD and Bim as negative controls. PC6-3 cells were differentiated in the presence of NGF for 7 days and then either maintained in the presence of NGF (+NGF) or withdrawn from NGF (-NGF) for 16 hours. The binding of p300 or CBP to the *bim* proximal promoter was studied by PCR amplification of the immunoprecipitated chromatin samples (Figure 4.4). The PCR primers previously used to study the binding of NF-Y to the ICB were also used for p300 and CBP: they amplify a 331 base pair region of the *bim*

Figure 4.2 The ICB is required for activation of the *bim* promoter by p300.

(A) Co-microinjection of CMVp300 or pRc/RSV-mCBP with *bim*-LUC. Sympathetic neurons were microinjected with *bim*-LUC at 10 ng/µl and pRL-TK at 5 ng/µl, along with CMVp300 or the control empty vector pcDNA3.1 at 50 ng/µl, or pRc/RSV-mCBP or the control empty vector pBJ9Ω at 50 ng/µl. Following injection the cells were maintained in medium containing NGF overnight, after which time luciferase activity was measured. Microinjection experiments were carried out 4 times and data is presented as the mean ± S.E. Co-microinjection of CMVp300 induces a significant activation of *bim*-LUC (**). Co-microinjection of pRc/RSV-mCBP also induces a significant activation of *bim*-LUC (*).

(B) Co-microinjection of CMVp300 with *bim*-LUC or *bim*-LUC CCAAT(-). Sympathetic neurons were microinjected with *bim*-LUC or *bim*-LUC CCAAT (-) at 10 ng/µl and pRL-TK at 5 ng/µl, along with CMVp300 or the control empty vector pcDNA3.1 at 50 ng/µl. Following injection the cells were maintained in medium containing NGF overnight, after which time luciferase activity was measured. Microinjection experiments were carried out 5 times and data is presented as the mean ± S.E. Co-microinjection of CMVp300 induces a significant activation of *bim*-LUC (**). Co-microinjection of CMVp300 does not activate *bim*-LUC CCAAT (-). As shown previously (Figure 3.4), bim-LUC CCAAT (-) has a significantly lower basal promoter level compared to *bim*-LUC (***).

A

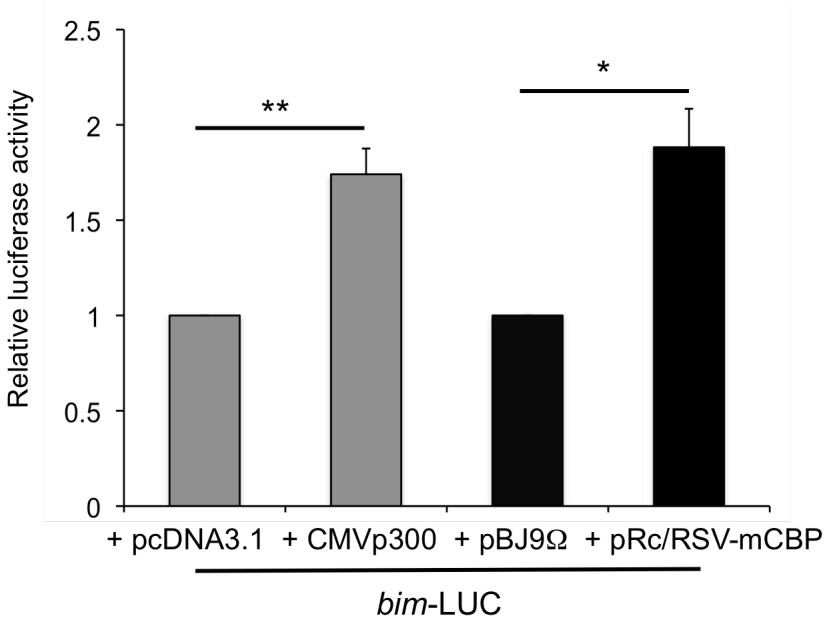
Relative luciferase activity
2.5
2
1.5
1
0.5
0
**
*
+ pcDNA3.1
+ CMVp300
+ pBJ9Ω
+ pRc/RSV-mCBP
bim-LUC

B

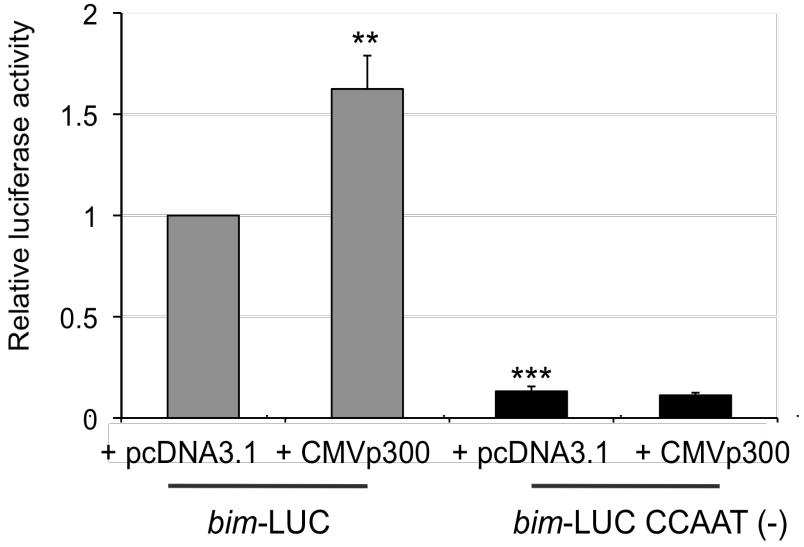
Relative luciferase activity
2
1.5
1
0.5
0
**
***
+ pcDNA3.1
+ CMVp300
+ pcDNA3.1
+ CMVp300
bim-LUC
bim-LUC CCAAT (-)

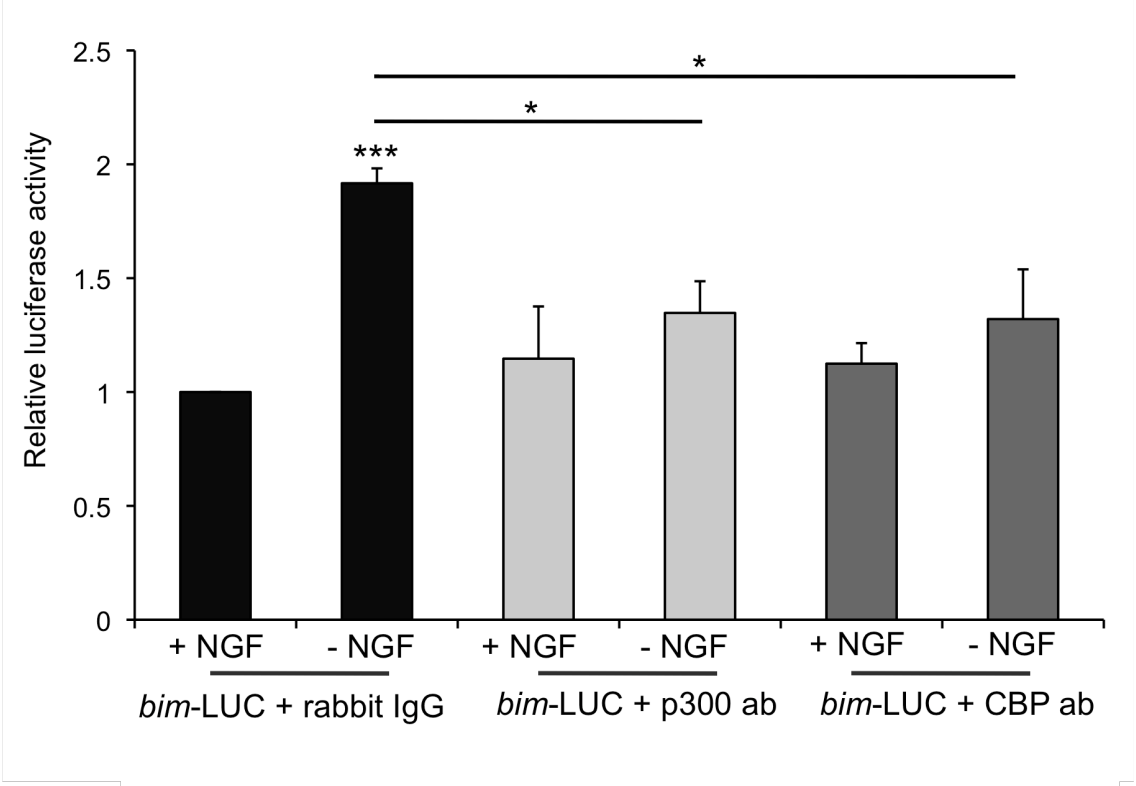

Figure 4.3 CBP and p300 are required for efficient activation of *bim*-LUC following NGF withdrawal.

Co-injection of p300 or CBP antibodies with *bim*-LUC. Sympathetic neurons were microinjected with *bim*-LUC at 10 ng/µl and pRL-TK at 5 ng/µl, together with the p300 (C-20: Sc-585 X) or CBP (C-20: Sc-583 X) antibodies or rabbit IgG as a control, each at 1 µg/µl. The cells were maintained in medium containing NGF (+NGF) or withdrawn from NGF (-NGF) for 16 hours, after which time luciferase activity was measured. Microinjection experiments were carried out 6 times and data is presented as the mean ± S.E. *Bim*-LUC is activated significantly following NGF withdrawal when co-injected with rabbit IgG (***). *Bim*-LUC is not activated significantly when co-injected with the p300 and CBP antibodies. There is a significant decrease in the induction of *bim*-LUC following NGF withdrawal when co-injected with the p300 antibody (*) and the CBP antibody (*), compared to the control rabbit IgG.

proximal promoter that includes the ICB (Figure 3.3A). The negative control antibodies, MyoD and Bim, immunoprecipitated background levels of *bim* promoter chromatin in the presence and absence of NGF. In the presence of NGF, there was some binding of p300 and CBP to the *bim* promoter but this was significantly enriched following NGF withdrawal (Figure 4.4A and B). Therefore, p300 and CBP are bound to the same region of the *bim* promoter as NF-Y and the affinity of this interaction increases following NGF withdrawal. Since the coactivators CBP and p300 do not contact the DNA directly, they must bind via proteins that are already bound to the *bim* promoter. We already know that mutation of the ICB abolishes the activation of the *bim*-LUC reporter by p300 (Figure 4.2) and that NF-Y is bound to the *bim* promoter in the presence and absence of NGF (Figure 3.3). Taken together, this data suggests that CBP/p300 may activate the *bim* promoter through protein-protein interactions with NF-Y bound to the ICB.

4.2.5 NF-Y can bind to CBP/p300 in the presence of NGF or following NGF withdrawal.

To confirm that NF-Y interacts with CBP/p300 in extracts from NGF-dependent cells, some co-immunoprecipitation (Co-IP) experiments were carried out (Figure 4.5). These were performed by Dr. Mark Kristiansen in our group. Nuclear extracts were prepared from PC6-3 cells differentiated in the presence of NGF for 7 days and then either maintained in the presence of NGF (+NGF) or withdrawn from NGF (-NGF) for 16 hours. Initially, +NGF and -NGF nuclear extracts were immunoprecipitated with antibodies against p300, CBP, NF-YA or rabbit IgG. Immunoblots were then carried out using an antibody against NF-YA (Figure 4.5A). There was a large amount of NF-YA protein detected in the input control lanes and with the immunoprecipitate from the NF-YA antibody. However, there was also NF-YA protein precipitated with antibodies against p300 and CBP, compared to the control rabbit IgG (Figure 4.5A). The experiment was then repeated by immunoprecipitating nuclear extracts with p300, CBP, NF-YA or rabbit IgG and then immunoblotting with antibodies against p300 or CBP (Figure 4.5B). There was a considerable amount of p300 or CBP protein present in the input control samples and this was easily detected in the immunoprecipitates from p300 or CBP, respectively. However, there was also p300 and CBP protein precipitated with

Figure 4.4 The binding of CBP and p300 to the *bim* promoter increases after NGF withdrawal.

(A) PC6-3 cells were differentiated in the presence of NGF for 7 days. The neuronally differentiated cells were then either maintained in the presence of NGF (+NGF) or withdrawn from NGF (-NGF) for 16 hours. After 16 hours, the cells were cross-linked with 1% formaldehyde and chromatin immunoprecipitations were performed using the p300 (C-20: Sc-585 X) or CBP (C-20: Sc-583 X) antibodies. Negative control reactions were carried out with a Bim (AB17003) antibody and a MyoD (M-318: Sc-760 X) antibody, respectively. ChIP samples were analysed by semi-quantitative PCR and a representative image is shown. The 1Kb+ DNA ladder was used as a molecular weight marker.

(C) PCR was quantitated at 28 cycles and the average amount of *bim* promoter DNA, precipitated by each antibody, was calculated. ChIP was performed 3 times and data is presented as the mean ± S.E. There is a significant increase in the amount of *bim* promoter DNA precipitated by the p300 (**) and the CBP (*) antibodies following NGF withdrawal (-NGF), compared to in the presence of NGF (+NGF).

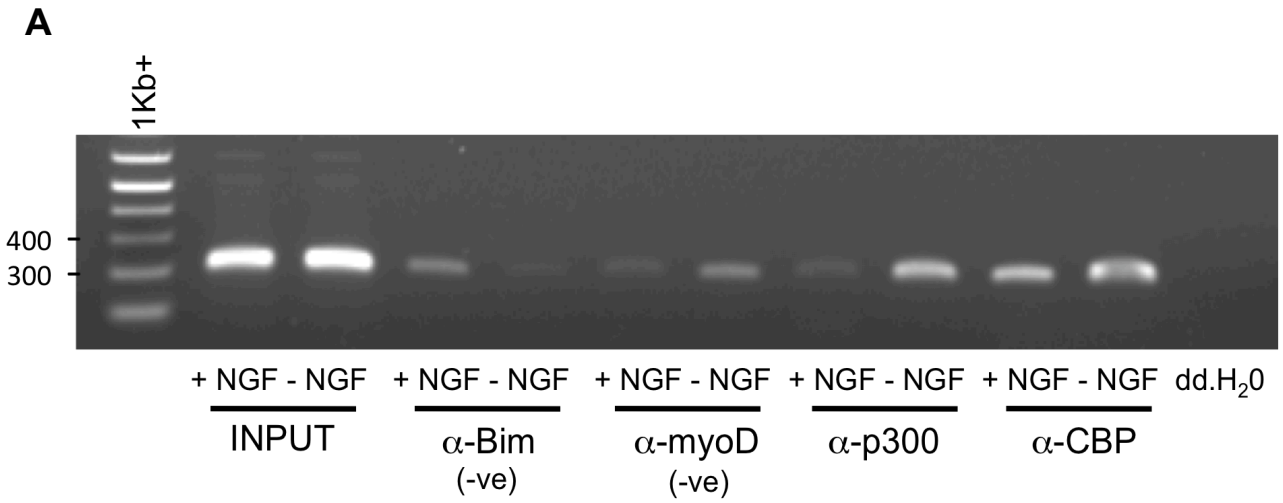
A
1Kb+
400
300
+ NGF - NGF
+ NGF - NGF
+ NGF - NGF
+ NGF - NGF
+ NGF - NGF
dd.H20
INPUT
α-Bim
(-ve)
α-myoD
(-ve)
α-p300
α-CBP

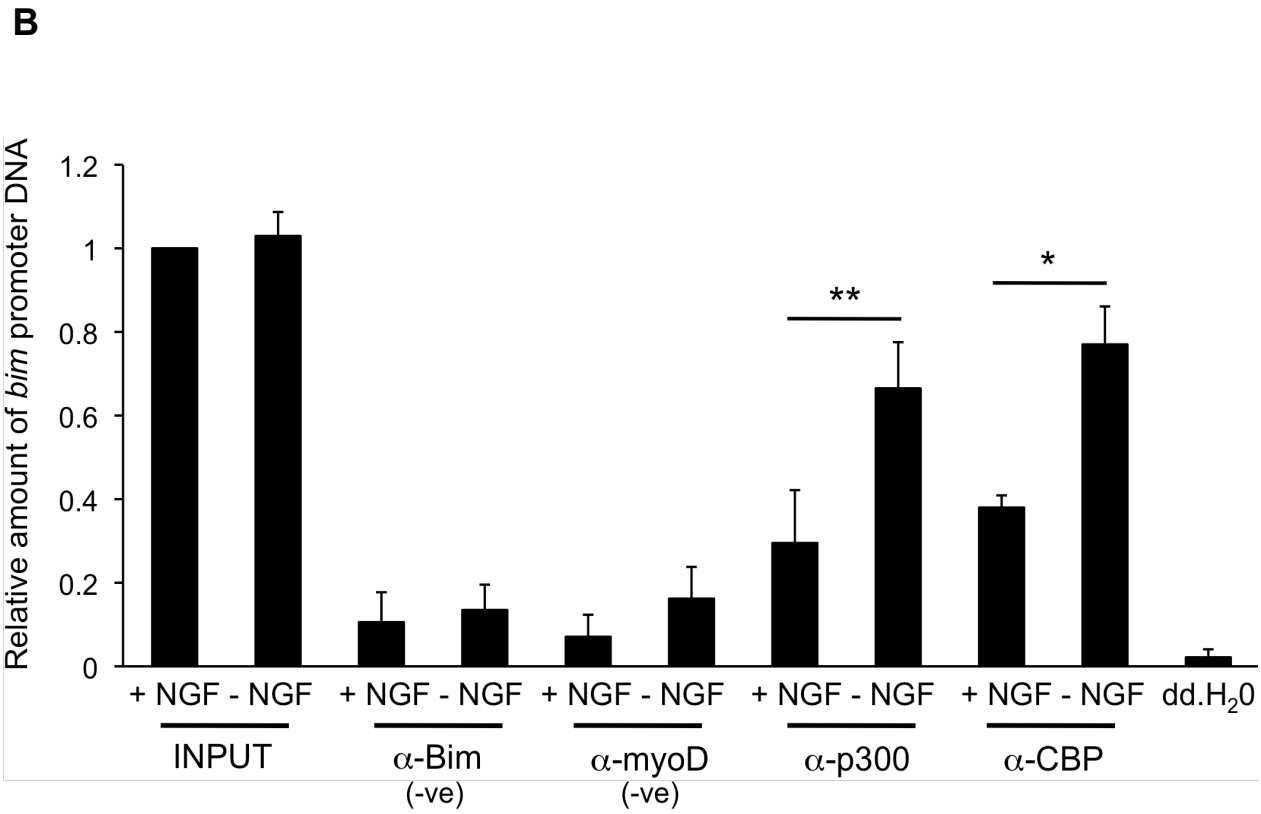
B
Relative amount of bim promoter DNA
1.2
1
0.8
0.6
0.4
0.2
0
**
*
+ NGF - NGF
+ NGF - NGF
+ NGF - NGF
+ NGF - NGF
+ NGF - NGF
dd.H20
INPUT
α-Bim
(-ve)
α-myoD
(-ve)
α-p300
α-CBP

the NF-YA antibody, compared to the control rabbit IgG (Figure 4.5B). There also appears to be a modest increase in the affinity of p300 and CBP for NF-Y and of NF-Y for p300 and CBP following NGF withdrawal (Figure 4.5A and B). These results demonstrate that NF-Y interacts with CBP and p300 *in vitro* in the presence of NGF and following NGF withdrawal.

Figure 4.5 NF-Y can bind to CBP/p300 in the presence of NGF or following NGF withdrawal.

(A) Co-immunoprecipitation of NF-Y with antibodies against p300 and CBP, respectively. Nuclear extracts were prepared from PC6-3 cells differentiated in the presence of NGF for 7 days and then either maintained in the presence of NGF (+NGF) or withdrawn from NGF (-NGF) for 16 hours. The nuclear extracts were immunoprecipitated with antibodies against p300 (C-20: Sc-585), CBP (C-20: Sc-583), NF-YA (H-209: Sc-10779) or rabbit IgG. Immunoblots were then carried out on the precipitated samples using an antibody against NF-YA (H-209: Sc-10779). Total ERK1/2 was used as a loading control (ERK1/2 antibody from Cell Signalling #9102). Several experiments were performed and representative blots are shown.

(B) Co-immunoprecipitation of p300 and CBP with an antibody against NF-Y. Nuclear extracts were prepared from PC6-3 cells differentiated in the presence of NGF for 7 days and then either maintained in the presence of NGF (+NGF) or withdrawn from NGF (-NGF) for 16 hours. The nuclear extracts were immunoprecipitated with antibodies against p300 (C-20: Sc-585), CBP (C-20: Sc-583), NF-YA (H-209: Sc-10779) or rabbit IgG. Immunoblots were then carried out on the precipitated samples using an antibody against p300 (C-20: Sc-585) or CBP (C-20: Sc-583), respectively. Total ERK1/2 was used as a loading control (ERK1/2 antibody from Cell Signalling #9102). Several experiments were performed and representative blots are shown.

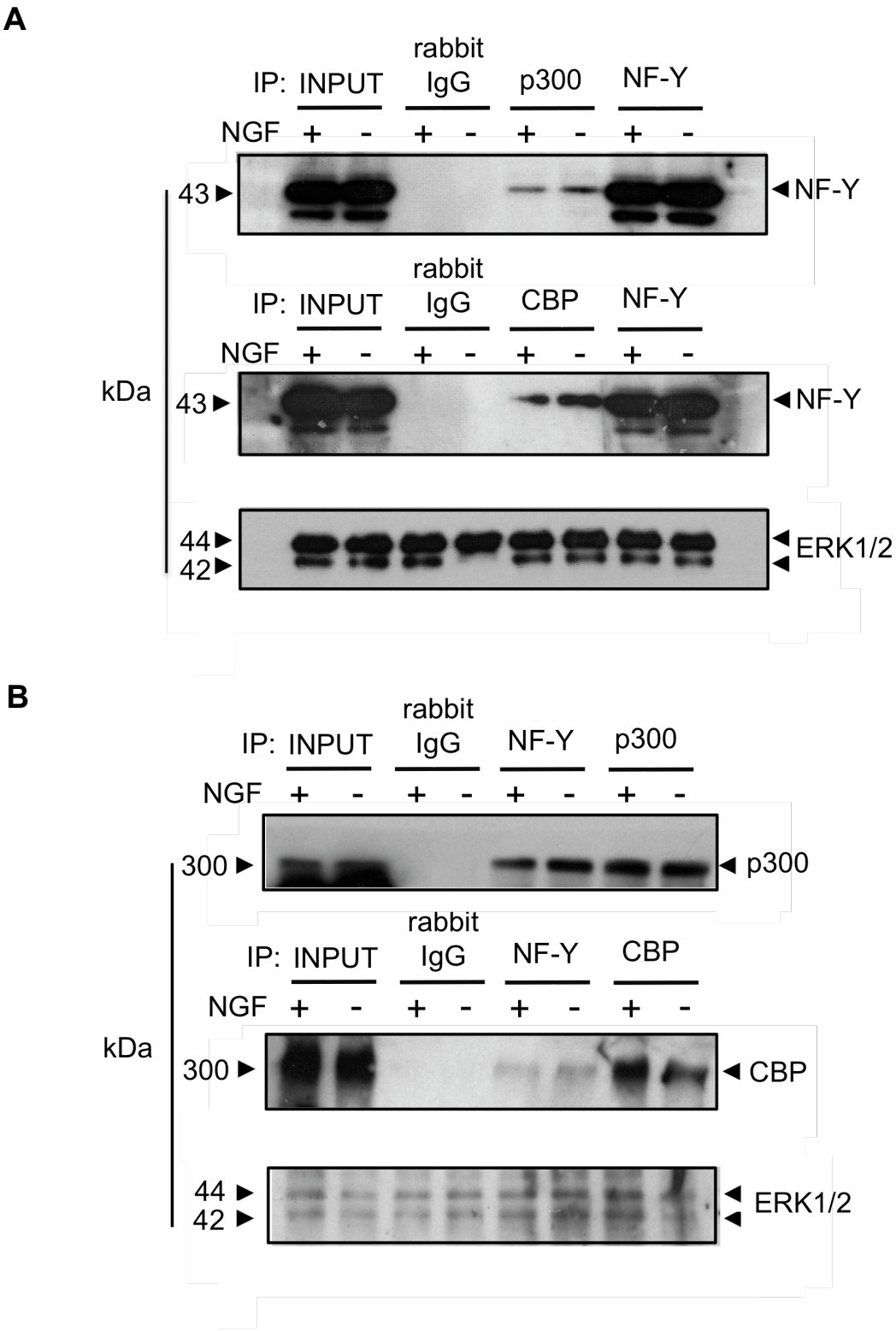
A
rabbit
IP: INPUT IgG p300 NF-Y
NGF + - + - + - + -
43
NF-Y
rabbit
IP: INPUT IgG CBP NF-Y
NGF + - + - + - + -
kDa
43
NF-Y
44
42
ERK1/2
B
rabbit
IP: INPUT IgG NF-Y p300
NGF + - + - + - + -
300
p300
rabbit
IP: INPUT IgG NF-Y CBP
NGF + - + - + - + -
kDa
300
CBP
44
42
ERK1/2

4.3 Discussion

I originally hypothesised that the coactivators CBP/p300 may be important for efficient activation of the *bim* promoter following NGF withdrawal in sympathetic neurons. Initially, I demonstrated that CBP and p300 are expressed in sympathetic neurons where they localise to the nucleus. There is no apparent change in the expression level of the proteins following NGF withdrawal, but since CBP and p300 are global coactivators then it is likely that they are involved in a number of transcriptional pathways in sympathetic neurons. It is therefore not surprising that there is no change in total protein levels when cells are deprived of NGF. I then overexpressed p300 or CBP in sympathetic neurons and found that this is sufficient to activate the *bim*-LUC reporter construct. Interestingly, overexpression of p300 does not activate the *bim*-LUC CCAAT(-) construct, thereby demonstrating that p300 requires the CCAAT box to be intact in order to activate *bim* transcription. Furthermore, in Chapter 3 I demonstrated that the mutated CCAAT box cannot bind NF-Y, so these results indicated that there may be an interaction between NF-Y and p300/CBP. In addition, a number of other studies have reported that NF-Y can recruit p300/CBP to the proximal promoters of different genes (Li *et al*., 1998; Franiello *et al*., 1999).

To further study the role of p300/CBP in this context, I performed some antibody co-injection experiments. Loss of p300 or CBP by the injection of specific antibodies significantly decreases the activation of the *bim*-LUC reporter construct following NGF withdrawal, indicating that p300 and CBP are important for efficient activation of the *bim* promoter following NGF withdrawal in sympathetic neurons. Again, as with NF-Y, it is possible that inhibition of CBP and p300 may have non-specific effects in sympathetic neurons, as the loss of CBP and p300 is likely to affect other promoters as well as *bim*. Nevertheless, this data indicates that CBP/p300 may play an important role in neuronal apoptosis induced by activation of the proapoptotic *bim* gene.

ChIP experiments were then performed and this data confirms that p300 and CBP can bind to the same region of the *bim* promoter as NF-Y, and that binding of both p300 and CBP increases significantly following NGF withdrawal. The ChIP method that

I have used has a long cross-linking time of 3 hours at room temperature. Therefore, proteins bound to proteins can be immunoprecipitated along with proteins bound to DNA. Since CBP and p300 do not contact the DNA directly, they must bind via proteins that are already bound to the *bim* promoter in this location. As the ICB must be intact for activation of *bim* by p300 then this data suggests that p300/CBP activates the *bim* promoter directly through NF-Y. As further evidence to support this hypothesis, co-IP experiments demonstrate that NF-Y can interact with p300 and CBP in nuclear extracts from neuronally differentiated PC12 cells.

Following NGF withdrawal, FOXO3a translocates from the cytoplasm into the nucleus and binds to the two conserved FOXO sites in the *bim* promoter (Gilley *et al*., 2003). The FOXO sites are located within a 300 base pair region either side of the ICB. NF-Y is bound to the *bim* promoter in the presence of NGF and following NGF withdrawal and is known to significantly distort DNA to facilitate protein-protein interactions between DNA-binding factors (Ronchi *et al*., 1995; Liberati *et al*., 1998; Mantovani *et al*., 1999). CBP/p300 binding to the *bim* promoter increases significantly after NGF deprivation and CBP/p300 can interact with NF-Y *in vitro*. It has previously been shown that CBP/p300 can also interact with FOXO3a, and the other regulatory factors such as Myb and c-Jun that activate *bim* transcription, in other systems (Lee *et al*., 1996; Giordano and Avantaggiati, 1999; Bessa *et al*., 2001; Mahmud *et al*., 2002; Perrot and Rechler, 2005). Therefore I hypothesise that following NGF withdrawal, NF-Y, FOXO3a, and perhaps other DNA-binding factors such as c-Jun, form a stereospecific interaction surface to recruit CBP/p300 (Figure 4.6). These interactions then form a stable multi-protein complex that may integrate the several signalling pathways that activate the *bim* promoter following NGF withdrawal in sympathetic neurons.

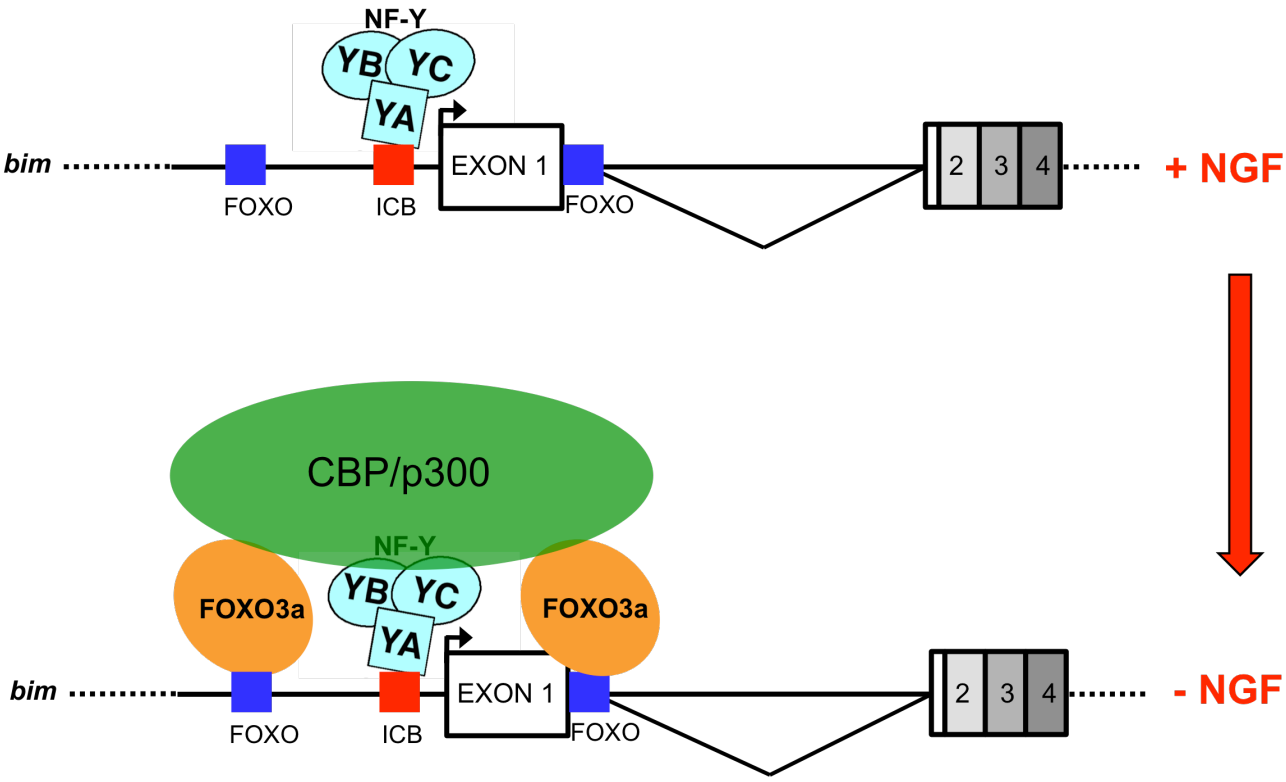

Figure 4.6 Model of the transcriptional activation of the *bim* promoter in sympathetic neurons in the presence of NGF and following NGF withdrawal.

In sympathetic neurons deprived of NGF, FOXO3a translocates from the cytoplasm into the nucleus and binds to the two conserved FOXO sites in the *bim* promoter (Gilley *et al*., 2003). CBP/p300 binding to the *bim* promoter increases significantly after NGF withdrawal and CBP/p300 can interact with NF-Y *in vitro*. CBP/p300 may also interact with FOXO3a and other regulatory factors that activate *bim* transcription. Therefore following NGF withdrawal, NF-Y and FOXO3a may recruit CBP/p300 to form a stable multi-protein complex that increases the transcriptional activation of *bim*.

Chapter 5: Investigating the mechanism by which the MEK/ERK pathway negatively regulates *bim* gene expression in sympathetic neurons.

5.1 Introduction

It is now apparent that the simultaneous induction of independent transcriptional pathways in neurons contributes to the increase in *bim* mRNA level after NGF withdrawal. The different signalling pathways that regulate *bim* expression control the activity of DNA-binding transcription factors that recognise elements located within the *bim* promoter or first intron, as discussed in the previous two chapters. However, relatively little is known about regulatory elements located elsewhere in the *bim* gene sequence. The multipart structure of *bim* is highly conserved between mammals with the mouse, rat and human genes sharing an identical exon/intron structure (Figure 1.7). Considering the number of mechanisms that have, so far, been identified to safeguard the inappropriate activation of *bim* in neurons, it is probable that there are additional regulatory elements located outside of the *bim* promoter and first intron that are also important.

Recent studies have provided evidence that Bim is not only regulated at the level of transcription and by post-translational modifications. Over the last decade it has become evident that eukaryotic gene expression is subject to additional control mechanisms via post-transcriptional processing. Here, a number of steps contribute to the formation of a mature mRNA. For example, alternative splicing can give rise to many different transcripts from a single pre-mRNA. While the 5′ untranslated region (UTR) is principally involved in controlling mRNA translation, the 3′ UTR regulates a range of processes that control the fate of an mRNA, such as mRNA localisation (Andreassi and Riccio, 2009). The discovery of the complex nature of the 3′ UTR has clarified why these non-coding regions are often so long and so important for the proper regulation of gene expression.

The 3′ UTR is often the target for post-transcriptional regulation by microRNAs and RNA-binding proteins. MicroRNAs (miRNAs) constitute a large

family of small, 20-24 nucleotide long, non-coding RNAs that have been identified as key regulators of almost every eukaryotic cellular process (Filipowicz *et al*., 2008). Mature miRNA molecules are partially complementary to sequences that are typically located within the 3′ UTR of an mRNA. Here, miRNAs control gene expression most-commonly by regulating mRNA translation or stability in the cytoplasm (Valencia-Sanchez *et al*., 2006; Pillai *et al*., 2007; Standart and Jackson, 2007). MiRNAs have been hailed as the 'regulators of the master regulators' since the up or down regulation of a single miRNA can have a profound effect on the normal function of a number of different genes. For example, an early study which targeted the muscle-specific miRNA, miR-1-2, for deletion revealed numerous essential functions in the heart including regulation of cardiac morphogenesis, electrical conduction and cell-cycle control (Zhao *et al*., 2007). Furthermore, mice with defects in the miRNA biogenesis pathway show early embryonic lethality indicating that miRNAs play a critical role in vertebrate development (Bernstein *et al*., 2003; Liu *et al*., 2004; Abbott *et al*., 2005). Recently, several groups have reported that *bim* is a target for regulation by miRNAs. For example, Bim expression is repressed by miR-17~92 during B cell development at the pro-B to pre-B transition and loss of miR-17~92 expression results in increased levels of Bim and inhibition of B cell development (Ventura *et al*., 2008).

In addition to miRNA binding sites, the 3′ UTR of an mRNA can contain a number of other sequences that mediate post-transcriptional regulation. AU-rich elements (AREs) are sequences rich in adenosine and uridine bases that typically target their mRNA for decay (Barreau *et al*., 2005). They are one of the most common destabilising elements and are frequently found in mRNAs that have a short half-life, for example those encoded by immediate early response genes such as *c-fos* (Chen *et al*., 1994; Chen and Shyu, 1995). ARE sequences often contain the AUUUA pentamer and can bind a number of different RNA-binding proteins (Roretz and Gallouzi, 2008). Furthermore, some examples of ARE-mediated decay have been linked to miRNAs (Jing *et al*., 2005; Vasudevan, 2007; von Roretz and Gallouzi, 2008). Studies with Baf-3 cells have revealed that *bim* mRNA is stabilised when cytokines are limiting and this regulation occurs via AREs found within the *bim* 3′ UTR (Matsui *et al*., 2007).

As well as sequences involved in post-transcriptional regulation, a number of important transcriptional control elements can be found within the genomic region that contains the 3′ UTR. Enhancer elements are generally a closely grouped cluster of transcription factor binding sites that act cooperatively to enhance transcription from a distal location. Enhancers are functionally similar to promoter elements but they may be located far from the core promoter, for example within introns or the 3′ UTR (Blackwood and Kadonaga, 1998; Lettice *et al*., 2003). It is thought that enhancer elements are brought into close proximity of the core promoter by 'DNA looping' (Szutorisz *et al*., 2005). Therefore, the orientation and spatial organisation of the transcription factor binding sites within an enhancer is often critical for its regulatory activity (Remenyi et al., 2004; Szutorisz *et al*., 2005). Silencer elements share many of the same properties as enhancer elements in that they are transcriptional elements that can be found far from the core promoter (Ogbourne and Antalis, 1998). Typically, silencers bind repressors, DNA-binding proteins that have a repressive effect on transcription. Repressors can recruit negative cofactors, corepressors, and in some cases the recruitment of different corepressors can change an activator into a repressor (Ogbourne and Antalis, 1998). It is unclear precisely how silencer elements function but it is generally accepted that they repress transcription by one or more of three mechanisms: by blocking the binding of an activator to DNA, by recruiting histone modifying enzymes that stabilise the chromatin structure, or by inhibiting pre-initiation complex formation (Chen and Widom, 2005; Maston *et al*., 2006).

The Raf-MEK-ERK pathway delivers important survival signals in a number of different cell types. Knockout mice with loss of *c-Raf-1* or *B-Raf* die as embryos with increased apoptosis in certain tissues (Wojnowski *et al*., 1997; Huser *et al*., 2001; Mikula *et al*., 2001). A number of papers have reported that the MEK1/2/ERK1/2 pathway negatively regulates the expression of Bim_{EL} (Ley *et al*., 2005a). However, it is not known whether the MEK/ERK pathways (either MEK1/2/ERK1/2 or MEK5/ERK5) control *bim* expression in an additional manner prior to the phosphorylation of Bim_{EL}.

Weston *et al*. (2003) showed that *bim* mRNA levels are upregulated following serum withdrawal in RR1 cells (a cell line expressing ΔRaf-1:ER*, the

conditionally active form of the Raf-1 protein kinase), but a mechanism was not investigated. Moreover, some preliminary experiments have suggested that the MEK/ERK pathway may play a role in the regulation of *bim* expression in sympathetic neurons. Dr. Jonathan Gilley, a previous member of our group, carried out some initial semi-quantitative RT-PCR experiments that indicated that the MEK/ERK pathway negatively regulates *bim* expression by an unknown mechanism (unpublished data). I wanted to further investigate this hypothesis in sympathetic neurons.

5.2 Results

5.2.1 The MEK/ERK pathway negatively regulates *bim* mRNA expression independently of the PI3-K pathway in sympathetic neurons.

To confirm the preliminary observation, made by Jonathan Gilley, that the MEK/ERK pathway negatively regulates *bim* expression, I carried out some semi-quantitative RT-PCR experiments. Sympathetic neurons were either maintained in medium containing NGF, withdrawn from NGF or treated with LY294002 (50 μM) in the presence of NGF or with U0126 (10 μM) in the presence of NGF. After 16 hours, total RNA was isolated and the amount of *bim* mRNA was analysed by semi-quantitative PCR relative to *neurofilament-M* mRNA (*neurofilament-M* was used as a house-keeping gene) (Figure 5.1A). It has been shown previously that the PI3-kinase (PI3-K) pathway negatively regulates *bim* expression via two conserved FOXO sites in the *bim* promoter and first intron (Gilley *et al*., 2003). As a positive control sympathetic neurons were treated with the PI3-K inhibitor LY294002. Upon treatment with LY294002 the level of *bim* mRNA increased by 2.2 fold (Figure 5.1B). This is consistent with previous data from Gilley *et al*. (2003). When I treated sympathetic neurons with the MEK/ERK inhibitor U0126 there was also a significant induction of *bim* mRNA, 2.25 fold (Figure 5.1B). This data confirms the hypothesis that the MEK/ERK pathway negatively regulates *bim* expression in sympathetic neurons. It is also important to note here that inhibition of either the PI3-K or the MEK/ERK pathway does not induce *bim* mRNA to the level that is seen after NGF withdrawal (Figure 5.1B). This is because full activation of *bim* following NGF withdrawal appears to require changes in several signalling pathways, as discussed in the previous two chapters.

The PI3-K and MEK/ERK signalling pathways are prosurvival pathways activated by the small G protein Ras following the binding of NGF to TrkA (Figure 5.2A). As a control experiment I wanted to confirm that phospho-ERK1/ERK2 levels are reduced when sympathetic neurons are treated with U0126. I therefore performed some immunoblots with extracts from sympathetic neurons either maintained in the presence of NGF or treated with increasing concentrations of U0126 in the presence of NGF (Figure

Figure 5.1 The MEK/ERK pathway negatively regulates *bim* mRNA expression in sympathetic neurons.

(A) Sympathetic neurons were either maintained in medium containing NGF, withdrawn from NGF for 16 hours, treated with the PI3-K inhibitor LY294002 at 50 μM or with the MEK/ERK inhibitor U0126 at 10 μM. LY294002 and U0126 were dissolved in DMSO and therefore equal volumes of DMSO were added to untreated cells (+NGF and -NGF). Cells were treated with LY294002 or U0126 for 16 hours in the presence of NGF. After 16 hours, total RNA was isolated and analysed by semi-quantitative RT-PCR. Representative images are shown for the *bim* and *neurofilament-M* mRNAs.

(B) Quantitation of RT-PCR in Figure 5.1 A. PCR was quantitated at 30 and 35 cycles and the average mRNA levels were calculated. Relative *bim* mRNA levels were calculated by normalising to the control *neurofilament-M*. The experiment was performed 6 times and data is presented as the mean ± S.E. Endogenous *bim* mRNA levels increase significantly following NGF withdrawal and treatment with LY294002, respectively (*). Treatment with U0126 also induces a significant increase in the level of *bim* mRNA (*).

A

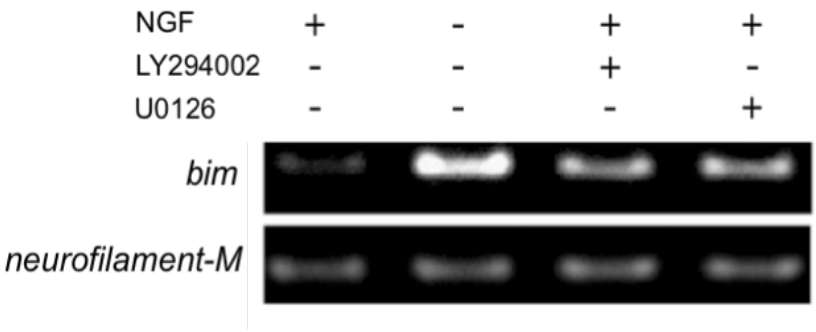
NGF + - + +
LY294002 - - + -
U0126 - - - +
bim
neurofilament-M

B

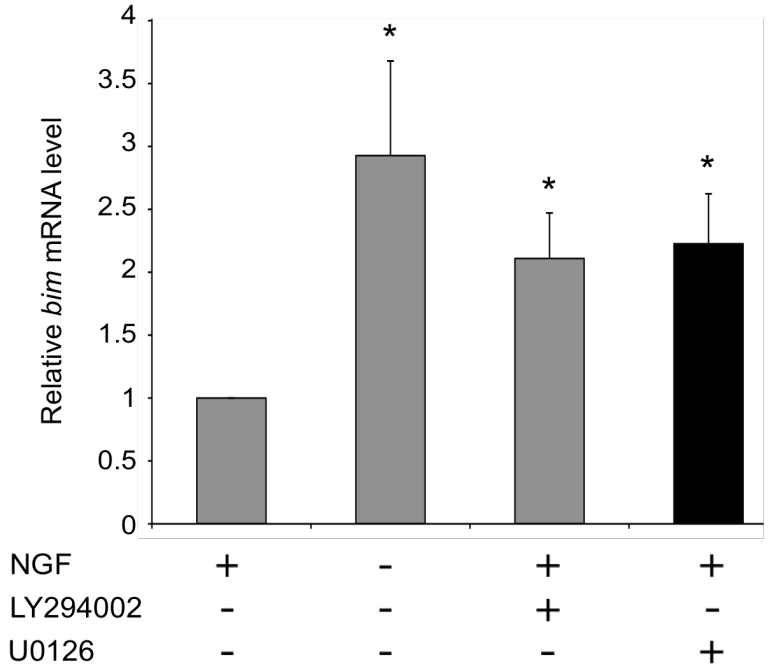
Relative bim mRNA level
4
3.5
3
2.5
2
1.5
1
0.5
0
*
*
*
NGF + - + +
LY294002 - - + -
U0126 - - - +

5.2B). Treatment of sympathetic neurons with U0126 at 10 μM strongly reduced levels of phospho-ERK, whereas ERK protein levels were not altered (Figure 5.2B). This data confirms that treatment of sympathetic neurons with U0126 at 10 μM inhibits MEK/ERK signalling. I then performed another control experiment to confirm that the PI3-K and MEK/ERK signalling pathways are largely independent of one another in sympathetic neurons and that the increase in *bim* mRNA following treatment with U0126, as shown in Figure 5.1, is independent of PI3-K signalling. Immunoblots were carried out with extracts from sympathetic neurons either maintained in the presence of NGF, withdrawn from NGF for 16 hours or treated with U0126 (10 μM) for 16 hours in the presence of NGF (Figure 5.2C). Phospho-Akt levels were high when neurons were maintained in the presence of NGF and there was no major change upon treatment with U0126 (Figure 5.2C). Gilley *et al*. (2003) showed that phospho-Akt levels fall in sympathetic neurons deprived of NGF. My data reproduces this result since phospho-Akt levels are low following NGF withdrawal whereas levels of Akt or ERK1/ERK2 are not altered (Figure 5.2C).

In conclusion, these results suggest that in sympathetic neurons the MEK/ERK pathway negatively regulates *bim* mRNA expression and this regulation is independent of PI3-K signalling.

5.2.2 The MEK/ERK pathway negatively regulates *bim* mRNA expression in sympathetic neurons via regulatory elements outside of the *bim* promoter and first intron.

To investigate the mechanism by which the MEK/ERK pathway negatively regulates *bim* expression in sympathetic neurons it was important to establish which regions of the *bim* gene mediate this effect. Initially, sympathetic neurons were microinjected with the *bim*-LUC reporter construct to determine whether there are any MEK/ERK-responsive elements within the 5.2 kb fragment of *bim* that is cloned in *bim*-LUC. This construct contains 2.5 kb of the *bim* promoter, the non-coding exon 1 and the 2.5 kb first intron. Following injection, the cells were either maintained in medium containing NGF, withdrawn from NGF or treated with LY294002 (50 μM) in the

Figure 5.2 The effect of U0126 on the phosphorylation of ERK 1/2 and Akt in sympathetic neurons.

(A) PI3-Kinase and ERK signalling pathways in sympathetic neurons. NGF activates the small G protein Ras via the tyrosine kinase receptor TrkA. Ras activates MEK/ERK1/2 signalling and this can be inhibited by treatment with the compound U0126. It is important to note that U0126 can also inhibit the related MEK5/ERK5 pathway. Ras also activates PI3-K/Akt signalling and this can be inhibited by treatment with the compound LY294002. Withdrawal of NGF leads to the dephosphorylation of ERK1/2 and Akt. The resulting decrease in Akt activity leads to a reduction in the phosphorylation of FOXO transcription factors, which can then translocate into the nucleus of sympathetic neurons (Gilley *et al*., 2003).

(B) Treatment of sympathetic neurons with 10 μM U0126 completely inhibits phosphorylation of ERK1/2. Immunoblots performed with whole cell extracts from sympathetic neurons maintained in the presence of NGF and then left untreated or treated with 5 μM, 10 μM, 20 μM or 40 μM U0126 for 16 hours are shown. Immunoblotting was performed with antibodies to detect total ERK1/2 (Cell Signalling #9102) and phospho-ERK1/2 (Cell Signalling #9101S). Several experiments were performed and representative blots are shown.

(C) Phosphorylation of Akt is not affected by treatment with U0126 in sympathetic neurons. Immunoblots performed with whole cell extracts from sympathetic neurons maintained in the presence of NGF, withdrawn from NGF for 16 hours, or treated with 10 μM U0126 for 16 hours in the presence of NGF are shown. Immunoblotting was carried out with antibodies to detect total Akt (Cell Signalling #9272), phospho-Akt (Cell Signalling #9271S) and total ERK1/2 (Cell Signalling #9102). Several experiments were performed and representative blots are shown.

U0126 was dissolved in DMSO and therefore an equal volume of DMSO was added to the untreated cells.

A

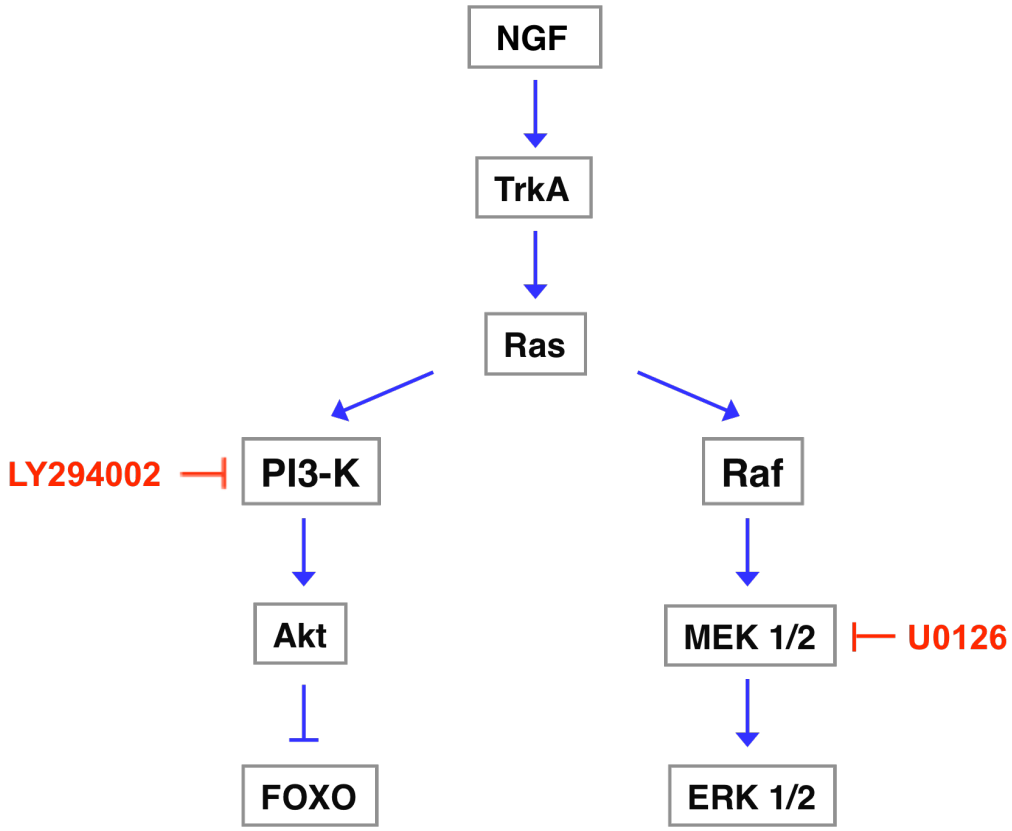
NGF
TrkA
Ras
LY294002
PI3-K
Raf
Akt
MEK 1/2
U0126
FOXO
ERK 1/2

B

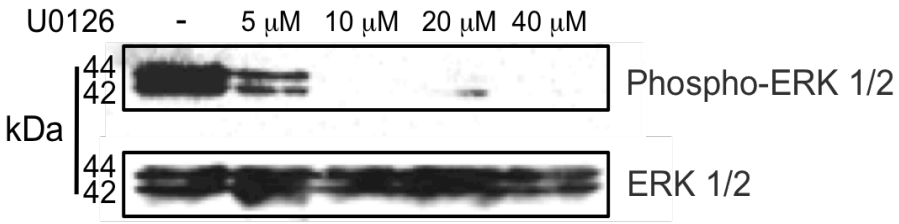
U0126 - 5 μM 10 μM 20 μM 40 μM
kDa
44
42
Phospho-ERK 1/2
44
42
ERK 1/2

C

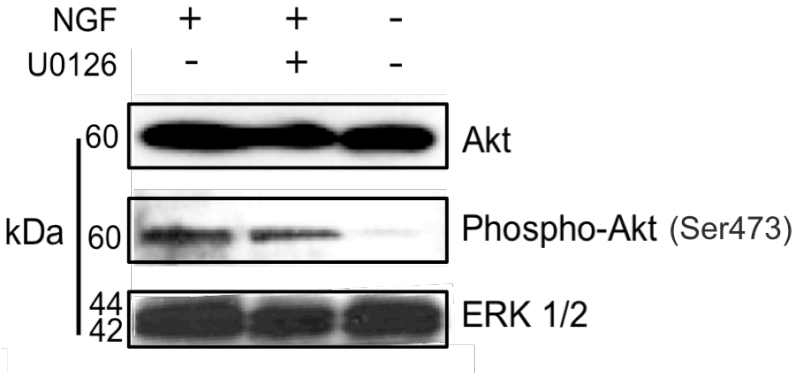
NGF + + -
U0126 - + -
kDa
60
Akt
60
Phospho-Akt (Ser473)
44
42
ERK 1/2

presence of NGF or with U0126 (10 μM) in the presence of NGF. After 16 hours relative luciferase activity was determined by the dual luciferase assay (Figure 5.3). Following NGF withdrawal *bim*-LUC was activated significantly to 1.7 fold (Figure 5.3). In dual luciferase assays, the induction of *bim*-LUC following NGF withdrawal varies from 1.5 fold to 2.5 fold in microinjected sympathetic neurons and a similar fold change in the level of the *bim*-LUC transcript has been measured by RT-PCR (Figure 3.4; Gilley *et al*., 2003; Gilley and Ham, 2005). However, the increase in the level of endogenous *bim* mRNA, measured by semi-quantitative RT-PCR, varies from 3 fold to 5 fold in sympathetic neurons (Figure 5.1; Whitfield *et al*., 2001; Gilley *et al*., 2003). Therefore, it is possible that there are some elements missing from the *bim*-LUC reporter construct that respond to NGF withdrawal. Treatment with LY294002 activated *bim*-LUC 2.9 fold since the two FOXO sites, which mediate the effect of inhibiting PI3-K signalling, are located within the region of the *bim* gene cloned into *bim*-LUC (Figure 5.3). However, when neurons were treated with U0126 there was no activation of *bim*-LUC (Figure 5.3). This data indicates that there are no MEK/ERK-responsive elements within the first 2.5 kb of the *bim* promoter, exon 1 or the first intron.

5.2.3 The *bim* 3′ UTR contains elements that are responsive to NGF withdrawal.

It is evident from Figure 5.3 that the region that mediates the regulation of *bim* by the MEK/ERK pathway is probably not located at the 5′ end of the *bim* gene. Therefore, I hypothesised that the *bim* 3′ UTR may contain the appropriate region since the 3′ UTR of an mRNA often contains a number of regulatory motifs that are important for modulating gene expression. Little is known about the *bim* 3′ UTR. It has been mapped for human and mouse *bim* and is ~4.2 kb and ~3.9 kb long, respectively. Initially, I mapped the rat *bim* 3′ UTR by 3′ RACE and found that it was 4239 bp long, a similar length to human *bim* and slightly longer than that of mouse *bim*. I used MacVector 6.5.3 software to briefly analyse the level of conservation of the *bim* 3′ UTR across species. I found that rat and mouse *bim* are highly homologous to each other throughout the 3′ UTR. Both rodents display some conservation with human

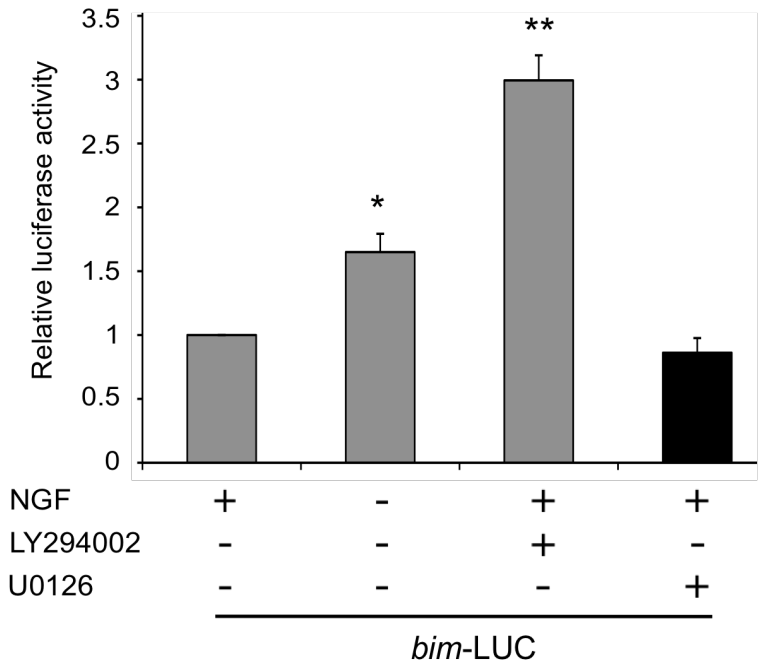

Figure 5.3 The MEK/ERK pathway negatively regulates *bim* mRNA expression in sympathetic neurons via regulatory elements outside of the *bim* promoter.

Sympathetic neurons were microinjected with *bim*-LUC at 10 ng/µl along with pRL-TK at 5 ng/µl. The cells were either maintained in medium containing NGF, withdrawn from NGF for 16 hours, treated with the PI3-K inhibitor LY294002 at 50 µM or with the MEK/ERK inhibitor U0126 at 10 µM. LY294002 and U0126 were dissolved in DMSO and therefore equal volumes of DMSO were added to untreated cells (+NGF and -NGF). Cells were treated with LY294002 or U0126 for 16 hours in the presence of NGF. After 16 hours, luciferase activity was measured. Microinjection experiments were carried out 4 times and data is presented as the mean ± S.E. *Bim*-LUC is activated significantly following NGF withdrawal and treatment with LY294002, respectively (* and **). Treatment with U0126 does not activate the *bim*-LUC reporter.

bim, particularly towards the 3′ end of the 3′ UTR where there is over 60% conservation between rat and human *bim* within the last 2 kb.

To determine if the 3′ UTR of *bim* is the region responsible for MEK/ERK regulation I constructed a *bim*-LUC+3′UTR reporter (Figure 5.4). Following 3′ RACE to determine the end point of the rat *bim* 3′ UTR, I amplified the region as two overlapping fragments by PCR (Figure 5.4). I then systematically cloned the two fragments into pGEM-T for sequence confirmation and the full-length rat *bim* 3′ UTR was assembled in pBluescript SK (Figure 5.4). Finally, the 4.3 kb rat *bim* 3′ UTR was sub-cloned into our *bim*-LUC reporter construct, downstream of luciferase and upstream of the SV40 late poly (A) signal (Figure 5.4). I decided to construct the *bim*-LUC+3′UTR reporter in a number of sequential steps following many unsuccessful attempts to directly clone the 3′ UTR into *bim*-LUC.

To compare the *bim*-LUC+3′UTR reporter to our original *bim*-LUC reporter, sympathetic neurons were microinjected with *bim*-LUC+3′UTR or *bim*-LUC, together with the control *Renilla* luciferase construct, pRL-TK. The injected cells were then either maintained in the presence of NGF (+NGF) or withdrawn from NGF (-NGF) for 16 hours, after which time relative luciferase activity was determined by the dual luciferase assay. Addition of the 3′ UTR greatly reduces the basal level of the *bim*-LUC reporter construct (Figure 5.5B). Therefore, this indicates that the *bim* 3′ UTR contains sequences that reduce luciferase activity either at the level of transcription, RNA stability or translation. Critically, addition of the 3′ UTR to the *bim*-LUC reporter significantly increases its induction from 1.8 fold to 3 fold, following NGF withdrawal (Figure 5.5C). This data suggests that the *bim* 3′ UTR contains elements that are responsive to NGF withdrawal. The *bim*-LUC+3′UTR construct may be more representative of endogenous *bim* than our original *bim*-LUC reporter since endogenous *bim* mRNA levels increase ~3 fold following NGF withdrawal (Figure 5.1).

Figure 5.4 Construction of the *bim*-LUC+3′ UTR reporter.

3′ RACE was performed on rat poly A+ RNA to determine the end point of the rat *bim* 3′ UTR. Once defined, the rat *bim* 3′ UTR was amplified by PCR as two overlapping fragments, a 2.57 kb fragment 1 (F1) and a 1.88 kb fragment 2 (F2). The two fragments were then cloned into pGEM-T using the pGEM-T easy vector system for DNA sequence confirmation. Fragment 1 was excised from pGEM-T using a SpeI restriction site at the 5′ end (the SpeI site was incorporated by PCR) and a unique BglII restriction site within the 3′ UTR. Fragment 2 was excised from pGEM-T using the same unique BglII restriction site and a SpeI restriction site at the 3′ end (the SpeI site was incorporated by PCR). The 4.3 kb rat *bim* 3′ UTR was assembled in pBluescript SK and then excised using SpeI and sub-cloned into *bim*-LUC using an XbaI restriction site. The *bim*-LUC reporter contains one other Xba1 restriction site (within *bim* intron 1) that was abolished by site-directed mutagenesis to leave the XbaI site used here as unique.

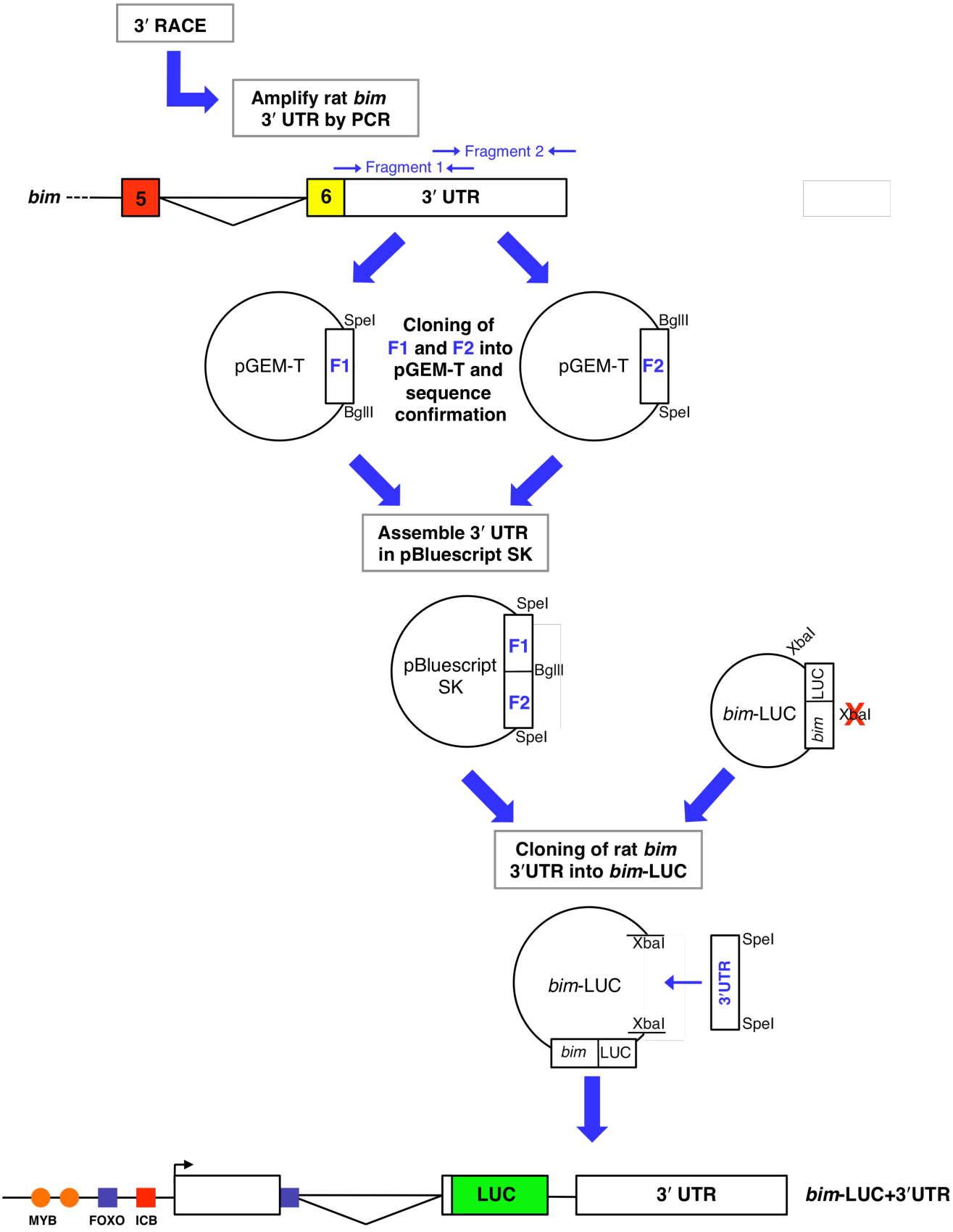
3′ RACE
Amplify rat bim 3′ UTR by PCR
Fragment 2
Fragment 1
bim
5
6
3′ UTR
pGEM-T
SpeI
F1
BglII
Cloning of F1 and F2 into pGEM-T and sequence confirmation
pGEM-T
BglII
F2
SpeI
Assemble 3′ UTR in pBluescript SK
pBluescript SK
SpeI
F1
BglII
F2
SpeI
XbaI
bim-LUC
LUC
bim
XbaI
Cloning of rat bim 3′UTR into bim-LUC
XbaI
bim-LUC
XbaI
bim
LUC
SpeI
3′UTR
SpeI
MYB
FOXO
ICB
LUC
3′ UTR
bim-LUC+3′UTR

Figure 5.5 The *bim* 3′ UTR contains additional sequences that respond to NGF withdrawal in sympathetic neurons.

Sympathetic neurons were microinjected with *bim*-LUC at 10 ng/μl or *bim*-LUC+3′UTR at 14 ng/μl, along with pRL-TK (5 ng/μl). The cells were maintained in medium containing NGF (+NGF) or withdrawn from NGF (-NGF) for 16 hours, after which time luciferase activity was measured. Microinjection experiments were carried out 5 times and data is presented as the mean ± S.E.

(A) Structure of the *bim*-LUC and *bim*-LUC+3′UTR reporters. The *bim*-LUC reporter contains 2.5 kb of the rat *bim* promoter, the non-coding Exon 1 and the 2.5 kb intron cloned upstream of the firefly luciferase gene. The *bim*-LUC+3′UTR reporter was constructed by cloning and inserting the 4.2 kb rat *bim* 3′ UTR into the *bim*-LUC reporter, upstream of the SV40 late poly (A) signal and downstream of the Luciferase reporter gene. The location of conserved FOXO binding sites, Myb binding sites and the ICB are shown.

(B) *Bim*-LUC is activated significantly following NGF withdrawal. Addition of the *bim* 3′ UTR significantly decreases the basal promoter level of *bim*-LUC (***).

(C) The basal levels of *bim*-LUC and *bim*-LUC+3′UTR were normalised to 1 and the induction factors of the two constructs were compared. Addition of the *bim* 3′ UTR significantly increases the induction of *bim*-LUC following NGF withdrawal (*).

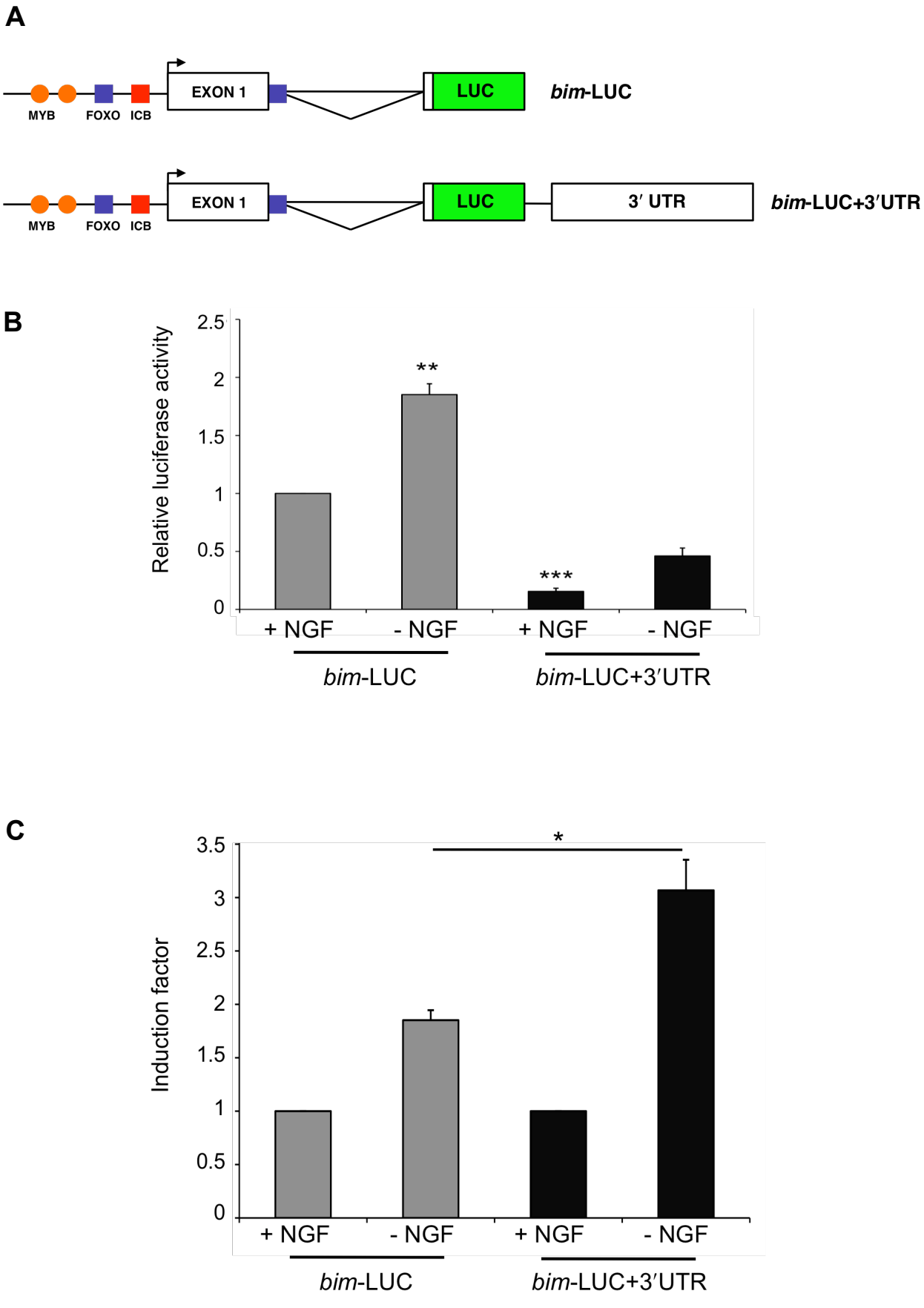
A
MYB
FOXO
ICB
EXON 1
LUC
bim-LUC
3′ UTR
bim-LUC+3′UTR
B
Relative luciferase activity
2.5
2
1.5
1
0.5
0
**
***
+ NGF
- NGF
+ NGF
- NGF
bim-LUC
bim-LUC+3′UTR
C
Induction factor
3.5
3
2.5
2
1.5
1
0.5
0
*
+ NGF
- NGF
+ NGF
- NGF
bim-LUC
bim-LUC+3′UTR

5.2.4 The *bim* 3′ UTR is a target of the MEK/ERK pathway in sympathetic neurons.

To answer the major question of whether the *bim* 3′ UTR mediates an effect by the MEK/ERK pathway, sympathetic neurons were microinjected with *bim*-LUC+3′UTR or *bim*-LUC, along with pRL-TK. Following injection, the cells were either maintained in medium containing NGF or treated with U0126 (10 μM) in the presence of NGF. After 16 hours, relative luciferase activity was determined by the dual luciferase assay (Figure 5.6). Following inhibition of the MEK/ERK pathway with U0126, *bim*-LUC was not significantly activated (Figure 5.6). This confirms my initial data that there are no MEK/ERK responsive elements at the 5′ of the *bim* gene. However, when *bim*-LUC+3′UTR was treated with U0126 there was a significant activation of the reporter to 2.5 fold (Figure 5.6B). Endogenous *bim* is activated following treatment with U0126 to 2.25 fold (Figure 5.1B). Therefore, this suggests that the regulation of *bim* mRNA level via the MEK/ERK-pathway is mediated by the 3′ UTR.

5.2.5 The role of conserved AU-rich elements in the *bim* 3′ UTR.

AU-rich elements (AREs) are typically found in the 3′ UTR of genes that require a very precise spatial and temporal expression pattern. AREs generally mediate the rapid degradation of an mRNA and this helps to ensure that in unstimulated cells there is a very low level of expression of a potent protein (Barreau *et al*., 2005). The rat *bim* 3′ UTR contains 10 AUUUA repeats whereas the human *bim* 3′ UTR and the mouse *bim* 3′ UTR contain 8 and 6, respectively. Many of the AREs in the *bim* 3′ UTR are conserved between rat and mouse although just 4 are conserved across rat, mouse and human *bim* (Figure 5.7A). Since the *bim* 3′ UTR contains a number of AREs, I wanted to investigate their role in *bim* expression in sympathetic neurons. I was also interested to establish whether there is a link between mRNA stability and the regulation of *bim* mRNA level by the MEK/ERK pathway. In order to generate *bim*-LUC+3′UTR(4xAREmut), a U to G point mutation was introduced at the central U of the 4 conserved AUUUA pentamers in the rat *bim* 3′ UTR, in the context of *bim*-LUC+3′UTR. Previous studies have shown that mutation of the central U of this type

Figure 5.6 The MEK/ERK pathway negatively regulates *bim* expression in sympathetic neurons via the 3′ UTR.

Sympathetic neurons were microinjected with *bim*-LUC at 10 ng/µl or *bim*-LUC+3′UTR at 14 ng/µl, along with pRL-TK (5 ng/µl). The cells were maintained in medium containing NGF and either left untreated (-U0126) or treated with U0126 (+U0126) for 16 hours, after which time luciferase activity was measured. Microinjection experiments were carried out 6 times and data is presented as the mean ± S.E. U0126 was dissolved in DMSO and therefore an equal volume of DMSO was added to the untreated cells.

(A) *Bim*-LUC+3′UTR is activated significantly following inhibition of the MEK/ERK pathway by treatment with U0126 (*). *Bim*-LUC is not activated significantly following treatment with U0126.

(B) The basal levels of *bim*-LUC and *bim*-LUC+3′UTR were normalised to 1 and the induction factors of the two constructs, following treatment with U0126, were compared. Addition of the *bim* 3′ UTR causes a significant increase in the induction of *bim*-LUC upon inhibition of the MEK/ERK pathway with U0126 (*).

A

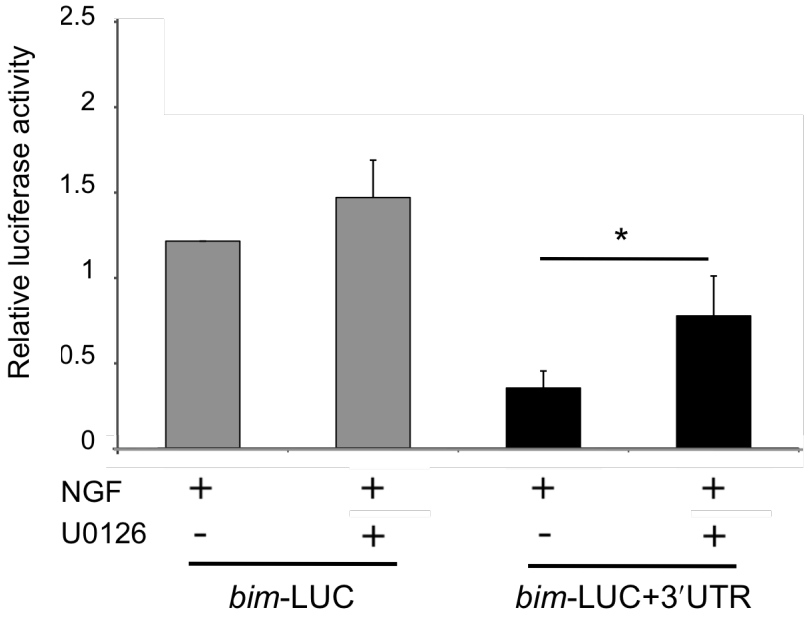
Relative luciferase activity
2.5
2
1.5
1
0.5
0
*
NGF + + + +
U0126 - + - +
bim-LUC
bim-LUC+3′UTR

B

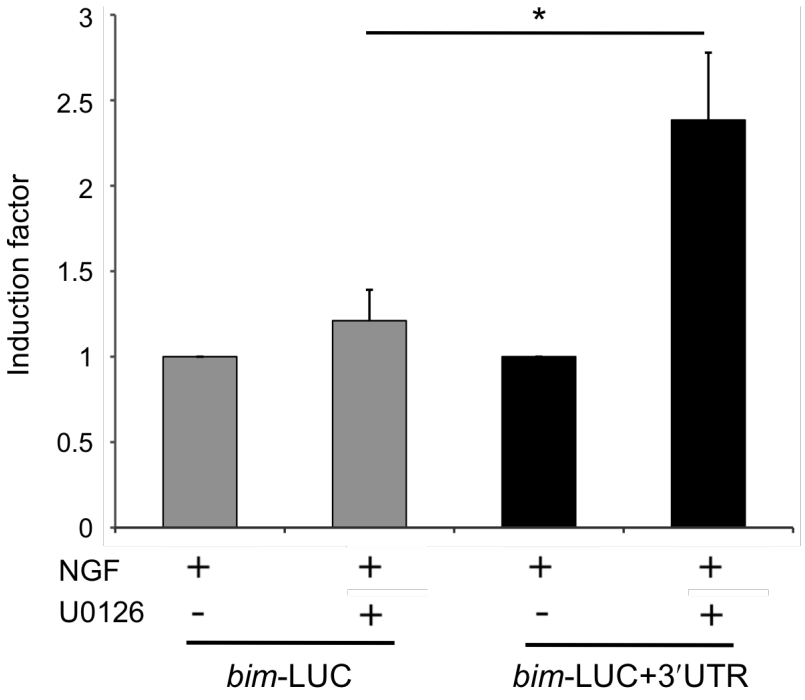
Induction factor
3
2.5
2
1.5
1
0.5
0
*
NGF + + + +
U0126 - + - +
bim-LUC
bim-LUC+3′UTR

of ARE results in a significant decrease in the destabilising efficiency of the ARE (Winzen *et al*., 2004). Sympathetic neurons were microinjected with *bim*-LUC, *bim*-LUC+3′UTR or *bim*-LUC+3′UTR(4xAREmut), along with pRL-TK. Following injection, the cells were either maintained in medium containing NGF or withdrawn from NGF. After 16 hours relative luciferase activity was determined by the dual luciferase assay (Figure 5.7). Mutation of the 4 AREs in the *bim* 3′ UTR (*bim*-LUC+3′UTR(4xAREmut) reporter) did significantly increase the basal level compared to the wild type construct (*bim*-LUC+3′UTR reporter), a 2.2 fold increase (Figure 5.7B). However, the basal level of the *bim*-LUC+3′UTR(4xAREmut) reporter was still greatly reduced compared to the *bim*-LUC reporter (Figure 5.7B). To further support the data in Figure 5.5, there was a significant increase in the activation of the *bim*-LUC+3′UTR reporter following withdrawal of NGF compared to the *bim*-LUC reporter (Figure 5.7C). Mutation of the 4 AREs in the *bim* 3′ UTR (the *bim*-LUC+3′UTR(4xAREmut) reporter) did result in a decrease in its activation compared to *bim*-LUC+3′UTR, but this difference was not significant (Figure 5.7C). Taken together this data suggests that the four conserved AREs partly contribute to the increased induction factor of *bim*-LUC+3′UTR. However, since mutation of the four AREs does not result in a significant decrease in the induction factor of *bim*-LUC+3′UTR and only has a modest effect on basal level, it is likely that there are additional elements in the *bim* 3′ UTR that control *bim* basal level and that are responsive to NGF withdrawal. These might be one or more of the non-conserved AREs in the rat *bim* 3′ UTR or other types of regulatory element.

5.2.6 The whole of the *bim* 3′ UTR is required for its effects on *bim*-LUC activity in sympathetic neurons.

As the next step to investigate the mechanism by which the *bim* 3′ UTR is negatively regulated by the MEK/ERK pathway, I decided to try to identify the general region of the 3′ UTR that is responsive to NGF withdrawal and a target of the MEK/ERK pathway. It is likely that this is the same region/effect, since MEK/ERK signalling is inhibited following NGF withdrawal, so this may account for the increased activation

Figure 5.7 The role of conserved AU-rich elements in the *bim* 3′ UTR.

(A) Schematic of the 3′ end of the *bim* gene. Coloured boxes indicate coding regions whereas white boxes indicated untranslated regions. The AU-rich elements that are conserved in rat, mouse and human *bim* are represented by grey bars. (Not to scale).

(B) The conserved AU-rich elements in the *bim* 3′ UTR contribute to the low basal level of the *bim*-LUC+3′UTR reporter. The four conserved AU-rich elements were mutated by site-directed mutagenesis, in the context of *bim*-LUC+3′UTR, to generate *bim*-LUC+3′UTR(4xAREmut). Sympathetic neurons were microinjected with *bim*-LUC at 10 ng/μl, or *bim*-LUC+3′UTR or *bim*-LUC+3′UTR(4xAREmut) at 14 ng/μl, along with pRL-TK (5 ng/μl). The cells were maintained in medium containing NGF (+NGF) or withdrawn from NGF (-NGF) for 16 hours, after which time luciferase activity was measured. Microinjection experiments were carried out 5 times and data is presented as the mean ± S.E. Following NGF withdrawal all 3 constructs are activated significantly (**), (*) and (*), respectively. Mutation of the 4 AU-rich elements significantly increases the basal level of *bim*-LUC+3′UTR (*).

(B) The conserved AU-rich elements in the *bim* 3′ UTR partly contribute to the induction of *bim* following NGF withdrawal. The basal level of the *bim*-LUC+3′UTR reporter The basal levels of *bim*-LUC, *bim*-LUC+3′UTR and *bim*-LUC+3′UTR(4xAREmut) were normalised to 1 and the induction factors of the three constructs were compared. There is a significant increase in the induction of *bim*-LUC+3′UTR compared to *bim*-LUC following NGF withdrawal (*). There is no significant difference in the induction factors between *bim*-LUC and *bim*-LUC+3′UTR(4xAREmut), or between *bim*-LUC+3′UTR and *bim*-LUC+3′UTR(4xAREmut).

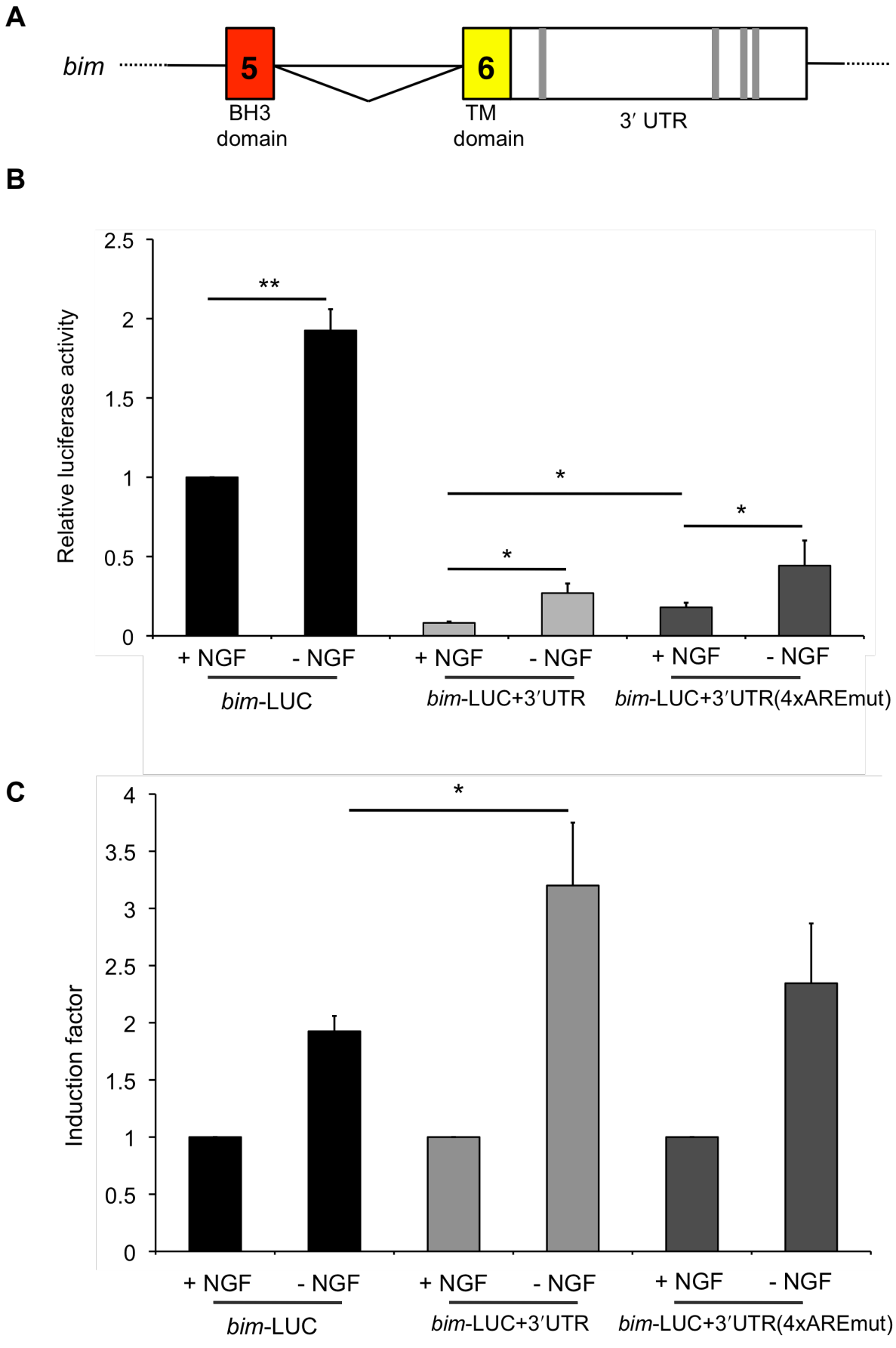
A
bim
5
6
BH3 domain
TM domain
3′ UTR
B
Relative luciferase activity
2.5
2
1.5
1
0.5
0
**
*
*
*
+ NGF
- NGF
+ NGF
- NGF
+ NGF
- NGF
bim-LUC
bim-LUC+3′UTR
bim-LUC+3′UTR(4xAREmut)
C
Induction factor
4
3.5
3
2.5
2
1.5
1
0.5
0
*
+ NGF
- NGF
+ NGF
- NGF
+ NGF
- NGF
bim-LUC
bim-LUC+3′UTR
bim-LUC+3′UTR(4xAREmut)

of *bim*-LUC+3′UTR compared to *bim*-LUC. Also, selectively inhibiting only the MEK/ERK pathway activates the *bim*-LUC+3′UTR reporter 2.5 fold, which is almost to the level of NGF withdrawal. To try to identify the relevant region of the 3′ UTR, I constructed a *bim*-LUC+3′UTR(F2) reporter construct that only contains the second half (F2) of the rat *bim* 3′ UTR. This 2.5 kb stretch of the *bim* 3′ UTR is highly conserved across species, thereby indicating that there may be important regulatory elements located there. Sympathetic neurons were microinjected with *bim*-LUC+3′UTR(F2) or *bim*-LUC, together with the control *Renilla* luciferase construct, pRL-TK. The injected cells were then either maintained in the presence of NGF (+NGF) or withdrawn from NGF (-NGF) for 16 hours, after which time relative luciferase activity was determined by the dual luciferase assay (Figure 5.8). Following NGF withdrawal both constructs were activated significantly, but there was only a moderate increase in the activation of *bim*-LUC+3′UTR(F2) compared to *bim*-LUC (Figure 5.8B). In addition to this, there was only a small decrease in the basal level of *bim*-LUC+3′UTR(F2) compared to *bim*-LUC (Figure 5.8A). This suggests that the whole of the *bim* 3′ UTR is required for its effects on *bim*-LUC activity in sympathetic neurons, since the *bim*-LUC+3′UTR(F2) reporter does not reproduce the properties of the *bim*-LUC+3′UTR reporter.

5.2.7 Regulation of *bim* expression by the MEK/ERK pathway is not an effect on mRNA stability in sympathetic neurons.

As the MEK/ERK-responsive elements are located within the *bim* 3′ UTR, initially I wanted to investigate a link with mRNA stability. However, it is evident that the four conserved AREs are not primarily responsible for this effect. In addition, TargetScan predicts that a large number of miRNA binding sites are located in the *bim* 3′ UTR so this would require extensive investigation. Therefore, before pursuing this hypothesis any further I decided to investigate whether the MEK/ERK pathway alters the stability of the endogenous *bim* mRNA in sympathetic neurons.

Sympathetic neurons were treated with actinomycin-D to inhibit transcription. Martin *et al*. (1988) found that the use of RNA and protein synthesis inhibitors protects sympathetic neurons against NGF withdrawal-induced death, and these results have

Figure 5.8 The whole of the *bim* 3′ UTR is required for its effects on *bim*-LUC activity in sympathetic neurons.

(A) The highly conserved fragment 2 (F2) of the *bim* 3′ UTR does not have the same effects on basal promoter activity and induction after NGF withdrawal as the full-length 3′ UTR. Sympathetic neurons were microinjected with *bim*-LUC at 10 ng/μl or *bim*-LUC+3′UTR (F2) at 14 ng/μl, along with pRL-TK (5 ng/μl). The cells were maintained in medium containing NGF (+NGF) or withdrawn from NGF (-NGF) for 16 hours, after which time luciferase activity was measured. Microinjection experiments were carried out 4 times and data is presented as the mean ± S.E. *Bim*-LUC and *bim*-LUC+3′UTR (F2) are both activated significantly following withdrawal of NGF (*). Although the basal activity of *bim*-LUC+3′UTR(F2) is 30% lower than *bim*-LUC this is difference is not significant.

(B) The basal levels of *bim*-LUC and *bim*-LUC+3′UTR (F2) were normalised to 1 and the induction factors of the two constructs were compared. Addition of the second half (F2) of the *bim* 3′ UTR does not significantly increase the induction of *bim*-LUC following withdrawal of NGF.

A

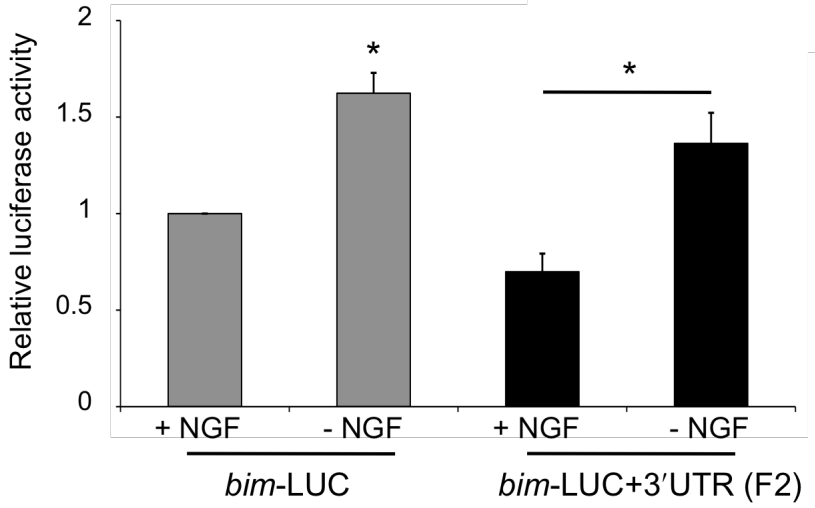
Relative luciferase activity
2
1.5
1
0.5
0
*
*
+ NGF
- NGF
+ NGF
- NGF
bim-LUC
bim-LUC+3′UTR (F2)

B

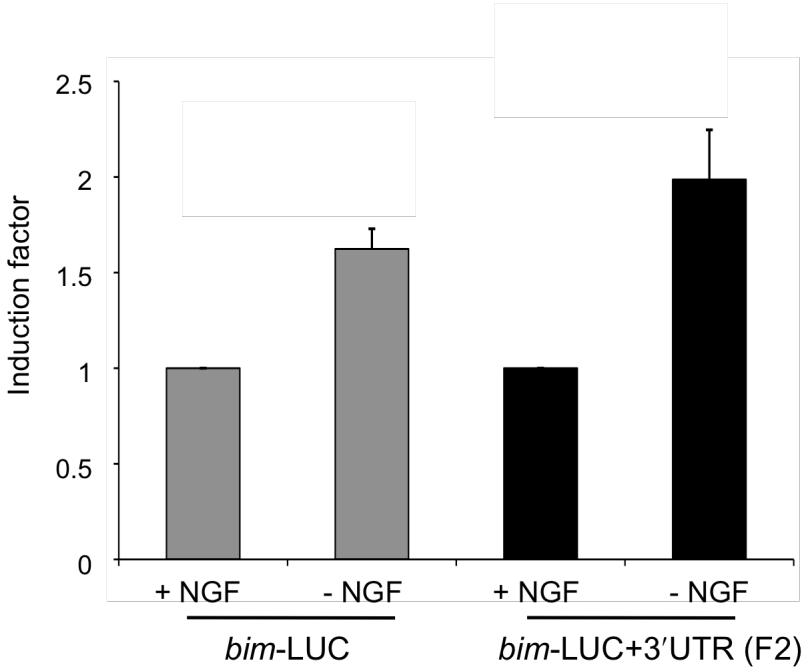
Induction factor
2.5
2
1.5
1
0.5
0
+ NGF
- NGF
+ NGF
- NGF
bim-LUC
bim-LUC+3′UTR (F2)

been reproduced by several other groups. In their study they used actinomycin-D at 0.1 μg/ml, therefore I also used this concentration of the inhibitor in these experiments. Initially, sympathetic neurons were treated with actinomycin-D over a time course from time point 0 hours to 16 hours, as 16 hours is the time point at which the original effect of U0126 was observed (Figure 5.1; Figure 5.6). Sympathetic neurons were either maintained in medium containing NGF (-U0126) or treated with U0126 at 10 μM in the presence of NGF (+U0126) (Figure 5.9). Actinomycin-D and U0126 were added to the cells together and then total RNA was isolated at the time points indicated (Figure 5.9A). The level of *bim* mRNA was analysed by Q-PCR relative to the level of the transcripts for the house-keeping genes *Hprt 1* and *Gapdh* (Figure 5.9). Both house-keeping genes behaved in a similar way as neither was affected by the addition of U0126 or actinomycin-D. Therefore only *bim* mRNA levels relative to *Hprt 1* are shown (Figure 5.9A, B and C). Following the addition of actinomycin-D, *bim* mRNA decays over the 16-hour time course in the absence of U0126 (Figure 5.9). The half-life of the rat *bim* mRNA appears to be between 2 and 4 hours in NGF-maintained sympathetic neurons (Figure 5.9A and B). Importantly, the addition of U0126 did not significantly increase the stability of the *bim* mRNA over the 16 hour time course (Figure 5.9A). To be certain that this was a representative result, I repeated the experiment by pre-treating sympathetic neurons with U0126 for 16 hours prior to the addition of actinomycin-D (for +U0126 conditions) (Figure 5.9B and C). This would therefore rule out the possibility that actinomycin-D was interfering with the activity of U0126. However, the same result was obtained with no significant difference in the stability of the *bim* mRNA in sympathetic neurons treated with or without U0126 (Figure 5.9B). I can therefore conclude that U0126 does not increase *bim* mRNA levels by altering mRNA stability, in sympathetic neurons.

The initial experiments with U0126 were performed by semi-quantitative RT-PCR (Figure 5.1). Q-PCR is a much more sensitive technique for determining mRNA levels than semi-quantitative RT-PCR, therefore it was important to reproduce my initial conclusions by Q-PCR. Following treatment with U0126 for 16 hours (+U0126), the level of *bim* mRNA is significantly elevated compared to the control cells (-U0126) (Figure 5.9C). At time point 0 (prior to the addition of actinomycin-D)

Figure 5.9 U0126 does not alter *bim* mRNA stability in sympathetic neurons.

(A) Sympathetic neurons were treated with actinomycin-D at 0.1 μg/ml in the presence of NGF. The cells were either maintained in medium containing NGF (-U0126) or treated with U0126 at 10 μM in the presence of NGF (+U0126). Actinomycin-D and U0126 were added to the cells together and then total RNA was isolated at time point 0 hours, 2 hours, 4 hours, 8 hours and 16 hours. The level of *bim* mRNA was analysed by Q-PCR relative to the level of the mRNAs encoded by the house-keeping genes *Hprt 1* and *Gapdh*. *Bim* mRNA levels relative to *Hprt 1* are shown here. Q-PCR experiments were carried out 5 times and data is presented as the mean ± S.E. There is no significant difference in the stability of *bim* mRNA in sympathetic neurons treated with or without U0126 over 16 hours.

(B) Sympathetic neurons were treated with actinomycin-D at 0.1 μg/ml in the presence of NGF. The cells were either maintained in medium containing NGF (-U0126) or treated with U0126 at 10 μM in the presence of NGF (+U0126). U0126 was added to the cells for 16 hours prior to the addition of actinomycin-D and U0126 together (for +U0126 conditions). Following addition of actinomycin-D, total RNA was isolated at time point 0 hours, 2 hours, 4 hours, 8 hours and 16 hours. The level of *bim* mRNA was analysed by Q-PCR relative to the house-keeping genes *Hprt 1* and *Gapdh*. *Bim* mRNA levels relative to *Hprt 1* are shown here. Q-PCR experiments were carried out 3 times and data is presented as the mean ± S.E. There is no significant difference in the stability of *bim* mRNA in sympathetic neurons treated with or without U0126 over 16 hours.

U0126 was dissolved in DMSO and therefore an equal volume of DMSO was added to untreated cells (-U0126).

(C) Q-PCR data from (B) with raw *bim* mRNA levels at timepoint 0 (+U0126 and -U0126 *bim* mRNA levels have not been normalised to 1). Treatment with U0126 for 16 hours elevates *bim* mRNA levels significantly (**).

A

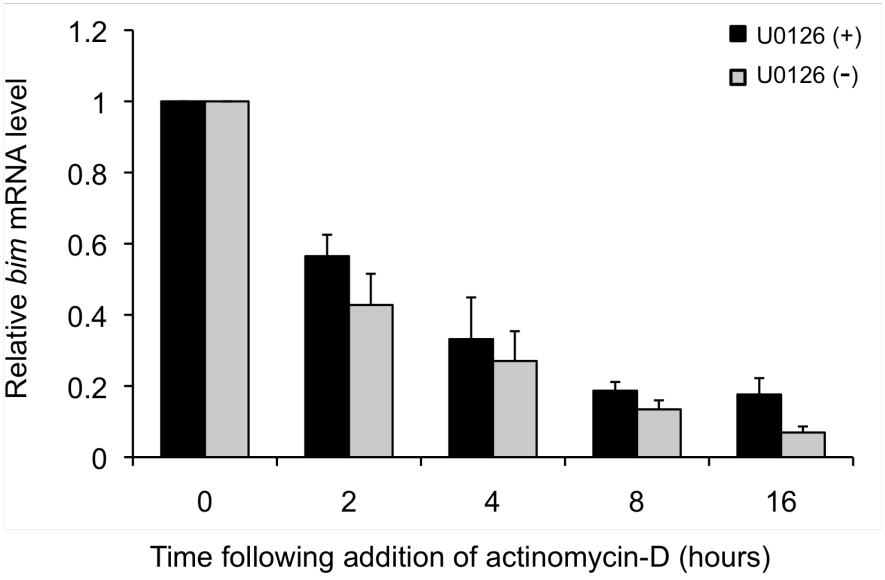
1.2
1
0.8
0.6
0.4
0.2
0
Relative bim mRNA level
U0126 (+)
U0126 (-)
0
2
4
8
16
Time following addition of actinomycin-D (hours)

B

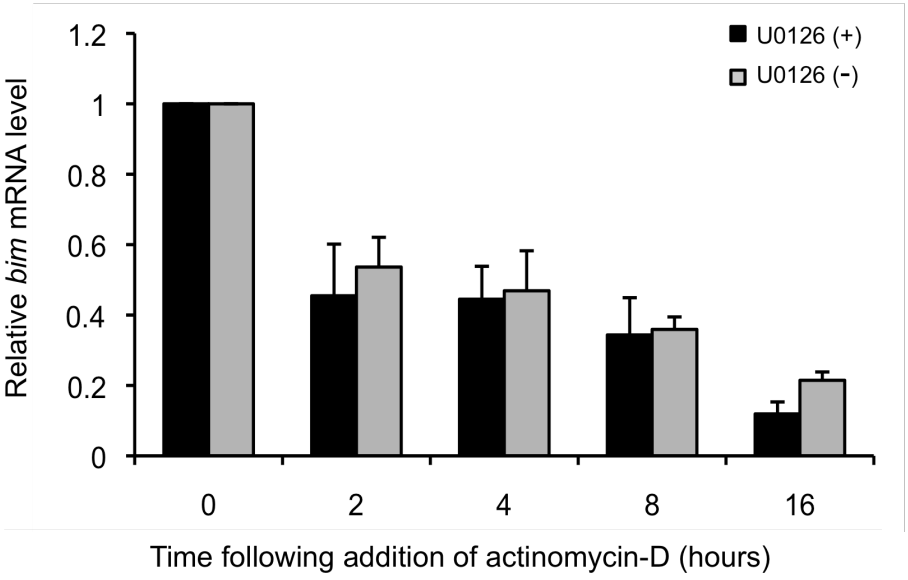
1.2
1
0.8
0.6
0.4
0.2
0
Relative bim mRNA level
U0126 (+)
U0126 (-)
0
2
4
8
16
Time following addition of actinomycin-D (hours)

C

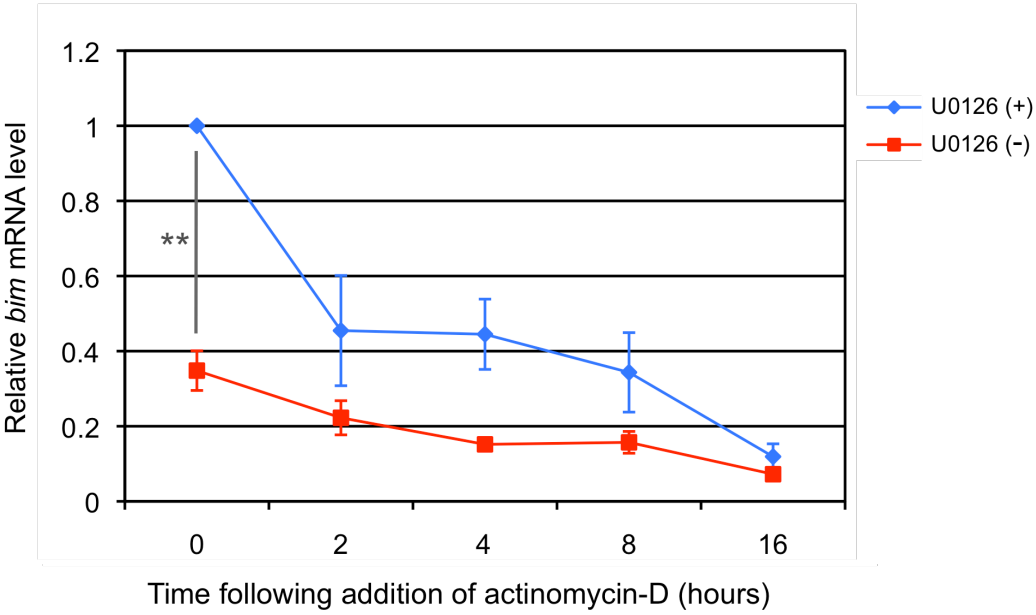
1.2
1
0.8
0.6
0.4
0.2
0
Relative bim mRNA level
**
U0126 (+)
U0126 (-)
0
2
4
8
16
Time following addition of actinomycin-D (hours)

bim mRNA levels are ~3 fold higher after 16 hours in the presence of U0126 (Figure 5.9C). Therefore, this result confirms my initial finding that the MEK/ERK pathway negatively regulates *bim* expression in sympathetic neurons.

5.3 Discussion

I have demonstrated that the MEK/ERK signalling pathway negatively regulates *bim* expression in sympathetic neurons via the *bim* 3′ UTR. This effect is independent of the PI3-K/Akt pathway and represses *bim* transcription in the presence of NGF (Figure 5.10).

After initially establishing that the 5′ end of the *bim* gene does not mediate the effect of the MEK/ERK pathway, I mapped the rat *bim* 3′ UTR by 3′ RACE and constructed a *bim*-LUC+3′UTR reporter construct to investigate this mechanism further (Figure 5.3; Figure 5.4). This proved to be a useful tool. Not only does it demonstrate that the *bim* 3′ UTR mediates the regulatory effect that is exerted on *bim* expression by MEK/ERK signalling, but this construct better represents the endogenous *bim* gene with low basal expression levels in the presence of NGF and an increased induction factor following NGF withdrawal, compared to our original *bim*-LUC reporter construct (Figure 5.5; Figure 5.6).

The 3′ UTR of a gene is often a target for post-transcriptional regulation by microRNAs and RNA-binding proteins. Therefore, I hypothesised that the MEK/ERK pathway may control *bim* expression at the level of mRNA stability or translation. I scanned the *bim* 3′ UTR using TargetScan software (Lewis *et al*., 2005) and found that the *bim* 3′ UTR contains hundreds of predicted miRNA binding sites. At that time there was no published work indicating that *bim* is a target for regulation by miRNAs and due to the scale of a miRNA study I decided to exam other possible regulatory mechanisms first. I found that the *bim* 3′ UTR contains a number of AU-rich elements (AREs), which are known to control the stability of an mRNA by targeting it for rapid degradation (Barreau *et al*., 2005; Roretz and Gallouzi, 2008). Matsui *et al*. (2007) also studied AU-rich elements in the *bim* 3′ UTR. They focused on 3 AREs within a 1 kb stretch of the *bim* 3′ UTR, these are the most 3′ out of the 4 conserved AREs that I investigated here (Figure 5.7). They used the Baf-3 cell line to show that heat shock cognate protein 70 (Hsc 70) binds to the AREs and enhances *bim* mRNA stability. They found that Hsc 70 is regulated by a number of different co-chaperones and these are regulated when cytokines activate Ras pathways. Since Ras is upstream of

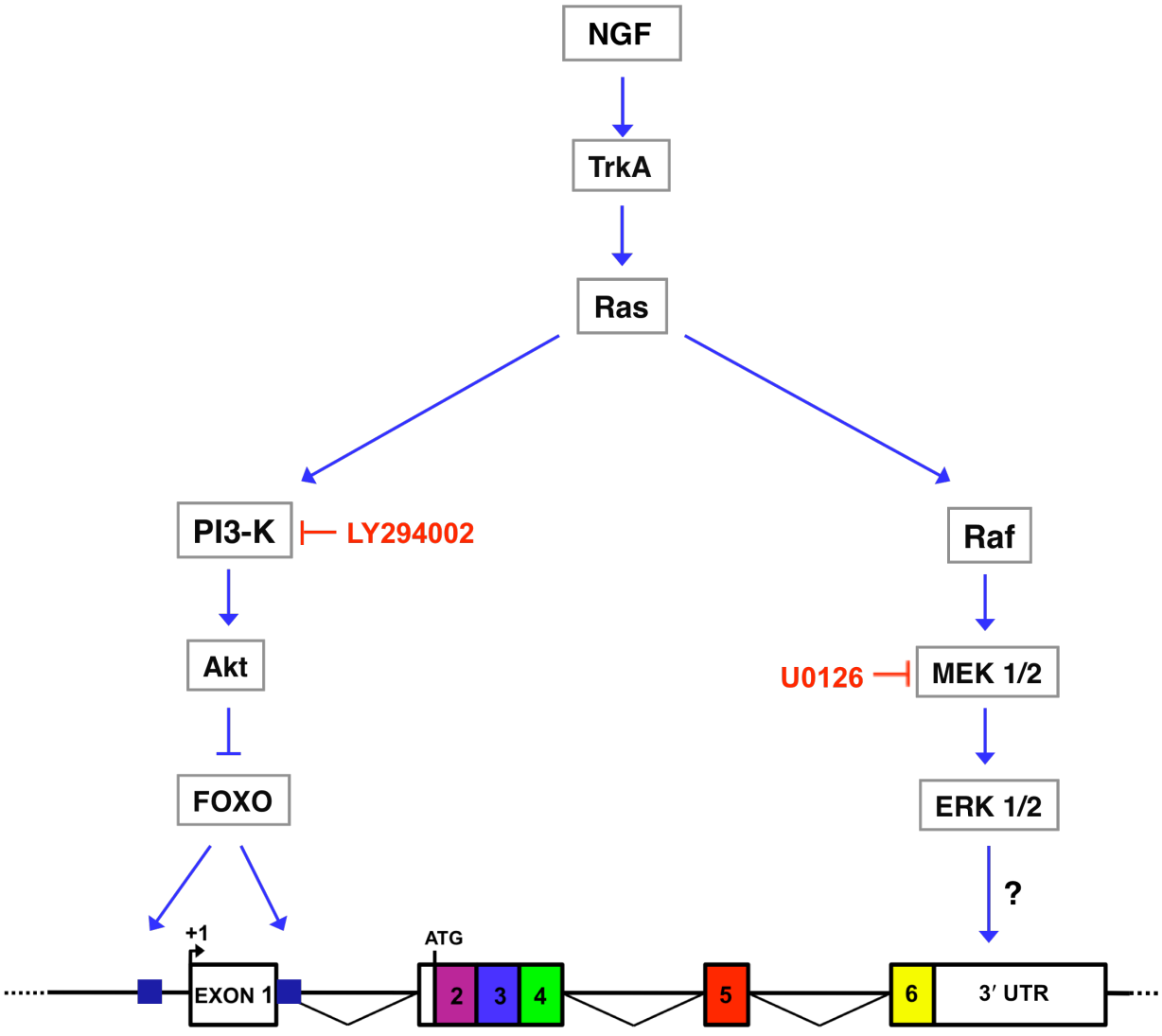

Figure 5.10 Model of the transcriptional regulation of *bim* expression by prosurvival signalling pathways in sympathetic neurons.

The MEK/ERK pathway negatively regulates *bim* expression at the level of transcription via the 3′ UTR by an unknown mechanism. PI3-K/Akt signalling inhibits FOXO transcription factors which can bind to conserved FOXO sites in the *bim* promoter, as indicated by the dark blue squares (Gilley *et al*., 2003). Both prosurvival pathways are activated following the binding of NGF to TrkA and act independently of each other to reduce *bim* expression.

MEK/ERK signalling it was possible that Matsui *et al*. had also been studying the negative regulation of *bim* by the MEK/ERK pathway. I found that mutation of the AREs described by Matsui *et al*. in the context of the *bim*-LUC+3′UTR construct, does partially reverse the increase in *bim* activation following NGF withdrawal conferred by the addition of the 3′ UTR, although this result was not significant. Therefore, it appears that the AREs studied by Matsui *et al*. do make some contribution to the induction of *bim* following NGF withdrawal in this context (Figure 5.7). Of course, it is possible that more than the 4 conserved AREs in the rat *bim* 3′ UTR may need to be mutated in order to see a striking effect. As the next step to investigate the mechanism by which the *bim* 3′ UTR is negatively regulated by the MEK/ERK pathway, I decided to try to identify the general region of the 3′ UTR that is responsive to NGF withdrawal. I found that the highly conserved second half of the *bim* rat 3′ UTR does not fully reproduce the effect of the whole region (Figure 5.8). Additionally, this data provides evidence that the mechanism I have investigated is not the same as that described by Matsui *et al*. (2007), since the 1 kb region of the *bim* 3′ UTR that they studied is within the 2.5 kb region that I studied here.

I found that *bim* mRNA levels are significantly elevated at 16 hours following addition of U0126 (Figure 5.1; Figure 5.9). Therefore, the mechanism by which the MEK/ERK pathway regulates *bim* expression must either be at the level of transcription or at the level of mRNA stability. I studied mRNA stability by treating sympathetic neurons with an inhibitor of transcription, actinomycin-D. I observed *bim* mRNA decay over a 16 hour time course and found that U0126 does not enhance *bim* mRNA stability (Figure 5.9). Taken together, my data indicates that the MEK/ERK pathway does not affect the stability of *bim* mRNA and therefore the mechanism that I have been investigating must be a transcriptional effect.

There are a number of important elements that can be found within genomic sequences that encode the 3′ UTR that contribute to the transcriptional regulation of a gene. Enhancer elements and silencer elements are transcriptional elements found far from the core promoter (Ogbourne and Antalis, 1998). Enhancer elements are generally one or more transcription factor binding sites that acting cooperatively and are able to interact with the core promoter by ‘DNA looping’ (Szutorisz *et al*., 2005).

Typically, silencer elements bind DNA-binding proteins that have a repressive effect on transcription (Ogbourne and Antalis, 1998). It is unclear whether the *bim* 3′ UTR harbours transcriptional enhancers and/or silencers and which of these are relevant in this context. However, based on what has been learned so far about the complex nature of the *bim* 3′ UTR, it is likely that there are a number of transcriptional elements within this 4.3 kb region. I found that the whole 3′ UTR is necessary to reproduce the full regulation of *bim* following NGF withdrawal (Figure 5.8), therefore there may be a number of transcriptional elements within the *bim* 3′ UTR that act cooperatively following the inhibition of the MEK/ERK pathway that occurs when sympathetic neurons are deprived of NGF, or treated with U0126.

As a further complication, U0126 also inhibits the most-recently identified member of the MAPK family, ERK5 (Balmanno and Cook, 2009). Previously there were no compounds that could distinguish between these two closely related MAPK signalling pathways. However, selective ERK1/ERK2 inhibitors have now been developed such as PD0325901 (Bain *et al*., 2007). Finegan *et al*. (2009) showed that the *in vitro* deletion of *erk5* in sympathetic neurons resulted in an increase in apoptosis. In contrast to my findings, Finegan *et al*. found that our *bim*-LUC reporter construct is activated when the PC6-3 subline of PC12 cells are treated with 10 μM U0126. However, the authors observed this effect following incubation with U0126 for 36 hours, replacing the inhibitor every 12 hours. In sympathetic neurons the level of *bim* RNA peaks at 16 hours after NGF withdrawal (Whitfield *et al*., 2001; Gilley *et al*., 2003). At 16 hours following treatment with U0126, I have shown that the *bim*-LUC reporter is not activated whereas the *bim*-LUC+3′UTR reporter is significantly activated (Figure 5.3, Figure 5.6). It is possible that the activation of *bim*-LUC after 36 hours incubation with U0126, as shown by Finegan *et al*. (2009) is an indirect effect.

Very recently Terasawa *et al*. (2009) also established a link between *bim* mRNA expression and MEK/ERK signalling. They used PC12 cells to identify a mechanism in which NGF withdrawal and subsequent inhibition of the MEK/ERK pathway leads to a decrease in the level of miR-221/222. The overexpression of miR-221 or miR-222 in PC12 cells suppressed the activity of a *bim*-LUC reporter construct that contained a 3′ region of the *bim* 3′ UTR. Taken together with my findings, this

suggests that MEK/ERK signalling can regulate *bim* expression at the level of transcription and at the level of mRNA stability/translation in neuronal cells.

Chapter 6: General discussion

Bim is a critical regulator of apoptosis in many cell types and as such, its deregulation has been implicated in certain human pathologies (Bouillet *et al*., 2001b; Biswas *et al*., 2007a; Doonan *et al*., 2007; McKerman and Cotter, 2007; Perier *et al*., 2007). Since the Bim protein was identified as a potent inducer of cell death via the intrinsic pathway there has been significant research into the different modes of Bim regulation. Consequently, it is now evident that a number of complex regulatory mechanisms are in place to constrain the expression and activity of the Bim protein and this has been complicated by the fact that many of these appear to be cell type specific. I have used the well-characterised model of NGF-dependent developing sympathetic neurons to further study the mechanisms by which the *bim* gene is regulated.

Until now, little was known about the function of the TATA-less *bim* proximal promoter. In this study I have shown that an NF-Y-binding CCAAT box controls the majority of *bim* basal promoter activity and that expression of a dominant negative NF-YA protein prevents the transcriptional activation of a *bim* reporter construct following NGF withdrawal. Moreover, NF-Y activity is required for the expression of the endogenous Bim protein and thereby contributes to apoptosis induced by NGF withdrawal. Additionally, I have demonstrated that the transcriptional coactivators CBP/p300 are required for efficient activation of *bim*-LUC when sympathetic neurons are deprived of NGF. My findings also indicate that CBP and p300 are recruited to the endogenous *bim* promoter in neuronally differentiated PC12 cells following NGF withdrawal, where they may interact with NF-Y to enhance *bim* transcription.

However, a number of unanswered questions remain. For example, does FOXO3a interact with CBP/p300 in this context? If my predicted model (Figure 4.6) is accurate then there should be limited interaction, if any, between CBP/p300 and FOXO3a in the presence of NGF, since active Akt phosphorylates FOXO3a, which would then be sequestered in the cytoplasm by 14-3-3 proteins (Gilley *et al*., 2003). Following NGF withdrawal FOXO3a translocates into the nucleus in sympathetic neurons where it would be able to bind to the two FOXO sites in the *bim* promoter and possibly interact with CBP/p300. Therefore, in NGF-deprived sympathetic neurons there should be a

significant increase in the amount of FOXO3a bound to CBP/p300 in the nucleus. Activation of the *bim* promoter by FOXO3a was previously studied by Gilley *et al*. (2003): These authors showed that the 5′ end of the *bim* gene contains two conserved FOXO sites, one in the promoter and one just downstream of exon 1, which can bind a GST-FOXO3a fusion protein *in vitro* in EMSA experiments. Essafi *et al*. (2005) also showed in BV137 cells (a human lymphoid CML cell line) that the upstream FOXO site can bind FOXO3a in ChIP experiments. However, it will be important to study whether the binding of FOXO3a to both FOXO sites increases after NGF withdrawal in neuronally differentiated PC12 cells. This would be predicted to be the case since it was necessary to mutate both FOXO sites in our *bim*-LUC reporter construct to significantly reduce the activation of *bim*-LUC, by overexpression of a constitutively active FOXO3a mutant and following NGF withdrawal (Gilley *et al*., 2003; Gilley and Ham, 2005). It would also be interesting to establish whether CBP/p300 interacts with the other transcription factors that bind to the *bim* promoter, for instance c-Jun. The role of c-Jun in NGF withdrawal-induced death and the induction of *bim* has been well documented (Estus *et al*., 1994; Ham *et al*., 1995; Xia *et al*., 1995; Virdee *et al*., 1997; Eilers *et al*., 1998; Harding *et al*., 2001; Harris and Johnson, 2001; Whitfield *et al*., 2001; Palmada *et al*., 2002; Besirli *et al*., 2005), and some conserved AP-1 binding sites located at the 5′ end of the *bim* gene are occupied by c-Jun in chromatin IP experiments (R. Randall, J. Gilley, R. Hughes and J. Ham, unpublished data). However, further work is necessary to understand the precise role of each of these AP-1 sites in *bim* promoter induction.

Previous studies have highlighted the importance of CBP/p300 in p53-dependent apoptosis (Goo and Roeder, 1997; Avantagiatti *et al*., 1999; Iyer *et al*., 2004). However, the work described here is one of the first studies to investigate the role of CBP/p300 in NGF withdrawal-induced cell death. By microinjecting specific antibodies I showed that both CBP and p300 contribute to the induction of the *bim*-LUC reporter construct after NGF withdrawal. However, in the future it will be important to show that CBP and p300 contribute to the induction of the endogenous *bim* gene in sympathetic neurons. One way to do this would be to isolate sympathetic neurons form $cbp^{FL/FL}$ and $p300^{FL/FL}$ mice and infect them with an adenovirus expressing CRE recombinase (Kasper *et al*., 2006). The

effect of the conditional knockout of the *cbp* and/or *p300* genes on Bim protein expression could then be measured.

The simultaneous interaction of multiple transcription factors with CBP/p300 has been proposed to contribute to transcriptional synergy (Vo and Goodman, 2001). Therefore, further Co-IP experiments to investigate the protein-protein interactions of CBP/p300 with FOXO3a, c-Jun and the Myb proteins, may yield interesting results. Further to this, it is possible that like the *IFN-β* promoter, the transcription factors known to occupy the *bim* promoter following NGF withdrawal, together with other transcriptional cofactors and the coactivators CBP/p300, form a multi-protein enhanceosome. The assembly of a number of regulatory proteins on the *IFN-β* promoter creates a stereospecific interaction surface for the recruitment of CBP/p300 and the basal transcription machinery (Kim *et al*., 1998; Merika *et al*., 1998; Wathelet *et al*., 1998; Yie *et al*., 1999). The resulting multi-protein structure, an enhanceosome, promotes pre-initiation complex formation and allows multiple rounds of transcription to proceed (Kim *et al*., 1998; Merika *et al*., 1998; Wathelet *et al*., 1998; Yie *et al*., 1999). Furthermore, NF-Y has been demonstrated to associate with the TATA-box binding protein (TBP), TBP-associated factors (TAFs) and TFIID and can therefore facilitate preinitiation complex formation and recruit RNA polymerase II to the promoters of CCAAT box-containing genes (Bellorini *et al*., 1997; Frontini *et al*., 2002; Kabe *et al*., 2005). Since *bim* lacks a TATA box, NF-Y bound to the ICB may well play a role in recruiting the basal transcription machinery to the *bim* promoter and initiating transcription from the major transcriptional start site, which is 29 bp downstream of the ICB in the rat *bim* gene.

I have shown that NF-Y binds to the *bim* promoter in the presence of NGF and following NGF withdrawal, but it is unclear whether NF-Y is the target of regulatory mechanisms other than direct protein-protein contact with CBP/p300. For instance, a number of reports have shown that NF-Y is a target for acetylation by CBP/p300 (Li *et al*., 1998; Franiello *et al*., 1999; Manni *et al*., 2008). In addition, the NF-YA subunit can be phosphorylated and a phosphorylation-deficient mutant form of NF-YA has impaired DNA-binding activity (Yun *et al*., 2003). It is not known whether NF-Y is regulated by post-translational modifications in sympathetic neurons or whether the state of the trimeric NF-Y protein changes following NGF withdrawal. However this could be

studied in the future by performing immunoblotting experiments with antibodies to each NF-Y subunit and extracts from sympathetic neurons cultured in the presence of NGF and following NGF withdrawal. Changes in the phosphorylation of the subunits might lead to changes in the mobility of NF-YA, B or C in SDS polyacrylamide gels. Furthermore, it will be interesting to determine whether other transcription factors, regulated by NGF withdrawal, bind to sites in the *bim* promoter that are immediately adjacent to the ICB. In some systems, NF-Y has been shown to bind cooperatively to the DNA with transcription factors whose activity is regulated by signalling pathways. For example, some promoters activated by ER stress contain ER stress-responsive elements that consist of a CCAAT box and adjacent ATF6 binding site. ATF6 is activated by ER stress and translocates into the nucleus where it binds cooperatively with NF-Y. Mutation of either the CCAAT box or ATF6 site in such promoters inhibits the response to ER stress (Yoshida *et al*., 2000).

My findings suggest that NF-Y is a critical regulator of *bim* expression in NGF withdrawal-induced apoptosis. However, is NF-Y important for *bim* expression in other systems considering that many of the regulatory mechanisms controlling *bim* activity appear to be cell type specific? As discussed previously, functional NF-Y levels are regulated by the concentration of the NF-YA subunit present within the cell, whereas NF-YB and NF-YC appear to be constitutively expressed in most cell types (Manni *et al*., 2008). This is why the YA13m29 mutant was generated to target NF-YA activity and also why I have focused on the NF-YA subunit in this study. *NF-YA* encodes two isoforms generated through alternative splicing (Mantovani, 1999). Zhu *et al*. (2003) demonstrated that the short transcript of NF-YA is highly expressed in immature c-kit^{+} bone marrow cells, but following haematopoietic differentiation, its expression declines rapidly. A later study from the same authors provided evidence that NF-Y might be a master gene in the processes of haematopoietic self-renewal and differentiation (Zhu et al., 2005). It would be interesting to examine whether *bim* expression also changes in these cells during this time when the cellular concentration of NF-YA becomes limiting. It would also be of interest to investigate whether NF-YA expression changes during the development of sympathetic neurons and which of two NF-YA transcripts is predominantly expressed in these cells. Furthermore, it is possible that other genes

involved in the cell death programme are NF-Y targets, since CCAAT boxes are present in around 30% of eukaryotic promoters and NF-Y is the major CCAAT-binding protein (Bucher, 1990; Mantovani, 1999).

Due to the well-established role of NF-Y in cell cycle control, and the potential role of NF-Y as a p53 target in oncogenesis, there has been increasing interest to develop small molecule drugs to inhibit NF-Y binding. Recently, GWL-78, a pyrrolobenzodiazepine-poly(*N*-methylpyrrole) conjugate, has been shown to inhibit NF-Y binding to CCAAT box sequences and also to displace NF-Y that is already bound to the promoter of CCAAT box-containing genes (Kotecha *et al*., 2008). This drug could provide a tool to further study the importance of NF-Y in neurons and other cell types.

As a second area of this study, I investigated the negative regulation of *bim* expression by the MEK/ERK signalling pathway in sympathetic neurons. I found that when sympathetic neurons are treated with the compound U0126, an inhibitor of the MEK/ERK pathway, the steady-state level of *bim* mRNA in the presence of NGF increases significantly. By mapping the rat *bim* 3′ UTR by 3′ RACE and generating a *bim*-LUC+3′UTR reporter construct, I localised the region responsive to MEK/ERK signalling to the 3′ UTR and investigated possible mechanisms for this regulation. Taken together, my data demonstrates that the MEK/ERK signalling pathway negatively regulates *bim* gene expression independently of the PI3-K/Akt pathway via the genomic region that contains the 3′ UTR in sympathetic neurons.

The precise mechanism by which the MEK/ERK signalling pathway represses *bim* expression in the presence of NGF remains unclear. I chose to investigate the role of conserved AU-rich elements in the *bim* 3′ UTR. However, the results were not entirely conclusive because mutation of the four conserved AREs only produced a partial effect. The results suggest that either the AREs located in the *bim* 3′ UTR do not play a major role, or that more of the 10 AUUUA repeats, found in the rat *bim* 3′ UTR, must be mutated to see a significant effect. This may well be the case since AREs are known to cooperate with each other for full function (Chen and Shyu, 1995). However, in contrast, class I AREs (individual, scattered AUUUA repeats), as identified within the *bim* 3′ UTR, tend to be present as no more than 3 functional binding sites (Chen and Shyu, 1995; Bakheet *et al*., 2006).

Despite the possible role of AU-rich elements in regulating *bim* expression, I obtained evidence that the MEK/ERK signalling pathway does not regulate *bim* mRNA stability in sympathetic neurons. Treatment of sympathetic neurons with U0126 and an inhibitor of transcription, actinomycin-D, demonstrated that inhibition of MEK/ERK signalling does not increase the stability of the *bim* mRNA over a 16 hour time course. Therefore, I can conclude that the mechanism that I have identified in sympathetic neurons is yet another means to control *bim* expression at the level of transcription, either through *cis*-acting enhancer or silencer elements within the *bim* 3′ UTR. In the future, transcription factor binding sites in the *bim* 3′ UTR could be identified and studied by using a similar approach as I have used to investigate the role of the NF-Y-binding CCAAT box in the *bim* proximal promoter. Since the only other reports to study the function of the *bim* 3′ UTR in regulating *bim* expression have been associated with *bim* mRNA stability, it is likely the mechanism that I have investigated here has not been observed in other cell types. Again, these findings prompt the question of whether this is a level of regulation that is specific to neuronal cells.

Further experiments will also determine which of the MAPK signalling pathways targets this region of the *bim* gene, since in sympathetic neurons both the MEK1/2/ERK1/2 and the MEK5/ERK5 signalling pathways are stimulated in response to NGF and are activated downstream from Ras (Kaplan and Miller, 2000; Wang and Tournier, 2006). A number of studies have described the importance of MEK1/2/ERK1/2 signalling in the post-translational control of the Bim protein in different cell types (Biswas and Greene, 2002; Luciano *et al*., 2003; Ley *et al*., 2004; Marani *et al*., 2004; Ley *et al*., 2005b; Ewings *et al*., 2007). The downstream transcriptional events involved in MEK5/ERK5 signalling in neurons are less well established, but recent data suggests that ERK5 may play an important role in neurotrophin-mediated survival, and deletion of the *erk5* gene results in a significant increase in apoptosis in developing sympathetic neurons (Finegan *et al*., 2009).

BH3-only proteins are ultimately the mediators of proapoptotic signals that predominantly activate the intrinsic pathway of apoptosis within a cell. Bim is one of the best-studied BH3-only proteins and consequently much has been learned about its role in the cell death programme. The diverse nature of the mechanisms that regulate *bim*

expression in different cell types suggests that the control of *bim* activity is multifaceted, and this therefore introduces a further level of complexity to the regulation of *bim* function in response to different apoptotic stimuli. It has previously been suggested that the *bim* promoter acts as a coincidence detector in neuronal cells (Biswas *et al*., 2007b). This may well be an accurate description in sympathetic neurons, in which multiple, seemingly non-redundant signalling pathways are involved in the activation of *bim* transcription and the loss of only one activating pathway is enough to significantly impair the induction of *bim* transcription in response to NGF withdrawal. Therefore, the highly complex and stringent nature of *bim* regulation in neurons ensures that apoptosis, and ultimately the suicide of a cell, is initiated only when absolutely necessary.

References

Abbott, A.L., Alvarez-Saavedra, E., Miska, E.A., Lau, N.C., Bartel, D.P., Horvitz, H.R. and Ambros, V. (2005) The let-7 MicroRNA family members mir-48, mir-84, and mir-241 function together to regulate developmental timing in Caenorhabditis elegans. *Developmental Cell*, **9**, 403-414.

Acehan, D., Jiang, X., Morgan, D.G., Heuser, J.E., Wang, X. and Akey, C.W. (2002) Three-dimensional structure of the apoptosome: implications for assembly, procaspase-9 binding, and activation. *Molecular Cell*, **9**, 423-432.

Ait-Si-Ali, S., Ramirez, S., Barre, F.X., Dkhissi, F., Magnaghi-Jaulin, L., Girault, J.A., Robin, P., Knibiehler, M., Pritchard, L.L., Ducommun, B. *et al*. (1998) Histone acetyltransferase activity of CBP is controlled by cycle-dependent kinases and oncoprotein E1A. *Nature*, **396**, 184-186.

Akiyama, T., Bouillet, P., Miyazaki, T., Kadono, Y., Chikuda, H., Chung, U.I., Fukuda, A., Hikita, A., Seto, H., Okada, T. *et al*. (2003) Regulation of osteoclast apoptosis by ubiquitylation of proapoptotic BH3-only Bcl-2 family member Bim. *The EMBO Journal*, **22**, 6653-6664.

Alberts, A.S., Geneste, O. and Treisman, R. (1998) Activation of SRF-regulated chromosomal templates by Rho-family GTPases requires a signal that also induces H4 hyperacetylation. *Cell*, **92**, 475-487.

Alderden, R.A., Mellor, H.R., Modok, S., Hambley, T.W. and Callaghan, R. (2006) Cytotoxic efficacy of an anthraquinone linked platinum anticancer drug. *Biochemical Pharmacology*, **71**, 1136-1145.

Ambrosini, G., Seelman, S.L. and Schwartz, G.K. (2009) Differentiation-related gene-1 decreases Bim stability by proteasome-mediated degradation. *Cancer Research*, **69**, 6115-6121.

Andreassi, C. and Riccio, A. (2009) To localize or not to localize: mRNA fate is in 3'UTR ends. *Trends in Cell Biology*, **19**, 465-474.

Antonsson, B., Montessuit, S., Lauper, S., Eskes, R. and Martinou, J.C. (2000) Bax oligomerization is required for channel-forming activity in liposomes and to trigger cytochrome c release from mitochondria. *The Biochemical Journal*, **345**, 271-278.

Antonsson, B., Montessuit, S., Sanchez, B. and Martinou, J.C. (2001) Bax is present as a high molecular weight oligomer/complex in the mitochondrial membrane of apoptotic cells. *The Journal of Biological Chemistry*, **276**, 11615-11623.

Arama, E., Bader, M., Srivastava, M., Bergmann, A. and Steller, H. (2006) The two Drosophila cytochrome C proteins can function in both respiration and caspase activation. *The EMBO Journal*, **25**, 232-243.

Arias, J., Alberts, A.S., Brindle, P., Claret, F.X., Smeal, T., Karin, M., Feramisco, J. and Montminy, M. (1994) Activation of cAMP and mitogen responsive genes relies on a common nuclear factor. *Nature*, **370**, 226-229.

Ashkenazi, A. and Dixit, V.M. (1998) Death receptors: signaling and modulation. *Science,* **281**, 1305-1308.

Avantaggiati, M.L., Ogryzko, V., Gardner, K., Giordano, A., Levine, A.S. and Kelly, K. (1997) Recruitment of p300/CBP in p53-dependent signal pathways. *Cell*, **89**, 1175-1184.

Bain, J., Plater, L., Elliott, M., Shpiro, N., Hastie, C.J., McLauchlan, H., Klevernic, I., Arthur, J.S., Alessi, D.R. and Cohen, P. (2007) The selectivity of protein kinase inhibitors: a further update. *The Biochemical Journal*, **408**, 297-315.

Bakheet, T., Williams, B.R. and Khabar, K.S. (2006) ARED 3.0: the large and diverse AU-rich transcriptome. *Nucleic Acids Research*, **34**, 111-114.

Bakhshi, A., Jensen, J.P., Goldman, P., Wright, J.J., McBride, O.W., Epstein, A.L. and Korsmeyer, S.J. (1985) Cloning the chromosomal breakpoint of t(14;18) human lymphomas:

clustering around JH on chromosome 14 and near a transcriptional unit on 18. *Cell*, **41**, 899-906.

Balmano, K. and Cook, S.J. (2009) Tumour cell survival signalling by the ERK1/2 pathway. *Cell Death and Differentiation*, **16**, 368-377.

Bamji, S.X., Majdan, M., Pozniak, C.D., Belliveau, D.J., Aloyz, R., Kohn, J., Causing, C.G. and Miller, F.D. (1998) The p75 neurotrophin receptor mediates neuronal apoptosis and is essential for naturally occurring sympathetic neuron death. *The Journal of Cell Biology*, **140**, 911-923.

Bannister, A.J., and Kouzarides, T. (1996) The CBP co-activator is a histone acetyltransferase. *Nature,* **384**, 641-643.

Barbacid, M. (1995) Neurotrophic factors and their receptors. *Current Opinion in Cell Biology*, **7**, 148-155.

Barde, Y.A. (1989) Trophic factors and neuronal survival. *Neuron*, **2**, 1525-1534.

Barreau, C., Paillard, L. and Osborne, H.B. (2005) AU-rich elements and associated factors: are there unifying principles? *Nucleic Acids Research*, **33**, 7138-7150.

Baskin-Bey, E.S., Washburn, K., Feng, S., Oltersdorf, T., Shapiro, D., Huyghe, M., Burgart, L., Garrity-Park, M., van Vilsteren, F.G., Oliver, L.K. *et al*. (2007) Clinical Trial of the Pan-Caspase Inhibitor, IDN-6556, in Human Liver Preservation Injury. *American Journal of Transplantation*, **7**, 218-225.

Becker, E.B., Howell, J., Kodama, Y., Barker, P.A. and Bonni, A. (2004) Characterization of the c-Jun N-terminal kinase-BimEL signaling pathway in neuronal apoptosis. *The Journal of Neuroscience*, **24**, 8762-8770.

Belliveau, D.J., Krivko, I., Kohn, J., Lachance, C., Pozniak, C., Rusakov, D., Kaplan, D. and Miller, F.D. (1997) NGF and neurotrophin-3 both activate TrkA on sympathetic neurons but differentially regulate survival and neuritogenesis. *The Journal of Cell Biology*, **136**, 375-388.

Bellorini, M., Lee, D.K., Dantonel, J.C., Zemzoumi, K., Roeder, R.G., Tora, L. and Mantovani, R. (1997) CCAAT binding NF-Y-TBP interactions: NF-YB and NF-YC require short domains adjacent to their histone fold motifs for association with TBP basic residues. *Nucleic Acids Research*, **25**, 2174-2181.

Benatti, P., Basile, V., Merico, D., Fantoni, L.I., Tagliafico, E. and Imbriano, C. (2008) A balance between NF-Y and p53 governs the pro- and anti-apoptotic transcriptional response. *Nucleic Acids Research*, **36**, 1415-1428.

Bernstein, E., Kim, S.Y., Carmell, M.A., Murchison, E.P., Alcorn, H., Li, M.Z., Mills, A.A., Elledge, S.J., Anderson, K.V. and Hannon, G.J. (2003) Dicer is essential for mouse development. *Nature Genetics*, **35**, 215-217.

Besirli, C.G., Wagner, E.F. and Johnson, E.M., Jr. (2005) The limited role of NH2-terminal c-Jun phosphorylation in neuronal apoptosis: identification of the nuclear pore complex as a potential target of the JNK pathway. *The Journal of Cell Biology*, **170**, 401-411.

Bessa, M., Saville, M.K. and Watson, R.J. (2001) Inhibition of cyclin A/Cdk2 phosphorylation impairs B-Myb transactivation function without affecting interactions with DNA or the CBP coactivator. *Oncogene*, **20**, 3376-3386.

Bhattacharjee, R.N., Underhill, C. and Torchia, J. (2001) Isolation of a p300/CBP cointegrator-associated protein coactivator complex. *Methods in Molecular Biology*, **176**, 249-260.

Bhattacharya A., Deng J.M., Zhang Z., Behringer R., de Crombrugghe B., Maity S.N. (2003). The B subunit of the CCAAT box binding transcription factor complex CBF (NF-YA) is essential for early mouse development and cell proliferation. *Cancer Research,* **63**, 8167-8172.

Bi, W., Wu, L., Coustry, F., de Crombrugghe, B., and Maity, S.N. (1997) DNA binding specificity of the CCAAT-binding factor CBF/NF-Y. *The Journal of Biological Chemistry,* **272**, 26562-26572.

Bilimoria, P. and Bonni A. (2008) Cultures of cerebellar granule neurons. *Cold Spring Harbor Laboratory Protocols*. doi:10.1101/pdb.prot5107.

Biswas, S.C. and Greene, L.A. (2002) Nerve growth factor (NGF) down-regulates the Bcl-2 homology 3 (BH3) domain-only protein Bim and suppresses its proapoptotic activity by phosphorylation. *The Journal of Biological Chemistry*, **277**, 49511-49516.

Biswas, S.C., Liu, D.X. and Greene, L.A. (2005) Bim is a direct target of a neuronal E2F-dependent apoptotic pathway. *The Journal of Neuroscience*, **25**, 8349-8358.

Biswas, S.C., Shi, Y., Sproul, A. and Greene, L.A. (2007) Pro-apoptotic Bim induction in response to nerve growth factor deprivation requires simultaneous activation of three different death signalling pathways. *The Journal of Biological Chemistry*, **282**, 29368-29374.

Biswas, S.C., Shi, Y., Vonsattel, J.P., Leung, C.L., Troy, C.M. and Greene, L.A. (2007) Bim is elevated in Alzheimer's disease neurons and is required for beta-amyloid-induced neuronal apoptosis. *The Journal of Neuroscience*, **27**, 893-900.

Blackwood, E.M. and Kadonaga, J.T. (1998) Going the distance: a current view of enhancer action. *Science,* **281**, 60-63.

Bodmer, J.L., Burns, K., Schneider, P., Hofmann, K., Steiner, V., Thome, M., Bornand, T., Hahne, M., Schroter, M., Becker, K. *et al*. (1997) TRAMP, a novel apoptosis-mediating receptor with sequence homology to tumor necrosis factor receptor 1 and Fas (Apo-1/CD95). *Immunity*, **6**, 79-88.

Bolognese, F., Wasner, M., Dohna, C.L., Gurtner, A., Ronchi, A., Muller, H., Manni, I., Mossner, J., Piaggio, G., Mantovani, R. *et al*. (1999) The cyclin B2 promoter depends on NF-Y, a trimer whose CCAAT-binding activity is cell-cycle regulated. *Oncogene*, **18**, 1845-1853.

Bonni, A., and Becker, E.B.E. (2006) Pin 1 mediates neural-specific activation of the mitochondrial apoptotic machinery. *Neuron* **49**, 655-662.

Borsello, T., Clarke, P.G., Hirt, L., Vercelli, A., Repici, M., Schorderet, D.F., Bogousslavsky, J. and Bonny, C. (2003) A peptide inhibitor of c-Jun N-terminal kinase protects against excitotoxicity and cerebral ischemia. *Nature Medicine*, **9**, 1180-1186.

Bouillet, P., Metcalf, D., Huang, D.C., Tarlinton, D.M., Kay, T.W., Kontgen, F., Adams, J.M. and Strasser, A. (1999) Proapoptotic Bcl-2 relative Bim required for certain apoptotic responses, leukocyte homeostasis, and to preclude autoimmunity. *Science*, **286**, 1735-1738.

Bouillet, P., Zhang, L.C., Huang, D.C.S., Webb, G.C., Bottema, C.D.K., Shore, P., Eyre, H.J., Sutherland, G.R., and Adams, J.M. (2001a) Gene structure, alternative splicing, and chromosomal localisation of pro-apoptotic Bcl-2 relative Bim. *Mammalian Genome,* **12**, 163-168.

Bouillet, P., Cory, S., Zhang, L.C., Strasser, A. and Adams, J.M. (2001b) Degenerative disorders caused by Bcl-2 deficiency prevented by loss of its BH3-only antagonist Bim. *Developmental cell*, **1**, 645-653.

Bouillet, P. and Strasser, A. (2002) BH3-only proteins - evolutionarily conserved proapoptotic Bcl-2 family members essential for initiating programmed cell death. *Journal of Cell Science*, **115**, 1567-1574.

Boyd, J.M., Gallo, G.J., Elangovan, B., Houghton, A.B., Maistrom, S., Avery, B.J., Ebb, R.G., Subramanian, T., Chittenden, T., and Lutz, R.J. (1995) Bik, a novel death-inducing protein shares a distinct sequence motif with Bcl-2 family proteins and interacts with viral and cellular survival-promoting proteins. *Oncogene* **11**, 1921-1928.

Bradford, M.M. (1976) A rapid and sensitive method for the quantitation of microgram quantities of protein utilizing the principle of protein-dye binding. *Analytical Biochemistry,* **72**: 248-254.

Brancolini, C., Benedetti, M. and Schneider, C. (1995) Microfilament reorganization during apoptosis: the role of Gas2, a possible substrate for ICE-like proteases. *The EMBO Journal*, **14**, 5179-5190.

Brennan, C., Rivas-Plata, K. and Landis, S.C. (1999) The p75 neurotrophin receptor influences NT-3 responsiveness of sympathetic neurons in vivo. *Nature Neuroscience*, **2**, 699-705.

Bucher, P. (1990) Weight matrix descriptions of four eukaryotic RNA polymerase II promoter elements derived from 502 unrelated promoter sequences. *Journal of Molecular Biology,* **212**, 563–578.

Caretti, G., Motta, M.C. and Mantovani, R. (1999) NF-Y associates with H3-H4 tetramers and octamers by multiple mechanisms. *Molecular and Cellular Biology*, **19**, 8591-8603.

Cavanaugh, J. E. (2004) Role of extracellular signal regulated kinase 5 in neuronal survival. *European Journal of Biochemistry*. **271**, 2056-2059.

Cazanave, S.C., Mott, J.L., Elmi, N.A., Bronk, S.F., Werneburg, N.W., Akazawa, Y., Kahraman, A., Garrison, S.P., Zambetti, G.P., Charlton, M.R. *et al*. (2009) JNK1-dependent PUMA expression contributes to hepatocyte lipoapoptosis. *The Journal of Biological Chemistry*, **284**, 26591-26602.

Chai, J., Du, C., Wu, J.W., Kyin, S., Wang, X. and Shi, Y. (2000) Structural and biochemical basis of apoptotic activation by Smac/DIABLO. *Nature*, **406**, 855-862.

Chai, J., Yan, N., Huh, J.R., Wu, J.W., Li, W., Hay, B.A. and Shi, Y. (2003) Molecular mechanism of Reaper-Grim-Hid-mediated suppression of DIAP1-dependent Dronc ubiquitination. *Nature Structural Biology*, **10**, 892-898.

Chan, H.M., and La Thangue, N.B. (2001) p300/CBP proteins: HATs for transcriptional bridges and scaffolds. *Journal of Cell Science,* **114**, 2363-2373.

Charriaut-Marlangue, C., Margaill, I., Represa, A., Popovici, T., Plotkine, M. and Ben-Ari, Y. (1996) Apoptosis and necrosis after reversible focal ischemia: an in situ DNA fragmentation analysis. *Journal of Cerebral Blood Flow & Metabolism*, **16**, 186-194.

Chen, C.Y., Chen, T.M. and Shyu, A.B. (1994) Interplay of two functionally and structurally

distinct domains of the c-fos AU-rich element specifies its mRNA-destabilizing function. *Molecular and Cellular Biology*, **14**, 416-426.

Chen, C.Y. and Shyu, A.B. (1995) AU-rich elements: characterization and importance in mRNA degradation. *Trends in Biochemical Sciences*, **20**, 465-470.

Chen, J.Z., Ji, C.N., Gu, S.H., Li, J.X., Zhao, E.P., Huang, Y., Huang, L., Ying, K., Xie, Y. and Mao, Y.M. (2004) Over-expression of Bim alpha3, a novel isoform of human Bim, result in cell apoptosis. *The International Journal of Biochemistry & Cell Biology*, **36**, 1554-1561.

Chen, L. and Widom, J. (2005) Mechanism of transcriptional silencing in yeast. *Cell*, **120**, 37-48.

Chen, L., Willis, S.N., Wei, A., Smith, B.J., Fletcher, J.I., Hinds, M.G., Colman, P.M., Day, C.L., Adams, J.M. and Huang, D.C. (2005) Differential targeting of prosurvival Bcl-2 proteins by their BH3-only ligands allows complementary apoptotic function. *Molecular Cell*, **17**, 393-403.

Cheng, E.H., Sheiko, T.V., Fisher, J.K., Craigen, W.J. and Korsmeyer, S.J. (2003) VDAC2 inhibits BAK activation and mitochondrial apoptosis. *Science,* **301**, 513-517.

Chipuk, J.E., Bouchier-Hayes, L. and Green, D.R. (2006) Mitochondrial outer membrane permeabilization during apoptosis: the innocent bystander scenario. *Cell Death and Differentiation*, **13**, 1396-1402.

Chipuk, J.E. and Green, D.R. (2008) How do BCL-2 proteins induce mitochondrial outer membrane permeabilization? *Trends in cell biology*, **18**, 157-164.

Cleary, M.L., Smith, S.D. and Sklar, J. (1986) Cloning and structural analysis of cDNAs for bcl-2 and a hybrid bcl-2/immunoglobulin transcript resulting from the t(14;18) translocation. *Cell*, **47**, 19-28.

Cottet, S. and Schorderet, D.F. (2009) Mechanisms of apoptosis in retinitis pigmentosa. *Current Molecular Medicine*, **9**, 375-383.

Coultas, L., Terzano, S., Thomas, T., Voss, A., Reid, K., Stanley, E.G., Scott, C.L., Bouillet, P., Bartlett, P., Ham, J. *et al*. (2007) Hrk/DP5 contributes to the apoptosis of select neuronal populations but is dispensable for haematopoietic cell apoptosis. *Journal of Cell Science*, **120**, 2044-2052.

Crowder, R.J. and Freeman, R.S. (1998) Phosphatidylinositol 3-kinase and Akt protein kinase are necessary and sufficient for the survival of nerve growth factor-dependent sympathetic neurons. *The Journal of Neuroscience*, **18**, 2933-2943.

Crowley, C., Spencer, S.D., Nishimura, M.C., Chen, K.S., Pitts-Meek, S., Armanini, M.P., Ling, L.H., McMahon, S.B., Shelton, D.L., Levinson, A.D. *et al*. (1994) Mice lacking nerve growth factor display perinatal loss of sensory and sympathetic neurons yet develop basal forebrain cholinergic neurons. *Cell*, **76**, 1001-1011.

Danial, N.N. and Korsmeyer, S.J. (2004) Cell death: critical control points. *Cell*, **116**, 205-219.

Das, C., Lucia, M.S., Hansen, K.C. and Tyler, J.K. (2009) CBP/p300-mediated acetylation of histone H3 on lysine 56. *Nature*, **459**, 113-117.

Datta, S.R., Katsov, A., Hu, L., Petros, A., Fesik, S.W., Yaffe, M.B. and Greenberg, M.E. (2000) 14-3-3 proteins and survival kinases cooperate to inactivate BAD by BH3 domain phosphorylation. *Molecular Cell*, **6**, 41-51.

DeCathelineau, A.M. and Henson, P.M. (2003) The final step in programmed cell death: phagocytes carry apoptotic cells to the grave. *Essays in biochemistry*, **39**, 105-117.

Deckwerth, T.L. and Johnson, E.M., Jr. (1993) Temporal analysis of events associated with programmed cell death (apoptosis) of sympathetic neurons deprived of nerve growth factor. *The Journal of Cell Biology*, **123**, 1207-1222.

Deckwerth, T.L., Elliott, J.L., Knudson, C.M., Johnson, E.M., Jr., Snider, W.D. and Korsmeyer, S.J. (1996) BAX is required for neuronal death after trophic factor deprivation and

during development. *Neuron*, **17**, 401-411.

Dehan, E., Bassermann, F., Guardavaccaro, D., Vasiliver-Shamis, G., Cohen, M., Lowes, K.N., Dustin, M., Huang, D.C., Taunton, J. and Pagano, M. (2009) betaTrCP- and Rsk1/2-mediated degradation of BimEL inhibits apoptosis. *Molecular Cell*, **33**, 109-116.

Delcroix, J.D., Valletta, J.S., Wu, C., Hunt, S.J., Kowal, A.S. and Mobley, W.C. (2003) NGF signaling in sensory neurons: evidence that early endosomes carry NGF retrograde signals. *Neuron*, **39**, 69-84.

Deppmann, C.D., Mihalas, S., Sharma, N., Lonze, B.E., Niebur, E. and Ginty, D.D. (2008) A model for neuronal competition during development. *Science,* **320**, 369-373.

Deshmukh, M., Vasilakos, J., Deckwerth, T.L., Lampe, P.A., Shivers, B.D. and Johnson, E.M., Jr. (1996) Genetic and metabolic status of NGF-deprived sympathetic neurons saved by an inhibitor of ICE family proteases. *The Journal of Cell Biology*, **135**, 1341-1354.

Deshmukh, M. and Johnson, E.M., Jr. (1998) Evidence of a novel event during neuronal death: development of competence-to-die in response to cytoplasmic cytochrome c. *Neuron*, **21**, 695-705.

Deshmukh, M., Du, C., Wang, X. and Johnson, E.M., Jr. (2002) Exogenous smac induces competence and permits caspase activation in sympathetic neurons. *The Journal of Neuroscience*, **22**, 8018-8027.

Deveraux, Q.L., Takahashi, R., Salvesen, G.S. and Reed, J.C. (1997) X-linked IAP is a direct inhibitor of cell-death proteases. *Nature*, **388**, 300-304.

Deveraux, Q.L., Roy, N., Stennicke, H.R., Van Arsdale, T., Zhou, Q., Srinivasula, S.M., Alnemri, E.S., Salvesen, G.S. and Reed, J.C. (1998) IAPs block apoptotic events induced by caspase-8 and cytochrome c by direct inhibition of distinct caspases. *The EMBO Journal*, **17**, 2215-2223.

Dhein, J., Walczak, H., Baumler, C., Debatin, K.M. and Krammer, P.H. (1995) Autocrine T-

cell suicide mediated by APO-1/(Fas/CD95). *Nature*, **373**, 438-441.

Di Agostino, S., Strano, S., Emiliozzi, V., Zerbini, V., Mottolese, M., Sacchi, A., Blandino, G., and Paggio, G. (2006) Gain of function of mutant p53: The mutant p53/NF-Y protein complex reveals an aberrant transcriptional mechanism of cell cycle regulation. *Cancer Cell* **10**, 191-202.

Didier, D.K., Schiffenbauer, J., Woulfe, S.L., Zacheis, M., and Schwartz, B.D. (1998) Characterisation of the cDNA encoding a protein binding to the major histocompatibility complex class II box. *Proceedings of the National Academy of Sciences of the United States of America*, **85**, 7322-7326.

Dijkers, P.F., Medema, R.H., Lammers, J.W., Koenderman, L. and Coffer, P.J. (2000) Expression of the pro-apoptotic Bcl-2 family member Bim is regulated by the forkhead transcription factor FKHR-L1. *Current Biology*, **10**, 1201-1204.

Dijkers, P.F., Birkenkamp, K.U., Lam, E.W., Thomas, N.S., Lammers, J.W., Koenderman, L. and Coffer, P.J. (2002) FKHR-L1 can act as a critical effector of cell death induced by cytokine withdrawal: protein kinase B-enhanced cell survival through maintenance of mitochondrial integrity. *The Journal of Cell Biology*, **156**, 531-542.

D'Mello, S.R., Galli, C., Ciotti, T. and Calissano, P. (1993) Induction of apoptosis in cerebellar granule neurons by low potassium: inhibition of death by insulin-like growth factor I and cAMP. *Proceedings of the National Academy of Sciences of the United States of America*, **90**, 10989-10993.

Donovan, N., Becker, E.B., Konishi, Y. and Bonni, A. (2002) JNK phosphorylation and activation of BAD couples the stress-activated signaling pathway to the cell death machinery. *The Journal of Biological Chemistry*, **277**, 40944-40949.

Doonan, F., Donovan, M., Gomez-Vicente, V., Bouillet, P. and Cotter, T.G. (2007) Bim expression indicates the pathway to retinal cell death in development and degeneration. *The Journal of Neuroscience*, **27**, 10887-10894.

Duckett, C.S., Li, F., Wang, Y., Tomaselli, K.J., Thompson, C.B. and Armstrong, R.C. (1998) Human IAP-like protein regulates programmed cell death downstream of Bcl-xL and cytochrome c. *Molecular and Cellular Biology*, **18**, 608-615.

Dudek, H., Datta, S.R., Franke, T.F., Birnbaum, M.J., Yao, R., Cooper, G.M., Segal, R.A., Kaplan, D.R. and Greenberg, M.E. (1997) Regulation of neuronal survival by the serine-threonine protein kinase Akt. *Science*, **275**, 661-665.

Edwards, S.N. and Tolkovsky, A.M. (1994) Characterization of apoptosis in cultured rat sympathetic neurons after nerve growth factor withdrawal. *The Journal of Cell Biology*, **124**, 537-546.

Eilers, A., Whitfield, J., Babij, C., Rubin, L.L. and Ham, J. (1998) Role of the Jun kinase pathway in the regulation of c-Jun expression and apoptosis in sympathetic neurons. *The Journal of Neuroscience*, **18**, 1713-1724.

Eilers, A., Whitfield, J., Shah, B., Spadoni, C., Desmond, H. and Ham, J. (2001) Direct inhibition of c-Jun N-terminal kinase in sympathetic neurones prevents c-jun promoter activation and NGF withdrawal-induced death. *Journal of Neurochemistry*, **76**, 1439-1454.

Ellis, H.M. and Horvitz, H.R. (1986) Genetic control of programmed cell death in the nematode C. elegans. *Cell*, **44**, 817-829.

Ellis, R.E., Yuan, J.Y. and Horvitz, H.R. (1991) Mechanisms and functions of cell death. *Annual Review of Cell Biology*, **7**, 663-698.

Erhardt, P., Tomaselli, K.J. and Cooper, G.M. (1997) Identification of the MDM2 oncoprotein as a substrate for CPP32-like apoptotic proteases. *The Journal of Biological Chemistry*, **272**, 15049-15052.

Ernfors, P., Lee, K.F., Kucera, J. and Jaenisch, R. (1994) Lack of neurotrophin-3 leads to deficiencies in the peripheral nervous system and loss of limb proprioceptive afferents. *Cell*, **77**, 503-512.

Essafi, A., Fernandez de Mattos, S., Hassen, Y.A., Soeiro, I., Mufti, G.J., Thomas, N.S., Medema, R.H. and Lam, E.W. (2005) Direct transcriptional regulation of Bim by FoxO3a mediates STI571-induced apoptosis in Bcr-Abl-expressing cells. *Oncogene*, **24**, 2317-2329.

Estus, S., Zaks, W.J., Freeman, R.S., Gruda, M., Bravo, R. and Johnson, E.M., Jr. (1994) Altered gene expression in neurons during programmed cell death: identification of c-jun as necessary for neuronal apoptosis. *The Journal of Cell Biology*, **127**, 1717-1727.

Estus, S., Tucker, H.M., van Rooyen, C., Wright, S., Brigham, E.F., Wogulis, M. and Rydel, R.E. (1997) Aggregated amyloid-beta protein induces cortical neuronal apoptosis and concomitant "apoptotic" pattern of gene induction. *The Journal of Neuroscience*, **17**, 7736-7745.

Ewings, K.E., Hadfield-Moorhouse, K., Wiggins, C.M., Wickenden, J.A., Balmanno, K., Gilley, R., Degenhardt, K., White, E. and Cook, S.J. (2007) ERK1/2-dependent phosphorylation of BimEL promotes its rapid dissociation from Mcl-1 and Bcl-xL. *The EMBO Journal*, **26**, 2856-2867.

Fagan, A.M., Zhang, H., Landis, S., Smeyne, R.J., Silos-Santiago, I. and Barbacid, M. (1996) TrkA, but not TrkC, receptors are essential for survival of sympathetic neurons in vivo. *The Journal of Neuroscience*, **16**, 6208-6218.

Faniello, M.C., Bevilacqua, M.A., Condorelli, G., de Crombrugghe, B., Maity, S.N., Avvedimento, V.E., Cimino, F. and Costanzo, F. (1999) The B subunit of the CAAT-binding factor NFY binds the central segment of the Co-activator p300. *The Journal of Biological Chemistry*, **274**, 7623-7626.

Farina, A., Manni, I., Fontemaggi, G., Tiainen, M., Cenciarelli, C., Bellorini, M., Mantovani, R., Sacchi, A. and Piaggio, G. (1999) Down-regulation of cyclin B1 gene transcription in terminally differentiated skeletal muscle cells is associated with loss of functional CCAAT-binding NF-Y complex. *Oncogene*, **18**, 2818-2827.

Filipowicz, W., Bhattacharyya, S.N. and Sonenberg, N. (2008) Mechanisms of post-transcriptional regulation by microRNAs: are the answers in sight? *Nature Reviews Genetics*,

9, 102-114.

Finegan, K,G., Wang, X., Lee, E.J., Robinson, A.C. and Tournier, C. (2009) Regulation of neuronal survival by the extracellular signal-related protein kinase 5. *Cell Death and Differentiation,* **16**, 674-83.

Forsburg, S.L. and Guarente, L. (1989) Identification and characterization of HAP4: a third component of the CCAAT-bound HAP2/HAP3 heteromer. *Genes and Development*. **3**, 1166-1178.

Frankowski, H., Missotten, M., Fernandez, P.A., Martinou, I., Michel, P., Sadoul, R. and Martinou, J.C. (1995) Function and expression of the Bcl-x gene in the developing and adult nervous system. *Neuroreport*, **6**, 1917-1921.

Frontini, M., Imbriano, C., diSilvio, A., Bell, B., Bogni, A., Romier, C., Moras, D., Tora, L., Davidson, I. and Mantovani, R. (2002) NF-Y recruitment of TFIID, multiple interactions with histone fold TAF(II)s. *The Journal of Biological Chemistry*, **277**, 5841-5848.

Fruman, D.A., Meyers, R.E. and Cantley, L.C. (1998) Phosphoinositide kinases. *Annual Review of Biochemistry*, **67**, 481-507.

Gajewski, T.F. and Thompson, C.B. (1996) Apoptosis meets signal transduction: elimination of a BAD influence. *Cell*, **87**, 589-592.

Gallo, V., Kingsbury, A., Balazs, R. and Jorgensen, O.S. (1987) The role of depolarization in the survival and differentiation of cerebellar granule cells in culture. *The Journal of Neuroscience*, **7**, 2203-2213.

Galonek, H.L. and Hardwick, J.M. (2006) Upgrading the BCL-2 network. *Nature Cell Biology*, **8**, 1317-1319.

Gavathiotis, E., Suzuki, M., Davis, M.L., Pitter, K., Bird, G.H., Katz, S.G., Tu, H.C., Kim, H., Cheng, E.H., Tjandra, N. *et al*. (2008) BAX activation is initiated at a novel interaction site. *Nature*, **455**, 1076-1081.

Gilbert, S.F. (2006) Developmental Biology, eighth edition. *Sinauer Associates, Massachusetts*.

Giles, R.H., Peters, D.J., Bruening, M.H. (1998). Conjunction dysfunction: CBP/p300 in human disease. *Trends in Genetics*. **14**,178-183.

Gilley, J., Coffer, P.J. and Ham, J. (2003) FOXO transcription factors directly activate bim gene expression and promote apoptosis in sympathetic neurons. *The Journal of Cell Biology*, **162**, 613-622.

Gilley, J. and Ham, J. (2005) Evidence for increased complexity in the regulation of Bim expression in sympathetic neurons: involvement of novel transcriptional and translational mechanisms. *DNA and Cell Biology*, **24**, 563-573.

Ginzinger, D.G. (2002) Gene quantification using real-time quantative PCR: an emerging technology hits the mainstream. *Experimental Hematology,* **30**, 503-512.

Giordano, A. and Avantaggiati, M.L. (1999) p300 and CBP: partners for life and death. *Journal of Cellular Physiology*, **181**, 218-230.

Glebova, N.O. and Ginty, D.D. (2004) Heterogeneous requirement of NGF for sympathetic target innervation in vivo. *Journal of Neuroscience*, **24**, 743-751.

Glebova, N.O. and Ginty, D.D. (2005) Growth and survival signals controlling sympathetic nervous system development. *Annual Review of Neuroscience*, **28**, 191-222.

Goodman, R. H., Smolik, S. (2000) CBP/p300 in cell growth, transformation, and development. *Genes and Development,* **14**: 1553-77.

Gomez-Bougie, P., Bataille, R. and Amiot, M. (2005) Endogenous association of Bim BH3-only protein with Mcl-1, Bcl-xL and Bcl-2 on mitochondria in human B cells. *European Journal of Immunology*, **35**, 971-976.

Greene, L.A. and Tischler, A.S. (1976) Establishment of a noradrenergic clonal line of rat adrenal pheochromocytoma cells which respond to nerve growth factor. *Proceedings of the National Academy of Sciences of the United States of America*, **73**, 2424-2428.

Greenlund, L.J., Korsmeyer, S.J. and Johnson, E.M., Jr. (1995) Role of BCL-2 in the survival and function of developing and mature sympathetic neurons. *Neuron*, **15**, 649-661.

Gross, A., Jockel, J., Wei, M.C. and Korsmeyer, S.J. (1998) Enforced dimerization of BAX results in its translocation, mitochondrial dysfunction and apoptosis. *The EMBO Journal*, **17**, 3878-3885.

Gu, W., Shi, X.L. and Roeder, R.G. (1997) Synergistic activation of transcription by CBP and p53. *Nature*, **387**, 819-823.

Gusmaroli, G., Tonelli, C. and Mantovani, R. (2001) Regulation of the CCAAT-Binding NF-Y subunits in Arabidopsis thaliana. *Gene*, **264**, 173-185.

Ham, J., Babij, C., Whitfield, J., Pfarr, C.M., Lallemand, D., Yaniv, M. and Rubin, L.L. (1995) A c-Jun dominant negative mutant protects sympathetic neurons against programmed cell death. *Neuron*, **14**, 927-939.

Ham, J., Towers, E., Gilley, J., Terzano, S. and Randall, R. (2005) BH3-only proteins: key regulators of neuronal apoptosis. *Cell Death and Differentiation*, **12**, 1015-1020.

Han, D.K., Chaudhary, P.M., Wright, M.E., Friedman, C., Trask, B.J., Riedel, R.T., Baskin, D.G., Schwartz, S.M. and Hood, L. (1997) MRIT, a novel death-effector domain-containing protein, interacts with caspases and BclXL and initiates cell death. *Proceedings of the National Academy of Sciences of the United States of America*, **94**, 11333-11338.

Harada, H., Quearry, B., Ruiz-Vela, A. and Korsmeyer, S.J. (2004) Survival factor-induced extracellular signal-regulated kinase phosphorylates BIM, inhibiting its association with BAX and proapoptotic activity. *Proceedings of the National Academy of Sciences of the United States of America*, **101**, 15313-15317.

Harding, T.C., Xue, L., Bienemann, A., Haywood, D., Dickens, M., Tolkovsky, A.M. and Uney, J.B. (2001) Inhibition of JNK by overexpression of the JNL binding domain of JIP-1 prevents apoptosis in sympathetic neurons. *The Journal of Biological Chemistry*, **276**, 4531-4534.

Harris, C.A. and Johnson, E.M., Jr. (2001) BH3-only Bcl-2 family members are coordinately regulated by the JNK pathway and require Bax to induce apoptosis in neurons. *The Journal of Biological Chemistry*, **276**, 37754-37760.

Heerssen, H.M., Pazyra, M.F. and Segal, R.A. (2004) Dynein motors transport activated Trks to promote survival of target-dependent neurons. *Nature Neuroscience*, **7**, 596-604.

Henderson, C. E., Bloch-Gallego, E and Camu, W. (1995) Purified embryonic motoneurons. In Nerve Cell Culture: A Practical Approach. J. Cohen and G. Wilkin, editors. *Oxford University Press, London*. 69-81.

Hengartner, M.O. (2000) The biochemistry of apoptosis. *Nature,* **407**, 770-6.

Hinds, M.G., Norton, R.S., Vaux, D.L. and Day, C.L. (1999) Solution structure of a baculoviral inhibitor of apoptosis (IAP) repeat. *Nature Structural Biology*, **6**, 648-651.

Hinds, M.G., Smits, C., Fredericks-Short, R., Risk, J.M., Bailey, M., Huang, D.C. and Day, C.L. (2007) Bim, Bad and Bmf: intrinsically unstructured BH3-only proteins that undergo a localized conformational change upon binding to prosurvival Bcl-2 targets. *Cell Death and Differentiation*, **14**, 128-136.

Hooft van Huijsduijnen, R., Li, X.Y., Black, D., Matthes, H., Benoist, C., and Mathis, D. (1990) Co-evolution from yeast to mouse: cDNA cloning of the two NF-Y (CP-1/CBF) subunits. *The EMBO Journal,* **9**, 3119-3127.

Hsu, Y.T. and Youle, R.J. (1997) Nonionic detergents induce dimerization among members of the Bcl-2 family. *The Journal of Biological Chemistry*, **272**, 13829-13834.

Hu, Q., and Maity, S.N. (2000) Stable expression of a dominant negative mutant of CCAAT binding factor/NF-Y in mouse fibroblast cells resulting in retardation of cell growth and inhibition of transcription of various cellular genes. *The Journal of Biological Chemistry,* **275**, 4435-4444.

Huang, E.J. and Reichardt, L.F. (2003) Trk receptors: roles in neuronal signal transduction. *Annual Review of Biochemistry*, **72**, 609-642.

Huser, M., Luckett, J., Chiloeches, A., Mercer, K., Iwobi, M., Giblett, S., Sun, X.M., Brown, J., Marais, R. and Pritchard, C. (2001) MEK kinase activity is not necessary for Raf-1 function. *The EMBO Journal*, **20**, 1940-1951.

Ibrado, A.M., Liu, L. and Bhalla, K. (1997) Bcl-xL overexpression inhibits progression of molecular events leading to paclitaxel-induced apoptosis of human acute myeloid leukemia HL-60 cells. *Cancer Research*, **57**, 1109-1115.

Imaizumi, K., Tsuda, M., Imai, Y., Wanaka, A., Takagi, T. and Tohyama, M. (1997) Molecular cloning of a novel polypeptide, DP5, induced during programmed neuronal death. *The Journal of Biological Chemistry*, **272**, 18842-18848.

Imaizumi, K., Benito, A., Kiryu-Seo, S., Gonzalez, V., Inohara, N., Lieberman, A.P., Kiyama, H. and Nunez, G. (2004) Critical role for DP5/Harakiri, a Bcl-2 homology domain 3-only Bcl-2 family member, in axotomy-induced neuronal cell death. *The Journal of Neuroscience*, **24**, 3721-3725.

Imbriano, C., Gurtner, A., Cocciarella, F., Di Agostino, S., Basile, V., Gostissa, M., Dobbelstein, M., Del Sal, G., Piaggio, G., and Mantovani, R. (2005) Direct p53 transcriptional repression: *In vivo* analysis of CCAAT-containing G_2/M promoters. *Molecular and Cellular Biology,* **25**, 3737-3751.

Inohara, N., Koseki, T., Hu, Y., Chen, S. and Nunez, G. (1997) CLARP, a death effector domain-containing protein interacts with caspase-8 and regulates apoptosis. *Proceedings of the National Academy of Sciences of the United States of America*, **94**, 10717-10722.

Inoue, Y., Itoh, Y., Abel, K., Okamoto, T., Daitoku, H., Fukamizu, A., Onozaki, K., and Hayashi, H. (2007) Smad3 is acetylated by p300/CBP to regulate its transactivation activity. *Oncogene,* **26**, 500-508.

Irmler, M., Thome, M., Hahne, M., Schneider, P., Hofmann, K., Steiner, V., Bodmer, J.L., Schroter, M., Burns, K., Mattmann, C. *et al*. (1997) Inhibition of death receptor signals by cellular FLIP. *Nature*, **388**, 190-195.

Iyer, N.G., Özdag, H., and Caldas, C. (2004) p300/CBP and cancer. *Oncogene,* **23**, 4225-4231.

Izumi, H., Molander, C., Penn, L., Ishisaki, A., Kohno, K., and Funa, K. (2001) Mechanism for the transcriptional repression by c-Myc on PDGF (&bgr;)-receptor. *Journal of Cell Science,* **114**, 1533-1544.

Jacobs, W.B., Govoni, G., Ho, D., Atwal, J.K., Barnabe-Heider, F., Keyes, W.M., Mills, A.A., Miller, F.D. and Kaplan, D.R. (2005) p63 is an essential proapoptotic protein during neural development. *Neuron*, **48**, 743-756.

Jeffers, J.R., Parganas, E., Lee, Y., Yang, C., Wang, J., Brennan, J., MacLean, K.H., Han, J., Chittenden, T., Ihle, J.N. *et al*. (2003) Puma is an essential mediator of p53-dependent and -independent apoptotic pathways. *Cancer Cell*, **4**, 321-328.

Jiang, M., Wei, Q., Wang, J., Du, Q., Yu, J., Zhang, L. and Dong, Z. (2006) Regulation of PUMA-alpha by p53 in cisplatin-induced renal cell apoptosis. *Oncogene*, **25**, 4056-4066.

Jing, Q., Huang, S., Guth, S., Zarubin, T., Motoyama, A., Chen, J., Di Padova, F., Lin, S.C., Gram, H. and Han, J. (2005) Involvement of microRNA in AU-rich element-mediated mRNA instability. *Cell*, **120**, 623-634.

Johnstone, R.W., Ruefli, A.A. and Lowe, S.W. (2002) Apoptosis: a link between cancer genetics and chemotherapy. *Cell*, **108**, 153-164.

Jost, P.J., Grabow, S., Gray, D., McKenzie, M.D., Nachbur, U., Huang, D.C., Bouillet, P., Thomas, H.E., Borner, C., Silke, J. *et al*. (2009) XIAP discriminates between type I and type II

FAS-induced apoptosis. *Nature*, **460**, 1035-1039.

Kabe, Y., Yamada, J., Uga, H., Yamaguchi, Y., Wada, T., and Handa, H. (2005) NF-Y is essential for the recruitment of RNA polymerase II and inducible transcription of several CCAAT box-containing genes. *Molecular and Cellular Biology*, **25**, 512-522.

Kamada, S., Kusano, H., Fujita, H., Ohtsu, M., Koya, R.C., Kuzumaki, N. and Tsujimoto, Y. (1998) A cloning method for caspase substrates that uses the yeast two-hybrid system: cloning of the antiapoptotic gene gelsolin. *Proceedings of the National Academy of Sciences of the United States of America*, **95**, 8532-8537.

Kapatos, G., Stegenga, S.L., and Hirayama, K. (2000) Identification and Characterization of Basal and Cyclic AMP Response Elements in the Promoter of the Rat GTP Cyclohydrolase I Gene. *The Journal of Biological Chemistry*, **275**, 5947-5957.

Kaplan, D.R., Martin-Zanca, D. and Parada, L.F. (1991) Tyrosine phosphorylation and tyrosine kinase activity of the trk proto-oncogene product induced by NGF. *Nature*, **350**, 158-160.

Kaplan, D.R. and Miller, F.D. (1997) Signal transduction by the neurotrophin receptors. *Current Opinion in Cell Biology*, **9**, 213-221.

Kaplan, D.R. and Miller, F.D. (2000) Neurotrophin signal transduction in the nervous system. *Current Opinion in Neurobiology*, **10**, 381-391.

Kasper, L.H., Fukuyama, T., Biesen M.A., Boussouar, F., Tong, C., de Pauw, A., Murray, P.J., van Deursen, J.M., Brindle, P.K. (2006) Conditional knockout mice reveal distinct functions for the global transcriptional coactivators CBP and p300 in T-cell development. *Moleculllar and Cellular Biology,* **26**, 789-809.

Kaufmann, S.H. (1989) Induction of endonucleolytic DNA cleavage in human acute myelogenous leukemia cells by etoposide, camptothecin, and other cytotoxic anticancer drugs: a cautionary note. *Cancer Research*, **49**, 5870-5878.

Kerr, J.F., Wyllie, A.H. and Currie, A.R. (1972) Apoptosis: a basic biological phenomenon

with wide-ranging implications in tissue kinetics. *British Journal of Cancer*, **26**, 239-257.

Kim, C.G., and Sheffery, M. (1990) Physical characterization of the purified CCAAT transcription factor, alpha-CP1. *The Journal of Biological Chemistry,* **5**, 13362-13369.

Kim, T. K., Kim, T. H., and Maniatis, T. (1998) Efficient recruitment of TFIIB and CBP-RNA polymerase II holoenzyme by an interferon-beta enhanceosome in vitro. *Proceedings of the National Academy of Sciences of the United States of America*. 95:12191-12196.

Kitson, J., Raven, T., Jiang, Y.P., Goeddel, D.V., Giles, K.M., Pun, K.T., Grinham, C.J., Brown, R. and Farrow, S.N. (1996) A death-domain-containing receptor that mediates apoptosis. *Nature*, **384**, 372-375.

Klesse, L.J., Meyers, K.A., Marshall, C.J. and Parada, L.F. (1999) Nerve growth factor induces survival and differentiation through two distinct signaling cascades in PC12 cells. *Oncogene*, **18**, 2055-2068.

Kolsch, W. (2000) Meaningful relationships: the regulation of the Ras/Raf/MEK/ERK pathway by protein interactions. *The Journal of Biochemistry,* **351**, 289-305.

Konishi, Y., Lehtinen, M., Donovan, N. and Bonni, A. (2002) Cdc2 phosphorylation of BAD links the cell cycle to the cell death machinery. *Molecular Cell*, **9**, 1005-1016.

Kotecha, M., Kluza, J., Wells, G., O'Hare, C.C., Forni, C., Mantovani, R., Howard, P.W., Morris, P., Thurston, D.E., Hartley, J.A. *et al*. (2008) Inhibition of DNA binding of the NF-Y transcription factor by the pyrrolobenzodiazepine-polyamide conjugate GWL-78. *Molecular Cancer Therapeutics*, **7**, 1319-1328.

Kothakota, S., Azuma, T., Reinhard, C., Klippel, A., Tang, J., Chu, K., McGarry, T.J., Kirschner, M.W., Koths, K., Kwiatkowski, D.J. *et al*. (1997) Caspase-3-generated fragment of gelsolin: effector of morphological change in apoptosis. *Science,* **278**, 294-298.

Kroemer, G. (1997) The proto-oncogene Bcl-2 and its role in regulating apoptosis. *Nature Medicine*, **3**, 614-620.

Kroemer, G. and Martin, S.J. (2005) Caspase-independent cell death. *Nature Medicine*, **11**, 725-730.

Kuida, K., Zheng, T.S., Na, S., Kuan, C., Yang, D., Karasuyama, H., Rakic, P. and Flavell, R.A. (1996) Decreased apoptosis in the brain and premature lethality in CPP32-deficient mice. *Nature*, **384**, 368-372.

Kung, A.L., Rebel, V.I., Bronson, R.T., Ch'ng L.E., Sieff, C.A., Livingston, D.M., and Yao, T.P. (2000) Gene dose-dependent control of haematopoiesis and haematologic tumour suppression by CBP. *Genes and Development,* **14**, 272-7.

Kuruvilla, R., Ye, H. and Ginty, D.D. (2000) Spatially and functionally distinct roles of the PI3-K effector pathway during NGF signaling in sympathetic neurons. *Neuron*, **27**, 499-512.

Kuwana, T., Mackey, M.R., Perkins, G., Ellisman, M.H., Latterich, M., Schneiter, R., Green, D.R. and Newmeyer, D.D. (2002) Bid, Bax, and lipids cooperate to form supramolecular openings in the outer mitochondrial membrane. *Cell*, **111**, 331-342.

Kuwana, T., Bouchier-Hayes, L., Chipuk, J.E., Bonzon, C., Sullivan, B.A., Green, D.R. and Newmeyer, D.D. (2005) BH3 domains of BH3-only proteins differentially regulate Bax-mediated mitochondrial membrane permeabilization both directly and indirectly. *Molecular Cell*, **17**, 525-535.

Lai, E.C. (2002) Micro RNAs are complementary to 3′ UTR sequence motifs that mediate negative post-transcriptional regulation. *Nature Genetics*. **30**, 363-4.

Lazebnik, Y.A., Cole, S., Cooke, C.A., Nelson, W.G. and Earnshaw, W.C. (1993) Nuclear events of apoptosis in vitro in cell-free mitotic extracts: a model system for analysis of the active phase of apoptosis. *The Journal of Cell Biology*, **123**, 7-22.

Leber, B., Lin, J. and Andrews, D.W. (2007) Embedded together: the life and death consequences of interaction of the Bcl-2 family with membranes. *Apoptosis*, **12**, 897-911.

LeBlanc, A.C. (2005) The role of apoptotic pathways in Alzheimer's disease neurodegeneration and cell death. *Current Alzheimer Research*, **2**, 389-402.

Lee, J.S., See, R.H., Deng, T. and Shi, Y. (1996) Adenovirus E1A downregulates cJun- and JunB-mediated transcription by targeting their coactivator p300. *Molecular and Cellular Biology*, **16**, 4312-4326.

Lee, S., Nakamura, E., Yang, H., Wei, W., Linggi, M.S., Sajan, M.P., Farese, R.V., Freeman, R.S., Carter, B.D., Kaelin, W.G., Jr. *et al*. (2005) Neuronal apoptosis linked to EglN3 prolyl hydroxylase and familial pheochromocytoma genes: developmental culling and cancer. *Cancer Cell*, **8**, 155-167.

Lei, K. and Davis, R.J. (2003) JNK phosphorylation of Bim-related members of the Bcl2 family induces Bax-dependent apoptosis. *Proceedings of the National Academy of Sciences of the United States of America*, **100**, 2432-2437.

Lenhard, B., Sandelin, A., Mendoza, L., Engstrom, P., Jareborg, N., and Wasserman, W.W. (2003) Identification of conserved regulatory elements by comparitive genome analysis. *Journal of Biology*, **2**:13.

Letai, A., Bassik, M.C., Walensky, L.D., Sorcinelli, M.D., Weiler, S. and Korsmeyer, S.J. (2002) Distinct BH3 domains either sensitize or activate mitochondrial apoptosis, serving as prototype cancer therapeutics. *Cancer Cell*, **2**, 183-192.

Lettice, L.A., Heaney, S.J., Purdie, L.A., Li, L., de Beer, P., Oostra, B.A., Goode, D., Elgar, G., Hill, R.E. and de Graaff, E. (2003) A long-range Shh enhancer regulates expression in the developing limb and fin and is associated with preaxial polydactyly. *Human Molecular Genetics*, **12**, 1725-1735.

Levi-Montalcini, R. (1987) The nerve growth factor 35 years later. *Science,* **237**, 1154-1162.

Lewis, B.P., Burge, C.B. and Bartel, D.P. (2005) Conserved seed pairing, often flanked by adenosines, indicates that thousands of human genes are microRNA targets. *Cell*, **120**, 15-20.

Ley, R., Balmanno, K., Hadfield, K., Weston, C. and Cook, S.J. (2003) Activation of the ERK1/2 signaling pathway promotes phosphorylation and proteasome-dependent degradation of the BH3-only protein, Bim. *The Journal of Biological Chemistry*, **278**, 18811-18816.

Ley, R., Ewings, K.E., Hadfield, K., Howes, E., Balmanno, K. and Cook, S.J. (2004) Extracellular signal-regulated kinases 1/2 are serum-stimulated "Bim(EL) kinases" that bind to the BH3-only protein Bim(EL) causing its phosphorylation and turnover. *The Journal of Biological Chemistry*, **279**, 8837-8847.

Ley, R., Ewings, K.E., Hadfield, K. and Cook, S.J. (2005a) Regulatory phosphorylation of Bim: sorting out the ERK from the JNK. *Cell Death and Differentiation*, **12**, 1008-1014.

Ley, R., Hadfield, K., Howes, E. and Cook, S.J. (2005b) Identification of a DEF-type docking domain for extracellular signal-regulated kinases 1/2 that directs phosphorylation and turnover of the BH3-only protein BimEL. *The Journal of Biological Chemistry*, **280**, 17657-17663.

Li, H., Zhu, H., Xu, C.J. and Yuan, J. (1998) Cleavage of BID by caspase 8 mediates the mitochondrial damage in the Fas pathway of apoptosis. *Cell*, **94**, 491-501.

Li, Q., Herrier, M., Landsberger, N., Kaludov, N., Ogryzko, V.V., Nakatani, Y., and Wolffe, A.P. (1998) *Xenopus* NF-Y pre-sets chromatin to potentiate p300 and acetylation-responsive transcription from the *Xenopus hsp70* promoter *in vivo*. *The EMBO Journal,* **17**, 6300-6315.

Liang, S.G., and Maity, S.N. (1998) Pathway of complex formation between DNA and three subunits of CBF/NF-Y. Photocross-linking analysis of DNA-protein interaction and characterization of equilibrium steps of subunit interaction and DNA binding. *The Journal of Biological Chemistry*, **273**, 31590-31598.

Liberati, C., Ronchi, A., Lievens, P., Ottolenghi, S. and Mantovani, R. (1998) NF-Y organizes the gamma-globin CCAAT boxes region. *The Journal of Biological Chemistry*, **273**, 16880-16889.

Liberati, C., di Silvio, A., Ottolenghi, S. and Mantovani, R. (1999) NF-Y binding to twin CCAAT boxes: role of Q-rich domains and histone fold helices. *Journal of Molecular Biology*,

285, 1441-1455.

Lindsten, T., Ross, A.J., King, A., Zong, W.X., Rathmell, J.C., Shiels, H.A., Ulrich, E., Waymire, K.G., Mahar, P., Frauwirth, K. *et al*. (2000) The combined functions of proapoptotic Bcl-2 family members bak and bax are essential for normal development of multiple tissues. *Molecular Cell*, **6**, 1389-1399.

Lipscomb, E.A., Sarmiere, P.D., Crowder, R.J. and Freeman, R.S. (1999) Expression of the SM-20 gene promotes death in nerve growth factor-dependent sympathetic neurons. *Journal of Neurochemistry*, **73**, 429-432.

Liu, J., Carmell, M.A., Rivas, F.V., Marsden, C.G., Thomson, J.M., Song, J.J., Hammond, S.M., Joshua-Tor, L. and Hannon, G.J. (2004) Argonaute2 is the catalytic engine of mammalian RNAi. *Science*, **305**, 1437-1441.

Liu, J.W., Chandra, D., Tang, S.H., Chopra, D. and Tang, D.G. (2002) Identification and characterization of Bimgamma, a novel proapoptotic BH3-only splice variant of Bim. *Cancer Research*, **62**, 2976-2981.

Livak, K.J. and Schmittgen, T.D. (2001) Analysis of relative gene expression data using real-time quantitative PCR and the 2(-Delta Delta C(T)) Method. *Methods*, **25**, 402-408.

Locksley, R.M., Killeen, N. and Lenardo, M.J. (2001) The TNF and TNF receptor superfamilies: integrating mammalian biology. *Cell*, **104**, 487-501.

Lonze, B.E., Riccio, A., Cohen, S. and Ginty, D.D. (2002) Apoptosis, axonal growth defects, and degeneration of peripheral neurons in mice lacking CREB. *Neuron*, **34**, 371-385.

Luciano, F., Jacquel, A., Colosetti, P., Herrant, M., Cagnol, S., Pages, G. and Auberger, P. (2003) Phosphorylation of Bim-EL by Erk1/2 on serine 69 promotes its degradation via the proteasome pathway and regulates its proapoptotic function. *Oncogene*, **22**, 6785-6793.

Luo, X., Budihardjo, I., Zou, H., Slaughter, C. and Wang, X. (1998) Bid, a Bcl2 interacting protein, mediates cytochrome c release from mitochondria in response to activation of cell

surface death receptors. *Cell*, **94**, 481-490.

Ma, C., Ying, C., Yuan, Z., Song, B., Li, D., Liu, Y., Lai, B., Li, W., Chen, R., Ching, Y.P. *et al*. (2007) dp5/HRK is a c-Jun target gene and required for apoptosis induced by potassium deprivation in cerebellar granule neurons. *The Journal of Biological Chemistry*, **282**, 30901-30909.

MacFarlane, M., Ahmad, M., Srinivasula, S.M., Fernandes-Alnemri, T., Cohen, G.M. and Alnemri, E.S. (1997) Identification and molecular cloning of two novel receptors for the cytotoxic ligand TRAIL. *The Journal of Biological Chemistry*, **272**, 25417-25420.

Mahmud, D.L., M, G.A., Deb, D.K., Platanias, L.C., Uddin, S. and Wickrema, A. (2002) Phosphorylation of forkhead transcription factors by erythropoietin and stem cell factor prevents acetylation and their interaction with coactivator p300 in erythroid progenitor cells. *Oncogene*, **21**, 1556-1562.

Majdan, M., Walsh, G.S., Aloyz, R. and Miller, F.D. (2001) TrkA mediates developmental sympathetic neuron survival in vivo by silencing an ongoing p75NTR-mediated death signal. *The Journal of Cell Biology*, **155**, 1275-1285.

Manni, I., Mazzaro, G., Gurtner, A., Mantovani, R., Haugwitz, U., Krause, K., Engeland, K., Sacchi, A., Soddu, S. and Piaggio, G. (2001) NF-Y mediates the transcriptional inhibition of the cyclin B1, cyclin B2, and cdc25C promoters upon induced G2 arrest. *The Journal of Biological Chemistry*, **276**, 5570-5576.

Manni, I., Caretti, G., Artuso, S., Gurtner, A., Emiliozzi, V., Sacchi, A., Mantovani, R. and Piaggio, G. (2008) Posttranslational regulation of NF-YA modulates NF-Y transcriptional activity. *Molecular Biology of the Cell*, **19**, 5203-5213.

Mantovani, R., Pessara, U., Tronche, F., Li, X.Y., Knapp, A.M., Pasquali, J.L., Benoist, C. and Mathis, D. (1992) Monoclonal antibodies to NF-Y define its function in MHC class II and albumin gene transcription. *The EMBO Journal*, **11**, 3315-3322.

Mantovani, R., Li, X.Y., Pessara, U., Hooft van Huisjduijnen, R., Benoist, C. and Mathis, D.

(1994) Dominant negative analogs of NF-YA. *The Journal of Biological Chemistry*, **269**, 20340-20346.

Mantovani, R., Bellorini, M., Zemzoumi, K., Farina, A., Berthelsen, J., and Piaggio. (1997). Cloning and expression of human NF-Y C. *Gene* **193**, 119-125.

Mantovani, R. (1998) A survey of 178 NF-Y binding CCAAT boxes. *Nucleic Acids Research*, **26**, 1135-1143.

Mantovani, R. (1999) The molecular biology of the CCAAT-binding factor NF-Y. *Gene*, **239**, 15-27.

Marani, M., Tenev, T., Hancock, D., Downward, J. and Lemoine, N.R. (2002) Identification of novel isoforms of the BH3 domain protein Bim which directly activate Bax to trigger apoptosis. *Molecular and Cellular Biology*, **22**, 3577-3589.

Marani, M., Hancock, D., Lopes, R., Tenev, T., Downward, J. and Lemoine, N.R. (2004) Role of Bim in the survival pathway induced by Raf in epithelial cells. *Oncogene*, **23**, 2431-2441.

Marsters, S.A., Sheridan, J.P., Pitti, R.M., Brush, J., Goddard, A. and Ashkenazi, A. (1998) Identification of a ligand for the death-domain-containing receptor Apo3. *Current Biology*, **8**, 525-528.

Martin, D.P., Schmidt, R.E., DiStefano, P.S., Lowry, O.H., Carter, J.G. and Johnson, E.M., Jr. (1988) Inhibitors of protein synthesis and RNA synthesis prevent neuronal death caused by nerve growth factor deprivation. *The Journal of Cell Biology*, **106**, 829-844.

Martin, L.J., Al-Abdulla, N.A., Brambrink, A.M., Kirsch, J.R., Sieber, F.E. and Portera-Cailliau, C. (1998) Neurodegeneration in excitotoxicity, global cerebral ischemia, and target deprivation: A perspective on the contributions of apoptosis and necrosis. *Brain Research Bulletin*, **46**, 281-309.

Martinez-Balbas, M., Bannister, A.J., Martin, K., Haus-Seuffert, P., Meisterernst, M. and Kouzarides, T. (1998) The acetyltransferase activity of CBP stimulates transcription. *The EMBO Journal*. **10**, 2886-2893.

Maston, G.A., Evans, S.K. and Green, M.R. (2006) Transcriptional regulatory elements in the human genome. *Annual Review of Genomics and Human Genetics*, **7**, 29-59.

Masuoka, H.C., Guicciardi, M.E. and Gores, G.J. (2009) Caspase inhibitors for the treatment of hepatitis C. *Clinics in Liver Disease*, **13**, 467-475.

Matsui, H., Asou, H. and Inaba, T. (2007) Cytokines direct the regulation of Bim mRNA stability by heat-shock cognate protein 70. *Molecular Cell*, **25**, 99-112.

Martin, D.P., Schmidt, R.E., DiStefano, P.S., Lowry, O.H., Carter, J.G. and Johnson, E.M., Jr. (1988) Inhibitors of protein synthesis and RNA synthesis prevent neuronal death caused by nerve growth factor deprivation. *The Journal of Cell Biology*, **106**, 829-844.

Martin, L.J., Al-Abdulla, N.A., Brambrink, A.M., Kirsch, J.R., Sieber, F.E. and Portera-Cailliau, C. (1998) Neurodegeneration in excitotoxicity, global cerebral ischemia, and target deprivation: A perspective on the contributions of apoptosis and necrosis. *Brain Research Bulletin*, **46**, 281-309.

Martin, L.J. (2001) Neuronal cell death in nervous system development, disease, and injury. *International Journal of Molecular Medicine*, **7**, 455-478

McKernan, D.P. and Cotter, T.G. (2007) A Critical role for Bim in retinal ganglion cell death. *Journal of Neurochemistry*, **102**, 922-930.

Merika, M., Williams, A.J., Chen, G., Collins, T., and Thanos, D. (1998) Recruitment of CBP/p300 by the IFN beta enhanceosome is required for synergistic activation of transcription. *Molecular Cell,* **1**, 277-287.

Merino, D., Giam, M., Hughes, P.D., Siggs, O.M., Heger, K., O'Reilly, L.A., Adams, J.M., Strasser, A., Lee, E.F., Fairlie, W.D. *et al*. (2009) The role of BH3-only protein Bim extends

beyond inhibiting Bcl-2-like prosurvival proteins. *The Journal of Cell Biology*, **186**, 355-362.

Mikecz, A., Zhang, S., Montminy, M., Tan, E.M., and Hemmerich, P. (2000) CREB-binding protein (CBP)/p300 and RNA polymerase II colocalise in transcriptionally active domains in the nucleus. *The Journal of Cell Biology,* **150**, 265-273.

Mikula, M., Schreiber, M., Husak, Z., Kucerova, L., Ruth, J., Wieser, R., Zatloukal, K., Beug, H., Wagner, E.F. and Baccarini, M. (2001) Embryonic lethality and fetal liver apoptosis in mice lacking the c-raf-1 gene. *The EMBO Journal*, **20**, 1952-1962.

Milligan, C.E., Prevette, D., Yaginuma, H., Homma, S., Cardwell, C., Fritz, L.C., Tomaselli, K.J., Oppenheim, R.W. and Schwartz, L.M. (1995) Peptide inhibitors of the ICE protease family arrest programmed cell death of motoneurons in vivo and in vitro. *Neuron*, **15**, 385-393.

Neame, S.J., Rubin, L.L. and Philpott, K.L. (1998) Blocking cytochrome c activity within intact neurons inhibits apoptosis. *The Journal of Cell Biology*, **142**, 1583-1593.

Neame, S.J., Whitfield, J. and Ham, J. (2004) Immunocytochemical techniques for studying apoptosis in primary sympathetic neurons. *Methods in Molecular Biology*, **282**, 169-177.

Nijhawan, D., Honarpour, N. and Wang, X. (2000) Apoptosis in neural development and disease. *Annual Review of Neuroscience*, **23**, 73-87.

O'Connor, L., Strasser, A., O'Reilly, L.A., Hausmann, G., Adams, J.M., Cory, S. and Huang, D.C. (1998) Bim: a novel member of the Bcl-2 family that promotes apoptosis. *The EMBO Journal*, **17**, 384-395.

Ogbourne, S. and Antalis, T.M. (1998) Transcriptional control and the role of silencers in transcriptional regulation in eukaryotes. *The Biochemical Journal*, **331,** 1-14.

Ogryzko, V.V., Schiltz, R.L., Russanova, V., Howard, B.H. and Nakatani, Y. (1996) The transcriptional coactivators p300 and CBP are histone acetyltransferases. *Cell*, **87**, 953-959.

Olesen, J. T., and Guarente, L. (1990). The HAP2 subunit of yeast CCAAT transcriptional activator contains adjacent domains for subunit association and DNA recognition: model for the HAP2/3/4 complex. *Genes and Development,* **4**, 1714-1729.

Oltersdorf, T., Elmore, S.W., Shoemaker, A.R., Armstrong, R.C., Augeri, D.J., Belli, B.A., Bruncko, M., Deckwerth, T.L., Dinges, J., Hajduk, P.J. *et al*. (2005) An inhibitor of Bcl-2 family proteins induces regression of solid tumours. *Nature*, **435**, 677-681.

Oppenheim, R.W. (1991) Cell death during development of the nervous system. *Annual Review of Neuroscience*, **14**, 453-501.

O'Reilly, L.A., Cullen, L., Visvader, J., Lindeman, G.J., Print, C., Bath, M.L., Huang, D.C. and Strasser, A. (2000) The proapoptotic BH3-only protein bim is expressed in hematopoietic, epithelial, neuronal, and germ cells. *The American Journal of Pathology*, **157**, 449-461.

Pajak, F., De Gois, S., Houhou, L., Vedrine, C., Mallet, J. and Berrard, S. (2003) Quantification of transcriptional activities of reporter gene constructs in primary cultures of sympathetic neurons. *Journal of Neuroscience Research*, **71**, 365-374.

Palmada, M., Kanwal, S., Rutkoski, N.J., Gustafson-Brown, C., Johnson, R.S., Wisdom, R. and Carter, B.D. (2002) c-jun is essential for sympathetic neuronal death induced by NGF withdrawal but not by p75 activation. *The Journal of Cell Biology*, **158**, 453-461.

Pan, G., O'Rourke, K., Chinnaiyan, A.M., Gentz, R., Ebner, R., Ni, J. and Dixit, V.M. (1997) The receptor for the cytotoxic ligand TRAIL. *Science*, **276**, 111-113.

Park, D.S., Morris, E.J., Stefanis, L., Troy, C.M., Shelanski, M.L., Geller, H.M. and Greene, L.A. (1998) Multiple pathways of neuronal death induced by DNA-damaging agents, NGF deprivation, and oxidative stress. *The Journal of Neuroscience*, **18**, 830-840.

Peart, M., and Prives, C. (2006). Mutant p53 gain of function: The NF-Y connection. *Cancer Cell* **10**: 173-174.

Perier, C., Bove, J., Wu, D.C., Dehay, B., Choi, D.K., Jackson-Lewis, V., Rathke-Hartlieb, S.,

Bouillet, P., Strasser, A., Schulz, J.B. *et al*. (2007) Two molecular pathways initiate mitochondria-dependent dopaminergic neurodegeneration in experimental Parkinson's disease. *Proceedings of the National Academy of Sciences of the United States of America*, **104**, 8161-8166.

Perkins, N.D., Felzien, L.K., Betts, J.C., Leung, K., Beach, D.H., and Nabel, G.J. (1997) Regulation of NF-B by cyclin-dependent kinases associated with the p300 coactivator. *Science,* **275**, 523-527.

Perrot, V. and Rechler, M.M. (2005) The coactivator p300 directly acetylates the forkhead transcription factor Foxo1 and stimulates Foxo1-induced transcription. *Molecular Endocrinology,* **19**, 2283-2298.

Petrij, F., Giles, R.H., Dauwerse, H.G., Saris, J.J., Hennekam, R.C., Masuno, M., Tommerup, N., van Ommen, G.J., Goodman, R.H., Peters, D.J., and Breuning, M.H. (1995) Rubinstein-Taybi syndrome caused by mutations in the transcriptional co-activator CBP. *Nature,* **376**, 348-351.

Pillai, R.S., Bhattacharyya, S.N. and Filipowicz, W. (2007) Repression of protein synthesis by miRNAs: how many mechanisms? *Trends in Cell Biology*, **17**, 118-126.

Pittman, R.N., Wang, S., DiBenedetto, A.J. and Mills, J.C. (1993) A system for characterizing cellular and molecular events in programmed neuronal cell death. *The Journal of Neuroscience*, **13**, 3669-3680.

Potts, P.R., Singh, S., Knezek, M., Thompson, C.B. and Deshmukh, M. (2003) Critical function of endogenous XIAP in regulating caspase activation during sympathetic neuronal apoptosis. *The Journal of Cell Biology*, **163**, 789-799.

Pozniak, C.D., Radinovic, S., Yang, A., McKeon, F., Kaplan, D.R. and Miller, F.D. (2000) An anti-apoptotic role for the p53 family member, p73, during developmental neuron death. *Science,* **289**, 304-306.

Putcha, G.V., Deshmukh, M. and Johnson, E.M., Jr. (1999) BAX translocation is a critical

event in neuronal apoptosis: regulation by neuroprotectants, BCL-2, and caspases. *The Journal of Neuroscience*, **19**, 7476-7485.

Putcha, G.V., Moulder, K.L., Golden, J.P., Bouillet, P., Adams, J.A., Strasser, A. and Johnson, E.M. (2001) Induction of BIM, a proapoptotic BH3-only BCL-2 family member, is critical for neuronal apoptosis. *Neuron*, **29**, 615-628.

Putcha, G.V., Harris, C.A., Moulder, K.L., Easton, R.M., Thompson, C.B. and Johnson, E.M., Jr. (2002) Intrinsic and extrinsic pathway signaling during neuronal apoptosis: lessons from the analysis of mutant mice. *The Journal of Cell Biology*, **157**, 441-453.

Putcha, G.V., Le, S., Frank, S., Besirli, C.G., Clark, K., Chu, B., Alix, S., Youle, R.J., LaMarche, A., Maroney, A.C. *et al*. (2003) JNK-mediated BIM phosphorylation potentiates BAX-dependent apoptosis. *Neuron*, **38**, 899-914.

Putcha, G.V. and Johnson, E.M., Jr. (2004) Men are but worms: neuronal cell death in C elegans and vertebrates. *Cell Death and Differentiation*, **11**, 38-48.

Puthakalath, H., Huang, D.C., O' Reilly, L.A., King, S.M., and Strasser, A. (1999) The proapoptotic activity of the Bcl-2 family member Bim is regulated by interaction with the dynein motor complex. *Molecular Cell,* **3**, 287- 296.

Puthalakath, H., Villunger, A., O'Reilly, L.A., Beaumont, J.G., Coultas, L., Cheney, R.E., Huang, D.C. and Strasser, A. (2001) Bmf: a proapoptotic BH3-only protein regulated by interaction with the myosin V actin motor complex, activated by anoikis. *Science,* **293**, 1829-1832.

Puthalakath, H., and Strasser, A. (2002) Keeping killers on a tight leash: Transcriptional and post-translational control of the pro-apoptotic family of BH3-only proteins. *Cell Death and Differentiation*, **9**, 505-512

Puthalakath, H., O'Reilly, L.A., Gunn, P., Lee, L., Kelly, P.N., Huntington, N.D., Hughes, P.D., Michalak, E.M., McKimm-Breschkin, J., Motoyama, N. *et al*. (2007) ER stress triggers apoptosis by activating BH3-only protein Bim. *Cell*, **129**, 1337-1349.

Qian, X., Riccio, A., Zhang, Y. and Ginty, D.D. (1998) Identification and characterization of novel substrates of Trk receptors in developing neurons. *Neuron*, **21**, 1017-1029.

Reed, J.C. (2002) Apoptosis-based therapies. *Nature Reviews Drug Discovery*, **1**, 111-121.

Remenyi, A., Scholer, H.R. and Wilmanns, M. (2004) Combinatorial control of gene expression. *Nature Structural & Molecular Biology*, **11**, 812-815.

Riccio, A., Pierchala, B.A., Ciarallo, C.L. and Ginty, D.D. (1997) An NGF-TrkA-mediated retrograde signal to transcription factor CREB in sympathetic neurons. *Science,* **277**, 1097-1100.

Riccio, A., Ahn, S., Davenport, C.M., Blendy, J.A. and Ginty, D.D. (1999) Mediation by a CREB family transcription factor of NGF-dependent survival of sympathetic neurons. *Science,* **286**, 2358-2361.

Riedl, S.J. and Salvesen, G.S. (2007) The apoptosome: signalling platform of cell death. *Nature Reviews*, **8**, 405-413.

Rodriguez, J. and Lazebnik, Y. (1999) Caspase-9 and APAF-1 form an active holoenzyme. *Genes & Development*, **13**, 3179-3184.

Rodriguez-Tebar, A., Dechant, G., Gotz, R. and Barde, Y.A. (1992) Binding of neurotrophin-3 to its neuronal receptors and interactions with nerve growth factor and brain-derived neurotrophic factor. *The EMBO Journal*, **11**, 917-922.

Romier, C., Cocchiarella, F., Mantovani, R. and Moras, D. (2003) The NF-YB/NF-YC structure gives insight into DNA binding and transcription regulation by CCAAT factor NF-Y. *The Journal of Biological Chemistry*, **278**, 1336-1345.

Ronchi, A., Bellorini, M., Mongelli, N. and Mantovani, R. (1995) CCAAT-box binding protein NF-Y (CBF, CP1) recognizes the minor groove and distorts DNA. *Nucleic Acids Research*, **23**, 4565-4572.

Roy, N., Deveraux, Q.L., Takahashi, R., Salvesen, G.S. and Reed, J.C. (1997) The c-IAP-1 and c-IAP-2 proteins are direct inhibitors of specific caspases. *The EMBO Journal*, **16**, 6914-6925.

Salsi, V., Caretti, G., Wasner, M., Reinhard, W., Haugwitz, U., Engeland, K. and Mantovani, R. (2003) Interactions between p300 and multiple NF-Y trimers govern cyclin B2 promoter function. *The Journal of Biological Chemistry*, **278**, 6642-6650.

Sattler, M., Liang, H., Nettesheim, D., Meadows, R.P., Harlan, J.E., Eberstadt, M., Yoon, H.S., Shuker, S.B., Chang, B.S., Minn, A.J. *et al*. (1997) Structure of Bcl-xL-Bak peptide complex: recognition between regulators of apoptosis. *Science,* **275**, 983-986.

Saunders, J.W., Jr. (1966) Death in embryonic systems. *Science,* **154**, 604-612.

Schlisio, S., Kenchappa, R.S., Vredeveld, L.C., George, R.E., Stewart, R., Greulich, H., Shahriari, K., Nguyen, N.V., Pigny, P., Dahia, P.L. *et al*. (2008) The kinesin KIF1Bbeta acts downstream from EglN3 to induce apoptosis and is a potential 1p36 tumor suppressor. *Genes & Development*, **22**, 884-893.

Schwarz, J.K., Deveto, S.H., Smith, E.J., Chellappan, S.P., Jakoi, L., and Nevins, J.R. (1993) Interactions of the p107 and Rb proteins with E2F during the cell proliferation response. *The EMBO Journal,* **12**, 1013-1020.

Schwartz, L.M., Smith, S.W., Jones, M.E. and Osborne, B.A. (1993) Do all programmed cell deaths occur via apoptosis? *Proceedings of the National Academy of Sciences of the United States of America*, **90**, 980-984.

Sedlak, T.W., Oltvai, Z.N., Yang, E., Wang, K., Boise, L.H., Thompson, C.B. and Korsmeyer, S.J. (1995) Multiple Bcl-2 family members demonstrate selective dimerizations with Bax. *Proceedings of the National Academy of Sciences of the United States of America*, **92**, 7834-7838.

Serra, E., Zemzoumi, K., di Silvio, A., Mantovani, R., Lardans, V. and Dissous, C. (1998) Conservation and divergence of NF-Y transcriptional activation function. *Nucleic Acids*

Research, **26**, 3800-3805.

Shi, Y. (2004) Caspase activation, inhibition, and reactivation: a mechanistic view. *Protein Science*, **13**, 1979-1987.

Shibue, T., Takeda, K., Oda, E., Tanaka, H., Murasawa, H., Takaoka, A., Morishita, Y., Akira, S., Taniguchi, T. and Tanaka, N. (2003) Integral role of Noxa in p53-mediated apoptotic response. *Genes & Development*, **17**, 2233-2238.

Shikama N., Lyon, J., and La Thangue, N.B. (1997) The p300/CBP family: integrating signals with transcription factors and chromatin. *Trends in Cell Biology,* **7**, 230-236.

Shikama, N., Chan, H.M., Krstic-Demonacos, M., Smith, L., Lee, C.W., Cairns, W. and La Thangue, N.B. (2000) Functional interaction between nucleosome assembly proteins and p300/CREB-binding protein family coactivators. *Molecular and Cellular Biology*, **20**, 8933-8943.

Shimizu, S., Eguchi, Y., Kosaka, H., Kamiike, W., Matsuda, H. and Tsujimoto, Y. (1995) Prevention of hypoxia-induced cell death by Bcl-2 and Bcl-xL. *Nature*, **374**, 811-813.

Shinjyo, T., Kuribara, R., Inukai, T., Hosoi, H., Kinoshita, T., Miyajima, A., Houghton, P.J., Look, A.T., Ozawa, K. and Inaba, T. (2001) Downregulation of Bim, a proapoptotic relative of Bcl-2, is a pivotal step in cytokine-initiated survival signaling in murine hematopoietic progenitors. *Molecular and Cellular Biology*, **21**, 854-864.

Sinha, S., Maity, S.N., Lu, J., and de Crombrugghe, B. (1995) Recombinant rat CBF-C, the third subunit of CBF/NFY, allows formation of a protein-DNA complex with CBF-A and CBF-B and with yeast HAP2 and HAP3. *Proceedings of the National Academy of Sciences of the United States of America*, **92**, 1624-1628.

Smeyne, R.J., Klein, R., Schnapp, A., Long, L.K., Bryant, S., Lewin, A., Lira, S.A. and Barbacid, M. (1994) Severe sensory and sympathetic neuropathies in mice carrying a disrupted Trk/NGF receptor gene. *Nature*, **368**, 246-249.

Soutoglou, E., Katrakili, N., and Talianidis, I. (2000) Acetylation regulates transcription factor activity at multiple levels. *Molecular Cell* **5**, 745-751.

Srinivasula, S.M., Ahmad, M., Ottilie, S., Bullrich, F., Banks, S., Wang, Y., Fernandes-Alnemri, T., Croce, C.M., Litwack, G., Tomaselli, K.J. *et al*. (1997) FLAME-1, a novel FADD-like anti-apoptotic molecule that regulates Fas/TNFR1-induced apoptosis. *The Journal of Biological Chemistry*, **272**, 18542-18545.

Srinivasula, S.M., Hegde, R., Saleh, A., Datta, P., Shiozaki, E., Chai, J., Lee, R.A., Robbins, P.D., Fernandes-Alnemri, T., Shi, Y. *et al*. (2001) A conserved XIAP-interaction motif in caspase-9 and Smac/DIABLO regulates caspase activity and apoptosis. *Nature*, **410**, 112-116.

Stahl, M., Dijkers, P.F., Kops, G.J., Lens, S.M., Coffer, P.J., Burgering, B.M. and Medema, R.H. (2002) The forkhead transcription factor FoxO regulates transcription of p27Kip1 and Bim in response to IL-2. *The Journal of Immunology*, **168**, 5024-5031.

Standart, N. and Jackson, R.J. (2007) MicroRNAs repress translation of m7Gppp-capped target mRNAs in vitro by inhibiting initiation and promoting deadenylation. *Genes & Development*, **21**, 1975-1982.

Stennicke, H.R. and Salvesen, G.S. (1999) Catalytic properties of the caspases. *Cell Death and Differentiation*, **6**, 1054-1059.

Strasser, A., Harris, A.W., Bath, M.L. and Cory, S. (1990) Novel primitive lymphoid tumours induced in transgenic mice by cooperation between myc and bcl-2. *Nature*, **348**, 331-333.

Straub, J.A., Lipscomb, E.A., Yoshida, E.S. and Freeman, R.S. (2003) Induction of SM-20 in PC12 cells leads to increased cytochrome c levels, accumulation of cytochrome c in the cytosol, and caspase-dependent cell death. *Journal of Neurochemistry*, **85**, 318-328.

Su, H., Trombly, M.I., Chen, J. and Wang, X. (2009) Essential and overlapping functions for mammalian Argonautes in microRNA silencing. *Genes & Development*, **23**, 304-317.

Su, M., Bansal, A.K., Mantovani, R., Sodek, J. (2005) Recruitment of NF-Y to the inverted CCAAT element (ICE) by the c-Jun and E1A stimulates basal transcription of the bone sialoprotein gene in osteosarcoma cells. *The Journal of Biological Chemistry,* **280**, 38365-38375.

Sun, C., Cai, M., Gunasekera, A.H., Meadows, R.P., Wang, H., Chen, J., Zhang, H., Wu, W., Xu, N., Ng, S.C. *et al*. (1999) NMR structure and mutagenesis of the inhibitor-of-apoptosis protein XIAP. *Nature*, **401**, 818-822.

Sun, C., Cai, M., Meadows, R.P., Xu, N., Gunasekera, A.H., Herrmann, J., Wu, J.C. and Fesik, S.W. (2000) NMR structure and mutagenesis of the third Bir domain of the inhibitor of apoptosis protein XIAP. *The Journal of Biological Chemistry*, **275**, 33777-33781.

Sun, Y.F., Yu, L.Y., Saarma, M., Timmusk, T. and Arumae, U. (2001) Neuron-specific Bcl-2 homology 3 domain-only splice variant of Bak is anti-apoptotic in neurons, but pro-apoptotic in non-neuronal cells. *The Journal of Biological Chemistry*, **276**, 16240-16247.

Susin, S.A., Lorenzo, H.K., Zamzami, N., Marzo, I., Snow, B.E., Brothers, G.M., Mangion, J., Jacotot, E., Costantini, P., Loeffler, M. *et al*. (1999) Molecular characterization of mitochondrial apoptosis-inducing factor. *Nature*, **397**, 441-446.

Suzuki, M., Youle, R.J. and Tjandra, N. (2000) Structure of Bax: coregulation of dimer formation and intracellular localization. *Cell*, **103**, 645-654.

Swope, D.L., Mueller, C.L., and Chrivia, J.C. (1996) CREB-binding protein activates transcription through multiple domains. *The Journal of Biological Chemistry,* **271**, 28138-28145.

Szutorisz, H., Dillon, N. and Tora, L. (2005) The role of enhancers as centres for general transcription factor recruitment. *Trends in Biochemical Sciences*, **30**, 593-599.

Takahashi, R., Deveraux, Q., Tamm, I., Welsh, K., Assa-Munt, N., Salvesen, G.S. and Reed, J.C. (1998) A single BIR domain of XIAP sufficient for inhibiting caspases. *The Journal of Biological Chemistry*, **273**, 7787-7790.

Tamm, I., Kornblau, S.M., Segall, H., Krajewski, S., Welsh, K., Kitada, S., Scudiero, D.A., Tudor, G., Qui, Y.H., Monks, A. *et al*. (2000) Expression and prognostic significance of IAP-family genes in human cancers and myeloid leukemias. *Clinical Cancer Research*, **6**, 1796-1803.

Tamm, I., Richter, S., Scholz, F., Schmelz, K., Oltersdorf, D., Karawajew, L., Schoch, C., Haferlach, T., Ludwig, W.D. and Wuchter, C. (2004) XIAP expression correlates with monocytic differentiation in adult de novo AML: impact on prognosis. *British Journal of Haematology*, **5**, 489-495.

Tanaka, Y., Naruse, I., Hongo, T., Xu, M.-J., Nakahata, T., Maekawa, T., and Ishii, S. (2000) Extensive brain hemorrhage and embryonic lethality in a mouse null mutant of CREB-binding protein. *Mechanisms of Development,* **95**, 133-145.

Tartaglia, L.A., Rothe, M., Hu, Y.F. and Goeddel, D.V. (1993) Tumor necrosis factor's cytotoxic activity is signaled by the p55 TNF receptor. *Cell*, **73**, 213-216.

Tatton, W.G., Chalmers-Redman, R., Brown, D. and Tatton, N. (2003) Apoptosis in Parkinson's disease: signals for neuronal degradation. *Annals of Neurology*, **5**, 61-70.

Taylor, R.C., Cullen, S.P. and Martin, S.J. (2008) Apoptosis: controlled demolition at the cellular level. *Nature Reviews*, **9**, 231-241.

Terasawa, K., Ichimura, A., Sato, F., Shimizu, K. and Tsujimoto, G. (2009) Sustained activation of ERK1/2 by NGF induces microRNA-221 and 222 in PC12 cells. *The FEBS Journal*, **276**, 3269-3276.

Testa, A., Donati, G., Yan, P., Romani, F., Huang, T.H., Vigano, M.A. and Mantovani, R. (2005) Chromatin immunoprecipitation (ChIP) on chip experiments uncover a widespread distribution of NF-Y binding CCAAT sites outside of core promoters. *The Journal of Biological Chemistry*, **280**, 13606-13615.

Thompson, C.B. (1995) Apoptosis in the pathogenesis and treatment of disease. *Science*, **267**,

1456-1462.

Tournier, C., and Wang, X. (2006) Regulation of functions by the ERK5 signalling pathway. *Cell Signalling,* **18**, 753-760.

Towers, E., Gilley, J., Randall, R., Hughes, R., Kristiansen, M. and Ham, J. (2009) The proapoptotic dp5 gene is a direct target of the MLK-JNK-c-Jun pathway in sympathetic neurons. *Nucleic Acids Research*, **37**, 3044-3060.

Tsujimoto, Y., Yunis, J., Onorato-Showe, L., Erikson, J., Nowell, P.C. and Croce, C.M. (1984) Molecular cloning of the chromosomal breakpoint of B-cell lymphomas and leukemias with the t(11;14) chromosome translocation. *Science,* **224**, 1403-1406.

U, M., Miyashita, T., Shikama, Y., Tadokoro, K. and Yamada, M. (2001) Molecular cloning and characterization of six novel isoforms of human Bim, a member of the proapoptotic Bcl-2 family. *FEBS Letters*, **509**, 135-141.

Uo, T., Kinoshita, Y. and Morrison, R.S. (2005) Neurons exclusively express N-Bak, a BH3 domain-only Bak isoform that promotes neuronal apoptosis. *The Journal of Biological Chemistry*, **280**, 9065-9073.

Valencia-Sanchez, M.A., Liu, J., Hannon, G.J. and Parker, R. (2006) Control of translation and mRNA degradation by miRNAs and siRNAs. *Genes & Development*, **20**, 515-524.

Van Delft, M.F., Wei, A.H., Mason, K.D., Vandenberg, C.J., Chen, L., Czabotar, P.E., Willis, S.N., Scott, C.L., Day, C.L., Cory, S. *et al*. (2006) The BH3 mimetic ABT-737 targets selective Bcl-2 proteins and efficiently induces apoptosis via Bak/Bax if Mcl-1 is neutralized. *Cancer Cell*, **10**, 389-399.

Varfolomeev, E., Blankenship, J.W., Wayson, S.M., Fedorova, A.V., Kayagaki, N., Garg, P., Zobel, K., Dynek, J.N., Elliott, L.O., Wallweber, H.J. *et al*. (2007) IAP antagonists induce autoubiquitination of c-IAPs, NF-kappaB activation, and TNFalpha-dependent apoptosis. *Cell*, **131**, 669-681.

Vasudevan, S., Tong, Y. and Steitz, J.A. (2007) Switching from repression to activation: microRNAs can up-regulate translation. *Science,* **318**, 1931-1934.

Ventura, A., Young, A.G., Winslow, M.M., Lintault, L., Meissner, A., Erkeland, S.J., Newman, J., Bronson, R.T., Crowley, D., Stone, J.R. *et al*. (2008) Targeted deletion reveals essential and overlapping functions of the miR-17 through 92 family of miRNA clusters. *Cell*, **132**, 875-886.

Villunger, A., Michalak, E.M., Coultas, L., Mullauer, F., Bock, G., Ausserlechner, M.J., Adams, J.M. and Strasser, A. (2003) p53- and drug-induced apoptotic responses mediated by BH3-only proteins puma and noxa. *Science* **302**, 1036-1038.

Virdee, K., Bannister, A.J., Hunt, S.P. and Tolkovsky, A.M. (1997) Comparison between the timing of JNK activation, c-Jun phosphorylation, and onset of death commitment in sympathetic neurones. *Journal of Neurochemistry*, **69**, 550-561.

Vo, N. and Goodman, R.H. (2001) CREB-binding protein and p300 in transcriptional regulation. *The Journal of Biological Chemistry*, **276**, 13505-13508.

Von Roretz, C. and Gallouzi, I.E. (2008) Decoding ARE-mediated decay: is microRNA part of the equation? *The Journal of Cell Biology*, **181**, 189-194.

Vucic, D. and Fairbrother, W.J. (2007) The inhibitor of apoptosis proteins as therapeutic targets in cancer. *Clinical Cancer Research*, **13**, 5995-6000.

Wajant, H. (2002) The Fas signaling pathway: more than a paradigm. *Science,* **296**, 1635-1636.

Wang, X., Merritt, A.J., Seyfried, J., Guo, C., Papadakis, E.S., Finegan, K.S., Kayahara, M., Dixon, J., Boot-Handford, R.P., Cartright, E.J., Mayer, U., and Tournier, C. (2005) Targeted deletion of mek5 causes early embryonic death and defects in the ERK5/MEF2 cell survival pathway. *Molecular and Cellular Biology*, **25**, 336-345.

Wang, X. and Tournier, C. (2006) Regulation of cellular functions by the ERK5 signalling pathway. *Cellular Signalling*, **18**, 753-760.

Wathelet, M.G., Lin, C.H., Parekh, B.S., Ronco, L.V., Howley, P.M. and Maniatis, T. (1998) Virus infection induces the assembly of coordinately activated transcription factors on the IFN-beta enhancer in vivo. *Molecular Cell*, **1**, 507-518.

Watson, F.L., Heerssen, H.M., Moheban, D.B., Lin, M.Z., Sauvageot, C.M., Bhattacharyya, A., Pomeroy, S.L. and Segal, R.A. (1999) Rapid nuclear responses to target-derived neurotrophins require retrograde transport of ligand-receptor complex. *The Journal of Neuroscience*, **19**, 7889-7900.

Wax, S.D., Rosenfield, C.L. and Taubman, M.B. (1994) Identification of a novel growth factor-responsive gene in vascular smooth muscle cells. *The Journal of Biological Chemistry*, **269**, 13041-13047.

Wei, M.C., Lindsten, T., Mootha, V.K., Weiler, S., Gross, A., Ashiya, M., Thompson, C.B. and Korsmeyer, S.J. (2000) tBID, a membrane-targeted death ligand, oligomerizes BAK to release cytochrome c. *Genes & Development*, **14**, 2060-2071.

Wei, M.C., Zong, W.X., Cheng, E.H., Lindsten, T., Panoutsakopoulou, V., Ross, A.J., Roth, K.A., MacGregor, G.R., Thompson, C.B. and Korsmeyer, S.J. (2001) Proapoptotic BAX and BAK: a requisite gateway to mitochondrial dysfunction and death. *Science,* **292**, 727-730.

Werlen, G., Hausmann, B., Naeher, D. and Palmer, E. (2003) Signaling life and death in the thymus: timing is everything. *Science,* **299**, 1859-1863.

Weston, C.R., Balmanno, K., Chalmers, C., Hadfield, K., Molton, S.A., Ley, R., Wagner, E.F. and Cook, S.J. (2003) Activation of ERK1/2 by deltaRaf-1:ER* represses Bim expression independently of the JNK or PI3K pathways. *Oncogene*, **22**, 1281-1293.

Whitfield, J., Neame, S.J., Paquet, L., Bernard, O. and Ham, J. (2001) Dominant-negative c-Jun promotes neuronal survival by reducing BIM expression and inhibiting mitochondrial cytochrome c release. *Neuron*, **29**, 629-643.

Whitfield, J., Neame, S.J. and Ham, J. (2004) Methods for culturing primary sympathetic

neurons and for determining neuronal viability. *Methods in Molecular Biology*, **282**, 157-168.

Wiggins, C.M., Band, H. and Cook, S.J. (2007) c-Cbl is not required for ERK1/2-dependent degradation of BimEL. *Cellular Signalling*, **19**, 2605-2611.

Wilkinson, J.C., Wilkinson, A.S., Scott, F.L., Csomos, R.A., Salvesen, G.S. and Duckett, C.S. (2004) Neutralization of Smac/Diablo by inhibitors of apoptosis (IAPs). A caspase-independent mechanism for apoptotic inhibition. *The Journal of Biological Chemistry*, **279**, 51082-51090.

Willis, S.N. and Adams, J.M. (2005) Life in the balance: how BH3-only proteins induce apoptosis. *Current Opinion in Cell Biology*, **17**, 617-625.

Willis, S.N., Fletcher, J.I., Kaufmann, T., van Delft, M.F., Chen, L., Czabotar, P.E., Ierino, H., Lee, E.F., Fairlie, W.D., Bouillet, P. *et al*. (2007) Apoptosis initiated when BH3 ligands engage multiple Bcl-2 homologs, not Bax or Bak. *Science,* **315**, 856-859.

Wilson, R., Goyal, L., Ditzel, M., Zachariou, A., Baker, D.A., Agapite, J., Steller, H. and Meier, P. (2002) The DIAP1 RING finger mediates ubiquitination of Dronc and is indispensable for regulating apoptosis. *Nature Cell Biology*, **4**, 445-450.

Winzen, R., Gowrishankar, G., Bollig, F., Redich, N., Resch, K. and Holtmann, H. (2004) Distinct domains of AU-rich elements exert different functions in mRNA destabilization and stabilization by p38 mitogen-activated protein kinase or HuR. *Molecular and Cellular Biology*, **24**, 4835-4847.

Wojnowski, L., Zimmer, A.M., Beck, T.W., Hahn, H., Bernal, R., Rapp, U.R. and Zimmer, A. (1997) Endothelial apoptosis in Braf-deficient mice. *Nature Genetics*, **16**, 293-297.

Wolter, K.G., Hsu, Y.T., Smith, C.L., Nechushtan, A., Xi, X.G. and Youle, R.J. (1997) Movement of Bax from the cytosol to mitochondria during apoptosis. *The Journal of Cell Biology*, **139**, 1281-1292.

Wong, C., Rougier-Chapman, E.M., Frederick, J.P., Datto, M.B., Liberati, N.T., Jian-Ming, L., and Xiao-Fan, W. (1999) Smad3-Smad4 and AP-1 complexes synergize in transcriptional activation of the c-Jun promoter by transforming growth factor. *Molecular and Cellular Biology,* **19**, 1821-1830.

Wright, K.L., Moore, T.L., Vilen, B.J., Brown, A.M., and Ting, J.P.-Y. (1995) Major histocompatibility complex class II-associated invariant chain gene expression is up-regulated by cooperative interactions of Sp1 and NF-Y. *The Journal of Biological Chemistry*, **270**, 20978-20986.

Wright, K.M., Vaughn, A.E. and Deshmukh, M. (2007) Apoptosome dependent caspase-3 activation pathway is non-redundant and necessary for apoptosis in sympathetic neurons. *Cell Death and Differentiation*, **14**, 625-633.

Wright, L.L., Cunningham, T.J., and Smolen, A.J. (1983) Developmental neuron death in the rat superior cervical sympathetic ganglion: cell counts and ultrastructure. *Journal of Neurocytology,* **12**, 727-738.

Wyllie, A.H., Kerr, J.F. and Currie, A.R. (1980) Cell death: the significance of apoptosis. *International Review of Cytology*, **68**, 251-306.

Wyttenbach, A. and Tolkovsky, A.M. (2006) The BH3-only protein Puma is both necessary and sufficient for neuronal apoptosis induced by DNA damage in sympathetic neurons. *Journal of Neurochemistry*, **96**, 1213-1226.

Xia, Z., Dickens, M., Raingeaud, J., Davis, R.J. and Greenberg, M.E. (1995) Opposing effects of ERK and JNK-p38 MAP kinases on apoptosis. *Science,* **270**, 1326-1331.

Xu, L., Lavinsky, R.M., Dasen, J.S., Flynn, S.E., McInerney, E.M., Mullen, T.M., Heinzel, T., Szeto, D., Korzus, E., Kurokawa, R. *et al*. (1998) Signal-specific co-activator domain requirements for Pit-1 activation. *Nature*, **395**, 301-306.

Xu, Y., Zhou, Y.L., Luo, W., Zhu, Q.S., Levy, D., MacDougald, O.A., Snead, M.L. (2006) NF-Y and CCAAT/enhancer-binding protein alpha synergistically activate the mouse amelogenin gene. *The Journal of Biological Chemistry*. **281**: 16090-8.

Yao, T.P., Oh, S.P., Fuchs, M., Zhou, N.D., Ch'ng, L.E., Newsome, D., Bronson, R.T., Li, E., Livingston, D.M., and Eckner R. (1998) Gene dosage-dependent embryonic development and proliferation defects in mice lacking the transcriptional integrator p300. *Cell,* **93**, 361-372.

Yan, N., Wu, J.W., Chai, J., Li, W. and Shi, Y. (2004) Molecular mechanisms of DrICE inhibition by DIAP1 and removal of inhibition by Reaper, Hid and Grim. *Nature Structural & Molecular Biology*, **11**, 420-428.

Yan, N. and Shi, Y. (2005) Mechanisms of apoptosis through structural biology. *Annual Review of Cell and Developmental Biology*, **21**, 35-56.

Yang, X., Chang, H.Y. and Baltimore, D. (1998) Essential role of CED-4 oligomerization in CED-3 activation and apoptosis. *Science,* **281**, 1355-1357.

Yang, X.J., Ogryzko, V.V., Nishikawa, J., Howard, B.H. and Nakatani, Y. (1996) A p300/CBP-associated factor that competes with the adenoviral oncoprotein E1A. *Nature*, **382**, 319-324.

Yankner, B.A. (1996) Mechanisms of neuronal degeneration in Alzheimer's disease. *Neuron*, **16**, 921-932.

Ye, H., Kuruvilla, R., Zweifel, L.S. and Ginty, D.D. (2003) Evidence in support of signaling endosome-based retrograde survival of sympathetic neurons. *Neuron*, **39**, 57-68.

Yie, J., Senger, K. and Thanos, D. (1999) Mechanism by which the IFN-beta enhanceosome activates transcription. *Proceedings of the National Academy of Sciences of the United States of America*, **96**, 13108-13113.

Yin, X.M., Wang, K., Gross, A., Zhao, Y., Zinkel, S., Klocke, B., Roth, K.A. and Korsmeyer, S.J. (1999) Bid-deficient mice are resistant to Fas-induced hepatocellular apoptosis. *Nature*,

400, 886-891.

Yoshida, E., Nakajima, T., Murakami, K. and Fukamizu, A. (1998) Identification of N-terminal minimal transactivation domain of CBP, p300 and caenorhabditis elegans homologues. *Gene*, **208**, 307-314.

Yoshida, H., Okada, T., Haze, K., Yanagi, H., Takashi, Y., Negishi, M., and Mori, K. (2000) ATF-6 activated by proteolysis binds in the presence of NF-Y (CBF) directly to the *cis*-acting element responsible for the mammalian unfolded protein response. *Molecular and Cellular Biology,* **20**, 6755-6767.

Youle, R.J. and Strasser, A. (2008) The BCL-2 protein family: opposing activities that mediate cell death. *Nature Reviews*, **9**, 47-59.

Yu, J., de Belle, I., Liang, H. and Adamson, E.D. (2004) Coactivating factors p300 and CBP are transcriptionally crossregulated by Egr1 in prostate cells, leading to divergent responses. *Molecular Cell*, **15**, 83-94.

Yu, J. and Zhang, L. (2008) PUMA, a potent killer with or without p53. *Oncogene*, **27:** 71-83.

Yuan, J. and Yankner, B.A. (2000) Apoptosis in the nervous system. *Nature*, **407**, 802-809.

Yuan, J. and Horvitz, H.R. (2004) A first insight into the molecular mechanisms of apoptosis. *Cell*, **116**, 53-56.

Yun, J., Chae, H.D., Choy, H.E., Chung, J., Yoo, H.S., Han, M.H. and Shin, D.Y. (1999) p53 negatively regulates cdc2 transcription via the CCAAT-binding NF-Y transcription factor. *The Journal of Biological Chemistry*, **274**, 29677-29682.

Yun, J., Chae, H.D., Choi, T.S., Kim, E.H., Bang, Y.J., Chung, J., Choi, K.S., Mantovani, R. and Shin, D.Y. (2003) Cdk2-dependent phosphorylation of the NF-Y transcription factor and its involvement in the p53-p21 signaling pathway. *The Journal of Biological Chemistry*, **278**, 36966-36972.

Zakrzewska, A., Schnell, P.O., Striet, J.B., Hui, A., Robbins, J.R., Petrovic, M., Conforti, L., Gozal, D., Wathelet, M.G. and Czyzyk-Krzeska, M.F. (2005) Hypoxia-activated metabolic pathway stimulates phosphorylation of p300 and CBP in oxygen-sensitive cells. *Journal of Neurochemistry*, **94**, 1288-1296.

Zhao, Y., Ransom, J.F., Li, A., Vedantham, V., von Drehle, M., Muth, A.N., Tsuchihashi, T., McManus, M.T., Schwartz, R.J. and Srivastava, D. (2007) Dysregulation of cardiogenesis, cardiac conduction, and cell cycle in mice lacking miRNA-1-2. *Cell*, **129**, 303-317.

Zhu, J., Giannola, D.M., Zhang, Y., Rivera, A.J. and Emerson, S.G. (2003) NF-Y cooperates with USF1/2 to induce the hematopoietic expression of HOXB4. *Blood*, **102**, 2420-2427.

Zhu, J., Zhang, Y., Joe, G.J., Pompetti, R. and Emerson, S.G. (2005) NF-Ya activates multiple hematopoietic stem cell (HSC) regulatory genes and promotes HSC self-renewal. *Proceedings of the National Academy of Sciences of the United States of America*, **102**, 11728-11733.